The Role of Nicotinamide N-Methyltransferase in Parkinson's Disease

Thomas, Martin Geoffrey

Awarding institution:
King's College London

The Role of Nicotinamide *N*-Methyltransferase in Parkinson's Disease

Martin Geoffrey Thomas

A Thesis Submitted in Partial Fulfilment for the Degree of Doctor of Philosophy

August 2014

King's College London

Institute of Pharmaceutical Science

London SE1 9NH

Abstract

Parkinson's disease (PD) is a progressive neurological movement disorder characterised by degenerating dopaminergic neurons in the midbrain's *substantia nigra pars compacta* (SNpc). In the majority of cases, PD is thought to be caused by a plethora of overlapping factors that combine to cause toxicity in SNpc neurons.

The enzyme nicotinamide *N*-methyltransferase (NNMT) is expressed at higher levels in the brain of PD patients. However, whether this association is indicative of a causative role in PD is unclear. The biochemical effects of NNMT expression were determined by comparing the NNMT-V5 expressing S.NNMT.LP cell line with its parent SH-SY5Y. Furthermore, the potential for NNMT to potentiate toxicity of β-carbolines (βC), a group of endogenous compounds with increased prevalence in PD, and 4-phenylpyridine (4PP), an environmental analogue of the neurotoxin 1-methyl-4-phenylpyridine, were determined by MTT and ATP assay. Finally, the ability of purified NNMT to metabolise the βC norharman (NH) *via* 2*N*-methylation was determined *via* enzyme assay and the toxicity of 2*N*-methylated NH (2-MeNH) was determined *via* MTT and ATP assay.

S.NNMT.LP cells contained a significantly higher ATP content than SH-SY5Y cells ($p < 0.01$). No difference was seen between S.NNMT.LP and SH-SY5Y toxicity to the βC tetrahydronorharman or 4PP. However, 200 μM NH significantly lowered ATP but not cell viability in S.NNMT.LP cells compared with SH-SY5Y ($p < 0.01$). NNMT was found to be capable of producing 2-MeNH from NH and S.NNMT.LP cells were

significantly protected from 2-MeNH toxicity ($p < 0.001$). Moreover, 2-MeNH was significantly less toxic to both cell lines than NH ($p < 0.05$). The metabolism of NH to 2-MeNH may, therefore, be a detoxification mechanism. Accordingly, the expression of NNMT in PD may be a protective response in PD by increasing ATP production and removing NH from the cytoplasm in favour of the less toxic 2-MeNH.

Acknowledgements

First and foremost I would like to thank the King's College London Graduate School for providing me with the funding to complete this PhD. Thanks also to Guarantors of Brain, Parkinson's UK and the King's College travel bursary scheme for allowing me to go all the way to New Orleans to present my work.

My utmost thanks go to Dr Richard Parsons who has guided me from day one and has been an excellent supervisor. In particular, I am very grateful for our great working relationship, the fact that he would always have an open mind towards my ideas and his good taste in whisky. My thanks also go to my second supervisor Dr David Barlow who guided us through the PhD process and helped me greatly with the statistical analysis of my data.

Thanks to Dan Asker, Calum King, Dr Helena Wong and Beatriz Padilla for never turning down a request and always giving me their time whenever I needed it. Thanks to Dr Khuloud Al-Jamal, Dr Julie Wang and Houmam Kafa for letting me use their equipment and helping me set up and troubleshoot my various protocols. Thanks to Dr David Mountford, Anna Pöschl and Ferdinand Fuchs for helping me with the chemical synthesis and always being responsive to my many questions. Thanks also to Dr Andrew Kicman for his help in arranging and setting up the mass spectrometry project and thanks to Anna Caldwell and Tobias Krams for carrying it out. Thanks to Michelle Zaso and Nicole Mendoza for helping me out in the lab and in cell culture. My thanks also go to Dr Elena Rosca for her help in optimising my toxicity assays and Matthijs van Haren, Prof Moinica Emanuelli and Dr Davide Sartini for helping me with the NNMT enzyme assay.

Thanks to all my friends and family who've been with me through all the ups and downs, weekend experiments and unplugged freezers of the last four years. In particular, I'd like to thank Bridie Dutton, Jo Muddle, Damian Rivett, Will Wild and Arcadia Woods for keeping me sane in FWB and sharing with me their own PhD experiences over many a lunchtime chat. Thanks also to Julia Mantaj for picking up the slack in the lab while I was writing and allowing me to keep in touch with my German roots. Finally, thanks to the three most important people in my life: my dad Geoff, my sister Jenny and my partner Arianna for being so caring and considerate during these 4 years and beyond. I truly appreciate all the support you've given me and I hope I've made you proud.

Table of Contents

Abstract 1

Acknowledgements 3

List of Figures 13

List of Tables 17

List of Abbreviations 18

1. Introduction 22

1.1. Introduction 23

1.1.1. Parkinson's disease prevalence and global impact 23

1.1.2. PD patients have an impaired ability to regulate movement 24

1.2. The pathophysiology of PD 30

1.2.1. Inherited vs non-inherited PD 30

1.2.1.1. SNCA 31

1.2.1.2. LRRK2 33

1.2.1.3. Parkin and PINK-1 33

1.2.1.4. Homologous mechanisms of familial and sporadic PD 34

1.2.2. The role of mitochondria in PD 35

1.2.2.1. Complex I deficiency 35

1.2.2.2. Iron accumulation 39

1.2.2.3. Impaired mitochondrial turnover 40

1.2.2.4. Mitochondria and ROS in PD: the chicken or the egg? 40

1.2.3. The susceptibility of dopaminergic neurons to damage 41

1.3. The cause(s) of PD 47

1.3.1. Aging 47

1.3.2. Environmental factors in PD development 49

1.3.3. The genetics of an un-genetic disease 51

1.3.3.1. Monogenic causes of sporadic PD 51

1.3.3.2. Genetic risk-factors for the development of sporadic PD 53

1.3.4. Nicotinamide N-methyltransferase is upregulated in PD 55

1.3.5. The activation of endogenous neurotoxins 59

1.3.5.1. The biosynthesis and environmental acquisition of βCs 59

1.3.5.2. βCs are potential pro-toxins in PD 60
1.3.5.3. The toxicity of N-methylated βCs 62
1.3.5.4. The identity of enzyme responsible for NH's N-methylations 63
1.4. The aims of the project 65
2. General Methods 66
2.1. Cell Culture 67
2.1.1. Maintenance and culture of cell lines 69
2.1.2. Cell trypsinisation, centrifugation and counting 69
2.1.3. Preparation of cell pellets for snap freezing 70
2.2. Western Blotting 71
2.2.1. Preparation of protein samples 73
2.2.2. Protein assay using the Lowry method 73
2.2.3. Preparation of samples for Western blotting 75
2.2.4. SDS – polyacrylamide gel electrophoresis (PAGE) 76
2.2.5. Semi-dry transfer of proteins to nitrocellulose membrane 76
2.2.6. Immunoblotting 78
2.3. RT-PCR 80
2.3.1. Isolation of cellular RNA 80
2.3.2. Reverse transcription of mRNA 81
2.3.3. PCR amplification of target cDNA 81
2.3.4. DNA gel electrophoresis 82
2.4. Toxicity Assays 83
2.4.1. Preparation of cultured cells for toxicity assays 84
2.4.2. Dosing 85
2.4.3. End-point analyses 87
2.4.3.1. MTT assay 87
2.4.3.2. ATP assay 88
2.4.4. Statistical analysis 89
2.4.4.1. Determination of individual dose toxicity 89
2.4.4.2. Determination of individual dose toxicity between cell lines 90
2.4.4.3. Determination and comparison of EC50s 91
3. Optimisation 94
3.1. Determination of appropriate cell viability assays 95
3.1.1. Introduction 95

3.1.1.1. The LDH assay 95

3.1.1.2. The MTT assay 96

3.1.1.3. The ATP assay 98

3.1.1.4. The balance between assay number and practicality 99

3.1.2. Methods 101

3.1.2.1. LDH assay optimisation 101

3.1.2.1.1. The effect of media supplements on the LDH assay 101

3.1.2.1.2. The dose-response effect of FBS-supplemented cell culture media on the LDH assay 102

3.1.2.2. MTT assay optimisation 102

3.1.2.2.1. The effect of FBS supplementation on cell viability via MTT reduction 102

3.1.2.3. ATP assay optimisation 103

3.1.2.3.1. Determination of the relationship between luminescence values, ATP concentration and cell viability 103

3.1.3. Statistical Analysis 103

3.1.4. Results 105

3.1.4.1. LDH assay optimisation 105

3.1.4.1.1. Media supplementation with phenol red and FBS increased absorbance in the LDH assay 105

3.1.4.1.2. Media supplementation with FBS increased LDH assay absorbance in a dose-dependent manner 107

3.1.4.2. MTT assay optimisation 108

3.1.4.2.1. FBS supplementation significantly affected cell viability 108

3.1.4.3. ATP assay optimisation 109

3.1.4.3.1. Luminescence values were proportional to ATP content and cell density in the ATP assay 109

3.1.5. Discussion 111

3.2. Determination of the appropriate cell density for toxicity assays 113

3.2.1. Introduction 113

3.2.2. Methods 115

3.2.3. Results 116

3.2.4. Discussion 118

3.3. Determination of the optimal incubation time for toxicity assays 120

3.3.1. Introduction 120

3.3.2. Methods 121
3.3.3. Results 122
3.3.3.1. Extending the incubation time to 5 days improved the dose-response curve in SH-SY5Y cells 122
3.3.3.2. The $EC50_{MTT}$ in S.NNMT.LP cells was significantly lower when the incubation time was extended to 5 days 124
3.3.4. Discussion 125
3.4. Characterisation of a positive control for the Western blotting of neuronal markers 128
3.4.1. Introduction 128
3.4.2. Methods 130
3.4.3. Results 132
3.4.4. Discussion 136
4. Characterisation of S.NNMT.LP cells 138
4.1. Introduction 139
4.2. Methods 142
4.2.1. Confirmation of NNMT-V5 expression 142
4.2.2. Validation of NNMT-V5 expression over time in S.NNMT.LP cells 144
4.2.3. Determination of cellular ATP concentration in S.NNMT.LP and SH-SY5Y incubated with 1 mM MeN 144
4.2.4. Measurement of oxygen consumption in S.NNMT.LP and SH-SY5Y incubated with 1 mM MeN 146
4.2.4.1. Culture of cells prior to the measurement of oxygen consumption 146
4.2.4.2. Measurement of oxygen consumption 146
4.2.5. Determination of mitochondrial membrane potential ($\Delta\psi_m$) in S.NNMT.LP and SH-SY5Y incubated with 1 mM MeN 147
4.2.6. Determination of neuronal lineage 149
4.2.7. Statistical analysis 149
4.3. Results 151
4.3.1. NNMT-V5 was expressed exclusively in S.NNMT.LP cells 151
4.3.2. NNMT-V5 expression did not vary with passage number 152
4.3.3. ATP concentration was significantly elevated in S.NNMT.LP cells and SH-SY5Y cells treated with 1 mM MeN compared to untreated SH-SY5Y 154
4.3.4. Oxygen consumption was significantly elevated in S.NNMT.LP cells and SH-SY5Y cells treated with 1 mM MeN 155

4.3.5. $\Delta\psi_m$ was not significantly different in SH-SY5Y cells treated with 1 mM MeN and S.NNMT.LP cells compared to untreated SH-SY5Y 157

4.3.6. NNMT-V5 expression did not induce a change in neuronal lineage in SH-SY5Y cells 158

4.4. Discussion 160

4.4.1. Confirmation and validation of NNMT-V5 expression 160

4.4.2. NNMT-V5-expression significantly enhanced cell viability, an effect mediated by MeN 162

4.4.3. The consequence of NNMT-V5 expression on neuronal lineage 164

4.4.4. Summary 166

5. The toxicity of βCs and 4PP in SH-SY5Y and S.NNMT.LP cells 167

5.1. Introduction 168

5.2. Methods 171

5.2.1. MTT assay of SH-SY5Y cells and S.NNMT.LP cells incubated with NH, THNH and 4PP 171

5.2.2. ATP assay of SH-SY5Y cells and S.NNMT.LP cells incubated with NH, THNH and 4PP 172

5.2.3. Statistical analysis 172

5.3. Results 173

5.3.1. No difference in cell viability between SH-SY5Y and S.NNMT.LP cells in response to NH, THNH and 4PP 173

5.3.1.1. NH 175

5.3.1.2. THNH 175

5.3.1.3. 4PP 175

5.3.1.4. Order of compound toxicity – MTT 176

5.3.2. S.NNMT.LP cells showed significantly greater decrease in ATP content and $EC50_{ATP}$ than SH-SY5Y cells in response to NH only 178

5.3.2.1. NH 180

5.3.2.2. THNH 180

5.3.2.3. 4PP 180

5.3.1.4. Order of compound toxicity – ATP 181

5.3.3. Toxicity differences existed between the MTT and ATP assays 183

5.4. Discussion 184

5.4.1. βC-toxicity in SH-SY5Y and S.NNMT.LP cells 184

5.4.2. 4PP-exposure in SH-SY5Y and S.NNMT.LP cells 187

5.4.3. The physiological relevance of the compound concentrations used in the study 189
5.4.4. Summary 191
6. The determination of the role of NNMT in 2-MeNH toxicity and biosynthesis 192
6.1. Introduction 193
6.2. Methods 195
6.2.1. Synthesis 195
6.2.1.1. Synthesis of 2-MeNH 195
6.2.1.2. Synthesis of 2,9-diMeNH 196
6.2.1.3. Confirmation of the identities of the synthetic products 198
6.2.1.3.1. NMR 198
6.2.1.3.2. Melting point analysis 198
6.2.1.3.3. Mass spectrometry 199
6.2.2. MTT assay of SH-SY5Y cells and S.NNMT.LP cells incubated with 2-MeNH ... 199
6.2.3. ATP assay of SH-SY5Y cells and S.NNMT.LP cells incubated with 2-MeNH 200
6.2.4. Determination of NNMT NH N-methyltransferase activity 200
6.2.4.1. Proof-of-concept study 200
6.2.4.2. Detection of 2-MeNH 203
6.2.4.2.1. Determination of 2-MeNH and THNH parent → product ion transitions 203
6.2.4.2.2. Sample preparation and LC-MS 203
6.2.4.2.3. Analysis of LC-MS data 205
6.2.4.3. Calculation of Michaelis-Menten kinetic parameters of NNMT NH 2-N-methylation 205
6.2.5. Statistical Analysis 206
6.3. Results 207
6.3.1. Analysis of syntheses: 2-MeNH 207
6.3.1.1. Characteristics of the synthetic product 207
6.3.1.2. NMR spectra for 2-MeNH matched those previously reported 207
6.3.1.3. The 2-MeNH mass to charge ratio (m/z) was confirmed using mass spectrometry 208
6.3.2. Analysis of syntheses: 2,9-diMeNH 210
6.3.2.1. Characteristics of the synthetic product 210
6.3.2.2. NMR spectra for 2,9-diMeNH did not match those previously reported 210
6.3.2. Toxicity assays of SH-SY5Y and S.NNMT.LP cells incubated with 2-MeNH 211

6.3.2.1. S.NNMT.LP cell viability was significantly less susceptible to the toxicity of 2-MeNH compared with SH-SY5Y cells 211
6.3.2.2. The ATP content of S.NNMT.LP cells was significantly protected against 2-MeNH compared with SH-SY5Y cells 216
6.3.3. Investigation of NNMT's NH 2N-methyltransferase activity 220
6.3.3.1. SRM transitions of 2-MeNH and THNH 220
6.3.3.2. Determination of NNMT NH 2N-methyltransferase specific activity 222
6.3.4. The kinetic parameters of NNMT NH 2N-methylation 223
6.4. Discussion 226
6.4.1. The synthesis of 2-MeNH, but not 2,9-diMeNH, was successful 226
6.4.2. S.NNMT.LP cell viability and ATP content were less susceptible to 2-MeNH toxicity than SH-SY5Y 228
6.4.3. NNMT has NH 2N-methyltransferase activity 232
6.4.4. Summary 236
7. Discussion 238
7.1. The contribution of the project towards establishing the role of NNMT in PD 239
7.1.1. Summary of the project thus far 239
7.1.2. The effects of NNMT expression on the cell 239
7.1.3. The effect of NNMT expression on the toxicity of NH 241
7.1.4. The NNMT-mediated conversion of NH to 2-MeNH may be a detoxification pathway 242
7.1.5. NNMT-V5 expression did not alter the toxicity of THNH and 4PP 245
7.1.6. Conclusions drawn from the project 247
7.2. Future work 248
7.2.1. Further studies using established methods 248
7.2.1.1. Optimisation of the NNMT enzyme assay 248
7.2.1.2. Synthesis of 2,9-diMeNH followed by repetition of enzyme assays and toxicity studies 248
7.2.1.3. Investigation of the mechanisms of βC toxicity/protection in S.NNMT.LP cells 249
7.2.1.4. Determination of NH 2N-methyltransferase activity in S.NNMT.LP cells 250
7.2.2. Improvement of physiological relevance via new methods 250
7.2.2.1. Repetition of toxicity assays using differentiated cells 250
7.2.2.1. Assessment of the effects of NNMT expression in vivo 253
7.3. Concluding remarks 254

References **256**

Appendix 1 ..... **276**

MTT data **277**

ATP data **283**

Appendix 2 ..... **289**

MTT data **290**

ATP data **292**

Appendix 3 ..... **294**

Appendix 4 ..... **298**

List of Figures

Figure 1.1. Dopaminergic neurons of the midbrain following tyrosine hydroxylase staining......25

Figure 1.2. The movement-signalling pathways of the brain's basal ganglia.. 26

Figure 1.3. The pigmentation of the midbrain is indicative of the presence of neuromelanin within the dopaminergic neurons of the SN......29

Figure 1.4. A histological image depicting a LB in the SN of a PD patient. 31

Figure 1.5. A Schematic representation of the 5 complexes of the mitochondrial electron transport chain. 36

Figure 1.6. Schematic representation of ROS generation by CxI......38

Figure 1.7. A computer-reconstructed axonal arbor of a single dopaminergic neuron from the SNpc of a rat brain. 42

Figure 1.8. NNMT catalyses the N-methylation of nicotinamide to 1-methyl-nicotinamide......56

Figure 1.9. The structural similarity between NH and MPP^+ following NH's *N*-methylation at the 2*N* position.....59

Figure 1.10 The methylation pathway of NH and 1,2,3,4-tetrahydroNH in the human brain. 61

Figure 2.1. A typical plate layout used for protein assays......74

Figure 2.2. An illustration of the gel "sandwich" used during the semi-dry transfer of protein bands from a 4-12% NuPage Bis-Tris SDS-PAGE gel to a nitrocellulose membrane. 77

Figure 2.3. 96-well plate layout used for MTT assays and ATP assays.....85

Figure 2.4. A schematic example of NH, THNH, 4-PP and 2-MeNH serial dilutions into a deep-well block.......86

Figure 3.1. Schematic representation of the relationship between LDH activity and formazan production in the LDH assay......96

Figure 3.2. Schematic representation of the conversion of MTT into purple formazan by various enzymes in the mitochondria and cytosol. 97

Figure 3.3. Schematic representation of the ATP luciferase assay.. 98

Figure 3.4. The effect of cell culture media supplements on the LDH cytotoxicity assay. 106

Figure 3.5. The effect of FBS-supplementation on the LDH-cytotoxicity assay. ... 107

Figure 3.6. The effect FBS on SH-SY5Y and S.NNMT.LP cell viability as measured by the MTT assay. 108

Figure 3.7. The linear relationship between ATP and luminescence and cell density and luminescence in the ATP assay. 110

Figure 3.8. The relationship between cell density and absorbance after 2 days and 5 days incubation as measured by the MTT assay. 117

Figure 3.9. Dose response curves of THNH following its incubation with SH-SY5Y cells and S.NNMT.LP cells. 123

Figure 3.10. Secondary antibody controls of SH-SY5Y, S.NNMT.LP, mouse brain in RIPA buffer and mouse brain in 1% triton-X in PBS. 133

Figure 3.11 Western blots of homogenised mouse brain, prepared in RIPA buffer or 1% Triton X-100 in PBS. 135

Figure 4.1. RT-PCR detection of NNMT-V5 expression in SH-SY5Y and S.NNMT.LP cell lines. 151

Figure 4.2. Western blot detection of NNMT-V5 and β-actin expression in S.NNMT cells and SH-SY5Y cells. 151

Figure 4.3. Western blots of recombinant NNMT expression and β-tubulin in SH-SY5Y cells and S.NNMT.LP cells. 153

Figure 4.4. NNMT-V5 protein expression as a function of passage number in S.NNMT.LP cells. 153

Figure 4.5. ATP concentrations within SH-SY5Y cells, SH-SY5Y cells supplemented with 1 mM MeN and S.NNMT.LP cells. 154

Figure 4.7. Typical trace of the oxygen consumption over time of SH-SY5Y cells, SH-SY5Y cells supplemented with 1 mM MeN and S.NNMT.LP cells. 156

Figure 4.6. The oxygen consumption of SH-SY5Y cells, SH-SY5Y cells incubated with 1 mM MeN, and S.NNMT.LP cells. 156

Figure 4.8. The mitochondrial membrane potential, as determined by JC-1 staining, in SH-SY5Y cells, SH-SY5Y cells supplemented with 1 mM MeN and S.NNMT.LP cells. 157

Figure 4.9. Western blots for various neuronal markers using protein samples derived from SH-SY5Y cells and S.NNMT.LP cells. 159

Figure 5.1. The structural similarity between 4PP and the MPP^+. 169

Figure 5.2. Dose response curves of NH, THNH and 4PP following their incubation with SH-SY5Y cells and S.NNMT.LP cells for 5 days (MTT assay). 174

Figure 5.3. Comparative toxicity curves of NH, 4PP and THNH in SH-SY5Y cells and S.NNMT.LP cells following a 5-day incubation (MTT assay).. 177

Figure 5.4. Dose response curves of NH, THNH and 4PP following their incubation with SH-SY5Y cells and S.NNMT.LP cells for 5 days (ATP assay). 179

Figure 5.5. Comparative toxicity curves of NH, 4PP and THNH in SH-SY5Y cells and S.NNMT.LP cells following a 5-day incubation (ATP assay). 182

Figure 6.1. The reaction conditions for the synthesis of 2-MeNH and 2,9-diMeNH. 194

Figure 6.2. The full scan spectrum of synthesised 2-MeNH following its infusion into a TSQ Triple quadrupole mass spectrometer. 209

Figure 6.3. The dose response curve of 2-MeNH toxicity towards SH-SY5Y cells and S.NNMT.LP cells after a 5 day incubation (MTT assay). 212

Figure 6.4. Comparative toxicity curves of NH and 2-MeNH in SH-SY5Y cells and S.NNMT.LP cells following 5-day incubations (MTT assay). 215

Figure 6.5. The dose response curve of 2-MeNH toxicity towards SH-SY5Y cells and S.NNMT.LP cells after a 5 day incubation (ATP assay). 216

Figure 6.6. Comparative toxicity curves of NH and 2-MeNH in SH-SY5Y cells and S.NNMT.LP cells following 5-day incubations (ATP assay). 219

Figure 6.7. Full scan spectrum of 2-MeNH m/z following fragmentation of the 183 m/z parent ion via MSMS. 221

Figure 6.8. The NNMT-mediated production of 2-MeNH over time 222

Figure 6.9. Michaelis-Menten plot of NH 2*N*-methyltransferase activity of NNMT. 223

Figure 6.10. Eadie-Hofstee plot of NH 2*N*-methyltransferase activity of NNMT. .224

Figure 6.11. Hanes-Woolf plot of NH 2*N*-methyltransferase activity of NNMT. ..224

List of Tables

Table 1.1. Known PD-causing genes that occur in sporadic PD. 52

Table 2.1. Commonly used solutions during cell culture. 68

Table 2.2. Components and abbreviations of the common reagents used during Western blotting. 72

Table 2.3. The compositions of various solutions used in toxicity assays. 86

Table 3.1. Antibodies and their dilutions used during Western blotting (neuronal markers). 131

Table 4.1. Antibodies and their dilutions used for Western blotting (NNMT expression and loading controls). 143

Table 4.2. PCR primer sequences and their product sizes. 143

Table 4.3. The compositions of solutions used during the determination of the biochemical effects of NNMT. 145

Table 6.1. The compositions of solutions used in the NNMT enzyme assay. 201

Table 6.2. The composition of 2-MeNH standards made from a 5 mg/mL stock of 2-MeNH in DMSO. 202

Table 6.3. The gradient conditions of the LC analysis of 2-MeNH following the NNMT enzyme assay. 204

Table 6.4 The dose-dependent effects of 2-MeNH on SH-SY5Y and S.NNMT.LP cell viability. 213

Table 6.5. The dose-dependent effects of 2-MeNH on the ATP content of SH-SY5Y and S.NNMT.LP cells. 217

Table 6.6. K_m and Vmax calculations from various plots of enzyme assay data for the determination of NNMT's NH 2*N*-methyltransferase activity. 225

List of Abbreviations

^{1}H-NMR – Proton NMR

2-MeNH – 2-methylnorharman

2,4-DNP – 2,4-dinitrophenol

2,9-diMeNH – 2,9-dimethylnorharman

4PP – 4-phenylpyridine

6OHDA – 6-hydroxydopamine

9-MeNH – 9-methylnorharman

^{13}C-NMR – Carbon NMR

ACN – Acetonitrile

βC – β-carboline

BSA – Bovine serum albumin

cDNA – Complimentary DNA

ChAT – Choline acetyltransferase

CoQ – Coenzyme Q

CSF – Cerebrospinal fluid

CxI – complex I of the mitochondrial respiratory chain

DAT – Dopamine transporter

DDT – Dithiothreitol

DMF – Dimethyl formamide

DMSO – dimethyl sulfoxide

DOPAL – 3,4-dihydroxyphenylacetaldehyde

Δψm – Mitochondrial membrane potential

EA – Ethyl acetate

ECL – Electrochemiluminescence

EDTA – ethylenediaminetetraacetic acid

FA – Formic acid

FBS – Fetal Bovine Serum

FMN – Flavin mononucleotide

GD – Gaucher's disease

GBA – Glucocerebrosidase

GBR 12909 – 1-[2-[bis(4-fluorophenyl)methoxy]ethyl)-4-(3-phenylpropyl)piperazine

GWAS – Genome-wide association study

HEK – Human embryonic kidney

HI – Heat-inactivated

HRP – Horseradish peroxidase

INMT – Indolethylamine *N*-methyltransferase

LB – Lewy Body

LC-MS – Liquid chromatography-mass spectrometry

LRRK2 – Leucine-rich repeat kinase 2

LDH – Lactate dehydrogenase

MAPT – Microtubule-associated protein tau

MeN – 1-methylnicotinamide

MI – Methyl iodide

MOPS – 3-(*N*-morpholino)propanesulfonic acid

MPP^+ – 1-methyl-4-phenylpyridine

MPTP – 1-methyl-4-phenyl-tetrahydropyridine

MSC – Microbiological safety cabinet

MTBST – Milk-Tris buffered saline-Triton X-100

mtDNA – Mitochondrial DNA

MTT – 3-(4,5-Dimethylthiazol-2-yl)-2,5-diphenyltetrazolium bromide

m/z – Mass-to-charge ratio

NADH – Nicotinamide adenine dinucleotide

NaH – Sodium hydride

NEAA – Non-essential amino acids

NH – Norharman

NNMT – Nicotinamide *N*-methyltransferase

NNMT-V5 – NNMT with a V5 tag at the C-terminus

NMR – Nuclear magnetic resonance

$O_2^{\bullet-}$ – Superoxide

PBS – Phosphate buffered saline

PCR – Polymerase chain reaction

PD – Parkinson's disease

PINK1 – Phosphatase and tensin homolog-induced putative kinase-1

PMSF – Phenylmethylsulfonyl fluoride

pNNMT.V5 – The plasmid encoding recombinant human NNMT

PNMT – Phenylethanolamine *N*-methyltransferase

RA – Retinoic acid

RIPA – Radioimmunoprecipitation assay

ROS – Reactive oxygen species

SAM – *S*-adenosylmethionine

SN – *Substantia nigra*

SNP – Single nucleotide polymorphism

SNpc – *Substantia nigra pars compacta*

SNpr – *Substantia nigra pars reticulata*

SRM – Selected reaction monitoring

TAE – Tris-acetate-EDTA

TBS – Tris buffered saline

TBST – Tris buffered saline-Triton X-100

TH – Tyrosine hydroxylase

THNH – Tetrahydro-norharman

TPH – Tryptophan hydroxylase

UCP – Uncoupling protein

$\mathbf{v_i}$ – Initial velocity

VTA – Ventral tegmental area

VPS35 – Vacuolar protein sorting 35

1. Introduction

1.1. Introduction

1.1.1. Parkinson's disease prevalence and global impact

Parkinson's disease (PD) is a progressive neurological movement disorder characterised by a number of motor and non-motor symptoms including bradykinesia, rigidity, depression and fatigue. PD prevalence increases with age and is expected to rise sharply in the near future as life expectancy increases, particularly in industrialised countries (de Lau & Breteler 2006, Dorsey *et al.* 2007, Lesage & Brice 2009, Kowal *et al.* 2013). Currently, estimates suggest that 1 in 100 people over 60 years of age have PD (de Lau & Breteler 2006, Kowal *et al.* 2013). As a consequence of the progressive increase in the proportion of elderly people within the populations of the world, this number is expected to more than double by 2030 (Dorsey *et al.* 2007).

The rising incidence of PD is expected to have profound economic consequences. Although there are difficulties associated with determining the economic burden of PD (Dodel *et al.* 2014), a recent, conservative, estimate of PD burden in the USA suggested that medical costs amounted to $14 billion in 2010 (Kowal *et al.* 2013). Furthermore, the non-medical costs of PD (for example, lost workforce productivity, disability benefit payments, professional care) were estimated to amount to an additional $6.3 billion.

In addition to the economic costs of PD, the disease also adds a large societal and emotional burden to PD patients and their friends and family. Consequently, PD is becoming an increasingly significant feature of many peoples' lives. As a result,

there is a growing need for more research into its mechanisms and potential treatment options as we progress through the 21st century.

1.1.2. PD patients have an impaired ability to regulate movement

Aside from a range of often difficult to distinguish non-motor symptoms (Chaudhuri, Healy & Schapira 2006), the defining, outwardly recognisable, features of PD include bradykinesia, rigidity, tremor and postural instability (Hirsch, Jenner & Przedborski 2013). These symptoms arise as a consequence of the main pathological hallmark of PD: the degeneration of the dopaminergic neurons in the brain's *substantia nigra pars compacta* (SNpc), a part of the basal ganglia in the midbrain (figure 1.1).

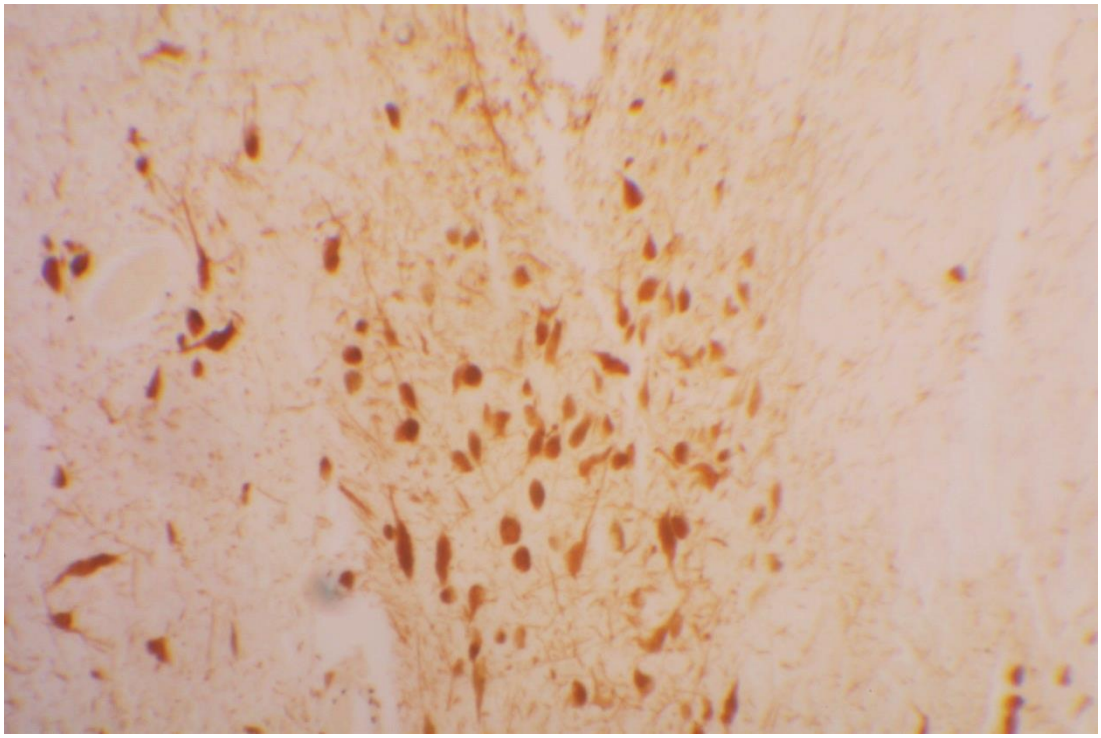

Figure 1.1. Dopaminergic neurons of the midbrain following tyrosine hydroxylase staining. Image kindly provided by Cindy Escobar (July 2014).

The degree of SNpc dopamine neuron loss varies with disease duration but is typically 80% at time of death with a 50% loss of dopamine in the striatum (Cheng, Ulane & Burke 2010). An illustration of the SNpc's role in movement-generation is shown in figure 1.2.

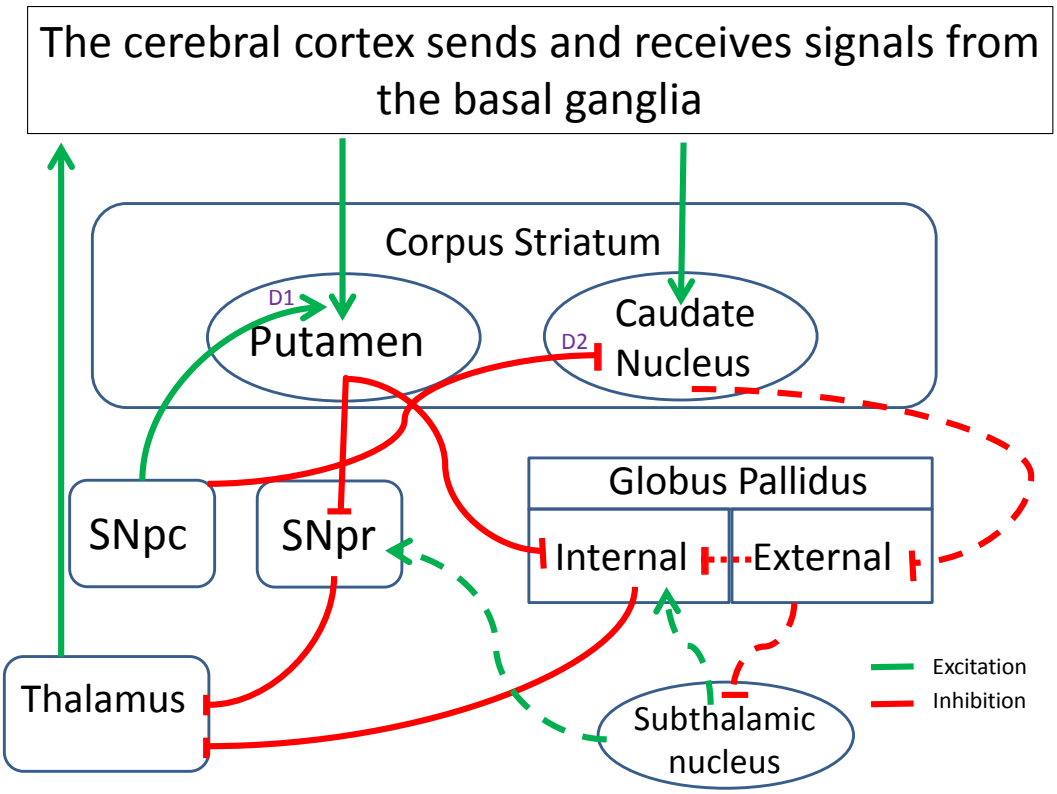

Figure 1.2. The movement-signalling pathways of the brain's basal ganglia. Signals are grouped into 2 pathways: the movement-generating direct pathway (solid lines) and the movement-inhibiting indirect pathway (dotted lines). Where pathways overlap (for example in the efferent signals from the SNpr and internal globus pallidus), a solid line is used. Signals in green are excitatory, while inhibitory signals are red. SNpc: substantia nigra pars compacta, SNpr: substantia nigra pars reticulata. D1 and D2 refer to the type of dopamine receptors located at the putamen and caudate nucleus respectively.

Movement-influencing signals in the basal ganglia can be grouped into 2 pathways: the movement-generating direct pathway and the movement-inhibiting indirect pathway. The direct pathway promotes movement by increasing thalamic-motor cortex signalling *via* its putamen-mediated disinhibition. On the other hand the indirect pathway dampens thalamic signalling by strengthening the inhibitory signals of the *substantia nigra pars reticulata* (SNpr) and the internal *globus pallidus*.

The SNpc plays a key role in modulating the strengths of these 2 pathways. Dopamine released by SNpc neurons at D1 receptors promotes activation of the direct pathway at the putamen. At the same time, dopamine also acts upon inhibitory D2 receptors at the caudate nucleus to inhibit the indirect pathway. The end result of dopamine's dual action is a movement-promoting signal being sent from the thalamus to the motor cortex and onwards to the periphery (Kandel, Schwartz & Jessel 2000, Purves *et al.* 2001).

Upon degeneration of the SNpc, the balance between these 2 pathways is disrupted, causing increased thalamic inhibition. In practice, this leads to a lowering of the body's ability to change conscious thought into movement. In particular, subtle movements, which the SNpc is especially capable of facilitating, become harder to perform, leading to the characteristically rigid movement patterns common in PD patients (Purves *et al.* 2001).

While degeneration of SNpc dopaminergic neurons is the most identifiable cause of PD and, indeed, the key factor of its movement-deteriorating pathology, there is growing evidence to suggest that PD is not simply a disorder affecting this single cell

population. Instead, there appear to be a number of additional cells, both neuronal and non-neuronal, and also beyond the SNpc, that appear to be subjected to their own pathologies. For example, it has been reported that α-synuclein deposition, a molecular hallmark of PD in dopaminergic neurons (discussed in more detail in section 1.2.1.1), can spread from cell to cell *via* the transcellular movement of α-synuclein (Braak *et al.* 2003, Kordower *et al.* 2008, Hirsch, Jenner & Przedborski 2013).

Accordingly, PD's pathological mechanisms can be categorised as "cell autonomous" or "non-cell autonomous". Cell autonomous processes are those that are occurring within the dopaminergic neurons of the SNpc, while the non-cell autonomous mechanisms cover the pathology outside of these neurons and the SNpc (Foltynie & Kahan 2013, Hirsch, Jenner & Przedborski 2013).

While the presence of non-cell autonomous mechanisms indicates that PD cannot be solely viewed as a disease of the SNpc, its degeneration remains the defining feature of PD pathology ((Triarhou 2002), figure 1.3).

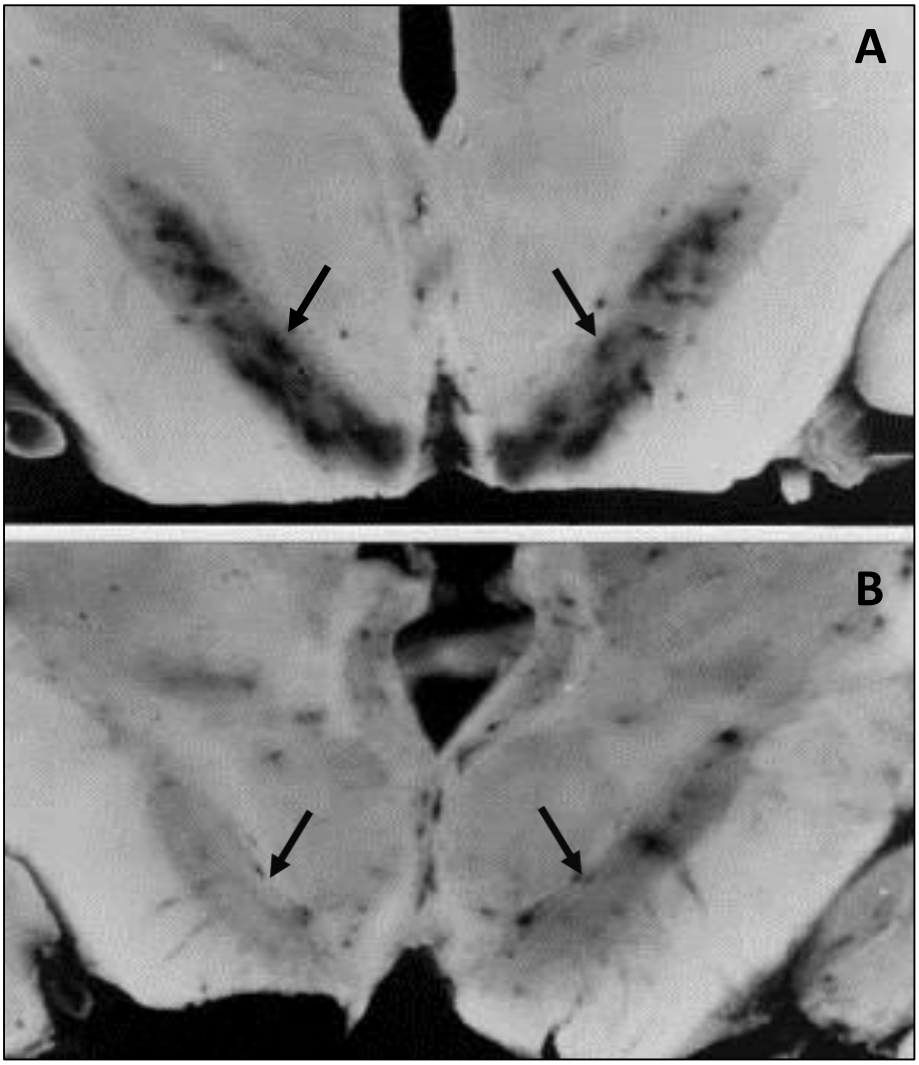

Figure 1.3. The pigmentation of the midbrain is indicative of the presence of neuromelanin (arrows) within the dopaminergic neurons of the SN (A). In PD, these neurons degenerate, resulting in a loss of pigmentation (B). Picture adapted from Triarhou 2002 with kind permission of Springer Science + Business Media.

Accordingly, further detailed discussion of non-cell autonomous mechanisms are beyond the scope of this review, which will initially focus on characterising the intracellular environment of degenerating dopaminergic neurons before discussing the factors that could be causing their pathology.

1.2. The pathophysiology of PD

1.2.1. Inherited *vs* non-inherited PD

Broadly speaking, PD can be classified into 2 categories: familial and sporadic. Familial PD refers to inherited forms of the disease that cluster within families. Due to the inherited nature of familial PD, its cause is often identifiable by the discovery of one or more mutated genes. On the other hand, people with sporadic PD do not appear to have a family history of the disease and, while some monogenic forms of sporadic PD do exist (discussed in more detail below), about 90% of PD cases occur idiopathically without a definable cause (Lesage & Brice 2009). However, while the cause of sporadic PD tends to be poorly defined, there is a large degree of physiological overlap between the monogenic and apparently non-genetic forms of PD. This has led to a large amount of research being undertaken into the genetic forms of the disease in an effort to understand the mechanisms that could also be occurring in sporadic PD.

1.2.1.1. SNCA

The *SNCA* gene encodes the protein α-synuclein and was the first gene to be directly associated with PD (Polymeropoulos *et al.* 1997). Mutations of *SNCA* include single point mutations and gene multiplications causing early onset autosomal-dominant PD (Lesage & Brice 2009, Puschmann 2013). *SNCA* mutations are characterised by α-synuclein accumulation into cellular structures known as Lewy bodies (LB, figure 1.4), a classical histological hallmark of both familial and sporadic PD (Ross *et al.* 2008).

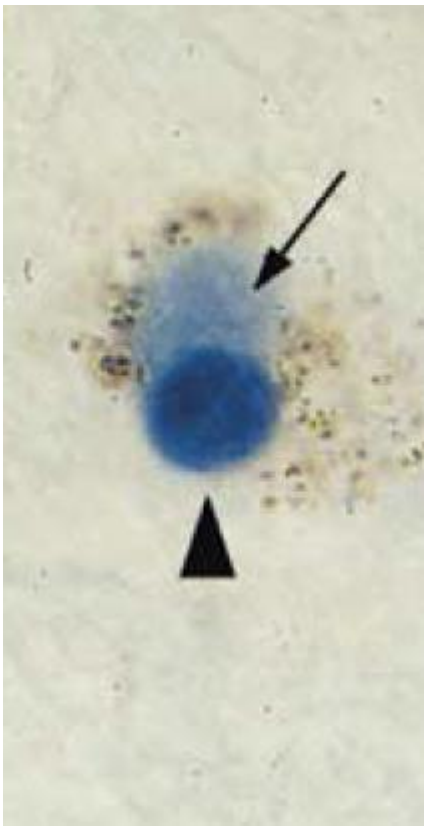

Figure 1.4. A histological image depicting a LB (arrowhead) in the SN of a PD patient. The single arrow is indicating a less well-defined feature known as a pale body. Imagine reproduced from Braak et al. 2003.

The role of α-synuclein in PD has not been fully established but it has recently been linked to lysosomal dysfunction leading to disrupted autophagy (Sidransky & Lopez 2012).

As mentioned in section 1.1.2, α-synuclein depositions in the form of LBs are able to spread across the brain *via* the physical movement of α-synuclein from cell to cell. The migration of LB pathology appears to occur in several stages. In fact, LB deposition has been found to begin in the medulla oblongata of the brainstem as well as in brain areas regulating olfaction, only later progressing to the midbrain and the SNpc. As the disease progresses, LB inclusions continue to progress beyond the SNpc, reaching the thalamus and parts of the cerebral cortex in late-stage PD (Braak *et al.* 2003). This phenomenon provides evidence of additional facets of PD occurring beyond the SNpc, often in a pre-clinical pathology. For example, patients who later go on to develop PD frequently complain of a reduced sense of smell (Doty 2012). Interestingly, while the extensive presence of LBs in PD justifies their status as disease hallmarks, LB pathology is not a PD-specific phenomenon. In fact, LBs also occur in Alzheimer's disease and Lewy body dementia, suggesting some form of mechanistic overlap within these 3 distinct diseases (Bras *et al.* 2014). As a consequence of this, it has been difficult to define the exclusive mechanistic role that α-synuclein plays in PD. However, the discovery that certain *SNCA* mutations trigger the disease indicates that α-synuclein, particularly in overabundance, has a PD-specific mode of action.

1.2.1.2. LRRK2

Mutations in the *LRRK2* gene, responsible for encoding the leucine-rich repeat kinase 2 (LRRK2), result in the development of late onset autosomal dominant PD (Lesage & Brice 2012), with the G2019S mutation of *LRRK2* being the most common PD-causing mutation (Puschmann 2013). The determination of LRRK2's role is still ongoing but it appears that, like α-synuclein, it is also involved in lysosome-mediated autophagy and it may also influence protein sorting by the Golgi (MacLeod *et al.* 2013). Furthermore, wild-type LRRK2 may be involved in protection of mitochondria from damage, with the G2019S mutation conferring an increased cellular vulnerability to mitochondrial damage (Saha *et al.* 2009).

1.2.1.3. Parkin and PINK-1

Mutations in the *parkin* gene account for the largest proportion of autosomal recessive PD (Dawson & Dawson 2010). In contrast to *SNCA* and *LRRK2*, the role of *parkin*, which encodes a protein of the same name, is quite well established. Parkin acts as a ubiquitin E3 protein ligase, and is involved in the tagging of proteins and organelles for degradation by autophagy (Shimura *et al.* 2000). In healthy cells, parkin functions as a quality control mediator of bioenergetics by relocating to dysfunctional mitochondria. Once there, it ubiquitinates proteins on the outer mitochondrial membrane, tagging the organelle for lysosomal degradation. In addition, parkin has also been linked to mitochondrial biogenesis and thus appears to play a role in all facets of mitochondrial turnover in the cell (Scarffe *et al.* 2014).

Parkin recruitment to the mitochondria is dependent upon another PD-linked gene: phosphatase and tensin homolog-induced putative kinase-1 (*PINK1*) (Vives-Bauza *et al.* 2010), mutations of which are the 2nd most common form of autosomal recessive PD (Lesage & Brice 2012). Accordingly, loss-of-function mutations of either parkin or PINK1 are associated with an accumulation of defective mitochondria and impaired cellular bioenergetics (Park *et al.* 2006, Hirsch, Jenner & Przedborski 2013, Scarffe *et al.* 2014).

1.2.1.4. Homologous mechanisms of familial and sporadic PD

Mutations of the above-mentioned genes constitute the bulk of the causative agents in familial PD. The intense study of these genes and their involvement in PD has not only led to a greater understanding of the genetic cases of PD but has also shed light on the potential mechanisms of sporadic cases. For example, α-synuclein accumulation into LBs is also a prevalent feature of sporadic PD, despite a lack of *SNCA* mutations (Ross *et al.* 2008). In addition, the *LRRK2*, *parkin* and *PINK1* mutation phenotypes all show great similarity to sporadic PD (Yao *et al.* 2004, Lesage & Brice 2009, Lesage & Brice 2012). In particular, the mitochondrial defects caused by mutations in these genes have resulted in a significant amount of research being carried out to investigate the relationship between the mitochondria and PD.

1.2.2. The role of mitochondria in PD

Whether as a consequence of specific gene mutations or arising sporadically, the organelle most centrally involved in PD is the mitochondria. The following section will highlight the key characteristics of the mitochondria that are affected in PD.

1.2.2.1. Complex I deficiency

ATP production by oxidative phosphorylation occurs *via* the sequential trafficking of electrons across the inner mitochondrial membrane. This process occurs in several stages, with electrons passing through multiple protein complexes associated with the mitochondrial inner membrane. The initial protein complex, complex I (CxI), catalyses the oxidation of nicotinamide adenine dinucleotide (NADH) to NAD^+. This reaction releases 2 electrons which are transferred to flavin mononucleotide (FMN) before being passed down the respiratory chain to other complexes (figure 1.5) (Smeitink, van den Heuvel & DiMauro 2001).

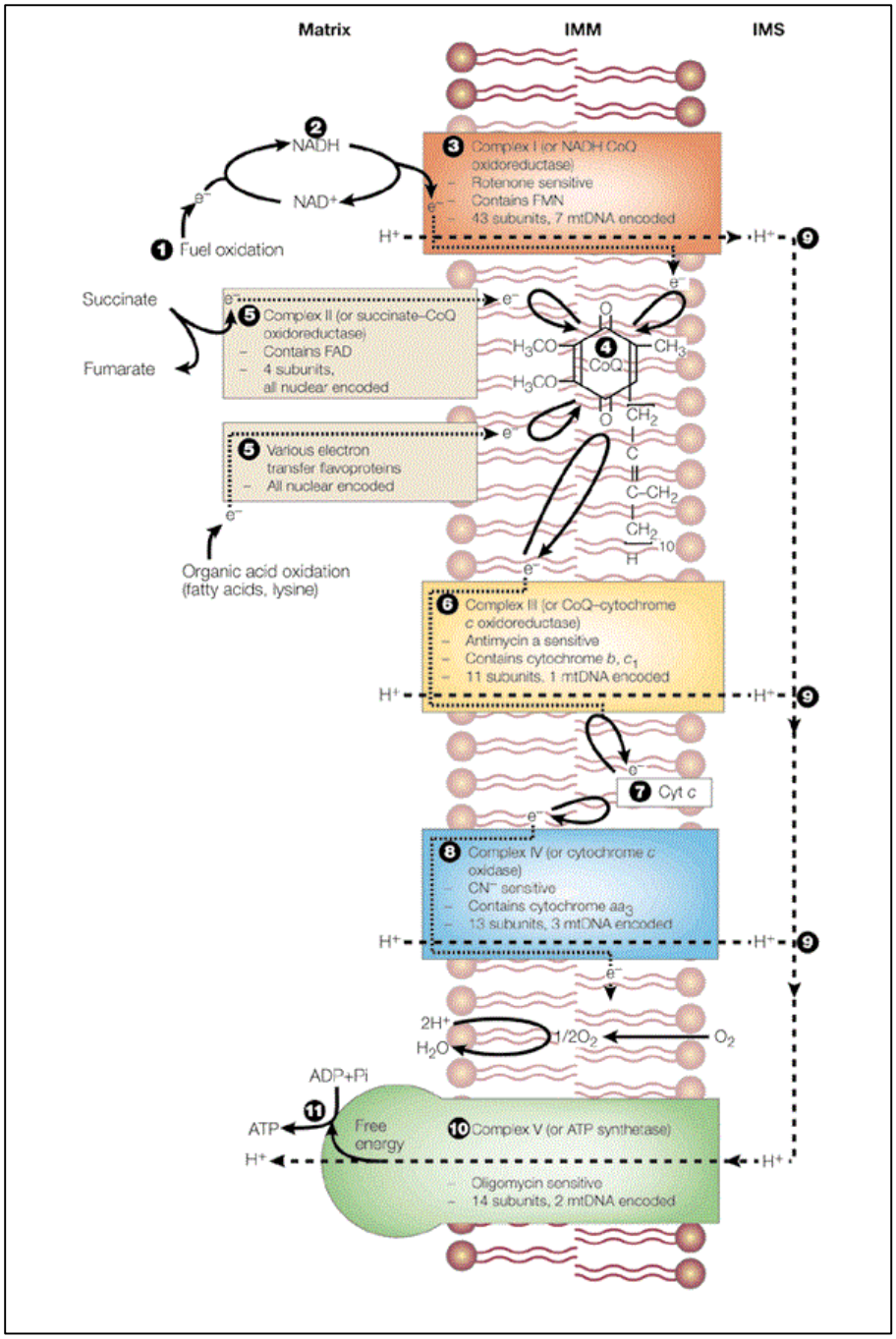

Figure 1.5. A Schematic representation of the 5 complexes of the mitochondrial electron transport chain. Beginning with CxI, the complexes pass electrons from NADH to molecular oxygen in a series of stages, providing the energy required to move protons from the mitochondrial matrix to the intermembrane space. The proton electrochemical gradient, established by this movement, is used by complex V to generate ATP. The numbers in the figure represent each stage of the process from the transfer of electrons onto NADH to the generation of ATP from complex V. reproduced from Smeitink, van den Heuvel and DiMauro 2001.

The first association between a disrupted mitochondrial function and PD arose from the report of mitochondrial CxI deficiency in the SNpc of patients that had died of sporadic PD (Schapira *et al.* 1989, Schapira *et al.* 1990). This deficiency does not appear to occur in all patients but amounts to an approximately 35% reduction in those affected (Schapira 2008). CxI deficiency has also been reported in familial PD (Palacino *et al.* 2004).

CxI inhibition reduces the flow of electrons through the respiratory chain and, thus, the amount of ATP that can be produced by oxidative phosphorylation (Exner *et al.* 2012). A reduction in cellular ATP has been shown to be a precursor to cell death (Eguchi, Shimizu & Tsujimoto 1997). Furthermore, dysfunctional CxI is associated with the increased production of reactive oxygen species (ROS), particularly the oxygen radical superoxide ($O_2^{\bullet -}$), which occurs following electron leakage from reduced FMN and the iron-sulphur centres of CxI (figure 1.6). This occurs as a result of a bottleneck effect that arises from the reduction in CxI's ability to pass on the electrons to complex III (Murphy 2009).

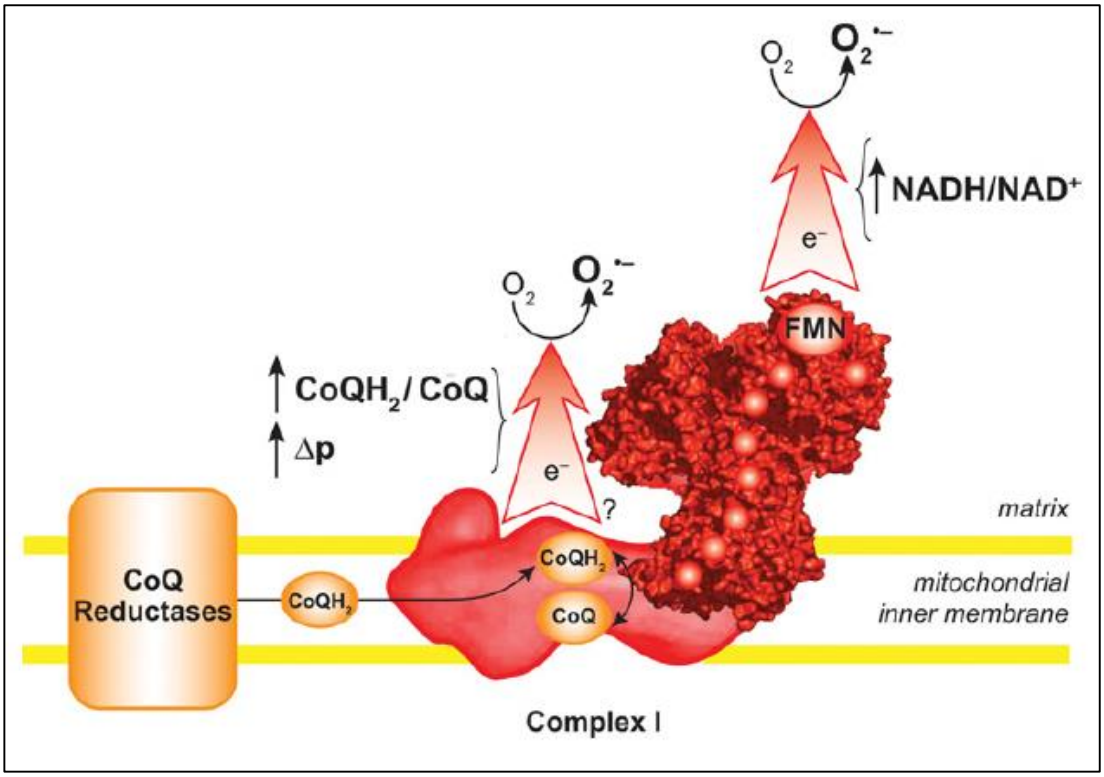

Figure 1.6. Schematic representation of ROS generation by CxI. The superoxide radical is generated primarily by electron leakage from reduced FMN but also occurs to a lesser extent from iron-sulphur centres (red circles). This form of ROS generation occurs following a reduction in CxI's ability to shuttle electrons onwards to coenzyme Q (CoQ) and the other complexes, a pathophysiological facet of PD. Electron leakage at CxI can also occur at the site of CoQ's reduction and arise when electrons begin to move back towards CxI. However, this type of superoxide production is not a factor in PD. Image reproduced from Murphy 2009.

ROS can trigger the activation of cell death signals and also react with, and damage, DNA. This is particularly true for mitochondrial DNA (mtDNA) which is located in the mitochondrial matrix, close to the site of ROS generation (Ott *et al.* 2007). The fact that mtDNA encodes many proteins of the respiratory chain, including 7 of CxI (Exner *et al.* 2012), implies that damage-induced mutations of CxI subunits could further impair their ability to efficiently transport electrons. This is supported by the finding that transfection of mtDNA from patients with reduced CxI activity into rho-zero A549 cells was able to transfer CxI deficiency (Gu *et al.* 1998). Accordingly, a vicious cycle can be established in which CxI deficiency and ROS production exacerbate each other, eventually leading to neuronal cell death *via* ATP depletion.

1.2.2.2. Iron accumulation

SNpc neurons are known to accumulate larger amounts of iron than other cells in the surrounding tissue (Dexter *et al.* 1987, Sofic *et al.* 1988, Dexter *et al.* 1989). In these neurons, iron accumulates and is sequestered into neuromelanin, a highly pigmented material which gives the SNpc a characteristically dark structure when viewed histologically (figure 1.3) (Gerlach *et al.* 2003). Under normal circumstances, iron accumulation and binding to neuromelanin is cytoprotective, preventing the release of free iron which can act as a catalyst for the production of highly reactive hydroxyl radicals (Zecca *et al.* 2008, Mochizuki & Yasuda 2012). However, in the presence of increased oxidative stress, for example caused by excessive mitochondrial ROS-generation, the binding of iron to neuromelanin is weakened,

facilitating its release and enhancing iron-mediated ROS production and damage (Zecca *et al.* 2008).

1.2.2.3. Impaired mitochondrial turnover

In order to maintain an efficient energy production within the cell, defective mitochondria, including those with CxI deficiency, require routine replacement. This typically occurs *via* a specialised form of autophagy, known as mitophagy (de Vries & Przedborski 2013). As mentioned above, loss of *parkin* and *PINK1* results in a reduction in the neuron's ability to recycle defective mitochondria.

The precise consequences of impaired mitophagy in PD are difficult to fully elucidate due to the fact that a lot of the studies investigating mitophagy in PD were conducted in non-mammalian (Poole *et al.* 2008, Liu & Lu 2010) and non-neuronal (Exner *et al.* 2007, Michiorri *et al.* 2010) cells. However, impaired mitophagy in PD is thought to result in the accumulation of defective mitochondria. Consequently, this would be expected to result in sub-optimal ATP synthesis, a failure to remove mtDNA mutations and increased ROS production, eventually leading to cell death (Chen & Chan 2009, de Vries & Przedborski 2013).

1.2.2.4. Mitochondria and ROS in PD: the chicken or the egg?

The mitochondria-associated deficiencies discussed above all result in the increased production of ROS. However, they can also arise as a result of ROS activity. Therefore, it is difficult to conclusively determine which factor, whether

mitochondrial dysfunction or a highly-oxidative environment, initiates this vicious cycle. However, as discussed in the following section, dopaminergic neurons possess a distinct intracellular environment that may hold the clues to what is occurring during the early stages of PD development.

1.2.3. The susceptibility of dopaminergic neurons to damage

Dopaminergic neurons in the brain are not created equal. In particular, there are 2 features that set SNpc dopaminergic neurons apart from the dopaminergic neurons of the nearby ventral tegmental area (VTA).

The first of these is the fact that SNpc neurons have a uniquely large axonal arbor (figure 1.7) (Matsuda *et al.* 2009, Bolam & Pissadaki 2012).

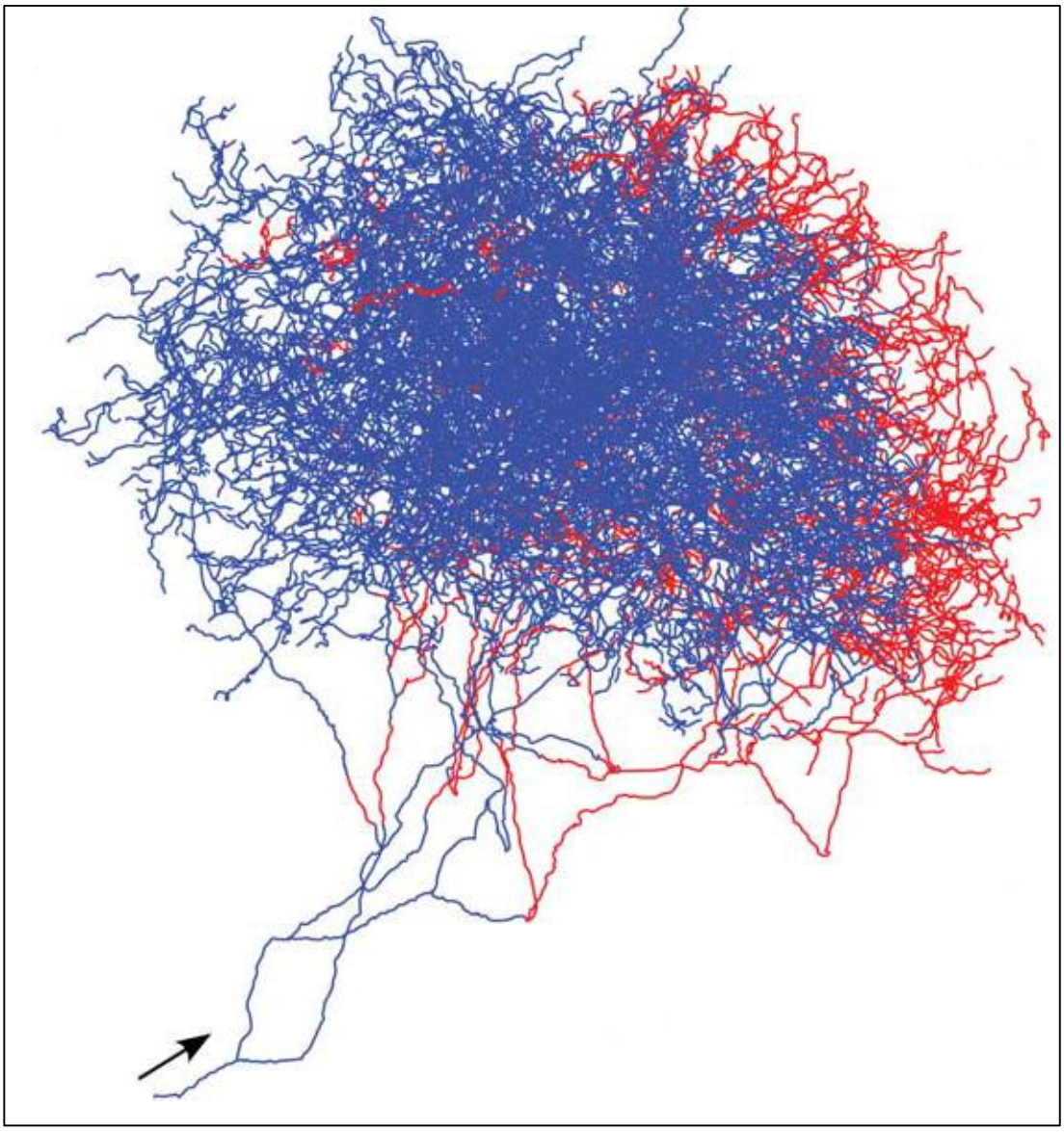

Figure 1.7. A computer-reconstructed axonal arbor of a single dopaminergic neuron from the SNpc of a rat brain. Red and blue lines represent axon fibres projecting to different sub-compartments of the striatum. The arrow indicates the direction of action potential propagation. Reproduced from Matsuda et al. 2009.

Calculations by Bolam and Pissadaki (2012) have estimated that dopaminergic neurons of the rat SNpc use their uncharacteristically large axons to innervate between 102,000 and 245,000 synapses per neuron. These figures are similar to the one proposed in another study (Andén *et al.* 1966). In contrast, Bolam and Pissadaki estimate that VTA neurons in the rat brain only contain up to 30,000 synapses per neuron. The relative bioenergetic cost of maintaining this huge number of synapses and an axon up to 78 cm long (Matsuda *et al.* 2009) will be substantial. ATP will be required to provide the energy for a large number of cellular factors including additional protein synthesis, organelle maintenance and intracellular signalling. More significantly, maintaining the membrane potential and axonal transport (all dependent upon ATP) across such a huge axon will lead to an extremely large energy demand. This, when scaled up to human SNpc axons, which are estimated to be in the region of 4.5 m long and innervate 10 times the number of synapses compared to rats (Bolam & Pissadaki 2012), is expected to result in a substantial energy burden that is unique to SNpc neurons. Furthermore, the dopaminergic neurons of the SNpc are non-myelinated (Pissadaki & Bolam 2013), further adding to additional ATP cost during action potential propagation (Attwell & Laughlin 2001).

Taken together, the morphological features of SNpc neurons create a phenomenal demand for ATP in order to maintain the successful innervation of their huge number of synapses. This large and sustained energy burden is likely to render SNpc dopaminergic neurons acutely susceptible to any form of insult or dysfunction that

reduces ATP production. Thus, it is possible that the unique morphological structure of these neurons contributes to their vulnerability towards degeneration in PD.

The second distinguishing feature of the dopaminergic neurons of the SNpc is related to their unique Ca^{2+}-conducting environment. Nigral dopaminergic neurons, unlike the dopaminergic neurons in the VTA, express a large amount of $Ca_v1.3$ L-type calcium channels, a relatively rare form of Ca^{2+}-channel found only in 10% of neurons in the brain (Surmeier *et al.* 2011). It appears that they use these channels to stimulate pacemaking Ca^{2+} oscillations in the absence of direct synaptic input. The pacemaking of the $Ca_v1.3$ L-type channels ensures that a slow but constant release of dopamine into the striatum occurs (Guzman *et al.* 2009). Another use for the Ca^{2+} oscillations could be the enhancement of dopamine synthesis which is thought to be linked to increased Ca^{2+} conductance (Mosharov *et al.* 2009). However, the physiological role of $Ca_v1.3$ in relation to the synthesis of dopamine is not thought to be that significant (Surmeier *et al.* 2011).

The increased Ca^{2+} conductance that is required to maintain neuronal pacemaking further enhances the already existent ATP-dependent burden on the neuron, as Ca^{2+} needs to be tightly regulated in order to prevent unwanted cell death (Orrenius, Zhivotovsky & Nicotera 2003). This requires the use of ATP-dependent active transport to move Ca^{2+} against its electrochemical gradient from the cytosol either out of the cell or into intracellular Ca^{2+} stores in the endoplasmic reticulum (Surmeier *et al.* 2011).

The increased ATP demand arising from the maintenance of cytosolic Ca^{2+} concentration will synergistically add to the ATP burden presented by Bolam and

Pissadaki (2012), as this will all take place across uncharacteristically large axons, further supporting the notion of dopaminergic neurons in the SNpc operating very close to the limit of their energy budget. In addition, the increased oxidative phosphorylation and mitochondrial shuttling of electrons required by these neurons to stay energetically viable will contribute to enhanced ROS production (Surmeier *et al.* 2012). Furthermore, increased Ca^{2+} conductance through $Ca_V1.3$ L-type channels has also been directly linked to ROS production (Guzman *et al.* 2010).

In addition to the points discussed above, the metabolism and oxidation of dopamine itself is thought to be toxic and, thus, contribute to the burden placed on SNpc neurons (Chen *et al.* 2008). Principally, dopamine-derived toxicity is mediated by its metabolite 3,4-dihydroxyphenylacetaldehyde (DOPAL) which is produced following the deamination of dopamine by monoamine oxidases A and B (Goldstein *et al.* 2013). DOPAL exerts toxicity in multiple ways including *via* its oxidation to a semiquinone radical (Anderson *et al.* 2011), DOPAL-mediated generation of highly reactive hydroxyl radicals (Li *et al.* 2001) and protein modification *via* the formation of adducts at lysine (DOPAL) and cysteine (DOPAL-quinone) residues (Rees *et al.* 2009).

DOPAL appears to be produced more readily in PD brains compared with non-PD controls. This is appears occur *via* 2 mechanisms. Firstly, vesicular uptake of dopamine in PD is estimated to be reduced by 89% at the putamen, the principal site of dopamine's action on the direct movement pathway (figure 1.2) (Goldstein *et al.* 2013). This will lead to less dopamine being packaged into synaptic vesicles and consequently less dopamine leaving the neurons *via* vesicle-mediated

exocytosis. The additional dopamine that remains in the cell is consequently metabolised to DOPAL. Secondly, activity of aldehyde dehydrogenase, the principal detoxifying enzyme of DOPAL, was estimated to be decreased by 70% in the PD putamen (Goldstein *et al.* 2013). This would prevent the removal of DOPAL from the cytosol, further prolonging and exacerbating DOPAL-mediated toxicity.

From the evidence discussed above, it appears that the increased energy demand, oxidative environment and toxic metabolite of dopamine inherently put SNpc neurons under a large degree of stress. Through time and in the presence of any additional stress factors, it appears that the SNpc cells are more likely than others to exceed their cytotoxic threshold. This could explain why SNpc neurons appear to show the most prominent toxicity in PD even when the mutations in PD-associated genes occur across the whole body. Accordingly, given the hypersusceptibility of these neurons, research into determining what is causing idiopathic PD should focus on identifying mechanisms that could contribute towards pushing SNpc neurons past their cytotoxic threshold. As discussed below, there are likely multiple, sometimes minor, overlapping factors that contribute to this as opposed to 1 underlying cause. Accordingly, this multiple-hit hypothesis could explain why defining a cause of PD has historically been difficult, as the diverse nature of these insults suggest that PD may in fact be an amalgamation of defects that only through time coalesce into 1 definable pathology.

1.3. The cause(s) of PD

1.3.1. Aging

The largest known risk factor for developing PD is age (Dexter & Jenner 2013). However, whether the aging process is itself causative of PD or whether PD-specific factors unrelated to general aging simply accumulate as people get older has been debated for some time. Some studies posit that aging and PD development occur *via* separate and distinct mechanisms, citing differences in the regional loss of dopamine within the striatum between PD and normal aging (Hornykiewicz 1989, Kish *et al.* 1992). However, Collier, Kanaan & Kordower (2011) argue that the use of more modern immunohistochemical techniques has enabled more accurate identification and quantification of dopaminergic neuron subpopulations (for example, SNpc versus VTA neurons), allowing the relationship between aging and PD to be revisited.

In a series of studies involving non-human primates, Collier and colleagues tested whether certain processes that occurred during normal aging overlapped with the development of PD (Collier, Kanaan & Kordower 2011). They discovered that the intensity of α-synuclein staining in SNpc tissue showed a significant positive correlation with age in normally aging primates. Furthermore, the distribution of α-synuclein staining amongst all dopaminergic neurons of the midbrain matched the distribution of immunoreactivity in PD, with the highest intensity being seen in SNpc neurons and negligible staining in the neurons of the VTA (Chu & Kordower 2007). Positive staining for α-synuclien was also associated with a loss of the

dopaminergic phenotype in those cells but, unlike in PD, was not found to correlate with dopaminergic neuron cell death (Chu & Kordower 2007).

Markers for oxidative stress were also found to increase with age and were highest in SNpc neurons of naturally aging primates compared with neurons of the VTA (Kanaan, Kordower & Collier 2008). These findings support the evidence presented in section 1.2.3 for an innate SNpc-specific vulnerability to oxidative stress. Based on these and additional data showing SNpc-specific increases in lysosomal dysfunction, inflammation and accumulation of misfolded proteins, Collier, Kanaan & Kordower (2011) hypothesised that the aging process lays the foundation for the development of PD, with the addition of multiple causative factors accelerating what is essentially a natural progression towards the disease.

This seems plausible, considering the overlapping mechanisms in both aging and PD. The histological differences between aging and PD SNpc neurons could therefore be made up by additional contributing factors to the aging process. However, the process of aging does not begin before the innately high energy demands in the SNpc neurons are established (see section 1.2.3). Thus, a more accurate hypothesis may be that the combination of innate SNpc neuronal susceptibility and the natural aging process combine to lay the foundation for PD with additional risk factors “filling in the blanks”.

1.3.2. Environmental factors in PD development

The first discovery, in the 1980s, that PD-like symptoms and SNpc degeneration can be caused by compounds originating outside of the body triggered a substantial paradigm shift, as scientists became aware of the fact that PD development can be influenced by environmental factors. 1-methyl-4-phenyl-tetrahydropyridine (MPTP) was discovered after illicit drug users injected themselves with a 1-methyl-4-propionoxypyridine solution that had become contaminated with MPTP during synthesis (Langston *et al.* 1983). The drug users rapidly developed parkinsonian symptoms which were later attributed to MPTP's active metabolite MPP^+ (Langston *et al.* 1984).

Since then, pesticides in particular have been investigated as potentially causative agents in PD (Wirdefeldt *et al.* 2011). While it has been difficult to fully determine which pesticides are involved in PD or indeed the disease-specific role of pesticides in general, they are generally considered to contribute to PD development (Wirdefeldt *et al.* 2011, Kamel 2013). A recent meta-analysis concluded that exposure to pesticides was, indeed, a risk factor for PD but that a dearth of high-quality studies prevented a cause-and-effect relationship from being confirmed (Pezzoli & Cereda 2013). Furthermore, future studies should focus on specific pesticides, rather than pesticide use in general, to elucidate which individual compounds are involved. The meta-analysis specifically implicated paraquat and maneb as pesticides directly associated with PD. In addition to paraquat and maneb, rotenone, a pesticide often used experimentally in both *in vitro* and *in vivo*

models of PD, has recently been associated with PD in a study of agricultural workers (Tanner *et al.* 2011).

While all have been implicated in PD, the 3 pesticides mentioned above have different mechanisms of action. Rotenone, like MPP^+, is an inhibitor of mitochondrial CxI and causes a reduction in ATP and also increases the production of ROS (Tanner *et al.* 2011). When used experimentally rotenone has been shown to cause PD-like symptoms *in vivo* (Martins *et al.* 2013). Paraquat, which also causes PD-like toxicity *in vivo* (Martins *et al.* 2013) is another mediator of ROS production but exerts its toxicity by facilitating the movement of electrons towards molecular oxygen, producing $O_2^{\bullet-}$ (Bus & Gibson 1984). The precise mechanism of maneb toxicity is unclear although it appears to disrupt the activity of proteins containing thiol groups (Roede & Jones 2014) and was found to inhibit aldehyde dehydrogenase (Fitzmaurice *et al.* 2014) suggesting that it may increase the presence of DOPAL in dopaminergic neurons. It too has been found to induce PD-like pathology *in vivo*, particularly in combination with paraquat (Thiruchelvam *et al.* 2000).

In addition to epidemiological evidence for the role of pesticides in PD, some studies have discovered potential associations between traumatic head injuries (Dick *et al.* 2007), organic solvents (Seidler *et al.* 1996), metals (Seidler *et al.* 1996) and magnetic fields (Noonan *et al.* 2002) and PD. However, the evidence in favour of these associations is currently thought to be inadequate (Wirdefeldt *et al.* 2011).

Overall, more research is required with potentially larger, better-quality studies to fully establish any association with PD. However, based on the evidence in favour of

pesticides, it is likely that exposure to certain chemicals could play a role as part of the multiple-hit hypothesis in PD.

1.3.3. The genetics of an un-genetic disease

Despite initially appearing to show almost no involvement, genetics in PD are becoming an increasingly attributable causative factor. As discussed in section 1.2.1, in a small number of cases, PD is identifiable by a specific genetic mutation that, in combination with the enhanced susceptibility of SNpc neurons (section 1.2.3), is capable of mediating dopaminergic neuron cell death. In spite of this, the majority of people develop PD pathology without a clearly definable genetic cause. This had led PD being considered a predominantly un-genetic disease (Lesage & Brice 2009). However, recent advances in the ability to screen large numbers of patients and identify common genetic traits have indicated that genetics in PD may play a greater role than previously assumed.

1.3.3.1. Monogenic causes of sporadic PD

Traditionally, monogenic PD has been identified *via* an association of the disease within a particular family. However, an increased frequency of studies involving the genetic screening of non-familial PD patients has led to a number of people with sporadic PD being found to possess PD-causing mutations (table 1.1) (Gilks *et al.* 2005, Klein *et al.* 2007, Lesage & Brice 2009, Lesage *et al.* 2011, Nalls *et al.* 2011, Lesage & Brice 2012).

Table 1.1. Known PD-causing genes that occur in sporadic PD. Adapted from Lesage and Brice 2012.

Gene	Inheritance	Type of PD
SNCA	Autosomal dominant	Early onset PD
parkin	Autosomal recessive	Early onset PD
LRRK2	Autosomal dominant	Late onset PD
VPS35 (Vacuolar protein sorting 35)	Autosomal dominant	Late onset PD

There are a number of explanations for this phenomenon. Firstly, *de novo* mutations, particularly in the autosomal-dominant *LRRK2* and *SNCA* genes, could account for the seemingly spontaneous occurrence of PD (Gilks *et al.* 2005, Puschmann 2013). Secondly, cases in which PD appears to have occurred sporadically may yet be due to the inheritance of PD-causing genes. This could arise due to the late onset of some PD mutation phenotypes such as the G2019S mutation of *LRRK2* (Lesage & Brice 2012). Accordingly, family members with this *LRRK2* mutation may die before the diagnosis of PD and/or identification of the mutation *via* genetic testing. In addition, penetrance of *LRRK2* mutations has been reported to be both incomplete and age-dependent, with penetrance even at 79 years of age not exceeding 75% (Healy *et al.* 2008). Both of the above-mentioned factors could lead to a misrepresentation of familial PD as sporadic, as a lack of

penetrance or death prior to PD development could lead to *LRRK2*-mediated PD appearing to skip generations despite its autosomal dominant nature.

Finally, a similar situation could arise with the autosomal-recessive forms of PD. While mutations in *parkin*, when inherited as homozygotes or compound heterozygotes (two different mutations of the same gene), show complete penetrance, the fact that they are only inherited 25% of the time from unaffected parents (due to the requirement for both recessive copies to be present) could lead to further cases of familial PD skipping multiple generations. This is particularly likely in smaller families where any Mendelian inheritance of PD-causing genes may be less obvious (Lesage & Brice 2012).

Interestingly, transgenic mouse models of these mutations often do not result in neuronal cell death (Blandini & Armentero 2012). Consequently, while these mutations are considered causative for PD in humans, they may do so by vastly increasing the susceptibility of SNpc neurons to additional stress as part of the multiple-hit hypothesis rather than by directly causing the toxicity themselves.

1.3.3.2. Genetic risk-factors for the development of sporadic PD

In addition to the identification of monogenic causes of PD, the use of genome-wide association studies (GWAS) has identified a number of genetic polymorphisms which have been found to enhance the probability of developing PD. GWAS allow associations to be made between specific genetic variants and PD, as they provide

the necessary, large sample size to find correlations between relatively infrequent mutations and disease prevalence.

Some of the genes considered risk factors for sporadic PD are the same genes responsible for the development of monogenic PD. For example, mutations in the *SNCA* promoter have been shown to increase the risk of developing PD but are not directly causative (Pals *et al.* 2004, Maraganore *et al.* 2006). Furthermore, a single nucleotide polymorphism (SNP) of the *SNCA* gene has also been linked to increased PD susceptibility (Goris *et al.* 2007). This SNP, called rs356219, has also been found to synergise with particular haplotype of mictrotubule-associated protein tau (*MAPT*), a gene normally associated with Alzheimer's disease (Myers *et al.* 2005). When these 2 polymorphisms are found together, Goris *et al.* (2007) determined that they approximately doubled the chance of developing PD.

LRRK2 has also been implicated as a susceptibility factor in idiopathic PD *via* SNPs known as rs1491942 and rs11564273 (Nalls *et al.* 2011). In addition, 2 other risk-enhancing polymorphisms (G2385R and R1628P), which are particularly prevalent in Asian populations, appear to confer up to 3-fold increased susceptibility to PD (Lesage & Brice 2009).

Despite the association of various established PD-genes with an increased susceptibility to the disease, mutations in the glucocerebrosidase (*GBA*) gene are thought to be the most common risk factors for the development of PD (Lesage *et al.* 2011). Homozygous mutations of *GBA* are responsible for the development of the autosomal-recessive Gaucher's disease (GD), a disorder characterised by abnormal storage and accumulation of glycolipids within lysosomes that most

commonly occurs outside of the CNS (Zimran 2011). Some homozygous GD patients have been shown to go on to develop early-onset PD (Tayebi *et al.* 2003). Interestingly, heterozygotes for *GBA* mutations don't develop GD but have, nevertheless, been found to have approximately a 5-fold greater chance of developing PD compared with people with wild type *GBA* (Sidransky *et al.* 2009), strongly suggesting that the GBA enzyme could be involved in the pathogenesis of the disease. This is thought to be manifest *via* some form of synergy with α-synuclein and its aggregation into Lewy bodies, but the precise mechanism is unclear (Sidransky & Lopez 2012).

The discovery of multiple genetic risk factors with overlapping physiological pathways in addition to the already established causative mutations suggests that genetics in PD could play a much larger role in PD than previously assumed. The role of genetics in PD is likely to grow in the near future as more powerful GWAS and meta-analyses are performed and more and more novel genes, some of which have not yet been characterised, are identified as potential mediators of PD susceptibility (Nalls *et al.* 2011). Together with additional, non-genetic, factors a picture is emerging of a disease that, in the majority of cases, has not one but multiple underlying causes.

1.3.4. Nicotinamide *N*-methyltransferase is upregulated in PD

Another factor found at significantly higher levels in PD patients is nicotinamide *N*-methyltransferase (NNMT). NNMT protein is expressed at higher levels in PD brains compared with controls (Parsons *et al.* 2002, Parsons *et al.* 2003) and in PD-

patients' cerebrospinal fluid (CSF) compared with controls (Aoyama *et al.* 2001). This increased expression occurs concomitantly with a shift towards higher NNMT activity in PD patients (Parsons *et al.* 2002), something which appears to be solely related to levels of mRNA as opposed to the presence of any gain-of-function mutations (Smith *et al.* 1998).

NNMT is an *S*-adenosylmethionine (SAM) dependent enzyme with a molecular weight of 29 kDa. It belongs to a family of 3 closely-related *N*-methyltransferases (Thompson & Weinshilboum 1998) and is most highly expressed in the cytosol of hepatocytes (Parsons *et al.* 2002). Its principal role in the body is the conversion of nicotinamide to 1-methylnicotinamide (MeN, Parsons *et al*. 2011, figure 1.8).

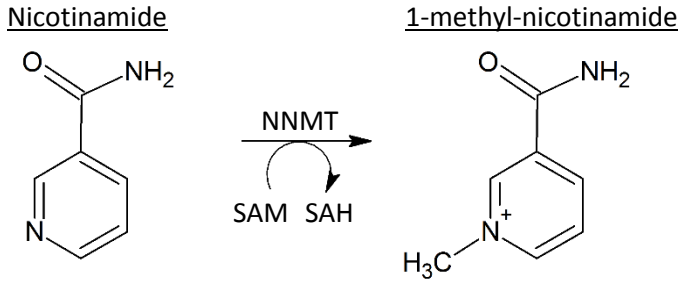

Figure 1.8. NNMT catalyses the N-methylation of nicotinamide to MeN. SAH = S-adenosylhomocysteine

The role of NNMT, which is also expressed in the dopaminergic neurons of the SNpc (Parsons *et al.* 2002), in PD is not yet fully established. However, it has been studied in diseases such as cirrhosis (Cuomo *et al.* 1994), hepatitis (Sternak *et al.* 2010), chronic obstructive pulmonary disease (Kim *et al.* 2010) and atherosclerosis (Mateuszuk *et al.* 2009) where it is involved in protecting diseased cells from

inflammation, oxidative damage and cell death. NNMT is also upregulated in cancer, where it promotes cell survival (Zhang *et al.* 2014) and tumourigenesis (Tang *et al.* 2011). The cytoprotection and cell survival effects seen in these diseases may occur as a result of NNMT-mediated activation of Akt signalling (Thomas *et al.* 2013). Akt signalling is anti-apoptotic and has been reported to be neuroprotective against experimental PD-causing toxins *in vivo* (Burke 2007). Furthermore, NNMT expression has been reported to protect mitochondria from toxic insult by MPP^+ and rotenone amongst others (Parsons *et al.* 2011, Milani, Ramsden & Parsons 2013). Consequently, NNMT in PD could be upregulated as a protective response to the underlying pathophysiology. However, this has not yet been verified and there are a number of hypotheses that suggest that NNMT may, in fact, play the opposite role in PD.

Firstly, an enhanced NNMT activity would be expected to increase the production of MeN and, thus, reduce the concentration of nicotinamide in the cytosol. Consequently, this would reduce the amount of nicotinamide that can be incorporated into NADH (Parsons *et al.* 2002, Parsons *et al.* 2003). A reduction in NADH availability would conceivably reduce the supply of electrons to the electron transport chain and, therefore, lower the eventual production of ATP. This could be particularly toxic to SNpc neurons due to their increased energy requirements described above.

Secondly, some studies suggest that MeN may, in fact, be toxic to cells. Fukushima *et al.* (1995) reported that MeN exposed to isolated mitochondrial CxI from bovine brains was toxic to the NDUFS3 subunit. It was speculated that MeN accepts

electrons from NADH and, thus, become a highly reactive free radical at the site of CxI. In support of this, the same group found that MeN injected stereotaxically into rat SN tissue significantly reduced striatal dopamine content compared with sham controls (Fukushima *et al.* 2002) and that MeN was significantly toxic to cultured mouse striatal neurons (Mori *et al.* 2012). However, it is important to note that the concentrations used in the Fukushima group's studies were extremely high, with toxic effects only reported at concentrations in excess of 10 mM, far higher than the tens of µM physiological range that was reported in rat brains (Erb *et al.* 1999). Another study using a high concentration (25 mM) of MeN did not report any toxicity towards rat cerebellar granule cells; in fact, the study reported that administration of 25 mM MeN was able to protect the cells against glutamate-induced excitotoxicity (Slomka *et al.* 2008). Moreover, MeN has been shown to be protective towards SH-SY5Y neuroblastoma cells at a concentration of 1 mM (Parsons *et al.* 2011), and concentrations below 1 mM were protective against liver damage (Sternak *et al.* 2010) and reduced inflammation *in vivo* (Chlopicki *et al.* 2007). Accordingly, conclusions regarding the toxicity of MeN should be viewed with reference to the experimental concentrations used.

Finally, and perhaps most intriguingly with regard to PD, NNMT has been found to have a wide substrate profile, being capable of catalysing the *N*-methylation of a number of compounds with pyridine moieties (Alston & Abeles 1988). This is of particular interest given that, as discussed in the following section, *N*-methylation of these moieties can vastly increase the toxicity of pyridine-containing compounds.

1.3.5. The activation of endogenous neurotoxins

1.3.5.1. The biosynthesis and environmental acquisition of βCs

A remarkable structural similarity exists between norharman (NH), the prototypical molecule of a group of compounds called β-carbolines (βC), and the neurotoxin MPP^+ (figure 1.9).

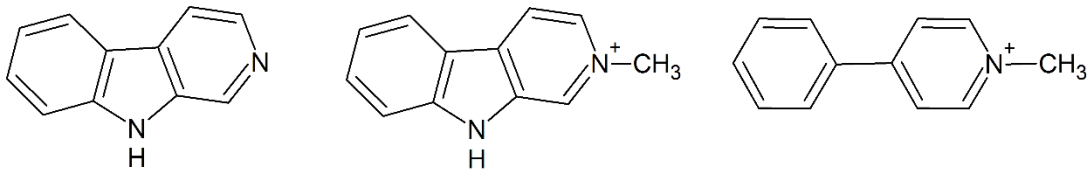

Norharman 2-methylnorharman 1-methyl-4-phenylpyridine

Figure 1.9. The structural similarity between NH and MPP^+ following NH's N-methylation at the 2N position

βCs are found endogenously in the human brain (Matsubara *et al.* 1993) where they are derived from the Pictet-Spengler condensation of tryptamine with acetaldehyde or pyruvic acid (Susilo *et al.* 1987, Susilo & Rommelspacher 1987, Stöckigt *et al.* 2011). They are also found in well-cooked food and drink such as meat, fish and roasted coffee, and also in tobacco smoke as high temperatures permit the pyrolysis of tryptophan and its condensation with aldehydes (Herraiz 2004). βCs acquired from environmental sources are able to cross the blood brain barrier (Fekkes & Bode 1993) a fact attributed to their hydrophobic structure (Matsubara *et al.* 1995). Due to their structural similarity to MPP^+, they are considered to be possible mediators of SNpc degeneration (Neafsey *et al.* 1989, Collins *et al.* 1992,

Bonnet *et al.* 2004, Hamann *et al.* 2006, Pavlovic *et al.* 2006, Wernicke *et al.* 2007) and have been shown to be elevated in the CSF of patients with PD compared to controls (Kuhn *et al.* 1996).

1.3.5.2. βCs are potential pro-toxins in PD

In order for NH to more accurately resemble MPP^+ it must be 2*N*-methylated and, thus, ionised, a process which has been shown to occur in the human brain (Matsubara, Collins & Neafsey 1992, Matsubara, Neafsey & Collins 1992, Gearhart *et al.* 2000). The conversion of NH to 2-methylNH (2-MeNH) facilitates entry into the cell *via* the dopamine transporter (DAT), the MPP^+ ion's primary point of entry into dopaminergic neurons (Wernicke *et al.* 2007). In contrast, NH is thought to enter the cell *via* passive diffusion. 2*N*-methylated βCs have been found at higher concentrations in PD CSF compared to healthy controls (Matsubara *et al.* 1995). As well as a 2*N*-methylation of βCs, a further 9*N*-methylation exclusive to 2-MeNH has been observed in the brain (Matsubara, Neafsey & Collins 1992, Matsubara *et al.* 1998, Gearhart *et al.* 2000). The proposed βC methylation pathway is shown in figure 1.10.

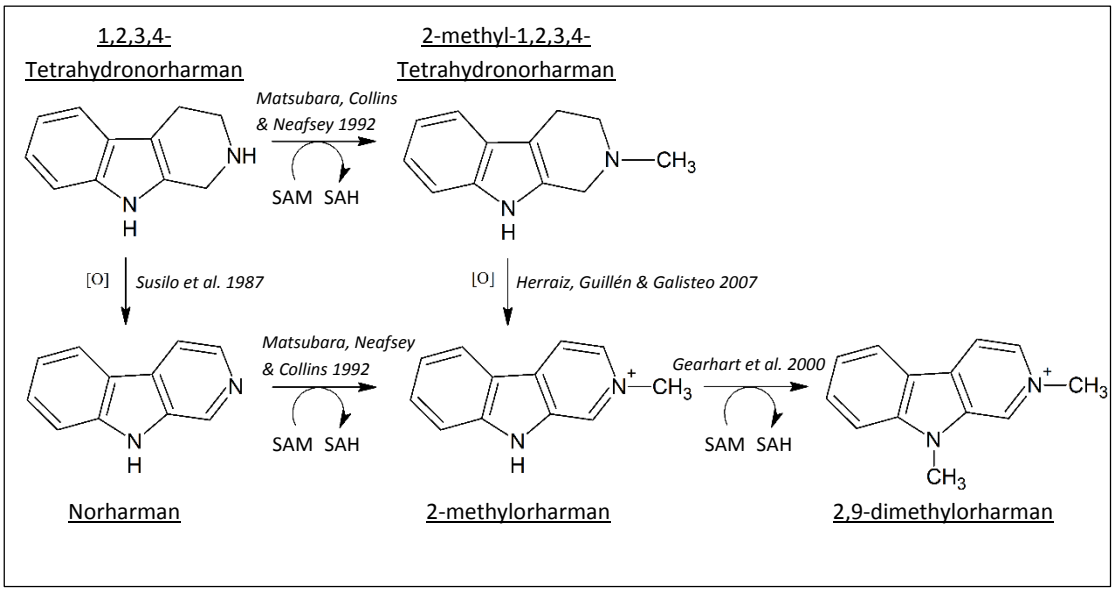

Figure 1.10 The methylation pathway of NH and 1,2,3,4-tetrahydroNH in the human brain. Image adapted from Matsubara, Collins & Neafsey 1992

In addition to NH, tetrahydroNH (THNH) is also of interest in PD. THNH is produced *via* the removal of a methyl group from 1-methylTHNH, which is the direct product of the Pictet-Spengler reaction of tryptamine in the brain (Susilo *et al.* 1987, Susilo & Rommelspacher 1987, Stöckigt *et al.* 2011). It is principally of interest in PD due to its status as a precursor for the biosynthesis of NH (Susilo *et al.* 1987) and also 2-MeNH *via* its own *N*-methylated intermediate (Matsubara, Collins & Neafsey 1992, Herraiz, Guillén & Galisteo 2007).

While the 2*N*-methylated form of NH and the di-methylated 2,9-dimethyl-NH (2,9-diMeNH) have been discovered *in vivo*, no evidence exists to support the existence of a 9*N*-monomethylated βC under physiological conditions (Matsubara, Collins &

Neafsey 1992, Gearhart *et al.* 2000). Instead, 9*N*-methylation has been found to occur only after 2*N*-methylation has taken place. It has been suggested that *N*-methylation at the 2*N* position confers sufficient nucleophilicity for further *N*-methylation at the 9*N* position to occur (Collins *et al.* 1992, Matsubara, Neafsey & Collins 1992).

1.3.5.3. The toxicity of N-methylated βCs

The toxicity of the *N*-methylated βCs has been studied extensively (Neafsey *et al.* 1989, Matsubara *et al.* 1998, Bonnet *et al.* 2004, Hamann *et al.* 2006, Pavlovic *et al.* 2006, Wernicke *et al.* 2007). While 2*N*-methylation has been shown to confer toxic properties and dopaminergic neuron specificity to most βCs, 9*N*-methylation of 2-MeNH appears to be a crucial step in toxicity potentiation as 2,9-diMeNH has been shown to be markedly more toxic than 2-MeNH in Neuro 2A cells (Bonnet *et al.* 2004), DAT-transfected and wild type human embryonic kidney (HEK) cells (Wernicke *et al.* 2007) and primary dopaminergic neurons (Hamann *et al.* 2006). In fact, 2,9-diMeNH has shown comparable toxicity to MPP^+ with a reduced reliance on DAT (Bonnet *et al.* 2004, Hamann *et al.* 2006, Wernicke *et al.* 2007). Despite a lowered DAT dependency relative to MPP^+, 2,9-diMeNH has been shown to be selective for dopaminergic neurons compared with other neurons and non-neuronal cells (Pavlovic *et al.* 2006).

N-methylated βCs, like MPP^+, are principally thought to act *via* inhibition of CxI of the mitochondrial respiratory chain, although weaker inhibition at complexes II and III have also been reported (Albores *et al.* 1990, Collins *et al.* 1992, Fields *et al.*

1992). The most recent support for this comes from Hamann *et al*. (2006) who exposed isolated mouse mesencephalic dopaminergic neurons to 2,9-diMeNH. Within 24 hours, a significant (30%) reduction in ATP was recorded alongside a significant rise in ROS to 250% of control. This occurred concomitantly with an increased production of lactate, suggesting that compensatory glycolysis had been initiated to account for the reduced aerobic ATP yield. Following these initial events, markers of both apoptotic (coordinated and mostly ATP-dependent) cell death and, later, necrotic (largely uncontrolled, often mediated by ATP depletion) cell death were present (Hamann *et al.* 2006). In addition to these *in vitro* findings, 2-MeNH and 2,9-diMeNH been shown to have *in vivo* toxicity to SNpc neurons (Neafsey *et al.* 1989, Neafsey *et al.* 1995, Pavlovic *et al.* 2006). Thus, *N*-methylated βCs are a PD-relevant neurotoxin that is produced in the brain from endogenously-occurring precursors.

1.3.5.4. The identity of enzyme responsible for NH's N-methylations

While many elements of 2,9-diMeNH's toxicity and biosynthesis have been confirmed, it is not fully established which enzyme or group of enzymes are capable of catalysing either of the *N*-methylations required for its production.

While studies investigating 9*N*-methyltransferase activity towards 2-MeNH have been performed (Gearhart *et al.* 2000), the enzyme responsible for producing 2,9-diMeNH has not been characterised and there are currently no suggested candidates for this reaction amongst known enzymes. It is also unclear whether one

or multiple enzymes are required for the initial 2*N*-methylation of NH followed by the 9*N*-methylation of 2-MeNH.

Gearhart, Neafsey & Collins (2002) discovered that purified phenylethanolamine *N*-methyltransferase (PNMT), an enzyme normally associated with adrenaline synthesis (Ziegler *et al.* 2002), has βC 2*N*-methyltransferase activity *via* its conversion of synthetic 9-methylNH (9-MeNH) to 2,9-diMeNH. However, the physiological relevance of this finding is unclear as 9-MeNH may not occur naturally in the brain (Matsubara, Neafsey & Collins 1992). While this finding suggests that PNMT may also convert NH to 2-MeNH, there was no evidence provided to support this. PNMT, which is found at its highest levels in the adrenal glands, has been detected in various parts of the brain including the SN (Kopp *et al.* 1979). In addition, it has been reported that PNMT-positive neurons in the brain are also lost during PD (Gai *et al.* 1993, Nagatsu & Sawada 2007). Taken together, these reports suggest that PNMT, in theory, could play role in PD progression by catalysing the primary step in the activation of NH toxicity.

In addition to PNMT, it has been speculated that NNMT may possess βC 2*N*-metyhyltransferase activity (Matsubara *et al.* 2002, Parsons *et al.* 2002, Parsons *et al.* 2003). As mentioned above, NNMT has been found to be upregulated in PD (Aoyama *et al.* 2001, Parsons *et al.* 2002, Parsons *et al.* 2003) and has been found to be capable of catalysing the *N*-methylation of numerous pyridine moieties in addition to nicotinamide (Alston & Abeles 1988). Furthermore, the expression of NNMT has been shown to be inversely proportional to disease duration (Parsons *et*

al. 2002). As such it is hypothesised that higher NNMT activity may result in the greater production of *N*-methylated βCs, particularly NH.

1.4. The aims of the project

The principal aim of the project was to determine the role of NNMT in PD. This was done in 3 primary studies. Firstly, the effects of NNMT expression on SH-SY5Y cells, a neuroblastoma cell line frequently used in *in vitro* PD studies (Xie, Hu & Li 2010), were determined in order to assess any inherent toxicity mediated by NNMT. Secondly, the susceptibility of NNMT-V5-expressing S.NNMT.LP cells versus non-expressing cells to NH, THNH and 2-MeNH toxicity was investigated. Finally, the ability of NNMT to catalyse NH 2*N*-methylation was investigated.

2. General Methods

The most commonly used methods and techniques are described in this chapter. Methods that were used less frequently will be described in detail in their relevant chapters.

2.1. Cell Culture

Unless otherwise stated, solutions referred to in the text were made according to table 2.1. All solutions were made in a class II microbiological safety cabinet (MSC).

Table 2.1. Commonly used solutions during cell culture.

Name	Abbreviation	Contents
Phosphate Buffered Saline	PBS	1 Tablet (Invitrogen, Paisley, UK) in 500 mL of deionised H2O and then autoclaved
Media for SH-SY5Y cells	SH media	90 mL of solution was removed from a 500 mL bottle containing a premixed formula of 1:1 Dulbecco's Modified Eagle Medium:F12 with phenol red (Sigma-Aldrich, Dorset, UK). Seventy five mL of fetal bovine serum (FBS, 15%, Sigma-Aldrich, Dorset, UK), 5 mL non-essential amino acids (1X), 5 mL L-glutamine (2mM), 5 mL of Penicillin/Streptomycin solution (100 Units/mL Penicillin, 100 µg/mL streptomycin, all Invitrogen, Paisley, UK) were added to the bottle and mixed.
Media for S.NNMT.LP cells	LP media	92.5 mL of liquid was removed from a 500 mL bottle containing a premixed formula of 1:1 Dulbecco's Modified Eagle Medium:F12 with phenol red (Sigma-Aldrich, Dorset, UK). Seventy five mL of fetal bovine serum (FBS, 15%, Sigma-Aldrich, Dorset, UK), 5 mL non-essential amino acids (1X), 5 mL L-glutamine (2mM) and 5 mL of Penicillin/Streptomycin solution (100 Units/mL Penicillin, 100 µg/mL streptomycin) and 2.5 mL of geneticin selection antibiotic (0.25 mg/mL, all Invitrogen, Paisley, UK) were added to the bottle and mixed.
Serum-free SH media	N/A	15 mL of liquid was removed from a 500 mL bottle containing a premixed formula of 1:1 Dulbecco's Modified Eagle Medium:F12 with phenol red (Sigma-Aldrich, Dorset, UK). Five mL non-essential amino acids (1X), 5 mL L-glutamine (2 mM) and 5 mL of Penicillin/Streptomycin solution (100 Units/mL Penicillin, 100 µg/mL streptomycin, all Invitrogen, Paisley, UK) were added to the bottle and mixed. hood.

2.1.1. Maintenance and culture of cell lines

Unless otherwise stated, all cells were incubated with 10 mL of cell line-appropriate media in 75 cm^2 flasks at 37°C and 5% CO_2 in an incubator (Panasonic Biomedical, Loughborough, UK). All cell manipulations were undertaken within a Class II MSC and all solutions were pre-warmed to 37^oC in a waterbath. Media was removed from the flasks every other day *via* aspiration, followed by the careful addition of 10 mL fresh media using a serological pipette.

2.1.2. Cell trypsinisation, centrifugation and counting

In order to prepare cells for experimentation, the following method was used. Once cells had reached approximately 85% confluence, the media was aspirated and the cells were washed gently by adding 5 mL of PBS. The PBS was aspirated followed by the addition of 2 mL of 0.25% trypsin (Invitrogen, Paisley, UK) to each flask. After incubating at room temperature for approximately 2 minutes, flasks were struck with the palm of the hand repeatedly to dislodge the cells from the growing surface. Trypsin was neutralised by adding 8 mL of media to the flask and pipetting up and down over the growing surface multiple times. The entire volume of the flask was then added to a 25 mL centrifuge tube and centrifuged for 5 minutes at 433 x *g* (Allegra X-22R centrifuge, Beckman Coulter, California, USA). The supernatant was aspirated and the pellet was resuspended by adding 10 mL of media directly onto the pellet and pipetting up and down repeatedly.

Viable cell number was determined *via* trypan blue exclusion. A 1:1 trypan blue (Sigma-Aldrich, Dorset, UK):cell suspension was made by adding 100 µL of the cell suspension to 100 µL trypan blue. The new suspension was mixed thoroughly before it was pipetted onto a haemocytometer. Under these conditions, viable cells are able to exocytose trypan blue and maintain a white appearance under a light microscope. This is not the case for dead or dying cells, which are unable to remove the dye and are, thus, stained blue. As a result, it was possible to identify and count only viable cells within 8 pre-determined grids of the haemocytometer under a microscope at 10x magnification. In order to remove bias, the same 8 grids were used each time and the initial grids were selected prior to viewing the slide under the microscope. The cell density (number of viable cells per mL) was then calculated using the following equation.

$$Cells/mL = \frac{total\ cells\ counted}{8} \times 20{,}000$$

The cell suspension was then diluted as necessary using media (desired cell densities are described in the individual assay descriptions) and added to the wells of the appropriate plate or flask for the assay using a repeat dispensing pipette.

2.1.3. Preparation of cell pellets for snap freezing

In order to prepare cells for RNA or protein extraction, cells were trypsinised and centrifuged as described above. After removal of the supernatant, pellets were resuspended in 10 mL of PBS before they were centrifuged again. This was done to ensure the removal of any excess protein or mRNA that may have been present in

any media residue. The supernatant was removed from the pellet and the cells were snap-frozen by immersion in liquid nitrogen. Frozen pellets were then transferred to a -80^{o}C freezer and stored until required.

2.2. Western Blotting

Unless otherwise stated, all solutions were prepared as described in table 2.2.

Table 2.2. Components and abbreviations of the common reagents used during Western blotting.

Name	Abbreviation	Contents
Tris Buffered Saline	TBS	6 g Trizma HCl (50 mM Tris, Sigma-Aldrich, Dorset, UK), 12 g Sodium Chloride (200 mM, Fisher Scientific, Loughborough, UK) dissolved in 500 mL, adjusted to pH 7.4. and made up to 1 L using deionised H_2O
Tris Buffered Saline-Triton X-100	TBST	1 L of TBS with 500 µL (0.05%) Triton X-100 (VWR, Leicestershire, UK)
Milk-Tris Buffered Saline-Triton X-100	MTBST	1 L of TBST with 50 g (5%) milk powder (Premier Foods, Hertforshire, UK)
Anode Buffer 1	AB1	18.15 g Tris base (0.3 M), 50 mL methanol (10%, both Fisher Scientific, Loughborough, UK) in 400 mL using deionised H_2O and adjusted to pH 10.4 and made up to 500 mL
Anode Buffer 2	AB2	1.51 g Tris base (25 mM), 50 mL methanol (10%) in 400 mL using deionised H_2O, adjusted to pH 10.4 and made up to 500 mL using deionised H_2O
Cathode Buffer	CB	1.51g Tris base (25 mM), 50 mL methanol (10%), 1.5g glycine (40 mM, Fisher Scientific, Loughborough, UK) in 400 mL using deionised H_2O, adjusted to pH 9.4. and made up to 500 mL
Radioimmuno-precipitation Buffer	RIPA buffer	5 ml of 1 M (157.6 g/L in water) Trizma HCL (50 mM, pH 7.4), 1 mL of 1% (v/v) Nonidet P40 (0.1%), 0.5 g 0.5% sodium deoxycholate (0.0025%), 15 mL of 1 M (58.4 g/L in water) sodium chloride (150 mM), 0.15 g ethylenediamine-tetraacetic acid (EDTA, 5 mM), 0.1 g 0.1% (w/v) Sodium dodecylsulphate (SDS, 0.0001%) made up to 100 mL with deionised water. This was the separated into 7 mL aliquots before a single tablet each of cOmplete Protease Inhbitor Cocktail (Roche, Burgess Hill, UK) and PhosSTOP (Roche, Burgess Hill, UK) was added.

2.2.1. Preparation of protein samples

Snap-frozen cell pellets were lysed by resuspension in 100 µL of either 1% Triton X-100 in PBS or RIPA buffer (Parsons *et al.* 2006, see table 2.2) as appropriate for the procedure. Samples were transferred into labelled 1.5 mL Eppendorf tubes and vortexed to further assist lysis. The samples were centrifuged at 16,160 x *g* for 10 minutes using a microcentrifuge (1-14 Microfuge, Sigma Centrifuges, Wem, UK) before the supernatants were transferred to clean 1.5 mL Eppendorf tubes. Two dilutions of each sample (1:10 and 1:20) were prepared (20 µL of each), using 1% Triton X-100 in PBS or RIPA buffer, for protein analysis. The remaining samples were kept on ice until further processing as described in section 2.2.3.

2.2.2. Protein assay using the Lowry method

Protein standards of 0 mg/mL, 0.2 mg/mL, 0.4 mg/mL, 0.6 mg/mL, 0.8 mg/mL, and 1.0 mg/mL bovine serum albumin (BSA) in 1% triton-X in PBS or RIPA buffer were prepared from a 10 mg/mL stock of BSA prepared in appropriate lysis buffer (1% triton-X in PBS or RIPA buffer) as follows:

- 1.0 mg/mL (90 µL lysis buffer + 10 µL stock)
- 0.8 mg/mL (92 µL lysis buffer + 8 µL stock)
- 0.6 mg/mL (94 µL lysis buffer + 6 µL stock)
- 0.4 mg/mL (96 µL lysis buffer + 4 µL stock)
- 0.2 mg/mL (98 µL lysis buffer + 2 µL stock)
- 0 mg/mL (100 µL lysis buffer)

A protein assay (Bio–Rad, Hemel Hempstead, UK), based on the method of Lowry (Lowry *et al.* 1951), was performed as per manufacturer's instructions. The assay measures a concentration-dependent colour change based upon the presence of a reduced Folin–Ciocalteu reagent which is produced following the copper-mediated oxidation of peptide bonds under alkaline conditions.

Solution A' was made by mixing 20 µL Solution S for every 1 mL of Solution A required. Five µL of each of the standard and diluted samples were transferred in triplicate to a 96-well plate (Thermo Scientific, Loughborough, UK). A typical example of the resulting plate layout is shown in figure 2.1.

	1	2	3	4	5	6	7	8	9	10	11	12
A				SH 1:10	SH 1:10	SH 1:10	0.0	0.0	0.0			
B				SH 1:20	SH 1:20	SH 1:20	0.2	0.2	0.2			
C				LP 1:10	LP 1:10	LP 1:10	0.4	0.4	0.4			
D				LP 1:20	LP 1:20	LP 1:20	0.6	0.6	0.6			
E							0.8	0.8	0.8			
F							1.0	1.0	1.0			
G												
H												

Figure 2.1. A typical plate layout used for protein assays. SH = SH-SY5Y, LP = S.NNMT.LP, 1:10 and 1:20 refer to the dilution factor of the samples in either RIPA buffer or 1% Triton X-100 in TBS. Numbers 0.0-1.0 are indicative of protein standard concentrations (in mg/mL) of BSA in RIPA buffer or 1% Triton X-100 in TBS.

Twenty five µL of solution A' were added to both sample and standard-containing wells using a multichannel pipette. The wells were then mixed thoroughly by placing the plate onto a vortexer. Two hundred µL of Solution B were then added to the wells using a multichannel pipette followed by additional mixing. The assay was incubated for 15 minutes at room temperature before absorbance was measured at 750 nm using a spectrophotometer (Perkin Elmer, Waltham, Massachusetts, USA). The absorbance values of the protein standards were then used to construct a calibration curve from which the protein content of the samples was calculated as µg/µL.

2.2.3. Preparation of samples for Western blotting

All samples were diluted to 3 µg of protein/µL using RIPA buffer before one volume of Laemmli sample buffer (Sigma-Aldrich, Missouri, USA) was added (final protein concentration 1.5 µg/µL), mixed and heated to 100^{o}C for 5 minutes using an Eppendorf heater (Grant Instruments, Shepreth, UK). This process denatures proteins and dissociates quaternary subunits by disrupting disulphide bridges and intramolecular bonds such as electrostatic interactions. As a consequence, protein separation during electrophoresis occurs primarily as function of protein size and not by quaternary structure.

2.2.4. SDS – polyacrylamide gel electrophoresis (PAGE)

A pre-cast 4-12% NuPage Bis-Tris SDS-PAGE gel was assembled and submerged in 1 L of 3-(*N*-morpholino)propanesulfonic acid (MOPS) buffer (both Invitrogen, Paisley, UK). Thirty µg of protein samples were loaded into the wells of the gel, along with 5 µL of *Strep*-tagged Precision Plus Protein markers (Bio–Rad, Hemel Hempstead, UK) which were added to the furthest well on the left hand side of the gel. Proteins were electrophoresed at 200V for 50 minutes.

2.2.5. Semi-dry transfer of proteins to nitrocellulose membrane

Samples were transferred onto a Hybond-ECL nitrocellulose membrane (Amersham Biosciences, Buckinghamshire, UK) using a semi-dry transfer method (Thomas *et al.* 2013) as described below.

Cathode buffer, anode buffer 1 and anode buffer 2 were poured into separate incubation trays before the gel was removed from the assembly and the gel plate opened. All wells were removed and the top left corner of the gel was cut off to assist the determination of the gel's orientation. The gel was carefully submerged into the cathode buffer and placed onto a rocking platform (Labnet International, New Jersey, USA) for at least 10 minutes to equilibrate the gel with the buffer. HybondECl nitrocellulose (GE Healthcare Life Sciences, Buckinghamshire, UK) was cut to the size of the filter paper, and was then rehydrated by submerging into deionised water for 2 minutes before being submerged in anode buffer 2 and

placed on a rocking platform for 5 minutes. A gel/membrane “sandwich” was then made on the anode of the transfer tank (Bio–Rad, Hemel Hempstead, UK) by submerging filter paper in buffers as detailed in figure 2.2. Once each piece filter paper had been placed, the sandwich was roller-pinned to remove air bubbles. The cathode plate was assembled, and proteins were transferred to the membrane at 19V for 36 minutes (1 gel) or 42 minutes (2 gels).

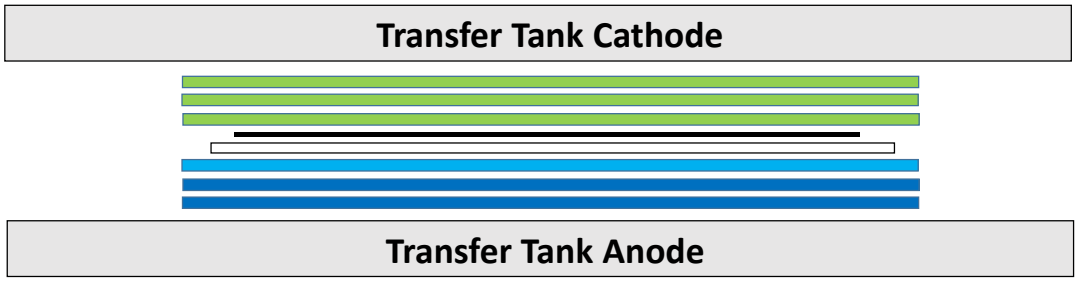

Figure 2.2 An illustration of the gel "sandwich" used during the semi-dry transfer of protein bands from a 4-12% NuPage Bis-Tris SDS-PAGE gel to a nitrocellulose membrane. The coloured layers represent Western blotting filter paper that had been submerged in appropriate buffer before being added onto the sandwich. From bottom to top: 2x anode buffer 1 (dark blue), 1x anode buffer 2 (light blue), nitrocellulose membrane (white), gel (black), 3x cathode buffer (green).

2.2.6. Immunoblotting

The gel-membrane layer was removed and the nitrocellulose membrane was cut to the size of the gel. Immunoblotting was performed using electrochemiluminescence (ECL)-based detection, as follows. Nitrocellulose membranes were transferred into sealed containers and blocked in MTBST for 2 hours on a rocking platform. This process allows proteins from the milk to attach themselves to any free binding sites on the nitrocellulose membrane, thus preventing any antibodies from later attaching themselves to the membrane non-specifically and reducing background staining. Membranes were incubated with primary antibody (diluted in MTBST) overnight at 4°C in a sealed 50 mL tube under constant rocking and rotation using a tube roller (Spiramix, Thermo Scientific, Loughborough, UK). The specific primary and secondary antibodies used for each Western blot are described in the relevant experimental chapters.

Following a 1 minute wash by submerging the blot in MTBST at room temperature under rocking conditions, the membranes were incubated for 2 hours in MTBST, while rocking at room temperature. This was followed by a co-incubation with a relevant secondary antibody-horseradish peroxidase (HRP) conjugate and a StrepTactin-HRP conjugate (1:4000, Bio–Rad, Hemel Hempstead, UK) in MTBST for 1 hour under the same conditions. The StrepTactin-HRP conjugate was added to bind to - and later visualise - the *Strep*-tagged protein markers. The secondary antibody solution was removed and the blot was washed with MTBST for 5 minutes by rocking at room temperature before the solution was removed again and the blot was washed twice with TBST for 5 minutes under the same conditions. The blot

was submerged in TBS while the ECL Select solution (GE Healthcare Life Sciences, Buckinghamshire, UK) was prepared by mixing equal volumes of solutions A and B as per manufacturer's instructions. The blot was removed from the TBS and any excess liquid was removed from the surface by applying the corner of the membrane to tissue paper. The membrane was covered with ECL solution and incubated at room temperature for 5 minutes, after which excess ECL reagent was removed as described above. Visualisation was performed using a ChemiDoc MP transilluminator (Bio–Rad, Hemel Hempstead, UK). In the event that membranes were to be re-used for reprobing with β-actin or β-tubulin loading control antibodies, stripping was performed by submerging membranes in Restore western blot stripping buffer (Thermo Scientific, Loughborough, UK) and rocking for 1 hour at 37^{o}C before rinsing and re-blocking for another hour prior to repeating the immunoblotting process.

Analysis of the blots was performed using ImageLab software (Bio–Rad, Hemel Hempstead, UK). Specifically, identification of band size was performed cross-referencing imaged bands with those of known size in the molecular weight marker lane. Quantification of band intensity was performed by dividing the integrated peak area of the desired band by the integrated peak area of the housekeeping gene β-tubulin to correct for protein loading.

2.3. RT-PCR

2.3.1. Isolation of cellular RNA

Extraction of RNA from snap-frozen cell pellets was performed using the Isolate RNA Mini Kit (Bioline, London, UK) as per manufacturer's instructions, with all steps undertaken within the confines of a PCR hood (SLEE, Mainz, Germany). Briefly, the pellet was resuspended *via* the addition of 400 µL Lysis Buffer R onto the pellet and pipetting up and down 10 times. The lysate was incubated at room temperature for 3 minutes. Spin Column R1 was placed into a collection tube and the lysate was pipetted into it. The Spin Column was centrifuged for 2 minutes at 10,000 x *g*, after which 400 µL of 70% ethanol was added to the filtrate and thoroughly mixed by pipetting up and down 10 times. The entire volume was then transferred into Spin Column R2, placed inside a new collection tube, and centrifuged at 10,000 x *g* for 2 minutes to bind RNA. Five hundred µL of Wash Buffer AR was added to the Spin Column which was then centrifuged at 10,000 x *g* for 1 minute. Seven hundred µL of Wash Buffer BR was added to the Spin Column which was again centrifuged at 10,000 x *g* for 1 minute. Using a fresh collection tube, the Spin Column was spun at 10,000 x *g* for 3 minutes to remove all traces of wash buffer. Finally, Spin Column R2 was placed in an Elution Tube, and 30 µL of RNase-free water was applied directly to the Spin Column membrane and incubated for 1 minute at room temperature, before RNA was eluted by centrifugation at 6,000 x *g* for 1 minute.

2.3.2. Reverse transcription of mRNA

mRNA was reverse-transcribed into complimentary DNA (cDNA) using the High Capacity RNA-to-cDNA kit (Life Technologies, Paisley, UK) as per manufacturer's instructions. Briefly, the extracted RNA (5 µL) was added to a mixture of nuclease-free water (4 µL, Roche, Burgess Hill, UK), reverse transcriptase buffer containing poly-dT primers (10 µL) and reverse transcriptase (1 µL) in a 0.2 mL thin-walled, dome-capped polymerase chain reaction (PCR) tube (Alpha Laboratories, Eastleigh, UK). The inclusion of poly-dT primers, as opposed to random hexamers, in the reaction buffer ensured that only full length mRNA was converted to cDNA. The solution was vortexed and briefly centrifuged to collect all the liquid at the bottom, before it was transferred to a thermal cycler (PCR Sprint, Thermo Scientific, Loughborough, UK) and incubated at 37 °C for 1 hour, after which the reaction was terminated by incubation for 5 minutes at 94 °C.

2.3.3. PCR amplification of target cDNA

cDNA samples were amplified using primer pairs designed using the Roche on-line universal probe library qPCR design tool (http://www.roche-applied-science.com/sis/rtpcr/upl/ezhome.htmL). Details of the specific primers pairs used for each target gene are described in the relevant experimental chapter.

PCR permits amplification of cDNA using DNA polymerase and primers for specific gene sequences to produce multiple copies of the desired gene. This is done in a temperature-controlled environment which permits melting of double stranded DNA, annealing of primers and DNA polymerase to the 2 single strands and

propagation of polymerase activity in both directions. The various temperature requirements for each stage are repeatedly cycled, allowing a large amount of specific cDNA replication from an initially small sample.

Following reverse transcription, cDNA samples were diluted 10-fold prior to amplification of target cDNA using the PlatinumTaq PCR kit (Invitrogen, Paisley, UK). The PCR reaction mixture was made by adding, into a 0.2 mL thin-walled dome-capped PCR tube: 2.5 µL of 10x reaction buffer, 0.5 µL of 10 mM deoxuribonucleotide triphosphate bases (0.2 mM final concentration), 0.75 µL of 50 mM $MgCl_2$ (1.5 mM final concentration), 0.625 µL of 10 µM forward primer (250 nM final concentration), 0.625 µL of 10 µM reverse primer (250 nM final concentration), 0.1 µL of 5 U/µL platinum Taq polymerase (0.02 U/µL final concentration) and 1 µL of cDNA sample, and made up to 25 µL using 18.9 µL of PCR-grade water (Roche, Burgess Hill, UK). A control reaction was performed using 1 µL of PCR-grade water, which had also undergone the procedures described in sections 2.3.1 and 2.3.2, in place of cDNA. PCR was then performed in a thermal cycler (PCR Sprint, Thermo Scientific, Loughborough, UK) using the cycling conditions as described in each experimental chapter. All samples were held at 4^{o}C once the reaction had been completed.

2.3.4. DNA gel electrophoresis

Confirmation of PCR success was performed using agarose gel electrophoresis. A 1.5% agarose gel was made by adding 50 mL of Tris-acetate-EDTA (TAE) buffer (Invitrogen, Paisley, UK) to 0.75 g of agarose (Sigma-Aldrich, Dorset, UK) inside a

conical flask and microwaving (Category E, Panasonic, Bracknell, UK) on maximum for 1 minute. The microwave was stopped every 20 seconds to allow the solution to be gently mixed. While the solution was cooling, the gel tray and electrophoresis equipment were assembled. An 8-well gel comb was placed into the gel tray, and once the solution was cool enough to hold, 2.5 µL of 10,000 x GelRed (Biotium, Cambridge, UK) were added and the flask was mixed gently. The solution was then poured into a gel tray and left to set for 30-40 minutes. The gel comb was removed and the gel was submerged in TAE buffer. Five µL PCR product was mixed, by pipetting, with 1 µL of 5x loading buffer (Thermo Scientific, Loughborough, UK) and was carefully loaded into a well on the gel. One µL of a 100bp ladder (Invitrogen, Paisley, UK) was diluted using 4 µL of TAE and 1 µL of loading buffer before 2 µL were added to the leftmost well of the gel. Samples were electrophoresed at 50V for 40 minutes and visualised, and digital images taken, using a uv-transilluminator (U:GENIUS, Syngene, Cambridge, UK). Band size was determined by comparison with the 100 bp ladder.

2.4. Toxicity Assays

Two measures of cell viability were used; (i) the ability of cells to reduce 3-(4,5-Dimethylthiazol-2-yl)-2,5-diphenyltetrazolium bromide (MTT) to formazan, and (ii) their intracellular ATP concentration. A more detailed explanation of the assays and their rationale can be found in section 3.1.1. A similar experimental procedure was followed for assays measuring cell viability *via* MTT reduction and ATP concentration. Unless otherwise stated, both assays followed the same procedure.

2.4.1. Preparation of cultured cells for toxicity assays

For MTT assays, clear, flat-bottomed 96-well plates were used (Thermo Scientific, Loughborough, UK). For ATP assays, white, flat bottomed 96-well plates (Greiner Bio-One Ltd, Stonehouse, UK), pre-treated with 100 µL of 0.01% poly-L-Lysine (Sigma-Aldrich, Poole, UK), were used which were prepared as follows. Following sterilisation of the white plate with 70% ethanol, poly-L-Lysine was pipetted into each well and incubated for 1 hour, after which it was removed and the plate was allowed to dry.

SH-SY5Y and S.NNMT.LP cells were trypsinised, pelleted and counted as described in Section 2.1.3. In order to minimise the time either cell line spent outside the incubator, all flasks were prepared one after the other rather than in parallel. This ensured that in studies comparing cell lines, both SH-SY5Y and S.NNMT.LP cells spent approximately equal time outside of the incubator prior to being seeded onto a plate.

Following the cell count, cells were diluted to an appropriate density as described in each experimental chapter. One hundred µL of diluted cell suspension was then added to a number of wells on a 96-well plate. In assays comparing SH-SY5Y and S.NNMT.LP cells, this process was then repeated for the remaining cell line, resulting in the plate layouts seen in figure 2.3. Each seeded plate was used to test 1 compound.

	1	2	3	4	5	6	7	8	9	10	11	12
A	SH	SH	SH	SH	LP	LP	LP	LP			SH*	SH*
B	SH	SH	SH	SH	LP	LP	LP	LP			LP*	LP*
C	SH	SH	SH	SH	LP	LP	LP	LP				
D	SH	SH	SH	SH	LP	LP	LP	LP	SH	SH	SH	SH
E	SH	SH	SH	SH	LP	LP	LP	LP	LP	LP	LP	LP
F	SH	SH	SH	SH	LP	LP	LP	LP				
G	SH	SH	SH	SH	LP	LP	LP	LP				
H	SH	SH	SH	SH	LP	LP	LP	LP				

	1	2	3	4	5	6	7	8	9	10	11	12
A	SH	SH	SH	LP	LP	LP					SH#	SH#
B	SH	SH	SH	LP	LP	LP					LP#	LP#
C	SH	SH	SH	LP	LP	LP						
D	SH	SH	SH	LP	LP	LP				SH	SH	SH
E	SH	SH	SH	LP	LP	LP				LP	LP	LP
F	SH	SH	SH	LP	LP	LP						
G	SH	SH	SH	LP	LP	LP						
H	SH	SH	SH	LP	LP	LP						

Figure 2.3. 96-well plate layout used for MTT assays (top panel) and ATP assays (bottom panel). SH = SH-SY5Y cells, LP = S.NNMT.LP cells. All wells in columns 1-8 were incubated with test compounds as described in section 2.4.2. Wells in rows D and E, columns 9-12 were used as untreated controls. * indicates control wells that did not receive MTT solution. # indicates cell-free control wells that contained only media of the indicated cell line.

2.4.2. Dosing

One hundred mM solutions of NH, 2-MeNH iodide, THNH, and 4-phenylpyridine (4PP) (table 2.3) were diluted in media to 2000 µM for 2-MeNH iodide (20 µL of solution in 1 mL of media), 800 µM (8 µL of solution in 1 mL of media) for NH and 1600 µM (16 µL of solution in 1 mL of media) for THNH and 4PP. Each dilution was pipetted directly into the top well of a v-bottomed, 96 deep-well block (Starlab, Milton Keynes, UK) as shown in figure 2.4.

Table 2.3. The compositions of various solutions used in toxicity assays.

Compound	Concentration	Composition
NH	100 mM	16.8 mg (Sigma-Aldrich, Dorset, UK) in 1 mL of DMSO (Sigma-Aldrich, Dorset, UK)
2-MeNH iodide	100 mM	31.0 mg (equivalent to 18.3 mg free base, synthesised according to chapter 6) in 1 mL of DMSO
THNH	100 mM	17.2 mg (Sigma-Aldrich, Dorset, UK) in 1 mL of DMSO
4-PP	100 mM	15.5 mg (Sigma-Aldrich, Dorset, UK) in 1 mL of DMSO
MTT	6 mg/mL	60 mg of MTT (Invitrogen, Paisley, UK) in 10 mL of PBS
MTT lysis buffer	N/A	25 g of SDS (10% w/v) dissolved in 125 mL of *N,N*-dimethylformamide (DMF, 50% v/v, both Sigma-Aldrich, Dorset, UK) and made up to 150 mL with deionised H2O.

	1	2	3	4	5	6	7	8	9	10	11	12
A	800 µM	800 µM	1600 µM	1600 µM	1600 µM	1600 µM	2000 µM	2000 µM				
B	400 µM	400 µM	800 µM	800 µM	800 µM	800 µM	1000 µM	1000 µM				
C	200 µM	200 µM	400 µM	400 µM	400 µM	400 µM	500 µM	500 µM				
D	100 µM	100 µM	200 µM	200 µM	200 µM	200 µM	250 µM	250 µM				
E	50 µM	50 µM	100 µM	100 µM	100 µM	100 µM	125 µM	125 µM				
F	25 µM	25 µM	50 µM	50 µM	50 µM	50 µM	62.5 µM	62.5 µM				
G	12.5 µM	12.5 µM	25 µM	25 µM	25 µM	25 µM	31.125 µM	31.125 µM				
H	6.25 µM	6.25 µM	12.5 µM	12.5 µM	12.5 µM	12.5 µM	15.563 µM	15.563 µM				

Figure 2.4. A schematic example of NH (columns 1-2), THNH (columns 3-4), 4-PP (columns 5-6) and 2-meNH (columns 7-8) serial dilutions into a deep-well block. The highest concentration for each compound was made by diluting a 100 mM solution into 1 ml of media. Serial dilutions were then performed by removing 500 µl of solution and adding it to the subsequent well containing 500 µl of media only. Odd numbered wells contained SH-SY5Y media while even rows contained S.NNMT.LP media.

Five hundred µL of appropriate media was added to rows B-H. Five hundred µL of each solution within row A was then removed and mixed by pipetting 10 times up and down into the wells of the row immediately below. This was then repeated with each subsequent row to produce 7 1:1 serial dilutions.

Media covering the cells in the plate was aspirated using a filterless 10 µL tip attached to the aspirator in order to minimise the contact between the aspirator and the growing surface. A multichannel pipette was used to add 100 µL of each individual concentration to all cells within plate row (n = 4 for the MTT assay, n = 3 for ATP assay, figure 2.3). Untreated (n = 4 for the MTT assay, n = 3 for ATP assay) and control wells were incubated with 100 µL media. Once cells had been dosed they were incubated for the required amount of time as detailed in the relevant experimental chapters.

2.4.3. End-point analyses

2.4.3.1. MTT assay

Following incubation as described in Section 2.4.2, the ability of the cells to reduce MTT to formazan was assessed as a measure of cell viability (Matharu *et al.* 2009). Ten µL of MTT solution (table 2.3) was added to each well, with the exception of the 2 no MTT control wells, using a repeat pipettor. The plate was then placed in the incubator for 4 hours.

Media was carefully aspirated from all the wells and 100 µL of lysis buffer (table 2.3) was added. The plate was then placed inside an Orbital Incubator SI50 (Stuart

Scientific, Stone, UK) at 150 rpm for 1 hour at 37^{o}C, after which absorbance was measured at 570nm using a spectrophotometer (Perkin Elmer, Massachusetts, USA). Results were calculated and expressed as described in section 2.5.4.

2.4.3.2. ATP assay

ATP content was assessed using the ATP-Glo kit (Biotium, California, USA) as previously described (Parsons *et al*. 2011). Briefly, ATP-Glo cocktail mix was made by dissolving 10 mg of D-luciferin in 1 mL of deionised water (final concentration 10 mg/mL). Eight hundred µL of D-luciferin solution was then added to 20 mL ATP assay buffer (final concentration 0.4 mg/mL D-luciferin). Two hundred µL of firefly luciferase was added to complete the cocktail.

After dosing as described in Section 2.4.2, plates were transferred without removal of media to a spectrophotometer equipped with an injector (Fluostar Omega, BMG Labtech, Buckinghamshire, UK). The spectrophotometer was programmed with the following protocol: injection of 100 µL of ATP-Glo cocktail, shake for 3 seconds, delay for 10 seconds and then measure luminescence for 10 seconds using a gain of 2000. All wells were sequentially injected and measured individually. Results were calculated and expressed as described in section 2.4.4.

In the event that absolute ATP values were to be determined *via* a calibration curve, a set of standards were made as follows:

- 10,000 pmol ATP: 5 µL of a 2 mM ATP solution was added to 995 µL of PBS
- 1000 pmol ATP: 100 µL of the above solution was added to 900 µL of PBS

- 100 pmol ATP: 100 µL of the above solution was added to 900 µL of PBS
- 10 pmol ATP: 100 µL of the above solution was added to 900 µL of PBS
- 1 pmol ATP: 100 µL of the above solution was added to 900 µL of PBS
- 0.1 pmol ATP: 100 µL of the above solution was added to 900 µL of PBS
- 0.01 pmol ATP: 100 µL of the above solution was added to 900 µL of PBS

One hundred µL of each standard were then loaded in triplicate onto the same white 96-well plate as the relevant experimental samples before the assay was performed as described above. Taking into account the addition of 1/10th of the stock solution of the standards into each well, the final amounts of ATP in each triplicate set of wells were 1000 pmol, 100 pmol, 10 pmol, 1 pmol, 0.1 pmol, 0.01 pmol, and 0.001 pmol. The calibration curve was constructed by creating a double log plot of luminescence against concentration of ATP. A line of best fit was then determined *via* linear regression.

2.4.4. Statistical analysis

All statistical analysis was performed using Graphpad Prism software (Graphpad, California, USA). In all cases $p < 0.05$ was taken as significant.

2.4.4.1. Determination of individual dose toxicity

In order to determine the overall effect of each, individual, compound dose on the viability (MTT reduction) and ATP content (ATP assay) of a single cell line, a 1-way repeated-measures ANOVA using blocked, mean data for each experimental repeat,

was performed with concentration as the independent variable and absorbance minus background (control wells with no MTT solution) or luminescence minus background (control wells with media only) as the dependent variable for the MTT and ATP assays respectively. Raw absorbance and luminescence values were used due to the requirement for ANOVA data to show an equal distribution of variability in the groups. Normalisation of data by expressing them as percentage of untreated (control) cells would, provided the control data were included, violate this assumption due to the fact that the untreated control would exist as 100% ± 0% (Lew 2007). Therefore, given that the aim of the test was to compare the effect of a particular dose versus untreated, raw data were used.

2.4.4.2. Determination of individual dose toxicity between cell lines

In order to determine whether SH-SY5Y and S.NNMT.LP cells exhibited significant differences in viability or ATP content at individual concentrations, a 2-way repeated-measures ANOVA using blocked, mean data for each experiment was performed with concentration and cell line as the two independent variables and data normalised as percentage of untreated (control) cells as the dependent variable. Data were normalised in order to take into account differences in baseline between both cell lines. Control data were not included in the analysis as, due to the normalisation process, these would violate the assumption of the ANOVA of an equal distribution of variability amongst the data. Data were blocked for individual experiments to take into account the week-to-week variation.

2.4.4.3. Determination and comparison of EC50s

In order to investigate the overall effect of a compound on a particular cell line, EC50s for each experiment were determined from dose-response curves as follows. Data were normalised as percentage of untreated (control) cells before concentration (in M) was log-transformed. These were then plotted using an XY scatter graph with log concentration as the independent variable and percentage of untreated (control) cells as the dependent variable. A non-linear regression analysis was then carried out using a log inhibitor *vs* response – variable slope model to the following equation:

$$Y = Bottom + \frac{Top - Bottom}{1 + 10^{(LogEC50 - X) * HillSlope}}$$

A constraint at Y = 0 was used due to the subtraction of background readings from all toxicity data. Two different EC50s can be calculated from this data. The first one, the relative EC50, is the point halfway between the top and the bottom of the plotted curve. The relative EC50 takes into account instances where the lowest concentrations of a compound achieve lower viability than untreated cells or instances where the lowest concentrations actually enhance the viability of the cells beyond 100%. While it can be of interest to take into account these effects at lower concentrations when determining general toxicity, the comparison of 2 separate relative EC50s is difficult, due to the fact that they could be derived from largely different areas of the y-axis. However, this is not the case for the absolute EC50. The absolute EC50 is determined by calculating the point on the x-axis (the log concentration), at which the curve intersects 50% viability (relative to untreated

cells) on the Y axis. Due to the desire to compare toxicity between cell lines using a fixed point of reference during our studies, only the absolute EC50s were determined. As a consequence, any further mention of EC50 will be in reference only to the absolute EC50. Furthermore, in order to differentiate between EC50s calculated following the MTT or ATP assays, the nomenclature $EC50_{MTT}$ and $EC50_{ATP}$ will be used in future chapters.

During statistical analysis, EC50s were generated and maintained in their log format due to the requirement for concentration to be log-transformed when constructing a dose-response curve. It was not considered to be statistically sound to perform statistics with the antilog of the logEC50s, due to the uneven symmetry that exists when a log standard error is anti-logged. For example, an EC50 of 1 µM +/- a standard error of 1 on the log scale, when anti-logged, will produce an EC50 with a negative error of 0.1 µM but a positive error of 10 µM. To avoid this skew, statistical analysis was performed using logEC50s, given that EC50s expressed this way show a normal distribution (Hancock *et al.* 1988). For ease of presentation and interpretation, where applicable, mean LogEC50 data were anti-logged to show the corresponding natural number. However, any statistical analysis concerning EC50s was exclusively carried out using log-transformed data.

In order to assess whether the overall toxicity of the tested compounds varied between cell lines, logEC50s were compared using a Student's *t*-test. In addition, $EC50_{MTT}$s generated for each compound/cell line were compared with their respective $EC50_{ATP}$s *via* a Student's *t*-test. This was done to determine whether a compound's toxicity varied depending on the assay. Finally, the relative order of

toxicity for all compounds used in a particular chapter was determined by comparing the $EC50_{MTT}$s and the $EC50_{ATP}$s in each cell line *via* either a Student's *t*-test (when comparing 2 compounds) or a 1-way ANOVA (when comparing 3 compounds).

3. Optimisation

In order to provide the most definitive answers to the research questions, a number of optimisation studies were performed. These were designed to determine the most appropriate toxicity assays for the cell lines used in the project, to determine the ideal conditions for maximising the production of relevant data in these assays and to develop a relevant and reliable positive control for Western blotting of neuronal markers. Therefore, this chapter has been presented as a collection of individual studies containing related optimisation experiments.

3.1. Determination of appropriate cell viability assays

3.1.1. Introduction

In vitro cytotoxicity can be determined in a number of ways. Some commonly used methods include the lactate dehydrogenase (LDH) assay, the MTT assay and the ATP assay.

3.1.1.1. The LDH assay

In healthy cells, LDH is located exclusively within the cytosol. However, during cell death, plasma membrane rupture leads to LDH leakage into the surrounding media. By measuring the amount of LDH that has been released from cells, the LDH assay reveals the extent of plasma membrane rupture and as such a measure of late-stage toxicity and cell death (Koh & Choi 1987). In practice, LDH presence in the media is determined *via* the measurement of the downstream production of a red formazan dye (figure 3.1).

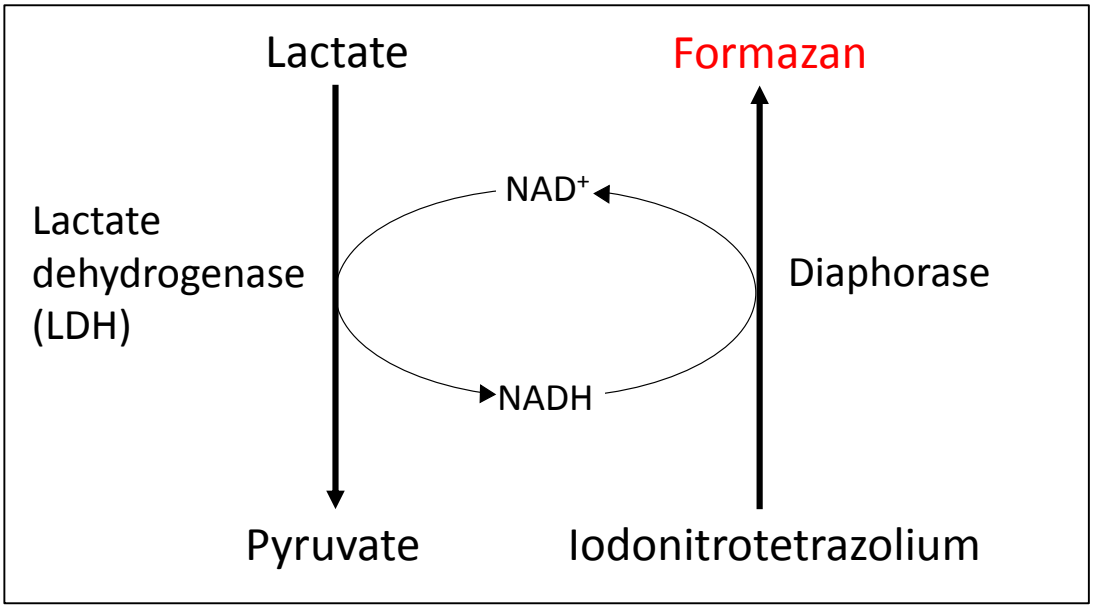

Figure 3.1. Schematic representation of the relationship between LDH activity and formazan production in the LDH assay. NADH produced via LDH activity is used by diaphorase to convert the colourless iodonitrotetrazolium into red formazan.

LDH catalyses the conversion of lactate to pyruvate, producing 1 NADH molecule as a result. NADH is then used by diaphorase, supplied with the assay kit, to convert colourless iodonitrotetrazolium to red formazan. The conversion is quantified *via* the measurement of absorbance at 490 nm. Thus, the production of formazan is directly dependent on LDH activity and, therefore, gives a quantitative measure of end-stage cytotoxicity.

3.1.1.2. The MTT assay

The MTT assay correlates cell viability with metabolic activity, *via* the reduction of the MTT dye into purple formazan (figure 3.2).

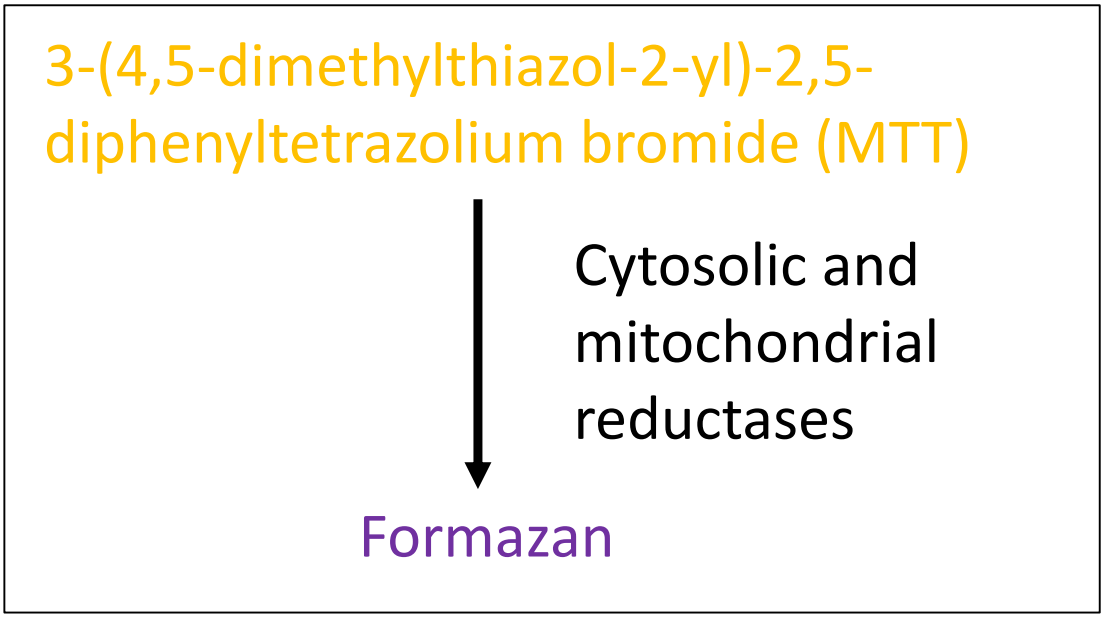

Figure 3.2. Schematic representation of the conversion of MTT into purple formazan by various enzymes in the mitochondria and cytosol.

The production of purple formazan is proportional to the cells' metabolic activity and is quantified by measuring absorbance at 570 nm. Contrary to popular belief, which states that this reduction is carried out by succinate dehydrogenase in the mitochondria and as such is an indicator of mitochondrial function (Kaneko *et al.* 1995, Satoh *et al.* 1996, van Meerloo, Kaspers & Cloos 2011), various reports suggest that the MTT assay is an indicator of the overall metabolic activity of the cell, as many additional cytosolic enzymes are able to catalyse MTT reduction (Berridge & Tan 1993, Liu *et al.* 1997, Bernas & Dobrucki 2002, Takahashi *et al.* 2002, Berridge, Herst & Tan 2005). In contrast to the LDH assay, the MTT assay can give an indication of an early-stage toxicity, as reduced metabolic activity will occur upstream of cell death (Fotakis & Timbrell 2006). However, the MTT assay can still demonstrate that cell death has occurred, as the lack of any detectable conversion of the MTT dye to formazan will be indicative of cessation of all metabolic activity.

3.1.1.3. The ATP assay

The measurement of intracellular ATP concentration, given its role as the principal energy store within the cell, is another commonly-used method for assessing cell viability (figure 3.3).

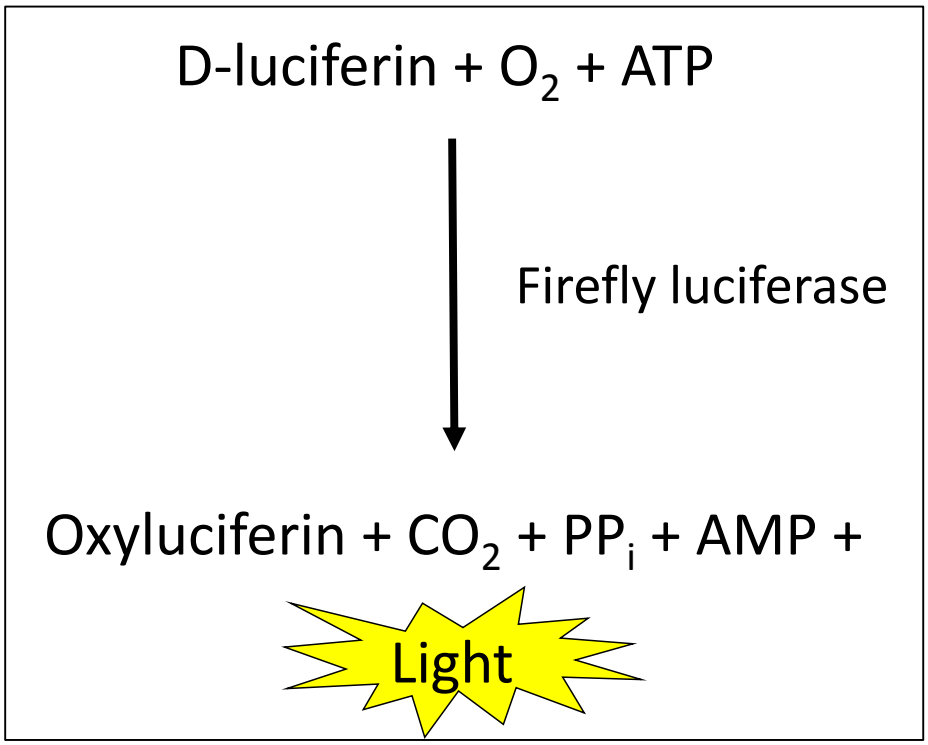

Figure 3.3. Schematic representation of the ATP luciferase assay. Intracellular ATP is directly proportional to the amount of light produced during the conversion of D-luciferin to oxyluciferin.

The assay involves the addition of a D-luciferin and firefly luciferase-containing solution to cells. This lyses the cells and provides firefly luciferase with intracellular ATP to drive the light-producing oxidation of D-luciferin. Thus, the amount of light produced is directly proportional to the amount of ATP contained within the cells. Viability studies involving the ATP assay can, therefore, give an indication of toxicity occurring *via* the depletion of ATP stores. In addition and similar to its MTT-based counterpart, the ATP assay can give an indication of toxicity prior to cell death, as the assay's high sensitivity allows it to rapidly detect changes in ATP content (Mueller, Kassack & Wiese 2004). The high sensitivity of the assay also allows the measurement of ATP levels in low numbers of cells, and is thus ideal for use with, for example, primary cultures where cell numbers may be low, or for high-throughput screening of 96-well based assays. The measurement of ATP as an indicator of cell viability/toxicity has been shown to correlate well with both cell proliferation and cytotoxicity of a number of different cell types (Crouch *et al.* 1993).

3.1.1.4. The balance between assay number and practicality

While each individual assay reveals different subtleties about what is causing cytotoxicity, performing multiple different assays for the same set of experiments is both time-consuming and expensive. However, solely relying on one method will only provide limited mechanistic information when cells undergo a toxic event. Also, it is possible that, in an assay assessing the effects of a compound on cell viability, the compound itself is interfering with the mechanism of the assay, for

example by inhibiting LDH or succinate dehydrogenase directly. Therefore, it was concluded that performing two cytotoxicity assays would provide a compromise: preventing excessive repetition, while also providing both confirmation of toxicity and additional mechanistic information about the stage of toxicity, whether very early (measured in the ATP assay), early to moderate (measured in the MTT assay) or late (measured in the LDH assay). Thus, the aim of this study was to determine which 2 of the above mentioned assays would be most suitable for assessing the viability of SH-SY5Y and S.NNMT.LP cell cultures.

3.1.2. Methods

3.1.2.1. LDH assay optimisation

3.1.2.1.1. The effect of media supplements on the LDH assay

In order to accurately quantify toxicity *in vitro*, it is important to ensure that there are no interfering factors in the cells' culture media. The possible interference of media components in the LDH assay was determined as follows. A 50 µL sample (in triplicate) of SH-SY5Y media was taken following each step of the media supplementation process (section 2.1, table 2.1) and added to a clear, flat-bottomed 96-well plate (Thermo Scientific, Loughborough, UK). Phenol red free Dulbecco's Modified Eagle Medium:F12 media (Sigma-Aldrich, Dorset, UK) was used for this process. In order to assess the effect of phenol red supplementation to the media, commercially-available Dulbecco's Modified Eagle Medium:F12 media containing phenol red (section 2.1, table 2.1) was used.

Cytoscan assay mix (G-Biosciences, St Louis, Missouri, USA) was made by dissolving the substrate mix in 11.4 mL of deionised water before adding 600 µL of assay buffer. Fifty µL of assay mix were then added to each well before incubating for 20 minutes at 37^{o}C. Absorbance at 490 nm was then measured using a spectrophotometer (Perkin Elmer, Waltham, Massachusetts, USA).

3.1.2.1.2. The dose-response effect of FBS-supplemented cell culture media on the LDH assay

Quantification of FBS-mediated interference in the LDH assay was determined by adding triplicate 50 µL samples of SH-SY5Y media containing 0%, 5%, 10%, and 15% FBS to a clear, flat-bottomed 96-well plate. Triplicate 50 µL samples of LDH enzyme (diluted 1:10,000 in PBS containing 1% bovine serum albumin) were also added to the plate as a positive control. The LDH assay was then carried out as described in section 3.1.2.1.1.

3.1.2.2. MTT assay optimisation

3.1.2.2.1. The effect of FBS supplementation on cell viability via MTT reduction

In order to determine the consequences of varying the FBS content in media upon cell viability, the following experiment was performed. SH-SY5Y and S.NNMT.LP cells in 15% FBS media were trypsinised, counted and seeded onto a 96-well plate at a density of 10,000 cells per well. Following an overnight incubation, all wells were washed with PBS before quadruplicate wells were given either serum-free media, media supplemented with 15% FBS, or media supplemented with 15% heat-inactivated (HI) FBS. The cells were then incubated for 48 hours before the MTT assay was performed as described in section 2.4.2.1.

3.1.2.3. ATP assay optimisation

3.1.2.3.1. Determination of the relationship between luminescence values, ATP concentration and cell viability

In order to confirm the proportional relationship between ATP content - as measured in the ATP assay - and cell viability, the following 2-part experiment was performed. Firstly, a set of ATP standards were made and luminescence was determined as described in section 2.4.3.2. Luminescence values and ATP content (in pmol) were expressed as a double-log plot. Secondly, SH-SY5Y and S.NNMT.LP cells were prepared for ATP assay as described in section 2.4.1. Cells were seeded at densities of 20,000, 40,000, and 80,000 cells per well. The plate was incubated overnight to allow the cells to settle before the ATP assay was performed as described in section 2.4.2.2. Cell number and luminescence values were plotted using a double-log plot.

3.1.3. Statistical Analysis

All statistical analyses were performed using Graphpad Prism software (Graphpad, California, USA). Effects of media components and FBS supplementation on the LDH assay were analysed using a 1-way ANOVA followed by a Dunnet post-test, comparing all columns against unsupplemented media. The effect of FBS supplementation on cell viability in the MTT assay was determined using a repeated measures 1-way ANOVA for each cell line followed by a Dunnet post-test comparing all columns against serum-free media. Data were matched by experimental repeat.

Finally, linearity of luminescence *vs* ATP concentration, and luminescence *vs* cell density, were determined *via* linear regression analysis.

3.1.4. Results

3.1.4.1. LDH assay optimisation

3.1.4.1.1. Media supplementation with phenol red and FBS increased absorbance in the LDH assay

The effect of media supplementation on absorbance at 490 nm is shown in figure 3.4. Supplementation of non-essential amino acids, L-glutamine or penicillin/streptomycin to phenol red-free media had no significant effect upon absorbance. However, addition of phenol red significantly increased absorbance (0.039 *vs* 0.067 ± 0.001, $p < 0.01$, n = 3). Addition of 15% FBS also significantly increased the absorbance of cell-free, media-only solutions (0.039 *vs* 0.53 ± 0.01, $p < 0.001$, n = 3).

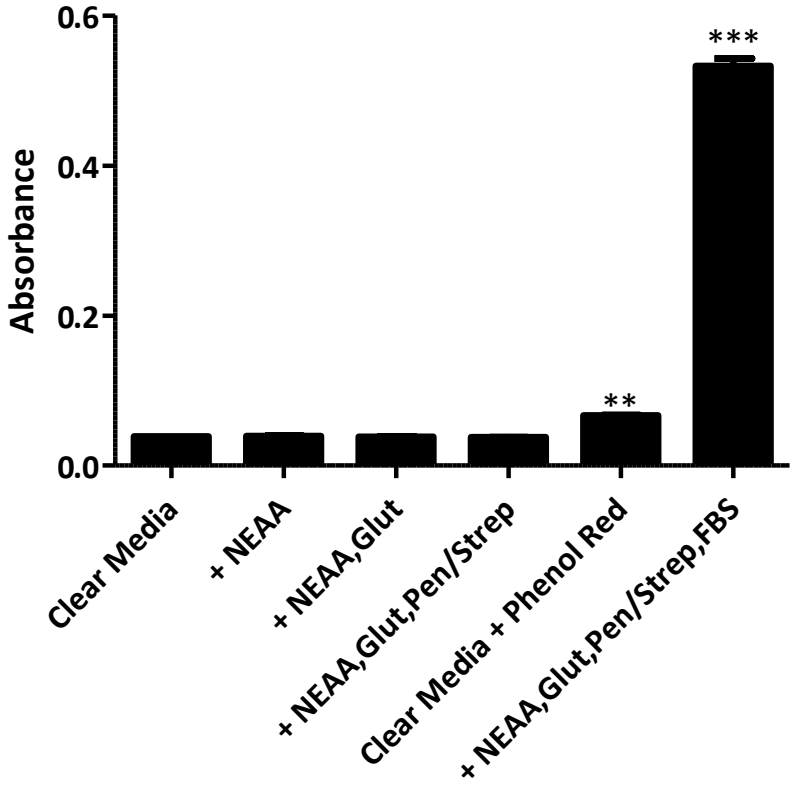

Figure 3.4. The effect of cell culture media supplements on the LDH cytotoxicity assay. All data are triplicate mean ± SEM. NEAA = non-essential amino acids, Glut = L-Glutamine, Pen/Strep = Penicillin/streptomycin, FBS = Fetal bovine serum. ** p < 0.01, *** p < 0.001, n = 3

3.1.4.1.2. Media supplementation with FBS increased LDH assay absorbance in a dose-dependent manner

Figure 3.5 shows the dose-dependent increase in absorbance following FBS supplementation. Absorbance was significantly increased following each subsequent addition of 5% FBS (serum free: 0.037 ± 0.001; 5% FBS: 0.20 ± 0.003; 10% FBS: 0.33 ± 0.003; 15% FBS: 0.46 ± 0.005, $p < 0.001$ for all, n = 3).

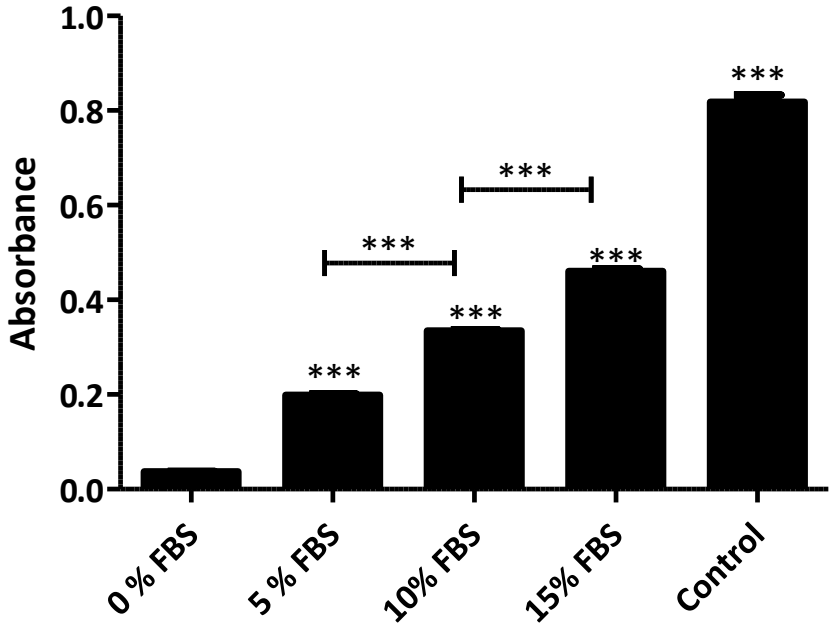

Figure 3.5. The effect of FBS-supplementation on the LDH-cytotoxicity assay. All data are triplicate mean ± SEM. Control consisted of diluted LDH enzyme solution only. *** p < 0.001, n = 3

3.1.4.2. MTT assay optimisation

3.1.4.2.1. FBS supplementation significantly affected cell viability

Cells cultured in 15% FBS for 48 hours showed significantly enhanced viability, as measured by the MTT assay, compared with cells grown in serum-free media (0.12 ± 0.05 *vs* 0.46 ± 0.16, 3.7-fold increase in absorbance, $p < 0.05$, n = 4 for SH-SY5Y cells; 0.06 ± 0.02 *vs* 0.18 ± 0.07, 3.9-fold increase in absorbance, $p < 0.05$, n = 4 for S.NNMT.LP cells, figure 3.6). No significant difference was seen between serum-free media and HI FBS-supplemented media for either cell line.

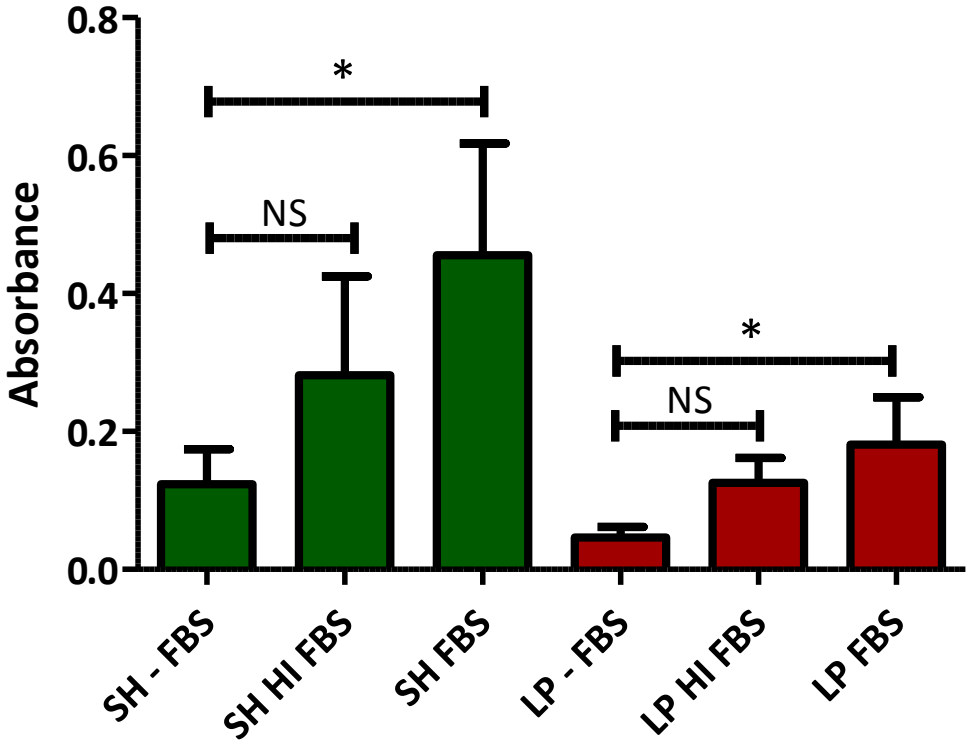

Figure 3.6. The effect FBS on SH-SY5Y (dark green, n = 4) and S.NNMT.LP (dark red, n = 4) cell viability as measured by the MTT assay. All data are mean ± SEM. – FBS = serum-free media, HI = media supplemented with 15% heat inactivated FBS, FBS = media supplemented with 15% FBS. * = p < 0.05 vs – FBS in the same cell line, NS = not significant vs – FBS in the same cell line.

3.1.4.3. ATP assay optimisation

3.1.4.3.1. Luminescence values were proportional to ATP content and cell density in the ATP assay

The effect of cell number on ATP content is shown in figure 3.7. A strong linear relationship was observed between ATP content and luminescence (r^2 = 0.998, figure 3.7A). A strong linear relationship was observed between SH-SY5Y (r^2 = 0.9998, figure 3.7B) and S.NNMT.LP (r^2 = 0.92, figure 3.7B) cell density compared with luminescence.

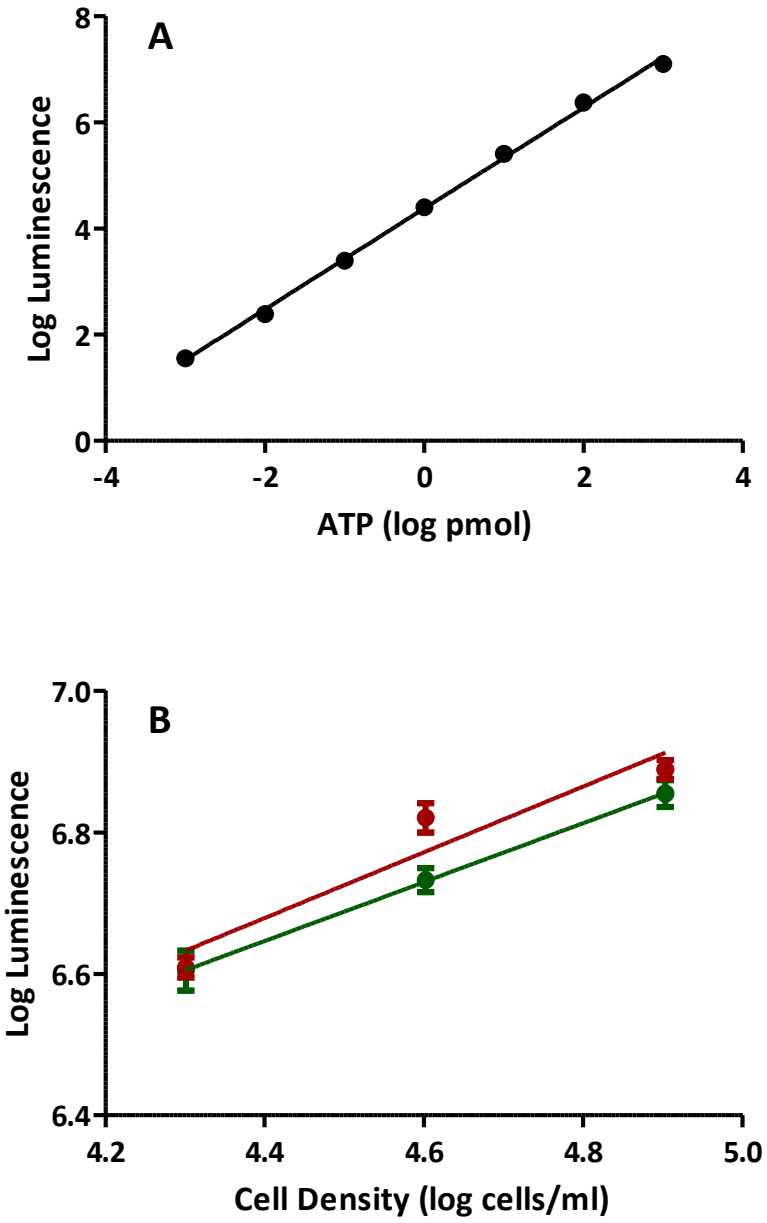

Figure 3.7. The linear relationship between ATP and luminescence (A) and cell density and luminescence (B) in the ATP assay. All data are mean ± SEM. Green circles = SH-SY5Y, red circles = S.NNMT.LP, n = 3

3.1.5. Discussion

Summary of key findings

- ***Absorbance in the LDH assay was significantly increased following the addition of FBS and phenol red***
- ***FBS increased the LDH assay absorbance in a dose-dependent manner***
- ***Cells cultured in media supplemented with 15% FBS, but not 15% HI FBS, showed significantly enhanced viability compared to cells with serum-free media***
- ***Luminescence in the ATP assay was directly proportional to ATP content and cell density***

The significant increase in absorbance observed following the addition of phenol red and FBS to the cell culture media suggested that these supplements had the potential to interfere with the LDH assay by increasing background absorbance, thus unfavourably decreasing the signal:noise ratio and the sensitivity of the assay. In the case of phenol red, this was most likely due to phenol red having an absorbance spectrum encompassing 490 nm (Baylor & Hollingworth 1990). On the other hand FBS, which showed dose-dependent interference, likely increased absorbance due to the presence of LDH within the serum (Van Der Helm 1962). The large response seen following FBS supplementation, particularly considering that both cell lines were routinely maintained in media supplemented with 15% FBS, was deemed to result in too great a background absorbance in the LDH assay.

One solution to this problem was to reduce the percentage of FBS or remove the FBS from the media in order to lower the background absorbance of the assay. However, given that the MTT assay demonstrated that there was a significant decrease in cell viability when FBS was removed from the media, doing so would have had physiological consequences for both cell lines due to the removal of growth factors (Honegger & Humbel 1986). This was also true of HI FBS which did not show significantly enhanced viability when compared with serum-free media. However, due to its alternate mechanism, the MTT assay would not be affected by the presence of LDH in FBS. This coupled with the finding that cell viability was at its highest when cells were cultured in 15% FBS media and the fact the MTT assay provides a more subtle, early indicator of toxicity than the LDH assay strongly suggested that the MTT assay was the more appropriate assay of the two for the purpose of the project.

The strong linearity between the ATP content of the standards and the measured luminescence confirmed the relationship between the two variables. Thus, the proportional increase in luminescence – and therefore ATP content – seen when luminescence was plotted against cell density also confirmed that the ATP content measured by the assay provided an accurate indicator of cell viability. Therefore, it appeared that both the MTT and ATP assays were suitable tools for the measurement of toxicity in both cell lines and could be used in later toxicity studies involving potential PD-causing agents.

3.2. Determination of the appropriate cell density for toxicity assays

3.2.1. Introduction

When establishing a toxicity profile, it is important to maximise the dynamic range between the upper and lower limits of toxicity in order to generate a well-described sigmoidal curve. Maximum toxicity can be achieved by increasing the compound's dose beyond the point at which all cells die. Achieving the highest possible viability - and thus the greatest dynamic range between upper and lower limits of the curve - can be achieved *via* the determination of the optimal cell density.

While signal intensity (in an assay that measures live cells) should increase in proportion with cell number, there will be a point at which this becomes saturated, i.e. the absorbance curve starts to plateau and no longer follows the Beer-Lambert law. Absorbance can be expressed by the following equation:

$$A = 2 - log\ \%\ T$$

where A is absorbance and log % T is the percentage of light that is transmitted through the sample logged to the base of 10. Accordingly, increasing the absorbance from 1 to 2 represents a reduction in transmittance from 10% to 1%. In many microplate readers, and indeed in the microplate readers utilised during the project, absorbance is only linear up to A = 2 due to the lack of accuracy in determining transmittances below 1%. Consequently, it is imperative for any assays involving absorbance measurements as endpoints to avoid over-seeding cells, as

the larger signal generated during the subsequent viability assay may lead to absorbances that exceed A = 2.

In addition to the instrumental issues with absorbance saturation, an excessively high cell density can lead to cells overgrowing, causing the rate at which the assay signal (e.g. MTT reduction) is produced to become saturated due to substrate depletion or difficulties in cell uptake due to the spatial interference from other cells. Overgrown cells could also lead to the masking of toxic effects *via* a similar mechanism, as cells that have been grown on top of by others may be spatially shielded from toxins. Finally, if the population is too dense, auto-toxicity may occur due to depletion of nutrients.

In order to determine the ideal cell seeding density for subsequent toxicity assays, a number of cell densities for incubations of 2 days and 5 days were tested for their ability to obtain a maximum signal without saturation of the MTT assay.

3.2.2. Methods

SH-SY5Y and S.NNMT.LP cells were trypsinised and counted as described in section 2.1.2. Cell suspensions were then seeded onto clear, flat-bottomed 96-well plates (Thermo Scientific, Loughborough, UK) at the following densities: for 2-day incubations cells were seeded at 5,000, 10,000, 20,000, 30,000, 40,000 and 50,000 cells per well, and for 5-day incubations cells were seeded at 5,000, 10,000, 20,000 and 40,000 cells per well. Following incubation, an MTT assay was performed as described in section 2.4.2.1.

3.2.3. Results

Following the 2 day incubation, absorbance at 570 nm increased in proportion with initial cell density (figure 3.8A). The peak absorbances of 1.30 ± 0.03 and 1.28 ± 0.03 for SH-SY5Y and S.NNMT.LP respectively were measured in the wells seeded with 50,000 cells but were only 6.6% and 2.7% respectively higher than the absorbances measured in wells seeded with 40,000 cells (1.22 ± 0.03 and 1.24 ± 0.03 for SH-SY5Y and S.NNMT.LP respectively).

Absorbance increased proportionally with cell density after 5 days in wells containing SH-SY5Y cells but not S.NNMT.LP cells (figure 3.8B). Absorbance in S.NNMT.LP cells increased proportionally from 5,000 cells/well to 20,000 cells/well but significantly decreased at 40,000 cells/well compared with 20,000 cells/well (0.91 ± 0.03 *vs* 0.77 ± 0.02, 22% loss, $p = 0.003$).

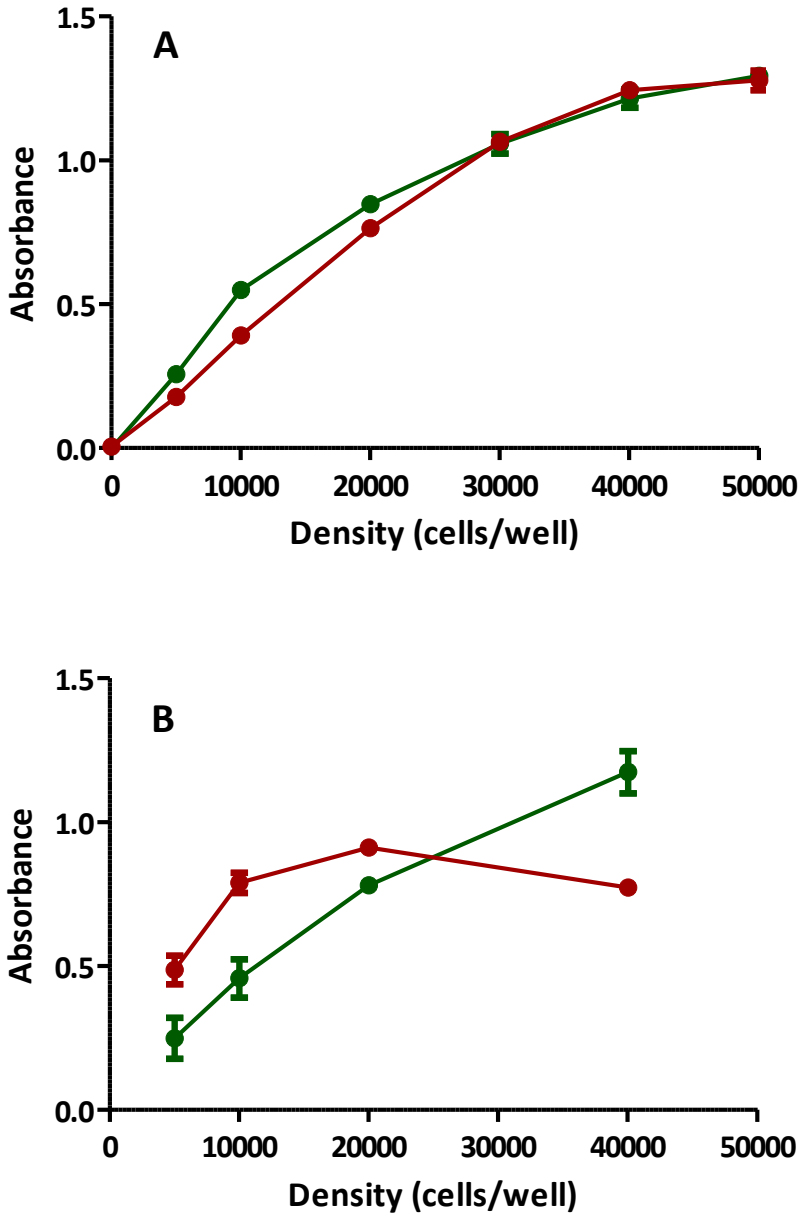

Figure 3.8. The relationship between cell density and absorbance after 2 days (A) and 5 days (B) incubation as measured by the MTT assay. All data are triplicate mean ± SEM. Green circles = SH-SY5Y, red circles = S.NNMT.LP

3.2.4. Discussion

Summary of key findings

- ***Absorbance increased in proportion with cell density for both cell lines after a 2-day incubation but showed only a marginal increase at the highest densities***
- ***Absorbance increased in proportion with cell density after a 5-day incubation for SH-SY5Y cells but not for S.NNMT.LP cells***

While the maximum absorbance after 2 days of incubation was achieved at 50,000 cells/well, the relatively small increase from 40,000 cells/well suggested that the absorbance may have been close to the saturation point. Thus, increasing the cell density beyond 40,000 cells/well for toxicity studies would have not only produced relatively trivial increases in absorbance, it could also have led to a masking of toxic effects as milder forms of toxicity may have remained undetected due to excess metabolic activity. Also, any potential detection of increased cell viability may also be compromised. As a consequence, 40,000 cells/well was the density chosen for 2 day assays.

For 5 day incubations, SH-SY5Y cells produced a peak absorbance at 40,000 cells/well. However, the fact that absorbance decreased when S.NNMT.LP density was increased to 40,000 cells/well suggested that using the higher density could cause S.NNMT.LP cells to become autotoxic. In addition, the longer incubation time and, thus, higher rates of cell division increased the possibility of overcrowding and/or instrumental absorbance saturation occurring during the incubation period.

Therefore, a lower density was considered. While 20,000 cells/well corresponded to the peak absorbance for S.NNMT.LP cells, it was not clear whether this density represented a point shortly after which absorbance was saturated. Fifteen thousand cells/well was considered to be an appropriate density, due to the combination of its close proximity to the peak absorbance of S.NNMT.LP cells and its presence within the linear, non-saturated portion of the curve for SH-SY5Y cells. In accordance with this, 15,000 cells/well was the density used in later 5-day toxicity assays.

3.3. Determination of the optimal incubation time for toxicity assays

3.3.1. Introduction

Due to the fact that age is the greatest risk factor in PD-development (Kieburtz & Wunderle 2013) it is important to model toxicity studies relevant to PD with as much of a long-term approach as possible. However, it is impractical to maintain proliferating cell lines in a constant environment for an extended period of time without introducing factors such as overcrowding and senescence. Nevertheless, it is important to expose cells to potential PD-causing compounds for as long as possible, given the likelihood that PD-relevant toxicity emerges over time. Thus, the applicability of 5-day *in vitro* toxicity assays was tested by comparing the results obtained following 5-day incubations with those from 2-day incubations.

3.3.2. Methods

SH-SY5Y and S.NNMT.LP cells were trypsinised and counted as described in section 2.4.1. Cell suspensions were then seeded into clear, flat-bottomed 96-well plates (Thermo Scientific, Loughborough, UK) at densities of 40,000 cells/well and 15,000 cells/well for 2-day and 5-day assays respectively. The plate layout described in section 2.4.1 was followed.

Following an overnight incubation, serial dilutions of THNH were made and transferred to cells in the plates according to the method described in section 2.4.2. Plates designated for 2-day assays were incubated for 48 hours before an MTT assay was performed (section 2.4.3.1). For the 5-day assays, the dosing procedure was repeated after an initial 48-hour incubation in order to replenish spent media. Plates were then incubated for an additional 72 hours before an MTT assay was performed.

Dose-response curves and log $EC50_{MTT}$s were determined as described in section 2.4.4.3.

3.3.3. Results

3.3.3.1. Extending the incubation time to 5 days improved the dose-response curve in SH-SY5Y cells

The dose-response curves for the 2-day and 5-day THNH incubations are shown in figure 3.9. Increasing the incubation time from 2 to 5 days increased the gradient of the linear portion of both dose-response curves. This occurred alongside an improvement in the r^2 of the SH-SY5Y curve (0.88 after 2 days vs 0.94 after 5 days) but not in the S.NNMT.LP cells (0.95 after 2 days vs 0.94 after 5 days).

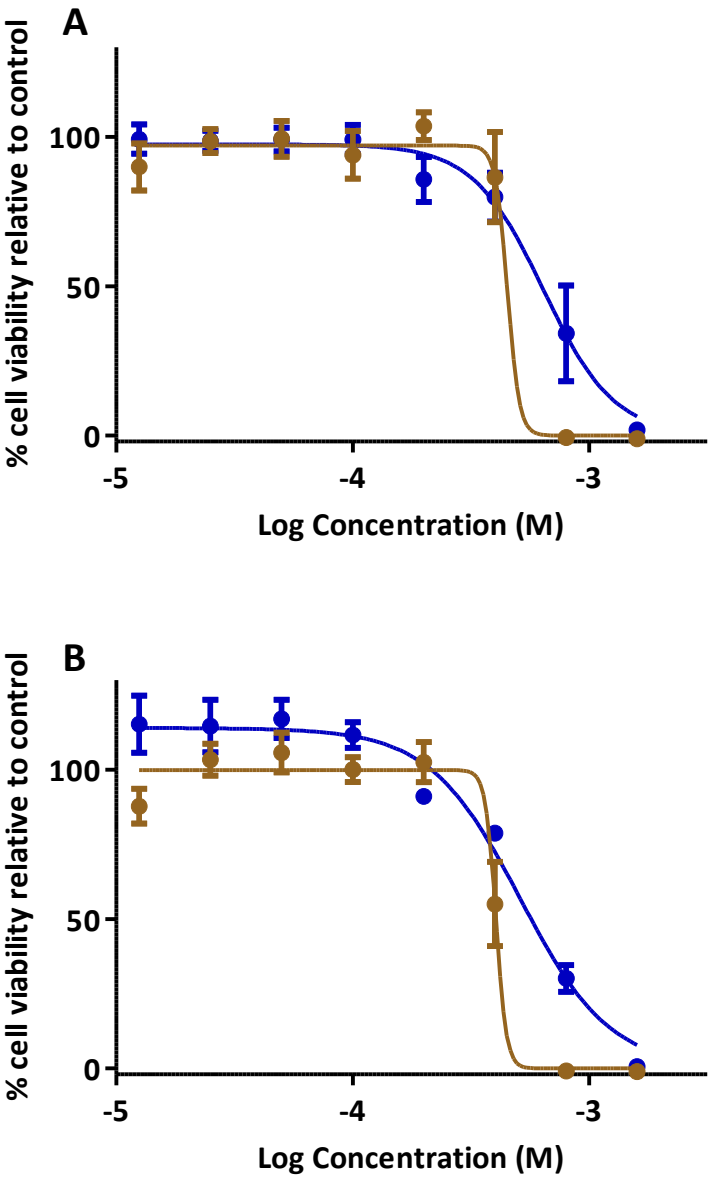

Figure 3.9. Dose response curves of THNH following its incubation with SH-SY5Y cells (A) and S.NNMT.LP cells (B). The duration of exposure was either 2 days (blue) or 5 days (brown). Cell viability was determined via MTT assay. All data are mean ± SEM, n = 3.

3.3.3.2. The $EC50_{MTT}$ in S.NNMT.LP cells was significantly lower when the incubation time was extended to 5 days

Increasing the incubation length from 2 to 5 days lowered the THNH log $EC50_{MTT}$ in each cell line. This difference was significant for S.NNMT.LP cells (2 day: -3.42 ± 0.02 (573 µM) *vs* µM 5 day: -3.39 ± 0.02 (410 µM), $p = 0.003$) but not for SH-SY5Y cells (2 day: -3.20 ± 0.07 (632 µM) *vs* µM 5 day: -3.43 ± 0.03 (454 µM), $p = 0.14$).

3.3.4. Discussion

Summary of key findings

- ***The $EC50_{MTT}$ of THNH was reduced in S.NNMT.LP cells after extending the incubation time***
- ***Extending the incubation time improved the r^2 of the SH-SY5Y dose-response curve***

Lengthening the incubation time resulted in a lowering of the THNH $EC50_{MTT}$. However, this change was only significant in S.NNMT.LP cells. This suggested that increasing the exposure time allowed more toxicity to manifest itself. While the $EC50_{MTT}$ was not significantly reduced in SH-SY5Y cells, the EC50 was reduced by 28% which matched the significant 28% reduction seen in S.NNMT.LP cells. Furthermore, the relatively low number of experimental repeats (n = 3) in this study may have contributed to the lack of statistical significance seen in the SH-SY5Y cells.

Whilst extending the incubation time did not have a significant effect on the THNH $EC50_{MTT}$ in SH-SY5Y cells, the overall toxicity profile of THNH in SH-SY5Y cells, with reference to the r^2, was improved. Accordingly, given both sets of data showing more pronounced toxicity at longer incubations, the incubation time for all future toxicity assays was increased to 5 days. In addition, in order to provide a more robust indication of toxicity, both in terms of the curve fit and EC50, the number of experimental repeats as shown in the experimental chapters 5 (n = 5) and 6 (n = 4) were increased.

While it is clear that an incubation time of 5 days may appear trivial in comparison to the 50 years over which neurotoxicity in idiopathic PD can develop, there are a number of reasons why this approach is justified.

Firstly, the overall life cycle of cells in culture is significantly shorter than that of neurons in the human brain. While a direct comparison (which itself will vary between cell lines and environmental conditions) between SH-SY5Y and S.NNMT.LP cells and neurons in the brain has not been reported, the relatively rapid decline in cell proliferation and viability seen from personal observations in these cells and as reported for other cell lines over successive passages (Hayflick 1965, Simons & Van den Broek 1970), is an indicator of an accelerated “aging” process of cells in culture compared to *in vivo*. Thus, in relative terms, incubating the cell lines with the compounds for 5 days *in vitro* was more physiologically relevant to the *in vivo* situation than incubating for only 2 days.

Secondly, the proliferating nature of both cell lines placed a practical constraint on the amount of time that cells could be incubated with their compounds before untreated controls became confluent. All toxicity assays were performed in 96-well plates to allow an entire experiment to be contained in 1 plate. This limited any spatial or environmental variability that could occur arise from using multiple plates, along with limiting physical damage to cells due to the splitting and reseeding process, which may be exacerbated if already under cytotoxic challenge. While longer incubations would have been possible using multiple 24-well plates, the introduction of additional variability that this would have caused was not considered to be of statistical best practice. Accordingly, 96-well plates were

considered to provide the best compromise between incubation length, absorbance strength and the number of possible experimental compound concentrations.

Finally, considering that these toxicity assays were principally designed to determine whether the expression of NNMT could alter cell toxicity in the presence βCs and 4PP, the incubation time was considered sufficient for any altered viability to become manifest. Should NNMT in fact be responsible for increased toxicity in the presence of these compounds, future studies would focus on maximising physiological relevance *via* the use of *in vivo* models.

3.4. Characterisation of a positive control for the Western blotting of neuronal markers

3.4.1. Introduction

In order to characterise whether enhanced NNMT expression in SH-SY5Y cells produced a change in neuronal lineage or general neuronal characteristics, the S.NNMT.LP cells' protein expression was investigated to determine whether they exhibited any altered expression of specific neuronal markers (chapter 4). For confirmatory purposes, this required a positive control against which bands on the Western blots could be compared. Mouse brain homogenate was considered to be the ideal candidate for this, given that this single control would express the entirety of the neuronal lineage spectrum required. Accordingly, a series of Western blots were performed to determine whether mouse brain homogenate could be used as a control for a variety of cell phenotype markers. These markers are, typically, enzymes involved in the biosynthetic pathway of the neurotransmitter of interest for a specific phenotype. Confirmation of expression of a particular enzyme is, thus, indicative of the phenotype in question.

Tyrosine hydroxylase (TH) is a commonly used neuronal marker for the expression of dopamine (Lopes *et al.* 2010, Korecka *et al.* 2013, Thomas *et al.* 2013). TH catalyses the conversion of L-tyrosine to L-dopa, the precursor to dopamine (Nagatsu 1995) and is, thus, expressed in dopaminergic areas of the brain such as the SN and the VTA, an area principally involved in the body's reward pathway (Fuxe 1965).

Phenylethanolamine *N*-methyltransferase (PNMT) is an enzyme involved in the downstream conversion of the dopamine metabolite noradrenaline/norepinephrine to adrenaline/epinephrine (Bülbring & Burn 1949). In the brain, PNMT is found mostly in the medulla oblongata, the arcuate nucleus of the hypothalamus and the SN (Kopp *et al.* 1979) and is indicative of an adrenergic phenotype.

Tryptophan hydroxylase (TPH) catalyses the rate-limiting step of serotonin synthesis (Grahame-Smith 1967). TPH exists as 2 isoforms, TPH1 and TPH2, with the former being expressed in the pineal gland and also in the gut and the latter being expressed exclusively in the brain, particularly the forebrain, midbrain and the hippocampus (Sakowski *et al.* 2006). Its presence is indicative of a serotonergic phenotype.

Choline acetyltransferase (ChAT) is responsible for catalysing the final step in the synthesis of acetylcholine (Nachmansohn & Berman 1946). ChAT expression in the human brain is principally located in the basal forebrain but it is also widely expressed in the basal ganglia and brainstem (Oda 1999) and is indicative of a cholinergic phenotype.

In addition to determining the expression of the cell-type markers, mouse brain homogenate was also investigated for the expression of the post-mitotic marker NeuN, a protein that is specific for neuronal maturity and thus a marker for the differentiation state of neuronally-derived cell lines such as SH-SY5Y and S.NNMT.LP (Agholme *et al.* 2010).

3.4.2. Methods

Mouse brains were obtained as snap-frozen hemispheres in liquid nitrogen from the Biological Services Unit, King's College London, from animals which had been culled using a Schedule 1 method as outlined in the Animal (Scientific Procedures) Act 1986. Tissues were prepared as previously described (Parsons *et al.* 2001). Briefly, tissue was homogenised in 10x volume of ice-cold RIPA buffer or 1% triton X-100 (approximately 400 µL) using 20 strokes of a Dounce homogeniser. Supernatant was centrifuged at 600 *x g* for 10 mins at 4^{o}C using a Sorval RT7 centrifuge (Thermo Scientific, Loughborough, UK), after which supernatant was collected and stored at -20^{o}C prior to protein concentration analysis as described in Section 2.2.2. Samples were subsequently prepared for Western blotting as described in section 2.2.3. Neuronal marker expression was assessed using primary antibodies against ChAT, TPH1, PNMT, TH and the post-mitotic neuronal marker NeuN, as outlined in Table 3.1.

Table 3.1. Antibodies and their dilutions used during Western blotting. Each primary antibody corresponded to a phenotypic cell marker: ChAT (acetylcholinergic); TPH1 (serotonergic); PNMT (adrenergic); TH (dopaminergic); NeuN (post-mitotic neurons). All secondary antibodies used were conjugated to horseradish peroxidase

Protein	Primary antibody	Secondary antibody
Choline acetyltransferase (ChAT)	Rabbit anti-ChAT (1:500, Source Bioscience, Nottingham, UK, GTX113163)	Goat anti-rabbit IgG (1:2000, Sigma-Aldrich, Dorset, UK, A8275)
NeuN	Rabbit anti-NeuN (1:100, Merck, Darmstadt, Germany, MAB377)	Goat anti-rabbit IgG (1:2000, Sigma-Aldrich, Dorset, UK, A8275)
Phenylethanolamine *N*-methyltransferase (PNMT)	Rabbit anti-PNMT (1:500, Source Bioscience, Nottingham, UK, GTX114098)	Goat anti-rabbit IgG (1:2000, Sigma-Aldrich, Dorset, UK, A8275)
Tryptophan hydroxylase 1 (TPH1)	Rabbit anti-TPH1 (1:500, Source Bioscience, Nottingham, UK, GTX109027)	Goat anti-rabbit IgG (1:2000, Sigma-Aldrich, Dorset, UK, A8275)
Tyrosine hydroxylase (TH)	Rabbit anti-TH (1:500, New England Biolabs, Hertfordshire, UK, #2792)	Goat anti-rabbit IgG (1:2000, Sigma-Aldrich, Dorset, UK, A8275)

In addition, a secondary antibody control, performed by blotting mouse brain protein along with SH-SY5Y and S.NNMT protein samples, with secondary antibody only was also performed to determine whether any non-specific binding of the secondary antibody was occurring.

3.4.3. Results

The Western blots for the secondary antibody controls are shown in figure 3.10. The secondary antibody control revealed non-specific bands occurring in the mouse brain samples at approximately 140 kDa and at 75 kDa. Accordingly, subsequent analysis discounted these bands from consideration.

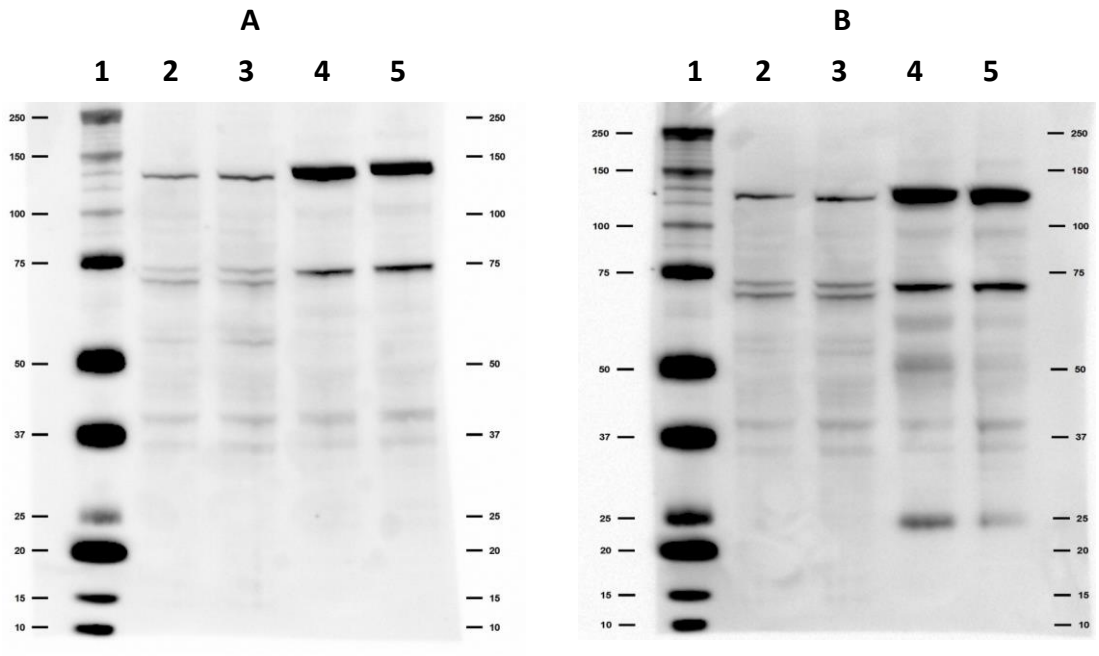

Figure 3.10. Secondary antibody controls of SH-SY5Y (lane 2), S.NNMT.LP (lane 3), mouse brain in RIPA buffer (lane 4) and mouse brain in 1% triton-X in PBS (lane 5). Blots were incubated with goat anti-rabbit IgG (A) or goat anti-mouse IgG (B) antibodies, diluted 1:2000 in MTBST, for 1 hour. Lane 1 comprises a series of Strep-tagged markers of known size (indicated) which were detected via the addition of Strep-Tactin-conjugated HRP.

The Western blots of the neuronal markers are shown in figure 3.11. NeuN was detected as a 45-50 kDa doublet which is in accord with its published size in the mouse brain (Dredge & Jensen 2011). This was also true for TH which was detected as a single band seen at approximately 58 kDa (Presgraves *et al.* 2004), ChAT which was detected as 2 bands at approximately 70 kDa (Misawa, Ishii & Deguchi 1992) and TPH which was detected as multiple bands just above 50 kDa (Sakowski *et al.* 2006). Finally, PNMT was detected as a single band at approximately 33 kDa, also in accord with published data (White & Lawson 1997). No clear difference in banding pattern was seen between RIPA buffer and 1% triton-X in PBS-treated homogenate.

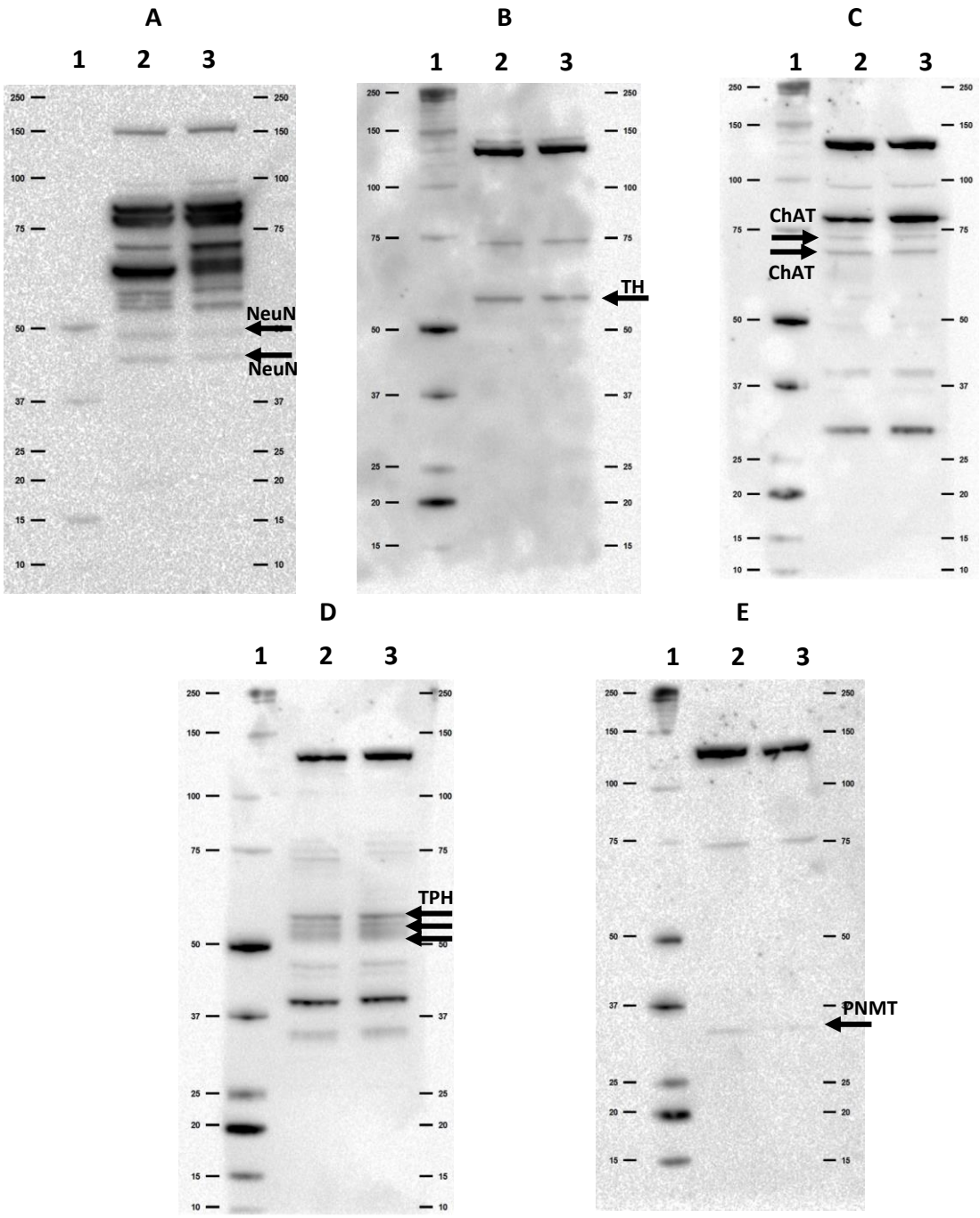

Figure 3.11 Western blots of homogenised mouse brain, prepared in RIPA buffer (lane 2) or 1% Triton X-100 in PBS (lane 3). Primary antibodies were anti-NeuN (1:100, A), TH (1:200, B), ChAT (1:500, C), TPH1 (1:500, D) and PNMT (1:500, E). The Secondary antibody for all cases was goat anti-rabbit IgG (1:2000). Lane 1 comprises a series of Strep-tagged markers of known size (indicated) which were detected via the addition of Strep-Tactin-conjugated HRP. Arrows indicate the identification of the relevant marker.

3.4.4. Discussion

Summary of key findings

- ***The secondary antibody controls revealed a subset of bands that occurred due to non-specific binding***
- ***Each primary antibody was capable of detecting the protein of interest***

The blots shown in figure 3.11 all contained multiple bands. Thus, it was necessary to cross-reference each blot with both the antibody manufacturers' information and available literature in order to determine which bands corresponded to the desired neuronal markers. Furthermore after cross referencing with the goat anti-rabbit IgG secondary antibody control (figure 3.10A), it appeared that the pronounced bands at approximately 140 kDa and 75 kDa appeared as a result of non-specific binding. Bands corresponding to this size in subsequent analyses were, thus, discounted.

Although more defined bands of greater size were seen in figure 3.11A, the double bands slightly below 50 kDa likely corresponded to NeuN (Dredge & Jensen 2011). Similar to the data shown here, Dredge and Jensen reported bands of approximately 66 kDa and between 70-90 kDa using an identical antibody but confirmed, *via* immunoprecipitation and mass spectrometry, that the doublet between 45-50 kDa was NeuN.

The single band seen at ~58 kDa in figure 3.11B matched the manufacturer's data (predicted size 58 kDa) and a previous report for the detection of TH (Presgraves *et*

al. 2004). Thus, this strongly indicated a successful identification of TH in the mouse brain samples. This was also true for ChAT (figure 3.11C), where the predicted target size of 70 kDa matched the two bands seen below the 75 kDa marker. The presence of more than one band can be explained by the presence of multiple splice variants of mouse ChAT (Misawa, Ishii & Deguchi 1992).

The multiple bands seen just above 50 kDa in figure 3.11D correspond to the TPH1 antibody manufacturer's predicted target size of 51 kDa. The additional bands seen at this size appear to be the result of cross-reactivity with the second isoform of tryptophan hydroxylase, TPH2 (Sakowski *et al*. 2006). Interestingly, it appears that TPH2 is the most predominant form of TPH in the brain, with TPH1 being expressed predominantly in the pineal gland which is not routinely considered to be part of the brain due to its localisation external to the blood brain barrier (Walther & Bader 2003). However, the positive detection in the Western blot suggests that the brain tissue obtained contained at least part of the pineal gland, and thus allowed for the detection of TPH1. Finally, the faint bands seen at ~33 kDa in figure 3.11E corresponded to the manufacturer's data and previously reported size for PNMT (White & Lawson 1997). Consequently, homogenised mouse brain provided a robust positive control for all of the phenotype markers under investigation. While no difference was seen between RIPA buffer and 1% Triton X-100 lysed samples, RIPA buffer was considered to be more desirable due to the presence of protease inhibitors minimising the likelihood of protein degradation.

4. Characterisation of S.NNMT.LP cells

4.1. Introduction

NNMT, responsible for the *N*-methylation of nicotinamide to MeN, is expressed at higher concentrations in the CSF of PD-patients (Aoyama *et al*. 2001) and in the brains of patients who had died of PD (Parsons *et al*. 2002, Parsons *et al*. 2003) compared to non-disease controls. In addition, Parsons *et al*. (2002) discovered that the level of expression of NNMT was inversely proportional to disease duration. Thus, it was suggested that NNMT may play a causative role in PD pathogenesis by facilitating the death of SNpc neurons.

There are three principal mechanisms by which NNMT is thought to increase toxicity (covered in detail in chapter 1). Firstly, NNMT may act as a catalyst for the *N*-methylation of βCs, a group of compounds found endogenously in the CNS (Deitrich & Erwin 1980, Susilo & Rommelspacher 1987, Matsubara *et al.* 1993, Matsubara *et al.* 1995, Kuhn *et al.* 1996) and in a variety of foods and tobacco smoke (Herraiz 2004, Crotti *et al.* 2010).

Secondly, increased NNMT activity may lead to an energy deficiency in the cell, as the metabolism of nicotinamide into MeN will reduce the availability of NADH and, thus, potentially reduce the supply of electrons to the ATP-generating electron transport chain (Parsons *et al*. 2002, Parsons *et al*. 2003). However, even though the expression of NNMT in SH-SY5Y cells was shown to decrease pyridine nucleotide (NAD^+ and NADH) concentrations, CxI activity was significantly increased (Parsons *et al*. 2011).

The third mechanism by which NNMT may exert toxicity is *via* increased MeN production. Studies by Fukushima *et al*. suggested that MeN was destructive to the

CxI subunit NDUFS3 (1995) and also significantly reduced rat striatal dopamine content (2002). However, the MeN concentrations in both studies were very high, the lowest being 10 mM, and conflict with the more-recent Parsons *et al.* (2011) study which showed that MeN was in fact neuroprotective at concentrations below 1 mM. Thus, more research is required to clarify the effects of NNMT on cell viability.

In order to determine whether increased NNMT expression is inherently toxic, the effects of NNMT expression upon SH-SY5Y cells, a cell line that does not express the enzyme (Parsons *et al*. 2011), were examined. Prior to the commencement of this study, a cell line (S.NNMT.LP) was generated by the stable transfection of SH-SY5Y human neuroblastoma cells with a plasmid encoding a recombinant human NNMT (pNNMT.V5). Translated protein from this plasmid contained a C-terminally fused V5 tag to allow for easy detection of recombinant protein (NNMT-V5).

In this chapter, recombinant NNMT-V5 expression was confirmed using Western blotting and RT-PCR and the absence of endogenous NNMT expression in SH-SY5Y cells was confirmed using RT-PCR. Subsequently, the effect of NNMT expression upon cellular ATP concentration, mitochondrial membrane potential and oxygen consumption were determined *via* a series of *in vitro* assays comparing SH-SY5Y cells with S.NNMT.LP cells. In addition, to identify whether any of the changes in mitochondrial function are mediated *via* increased MeN production, experiments were also performed in SH-SY5Y cells incubated with 1 mM MeN for 24 hours, a concentration shown in several studies to not be toxic and to have cytoprotective effects in this and other cell-types (Chlopicki *et al*. 2007, Sternak *et al*. 2010,

Parsons *et al*. 2011). Finally, the consequences of NNMT expression upon neuronal lineage and differentiation were investigated *via* Western blotting.

4.2. Methods

4.2.1. Confirmation of NNMT-V5 expression

In order to confirm that SH-SY5Y cells were successfully transfected with the pNNMT.V5 plasmid and that, consequently, recombinant NNMT-V5 protein was being produced by S.NNMT.LP cells, Western blotting and RT-PCR were performed as described in sections 2.2 and 2.3 respectively. Mouse anti-V5 and mouse anti-β-actin (table 4.1), were used for Western blotting, while primers for NNMT and β-actin (table 4.2), were used for RT-PCR. The PCR temperature cycling conditions were as follows: 94°C for 5 minutes followed by 30 cycles of 94°C for 30 seconds, 55°C for 30 seconds, and 72°C for 1 minute. The procedure was concluded with a final extension step at 72°C for 5 minutes.

Table 4.1. Antibodies and their dilutions used for Western blotting. All secondary antibodies used were conjugated to horseradish peroxidase

Protein	Function	Primary antibody	Secondary antibody
β-actin	Loading control	Mouse anti-β-actin (1:1000, Source Bioscience, Nottingham, UK, ABE933)	Goat anti-mouse IgG (1:5000, Sigma-Aldrich, Dorset, UK, A4416)
β-tubulin	Loading control	Mouse anti-β-tubulin (1:200, Abcam, Cambridge, UK, ab7792)	Goat anti-mouse IgG (1:5000, Sigma-Aldrich, Dorset, UK, A4416)
NNMT-V5 (recombinant)	Confirmation of NNMT-V5 expression	Mouse anti-V5 (1:2000, Abcam, Cambridge, UK, ab27671)	Goat anti-mouse IgG (1:5000, Sigma-Aldrich, Dorset, UK, A4416)

Table 4.2. PCR primer sequences and their product sizes. F = forward primer, R = reverse primer

Gene	GenBank accession number	Sequence	Target bases	Product size
β-*actin*	NM_001101.3	F: GGCATCCTCACCCTGAAGTA R: GGGTGTTGAAGGTCTCAAAA	271-473	203 bp
NNMT	NM_006169.2	F: TGGCCCCACTATCTATCAGC R: CCTCTTTCACAGCAGCCTCT	192-692	491 bp

4.2.2. Validation of NNMT-V5 expression over time in S.NNMT.LP cells

NNMT-V5 protein expression was assessed in S.NNMT.LP cells of varying passage numbers to determine whether the expression of NNMT-V5 remained stable with length of time in culture. Western blots were performed with proteins from S.NNMT.LP of passages 10 (twice), 12, 16, 19 and 21 along with SH-SY5Y of passage number 28, with β-tubulin used as loading control. Densitometry of detected bands was performed using Image Lab (Bio–Rad, Hemel Hempstead, UK), and the ratio of NNMT-V5:β-tubulin expression was calculated and expressed as absorbance units.

4.2.3. Determination of cellular ATP concentration in S.NNMT.LP and SH-SY5Y incubated with 1 mM MeN

In light of previous studies which demonstrated an increase in CxI activity in S.NNMT.LP cells (Parsons *et al*. 2011), it was decided to determine whether this translated into a corresponding increase in ATP synthesis. SH-SY5Y and S.NNMT.LP cells were trypsinised, counted and seeded as described in section 2.4.1 at a density of 7,500 cells per well. SH-SY5Y cells were seeded into 8 wells of the plate while S.NNMT.LP cells were seeded into 4 wells.

Following an overnight incubation, the media from 4 SH-SY5Y- and 4 S.NNMT.LP-containing wells was aspirated and replaced with 100 µL of fresh media. The remaining 4 SH-SY5Y-seeded wells were aspirated and replaced with media

supplemented with 1 mM MeN (table 4.3). Two wells containing media only were used as background controls.

Table 4.3. The compositions of solutions used during the determination of the biochemical effects of NNMT.

Compound	Concentration	Method
MeN	1 mM	17.3 mg (Sigma-Aldrich, Dorset, UK) in 1 mL of SH-SY5Y media, syringe-filtered and diluted 1:100 in SH-SY5Y media.
2,4-dinitrophenol (2,4-DNP)	1mM	9 mg (Sigma-Aldrich, Dorset, UK) in 1 mL of DMSO, diluted 1:50 in media to produce the final solution.
Oligomycins A, B, and C	250 µg/mL	2.5 mg (Sigma-Aldrich, Dorset, UK) in 10 mL of DMSO.
Mannitol	0.3 M	54.7 g mannitol (0.3 M,), 0.76 g potassium chloride (10 mM), 0.48 g magnesium chloride (5 mM) and 1.36 g potassium phosphate (10 mM, all Sigma-Aldrich, Dorset, UK) in 900 mL deionised H2O adjusted to pH 7.4 before being made up to 1 L.

Cells were incubated for 24 hours before intracellular ATP content was determined *via* ATP assay (section 2.4.3.2). In addition to the samples, a set of ATP standards (section 2.4.3.2) was also produced and assayed in order to construct a calibration curve which was used to determine the absolute ATP content within cells. Protein content was also measured in all samples as described in section 2.2.2. The protein and ATP content of the wells were then used to calculate ATP concentration, expressed as pmols ATP/mg protein ± SD.

4.2.4. Measurement of oxygen consumption in S.NNMT.LP and SH-SY5Y incubated with 1 mM MeN

4.2.4.1. Culture of cells prior to the measurement of oxygen consumption

In order to determine whether the increase in CxI activity previously reported (Parsons *et al*. 2011), and whether any changes in cellular ATP concentration observed in this study, were due to changes in the rate of oxidative phosphorylation, the rate of cellular O_2 consumption was measured. SH-SY5Y and S.NNMT.LP cells were cultured in 75 cm^2 tissue culture flasks until they reached the log phase of growth (corresponding to 65-70% confluence). Media was aspirated, cells were washed with 5 mL PBS, and 10 mL of appropriate media were added to 1 flask of SH-SY5Y and 1 flask of S.NNMT.LP cells (6 x 10^6 cells). An additional flask of SH-SY5Y cells was were incubated with 10mL of media supplemented with 1 mM MeN. All cells were subsequently incubated at 37^oC and 5% CO_2 for 24 hours.

4.2.4.2. Measurement of oxygen consumption

Oxygen concentration, using a method adapted from Kwok *et al.* (2010), was measured using a Clarke Electrode, with a waterjacket heated to 37^oC and calibrated to 100% O_2 content using cell line-appropriate culture media.

Briefly, after 24 hours incubation, cells were trypsinised and pelleted (section 2.1.2) before being resuspended in 1 mL of a mannitol solution (table 4.3). One hundred µL of the cell suspension was taken as an aliquot in order to measure protein

concentration (section 2.2.2). Eight hundred µL of the remaining cell suspension was added to 200 µL of mannitol buffer, mixed by pipetting and then transferred to the calibrated electrode chamber, after which measurements were taken for 3 minutes using a chart recorder. Twenty µL of oligomycin solution (final concentration 5 µg/mL, table 4.3) was added and oxygen concentration was measured for a further 3 minutes, after which 20 µL of 2,4-DNP solution (final concentration 1 mM, table 4.3) was added and measurements were taken for a final 3 minutes. Once the measurements were completed, the chamber was rinsed 5 times with deionised water before the procedure was repeated for the next cell suspension. Following the experiment and the conclusion of the protein assay, the rate of oxygen consumption was calculated and expressed as percent oxygen consumption/min/mg protein ± SD.

4.2.5. Determination of mitochondrial membrane potential ($\Delta\psi_m$) in S.NNMT.LP and SH-SY5Y incubated with 1 mM MeN

In order to determine whether the previously reported differences in CxI activity, and any differences in ATP production and oxygen consumption observed in this study, had any effect on the membrane potential of the cells' mitochondria, $\Delta\psi_m$ was measured. $\Delta\psi_m$ is used as an indicator of mitochondrial function, with a depolarised $\Delta\psi_m$ indicating a disrupted ATP-producing capacity *via* a reduction in proton motive force (Beltran *et al.* 2000). Accordingly, a high $\Delta\psi_m$ can be indicative of increased ATP production *via* enhanced proton movement across into the mitochondrial intermembrane space (Chen 1988). However, an excessively

hyperpolarised $\Delta\psi_m$ can also lead to the production of ROS (Votyakova & Reynolds 2001). Thus, it is imperative for cells to maintain $\Delta\psi_m$ at its most efficient ATP-producing state.

The cationic dye JC-1 allows measurement of $\Delta\psi_m$ by forming aggregates with intense red fluorescence inside mitochondria with high $\Delta\psi_m$. At lower $\Delta\psi_m$, JC-1 remains in its monomeric form and fluoresces green. Thus the ratio of red:green fluorescence can be used to determine $\Delta\psi_m$.

SH-SY5Y and S.NNMT.LP cells were trypsinised, counted and seeded into the wells of a black, poly-L-Lysine-coated flat bottomed 96-well plate (Greiner Bio-One Ltd, Stonehouse, UK) at a density of 7,500 cells per well. SH-SY5Y cells were seeded into 12 wells per plate and S.NNMT.LP cells were seeded into 4 wells. The 4 additional wells seeded with SH-SY5Y cells were required for the use of a positive control (described below).

Following overnight incubation, 4 of the wells containing SH-SY5Y cells and the S.NNMT.LP cells were given 100 µL of fresh media. Four of the remaining SH-SY5Y-seeded wells were given media supplemented with 1 mM MeN. The final 4 SH-SY5Y-seeded wells were given media containing 1 mM of 2,4-DNP, a mitochondrial uncoupler which depolarises $\Delta\psi_m$, as a positive control. The plate was subsequently incubated for 24 hours, after which staining was performed as per manufacturer's instructions (Cayman Chemical Company, Ann Arbor, MI, USA). Briefly, 10 µL of JC-1 reagent (diluted 1:10 in media appropriate for the cell line) was added to each well. Cells were then incubated for 15 minutes before the plate was centrifuged at 400 x *g* for 5 minutes (Allegra X-22R centrifuge, Beckman Coulter, California, USA). The

media was then aspirated and the cells washed twice with 200 µL of Assay Buffer, with centrifugation each time. One hundred µL of Assay Buffer was added to each well and fluorescence was measured using a Fluostar Optima fluorescence plate reader (BMG Labtech, Offenburg, Germany) with an excitation wavelength of 544 nm and an emission wavelength of 590 nm for the red JC-1 aggregates, and an excitation wavelength of 485 nm and an emission wavelength of 520 nm for the green JC-1 monomers. Two wells containing assay buffer only were used as background fluorescence controls. Fluorescence readings were corrected for background fluorescence and expressed as red:green ratio ± S.D.

4.2.6. Determination of neuronal lineage

In order to investigate whether NNMT expression influences neuronal lineage and neuronal differentiation, Western blots comparing a range of neuronal markers specific for neuronal cell-type plus the post-mitotic marker NeuN, were performed with SH-SY5Y and S.NNMT.LP cells as described in section 2.2. Mouse brain homogenate was used as a positive control for all neuronal lineage and post-mitotic markers. β-tubulin was used as a loading control (table 4.1).

4.2.7. Statistical analysis

Statistical analyses were performed using Prism (Graphpad, CA, USA). Differences between SH-SY5Y, SH-SY5Y supplemented with MeN and S.NNMT.LP cells were analysed using 1-way ANOVA followed by Dunnet or Tukey post-tests. The analysis

of whether NNMT-V5 expression varied with passage number was undertaken using a Spearman's rank correlation of passage number against NNMT-V5 expression normalised to β-tubulin.

4.3. Results

4.3.1. NNMT-V5 was expressed exclusively in S.NNMT.LP cells

Confirmation of NNMT-V5 mRNA and protein expression exclusively in S.NNMT.LP cells was demonstrated using RT-PCR (figure 4.1) and Western blot (figure 4.2).

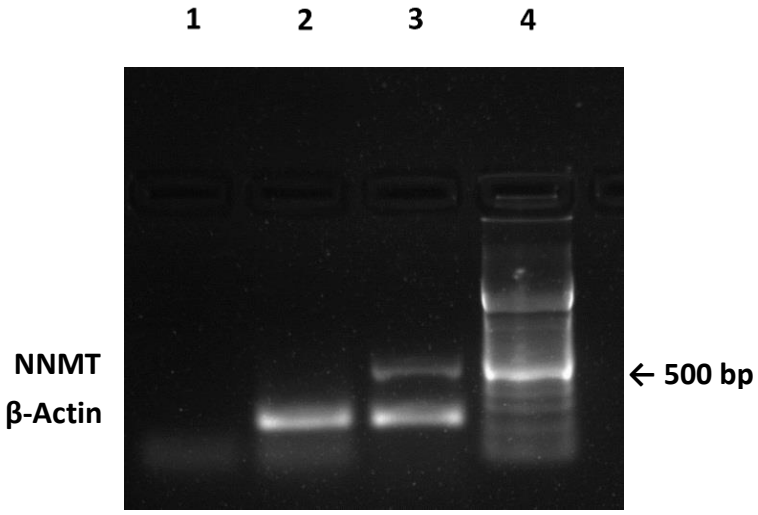

Figure 4.1. RT-PCR detection of NNMT-V5 expression in SH-SY5Y and S.NNMT.LP cell lines. Samples used were RT blank (1), SH-SY5Y cDNA (2), and S.NNMT.LP cDNA (3), 100 base pair ladder (4). NNMT and actin labels correspond to the appropriate band sizes for their respective PCR products. The 500 bp label points to the band in the ladder lane with base pair size of 500.

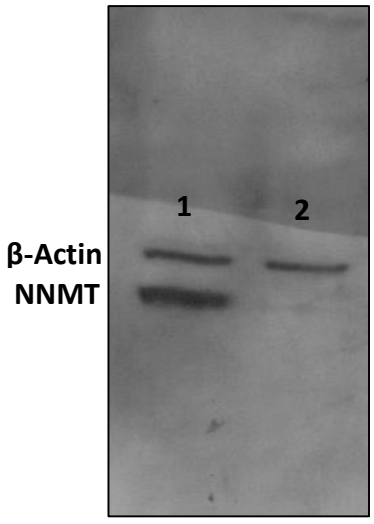

Figure 4.2. Western blot detection of NNMT-V5 and β-actin expression in S.NNMT cells (1) and SH-SY5Y cells (2).

NNMT mRNA was detected as a single ~490 bp PCR product in S.NNMT.LP cells only, with β-actin detected as a single ~200 bp PCR product in both S.NNMT.LP and SH-SY5Y, demonstrating the expression of recombinant NNMT mRNA in S.NNMT.LP only. Furthermore, the lack of NNMT mRNA in SH-SY5Y cells demonstrated the lack of endogenous expression of NNMT in SH-SY5Y cells, as the assay was designed to detect both endogenous and plasmid-derived NNMT mRNA.

NNMT-V5 protein was detected as a ~30 kDa band in S.NNMT.LP cells only, with β-actin detected as ~40 kDa band in both S.NNMT.LP and SH-SY5Y, demonstrating the expression of recombinant NNMT-V5 protein in S.NNMT.LP only.

4.3.2. NNMT-V5 expression did not vary with passage number

Having demonstrated that NNMT-V5 was expressed solely in S.NNMT.LP, it was decided to determine whether NNMT-V5 expression varied with increasing passage number. Although NNMT-V5 expression showed minor variations between samples of differing passage numbers (figure 4.3), a Spearman's rank correlation analysis demonstrated that there was no correlation between NNMT-V5 expression and passage number ($r = -0.1$, $p = 0.95$, figure 4.4).

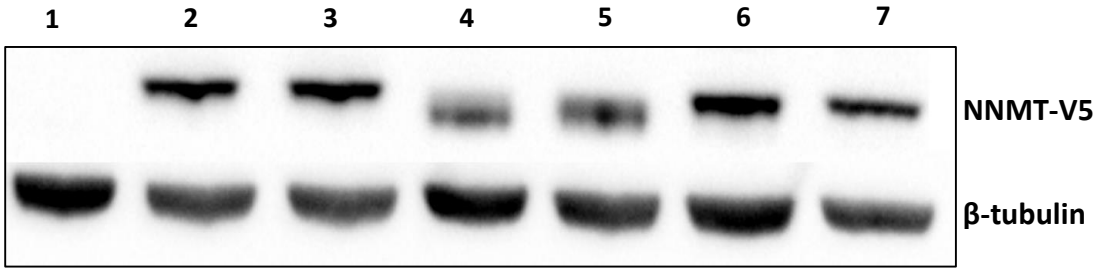

Figure 4.3. Western blots of recombinant NNMT expression (via anti-V5 antibody, top) and β-tubulin (bottom) in SH-SY5Y cells (1, control) and S.NNMT.LP cells of passage 10A (2), passage 10B (3), passage 12 (4), passage 16 (5), passage 19 (6) and passage 21 (7).

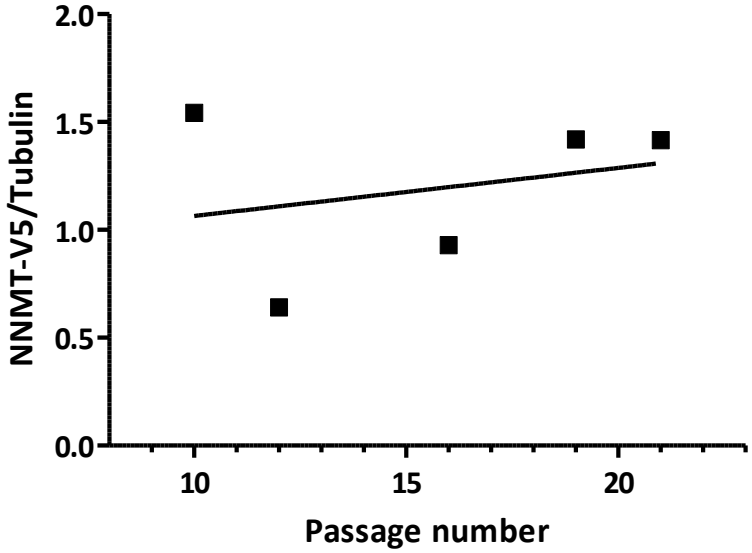

Figure 4.4. NNMT-V5 protein expression as a function of passage number in S.NNMT.LP cells. The relationship between passage number and NNMT-V5 expression was analysed using a Spearman's rank correlation. No correlation was found between the two variables (r = -0.1, P = 0.95). The line represents a line of best fit with a r^2 of 0.07.

4.3.3. ATP concentration was significantly elevated in S.NNMT.LP cells and SH-SY5Y cells treated with 1 mM MeN compared to untreated SH-SY5Y

As shown in figure 4.5, S.NNMT.LP cells and SH-SY5Y cells supplemented with 1 mM MeN contained a significantly higher (311.56 ± 53.19 pmols/mg protein and 310.95 ± 58.12 pmols/mg protein respectively; both $p < 0.01$, n = 4) concentration of ATP compared to untreated SH-SY5Y cells (150.81 ± 12.02 pmols/mg protein, n = 4).

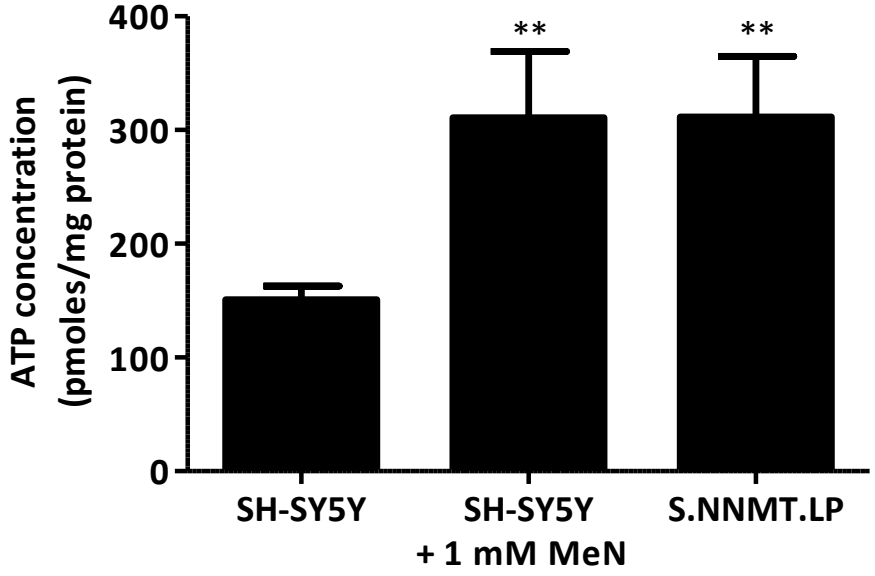

Figure 4.5. ATP concentrations within SH-SY5Y cells, SH-SY5Y cells supplemented with 1 mM MeN and S.NNMT.LP cells. All data are mean ± SD. ** p < 0.01 vs SH-SY5Y. Statistical analysis was performed using a 1-way ANOVA followed by a Dunnet post-test, n = 4.

4.3.4. Oxygen consumption was significantly elevated in S.NNMT.LP cells and SH-SY5Y cells treated with 1 mM MeN

Oxygen consumption was significantly increased in both 1 mM MeN-supplemented SH-SY5Y cells (4.49 ± 0.45 % O_2/min/mg protein, $p < 0.05$, n = 4) and in S.NNMT.LP cells (4.97 ± 0.50 % O_2/min/mg protein, $p < 0.01$, n = 4) compared with untreated SH-SY5Y cells (3.00 ± 0.25 % O_2/min/mg protein, n = 4, figure 4.6). Oxygen consumption decreased upon addition of oligomycin, and increased upon addition of 2,4-DNP (figure 4.7), in accord with their effects upon the mitochondrial respiratory chain.

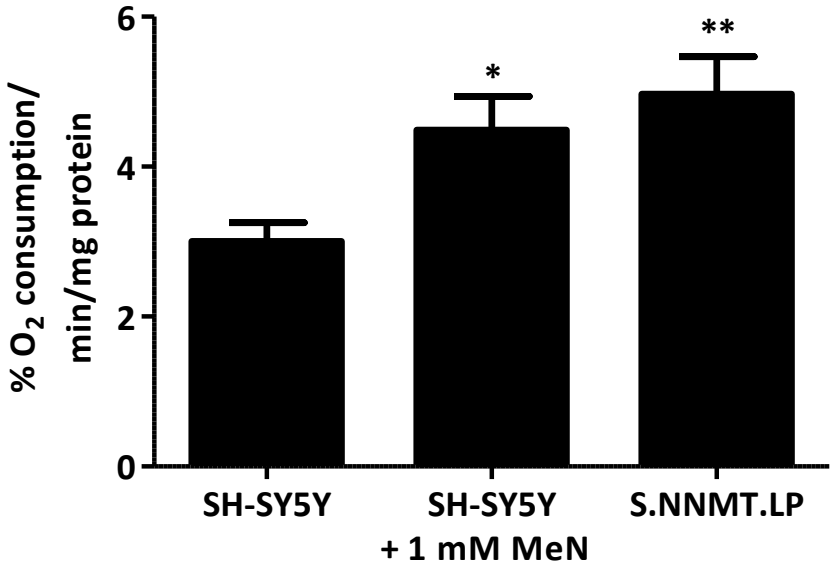

Figure 4.6. The oxygen consumption of SH-SY5Y cells, SH-SY5Y cells incubated with 1 mM MeN, and S.NNMT.LP cells. All data are mean ± SD. * p < 0.05, ** p < 0.01 vs SH-SY5Y. Statistical analysis was performed using a 1-way ANOVA followed by a Dunnet post-test, n = 4.

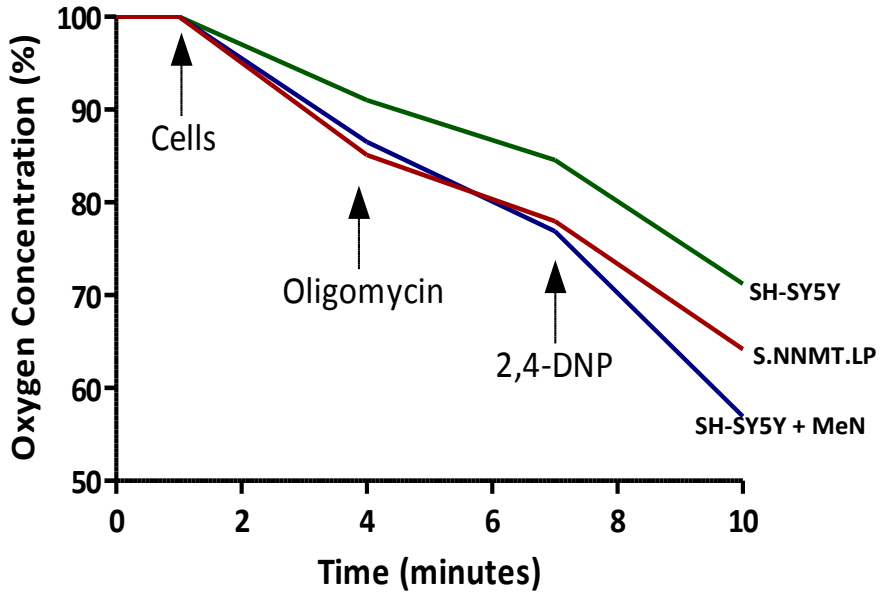

Figure 4.7. Typical trace of the oxygen consumption over time of SH-SY5Y cells (green), SH-SY5Y cells supplemented with 1 mM MeN (blue) and S.NNMT.LP cells (red).

4.3.5. $\Delta\psi_m$ was not significantly different in SH-SY5Y cells treated with 1 mM MeN and S.NNMT.LP cells compared to untreated SH-SY5Y

$\Delta\psi_m$ was not significantly different in either 1 mM MeN-supplemented SH-SY5Y cells or in S.NNMT.LP cells, compared to untreated SH-SY5Y (Figure 4.8, n = 3). $\Delta\psi_m$ was significantly decreased in SH-SY5Y cells in the presence of 2,4-DNP (63.46 ± 3.26 *vs* 31.66 ± 5.61, $p < 0.01$, n = 3), thus confirming that the assay had successfully measured cellular $\Delta\psi_m$.

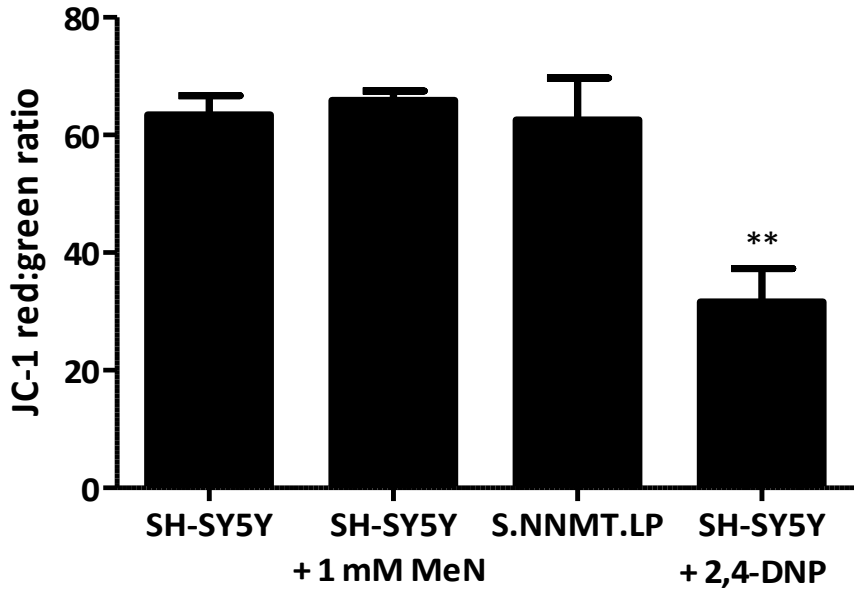

Figure 4.8. The mitochondrial membrane potential, as determined by JC-1 staining, in SH-SY5Y cells, SH-SY5Y cells supplemented with 1 mM MeN and S.NNMT.LP cells. SH-SY5Y cells exposed to 2,4-DNP were used as a control. All data are mean ± SEM. ** p < 0.01 vs SH-SY5Y. Statistical analysis was performed using a 1-way ANOVA followed by a Dunnet post-test, n = 3

4.3.6. NNMT-V5 expression did not induce a change in neuronal lineage in SH-SY5Y cells

Both SH-SY5Y and S.NNMT.LP samples were positive for the neuronal markers of acetylcholine (ChAT) and serotonin (TPH, figure 4.9). ChAT was detected in both cell lines as a protein of approximately 70 kDa while the 2 bands seen at approximately 50 kDa corresponded to the presence of both TPH isoforms. The larger band of the 45-50 kDa NeuN doublet was observed in SH-SY5Y and S.NNMT.LP cells. No gross change was seen in the expression of neuronal markers between SH-SY5Y and S.NNMT.LP cells. TH and PNMT were not detected in either SH-SY5Y or S.NNMT.LP cells.

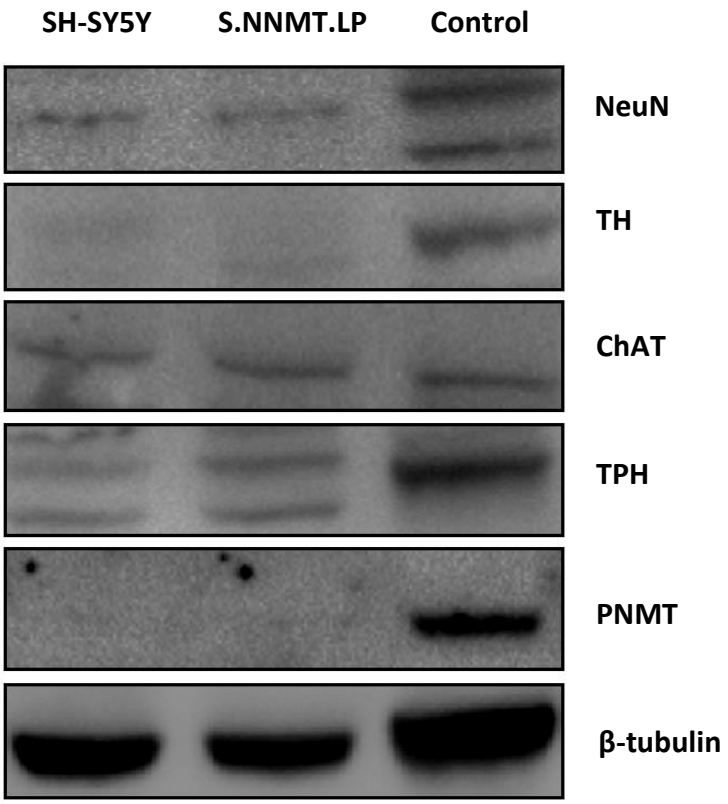

Figure 4.9. Western blots for various neuronal markers using protein samples derived from SH-SY5Y cells and S.NNMT.LP cells. Control samples comprised mouse brain.

4.4. Discussion

Summary of key findings

- ***NNMT-V5 expression was confirmed in S.NNMT.LP cells and did not vary with increasing passage number***
- ***ATP concentration and oxygen consumption were significantly higher in S.NNMT.LP cells and SH-SY5Y cells supplemented with 1 mM MeN, compared with SH-SY5Y cells alone***
- ***Both SH-SY5Y and S.NNMT.LP cells expressed markers for acetylcholinergic, serotonergic phenotypes and the post-mitotic marker NeuN but markers for dopamine and adrenaline were not detected***
- ***There was no change in the relative expressions of the markers between cell lines***

4.4.1. Confirmation and validation of NNMT-V5 expression

The presence of NNMT mRNA and NNMT-V5 protein in S.NNMT.LP cells but not in SH-SY5Y cells demonstrated that the S.NNMT.LP cell line expressed NNMT-V5. Furthermore, the differences in NNMT expression provide a more effective knock-in (S.NNMT.LP) and knock-out (SH-SY5Y) model than would be possible using siRNA silencing, which is considered successful when gene expression is reduced by 70% (Hood 2004). This allowed an effective study of the effects of NNMT expression to be conducted. Furthermore, the level of NNMT activity shown in S.NNMT.LP cells was similar to that observed in the cerebellum of PD patients (Parsons *et al*. 2002,

Parsons *et al*. 2011). Thus, the S.NNMT.LP cell line represents a disease-relevant model of NNMT expression.

While NNMT-V5 expression did not appear to vary with passage number, expression was lower in 2 samples (P12 and P16). This appeared to be related to the length of time between the thawing of liquid nitrogen-stored cells and the centrifugation and snap-freezing of cell pellets. The P12 and P16 samples were derived from cells which had been rejuvenated but had not undergone a subsequent passage, and as such were only a week or so in culture following their removal from storage. In contrast, other samples were obtained from cells which had been in culture for a number of passages. Accordingly, the 2 samples with the lowest NNMT-V5 expression were derived from cells which had spent the shortest amount of time in culture following thawing. Thus, it appears that it may take over a week for cellular NNMT expression to reach its peak after rejuvenation of cells from liquid nitrogen storage.

There is currently no study in the literature investigating this phenomenon, and although it is considered good scientific practice to allow cells to undergo at least one passage prior to experimental use, this is the first, to the author's knowledge, experimental demonstration of this phenomenon. Consequently, any further experiments conducted with S.NNMT.LP cells were performed only with cells that had spent over a week in culture and had undergone at least one passage.

4.4.2. NNMT-V5-expression significantly enhanced cell viability, an effect mediated by MeN

In order to assess the biochemical effects of NNMT-V5 expression, ATP production, oxygen consumption and $\Delta\psi_m$ were measured and compared in SH-SY5Y and S.NNMT.LP cells. ATP production was higher in S.NNMT.LP cells and SH-SY5Y cells incubated with 1mM MeN. The oxygen consumption of S.NNMT.LP cells and 1mM MeN-supplemented SH-SY5Y cells was also significantly increased and was likely elevated as a result of increased mitochondrial respiration as evidenced by the effect of oligomycin and 2,4-DNP controls. Oligomycin inhibits the synthesis of ATP at complex V and, thus, reduces the cellular requirement to consume oxygen (Kwok *et al*. 2010). Accordingly, the addition of oligomycin reduced the rate of oxygen consumption measured in the trace. On the other hand, 2,4-DNP, as a mitochondrial uncoupler, greatly enhances mitochondrial oxygen consumption as the cell must compensate for the loss in $\Delta\psi_m$. It does so by increasing electron transport through complexes I-V a process which requires higher rates of oxygen consumption, which was replicated in the traces obtained. Thus, the data confirm that the oxygen consumption seen in the experiment was occurring due to mitochondrial respiration. As such, these results demonstrate that the increase in ATP production observed arose from an increase in mitochondrial respiratory chain activity.

The increased ATP concentration and oxygen consumption in S.NNMT.LP cells and 1mM MeN-supplemented SH-SY5Y cells was unexpected, considering the hypothesis that the presence of NNMT would lead to a lowering of the cellular ATP

supply *via* the removal of NADH from the cell. Instead, whilst NNMT-V5 expression has indeed been shown to reduce the synthesis of NADH in SH-SY5Y cells (Parsons *et al*. 2011), it is clear that this decrease in NADH was not detrimental to the function of the mitochondria in terms of ATP and oxygen consumption.

The combination of an increased CxI activity, oxygen consumption and the resulting ATP synthesis are potentially indicative of an increased proton motive force and were, thus, expected to manifest as an increase in $\Delta\psi_m$. However, this was surprisingly not the case. The lack of change in $\Delta\psi_m$, despite the aforementioned increases, may be attributable to an elevated expression of mitochondrial uncoupling proteins (UCPs). The uncoupling process mediated by UCPs allows protons to pass down their electrochemical gradient without entering ATP synthase. This results in a lowering of $\Delta\psi_m$ but also limits the generation of ROS which readily occurs at high $\Delta\psi_m$ (Votyakova & Reynolds 2001). UCPs in the CNS are thought to counteract neuronal ROS production that occurs concomitantly with ATP synthesis (Andrews, Diano & Horvath 2005). In addition, overexpression of UCP5 in SH-SY5Y cells was shown to be protective upon MPP^+ exposure *via* a reduction in ROS and maintenance of ATP levels (Ho *et al.* 2006, Kwok *et al.* 2010). Thus, it is speculated that the lack of altered $\Delta\psi_m$ may have arisen due to an induction of one or more UCPs in order to counteract the elevated ROS production that may occur as a consequence of enhanced ATP synthesis. Further studies are needed to confirm this hypothesis.

In addition to these data, other studies using this knock-in/knock-out model have shown that S.NNMT.LP cells were significantly protected against the toxicity of a

variety of mitotoxins such as MPP+, rotenone, 2,4-DNP and 6-hydroxydopamine in comparison to SH-SY5Y cells, again mediated *via* an increase in MeN production (Parsons *et al.* 2011, Milani, Ramsden & Parsons 2013). These findings are supported by numerous other studies which have shown that increased NNMT expression, and MeN production, is cytoprotective in other cells (Cuomo *et al.* 1994, Kim *et al.* 2010, Sternak *et al.* 2010, Ulanovskaya, Zuhl & Cravatt 2013, Zhang *et al.* 2014).

Taken together, these data suggest that the expression of recombinant NNMT-V5 increases the viability of SH-SY5Y cells, an effect mediated by increased MeN production. Thus, the hypotheses that NNMT causes toxicity *via* NADH depletion or the increased production of toxic MeN were rejected. Instead, these data and data published in other studies (Cuomo *et al.* 1994, Kim *et al.* 2010, Parsons *et al.* 2011, Milani, Ramsden & Parsons 2013, Ulanovskaya, Zuhl & Cravatt 2013) support the hypothesis that the induction of NNMT expression is, in fact, a cytoprotective response towards cells. In light of the discovery that NNMT is upregulated in PD (Aoyama *et al*. 2001, Parsons *et al*. 2002, Parsons *et al*. 2003), this may be, therefore, occurring as a neuroprotective response to the underlying pathogenic process rather than contributing towards disease pathogenesis.

4.4.3. The consequence of NNMT-V5 expression on neuronal lineage

NNMT expression did not appear to alter the neuronal lineage of SH-SY5Y cells. It also did not appear to alter the expression of NeuN and, thus, does not appear to

play a role in the neuronal differentiation of SH-SY5Y cells. Interestingly, neither SH-SY5Y cells nor S.NNMT.LP cells appeared to express TH. While some groups report that SH-SY5Y cells do in fact express TH, whether undifferentiated (Constantinescu *et al.* 2007, Korecka *et al.* 2013) or following a differentiation protocol (Lopes *et al.* 2010), a number of personal disclosures from colleagues report a lack of TH expression in SH-SY5Y cells. The reason for these divergent opinions may be the geographical origin of particular batches of SH-SY5Y cells, or selection pressures from divergent protocols for culturing SH-SY5Y cells.

While the lack of TH expression in our cells will not correspond to ideal physiological relevance for PD, the production of this knock-in/knock-out model for NNMT expression allows the effective study of the biochemical consequences of NNMT. As such, subsequent investigations need to be undertaken in animal models, both transgenic and non-transgenic, to investigate the relevance of NNMT within an intact CNS.

While NNMT-V5 expression did not appear to alter neuronal phenotype or differentiation state, a paper published using data from this study (Thomas *et al*. 2013) reported that NNMT expression resulted in the induction of EFNB2 and AKt cell signalling pathways, leading to increased neurite and synapse formation. Coupled with increased ATP synthesis, which will be required for the maintenance of axonal transport down these nascent neurites, this suggests a role for NNMT in neuronal function rather than phenotypic differentiation.

4.4.4. Summary

In conclusion, NNMT-V5 expression increased the ATP content of SH-SY5Y cells, a process mediated by increased MeN production. These data, and supporting data from other studies, suggest that NNMT may play a protective role in PD. However, while NNMT expression may have been protective in and of itself, the possibility of interaction with the proposed protoxic β-carbolines cannot be ruled out. The potential for NNMT to interact with these compounds will be discussed in subsequent chapters.

5. The toxicity of βCs and 4PP in SH-SY5Y and S.NNMT.LP cells

5.1. Introduction

The previous chapter discussed how inducing NNMT expression in SH-SY5Y cells enhanced their viability and protected them from toxic insult. While this appears to suggest that NNMT expression may be beneficial to cell survivability, there is presently no data investigating NNMT's potential bioactivation of βCs, which are also increased in PD (Kuhn *et al*. 1996).

βCs, as discussed in chapter 1, are an endogenous group of compounds produced in the brain following the metabolism of tryptamine *via* the Pictet-Spengler reaction (Susilo *et al.* 1987, Susilo & Rommelspacher 1987, Stöckigt *et al.* 2011). They are also present in various foods such as cooked meat and fish and are a constituent of tobacco smoke. In both cases they are produced following the pyrolysis of tryptophan and its condensation with aldehydes (Herraiz 2004). They, particularly NH, are of particular interest in PD because of their structural similarity to MPP^+ (section 1.3.5.1, figure 1.9). In fact, *N*-methylation of βCs to form toxic β-carbolinium ions has been demonstrated in human brain homogenate (Matsubara, Collins & Neafsey 1992, Matsubara, Neafsey & Collins 1992, Gearhart *et al.* 2000) and this *N*-methylation appears to more readily occur in PD patients (Matsubara *et al*. 1995). However, the identity of an enzymatic catalyst for the reaction at either the 2*N* or 9*N* position is still unknown. Thus, it was hypothesised that, given NNMT's elevation in PD (Parsons *et al*. 2002, Parsons *et al*. 2003) and its ability to *N*-methylate pyridine groups (Alston and Abeles 1988), NNMT may be a catalyst for this reaction. Even if this were not the case, the simultaneously increased presence of both NNMT and the βCs in PD warranted investigating. Indeed, the induction of

NNMT expression in PD may cause cells to interact differently with βCs, independently of whether or not NNMT can catalyse βC-*N*-methylation. For example, if the protective effects of NNMT expression seen in chapter 4 persist following βC exposure, this would add additional support to the theory that NNMT is protective in PD. Accordingly, the susceptibility of the NNMT-expressing S.NNMT.LP cells to 2 βCs (NH and THNH) was compared with that of the non-NNMT-expressing SH-SY5Y cells *via* the MTT and ATP toxicity assays.

In addition to βCs, another compound of interest is 4PP. Although apparently lacking in PD-specific toxicity itself (Irwin, Langston & DeLanney 1987, Perry *et al.* 1987), 4PP is the closest non-methylated analogue to MPP^+ (figure 5.1).

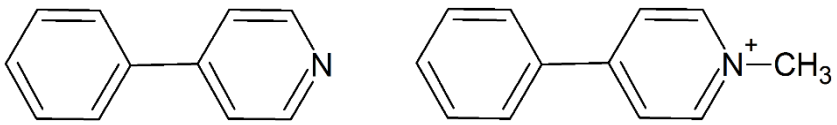

Figure 5.1. The structural similarity between 4PP (left) and the MPP^+ (right)

Unlike the βCs, 4PP is not produced endogenously. However it has been identified as a constituent of oranges (Thomas & Bassols 1992), mint (Snyder & D'Amato 1985) and also cigarette smoke (Heckman & Best 1981) and should readily cross the blood brain barrier due to its small size and hydrophobic nature (predicted logP = 2.59 ± 0.24 http://www.chemspider.com/Chemical-Structure.13062.html). Once inside the brain, 4PP may act as an extremely potent pro-toxin in patients with elevated levels of *N*-methylation activity, for example *via* the increased expression of NNMT. Thus, in addition to investigating S.NNMT.LP and SH-SY5Y cells for their susceptibility to βCs, they were also investigated for their susceptibility to 4PP.

5.2. Methods

5.2.1. MTT assay of SH-SY5Y cells and S.NNMT.LP cells incubated with NH, THNH and 4PP

SH-SY5Y and S.NNMT.LP cells were prepared for MTT assays as described in section 2.4.1. Cells were seeded at a density of 15,000 cells/well, following the plate layout described in figure 2.3.

Solutions of NH, THNH and 4PP were made according to section 2.4.2, table 2.3. The dosing procedure (also in section 2.4.2) was followed, resulting in both cell lines being exposed to 8 different concentrations:

- NH: 800 µM, 400 µM, 200 µM, 100 µM, 50 µM, 25 µM, 12.5 µM, 6.25 µM
- THNH: 1600 µM, 800 µM, 400 µM, 200 µM, 100 µM, 50 µM, 25 µM, 12.5 µM
- 4PP 1600 µM, 800 µM, 400 µM, 200 µM, 100 µM, 50 µM, 25 µM, 12.5 µM

All plates were then placed into the incubator for 48 hours before the dosing process was repeated again and the plates were incubated for a further 72 hours, making a total of 120 hours incubation.

Toxicity, *via* MTT assay, was assessed using the method described in section 2.4.3.1.

5.2.2. ATP assay of SH-SY5Y cells and S.NNMT.LP cells incubated with NH, THNH and 4PP

SH-SY5Y and S.NNMT.LP cells were prepared for ATP assay as described in section 2.4.1. Cells were seeded and incubated with NH, THNH and 4PP as described in Section 5.2.1.

Toxicity, *via* ATP assay, was assessed using the method described in section 2.4.3.2.

5.2.3. Statistical analysis

Data were analysed as described in section 2.4.4.

5.3. Results

5.3.1. No difference in cell viability between SH-SY5Y and S.NNMT.LP cells in response to NH, THNH and 4PP

Dose-response curves of the MTT assays, derived from the mean data of each experimental repeat (n = 5), are shown in figure 5.2. The dose-response curves for each experiment, which were used to generate 1 $EC50_{MTT}$ and 1 set of mean data per cell line, are shown in Appendix 1.

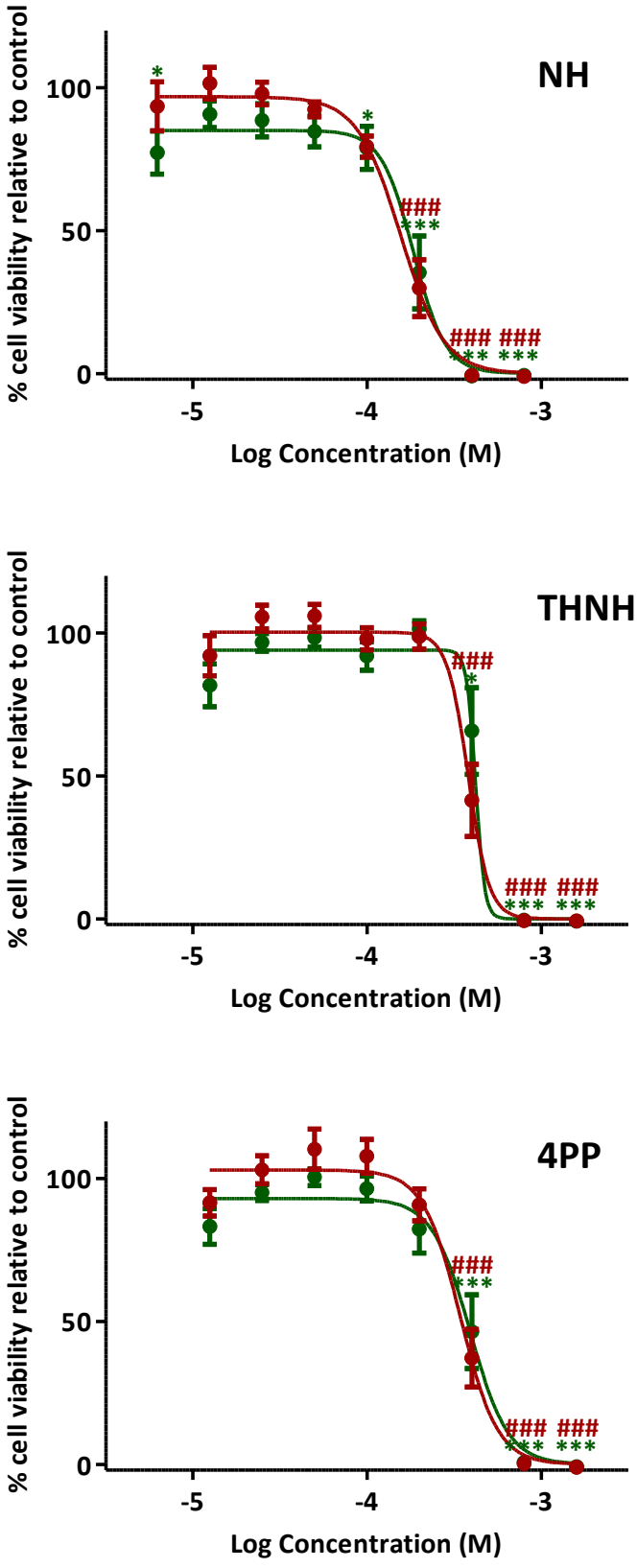

Figure 5.2. Dose response curves of NH, THNH and 4PP following their incubation with SH-SY5Y cells (green circles) and S.NNMT.LP cells (red circles) for 5 days. Cell viability was determined via MTT assay. All data are mean ± SEM, n = 5. * = p < 0.05 vs untreated SH-SY5Y, *** = p < 0.001 vs untreated SH-SY5Y, ### = p < 0.001 vs untreated S.NNMT.LP.

5.3.1.1. NH

NH was toxic to SH-SY5Y cells at concentrations of 100 µM ($p < 0.05$) and 200 µM, 400 µM and 800 µM (all $p < 0.001$). NH also caused significant toxicity to SH-SY5Y cells at the lowest dose, 6.25 µM ($p < 0.05$). In S.NNMT.LP cells, NH was toxic at concentrations of 200 µM, 400 µM and 800 µM (all $p < 0.001$). No significant difference in toxicity was seen between cell lines at any individual dose. The log $EC50_{MTT}$s (in M) for SH-SY5Y and S.NNMT.LP cells exposed to NH were -3.79 ± 0.06 (equivalent to 162 µM) and -3.81 ± 0.05 (equivalent to 155 µM) respectively. The difference between the 2 log $EC50_{MTT}$s was not significant ($p = 0.78$).

5.3.1.2. THNH

THNH was toxic to SH-SY5Y cells at concentrations of 400 µM ($p < 0.05$), 800 µM and 1600 µM (both $p < 0.001$). In S.NNMT.LP cells, THNH was also toxic at concentrations of 400 µM, 800 µM and 1600 µM (all $p < 0.001$). No significant difference in toxicity was seen between cell lines at any individual dose. The log $EC50_{MTT}$s (in M) for SH-SY5Y and S.NNMT.LP cells exposed to THNH were -3.37 ± 0.02 (equivalent to 427 µM) and -3.44 ± 0.04 (equivalent to 363 µM) respectively. The difference between the two log $EC50_{MTT}$s was not significant ($p = 0.19$).

5.3.1.3. 4PP

4PP was toxic to SH-SY5Y cells at concentrations of 400 µM, 800 µM and 1600 µM (all $p < 0.001$). In S.NNMT.LP cells, 4PP was also toxic at concentrations of 400 µM,

800 µM and 1600 µM (all $p < 0.001$). No significant difference in toxicity was seen between cell lines at any individual dose. The log $EC50_{MTT}$s (in M) for SH-SY5Y and S.NNMT.LP cells exposed to 4PP were -3.47 ± 0.04 (equivalent to 339 µM) and -3.48 ± 0.03 (equivalent to 331 µM) respectively. The difference between the two log $EC50_{MTT}$s was not significant ($p = 0.85$).

5.3.1.4. Order of compound toxicity – MTT

Overall, NH was most toxic to both cell lines, followed by 4PP and THNH as illustrated by the $EC50_{MTT}$s (-3.79 ± 0.06 (162 µM), -3.47 ± 0.04 (339 µM) and -3.37 ± 0.02 (427 µM) respectively for SH-SY5Y and -3.81 ± 0.05 (155 µM), -3.48 ± 0.03 (331 µM) and -3.44 ± 0.04 (363 µM) respectively for S.NNMT.LP) and figure 5.3, which shows the comparative toxicity profiles of all 3 compounds within each cell line. NH log $EC50_{MTT}$ was significantly lower than both THNH and 4PP in both cell lines ($p < 0.001$ for all). No statistical difference was seen between 4PP and THNH $EC50_{MTT}$s.

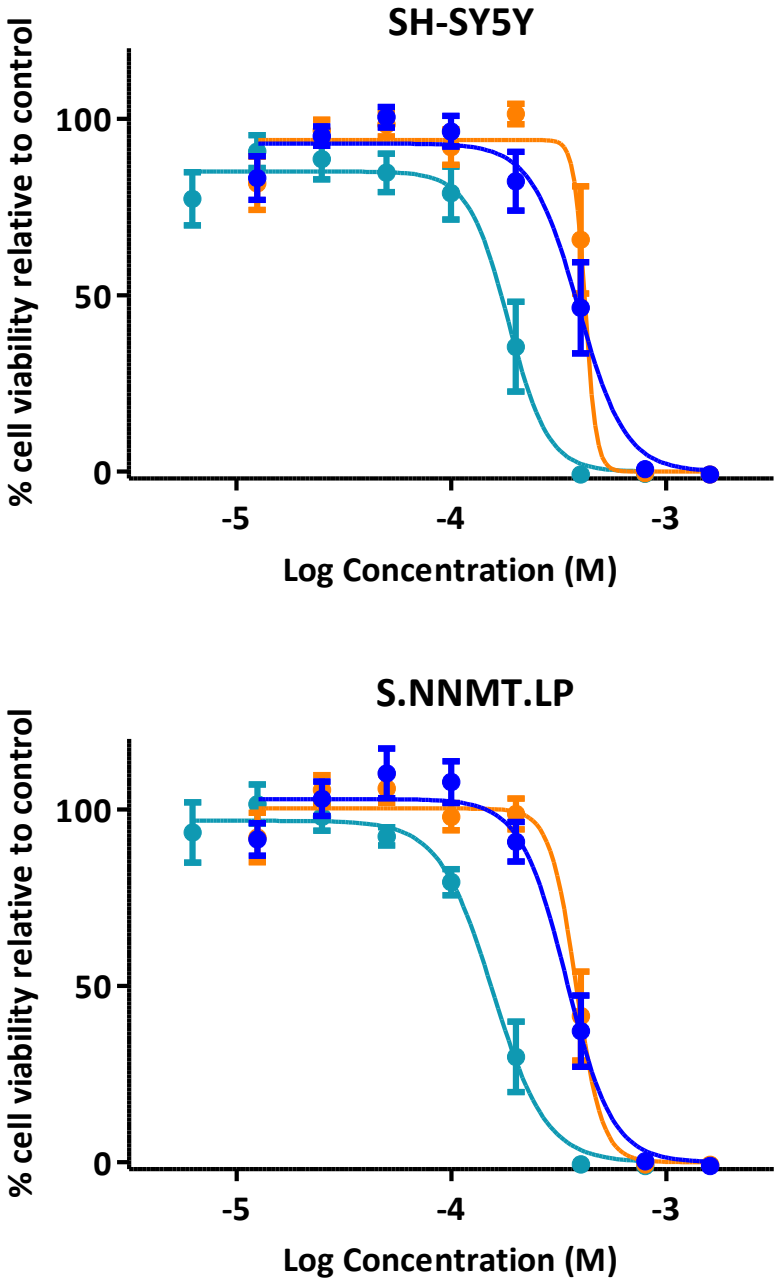

Figure 5.3. Comparative toxicity curves of NH (turquoise), 4PP (blue) and THNH (orange) in SH-SY5Y cells (top) and S.NNMT.LP cells (bottom) following a 5-day incubation. Cell viability was determined via MTT assay. All data are mean ± SEM, n = 5.

5.3.2. S.NNMT.LP cells showed significantly greater decrease in ATP content and $EC50_{ATP}$ than SH-SY5Y cells in response to NH only

Dose-response curves of the ATP assays, derived from the mean data of each experimental repeat (n = 5), are shown in figure 5.4. The dose-response curves for each experiment, which were used to generate 1 $EC50_{ATP}$ and 1 set of mean data per cell line, are shown in Appendix 1.

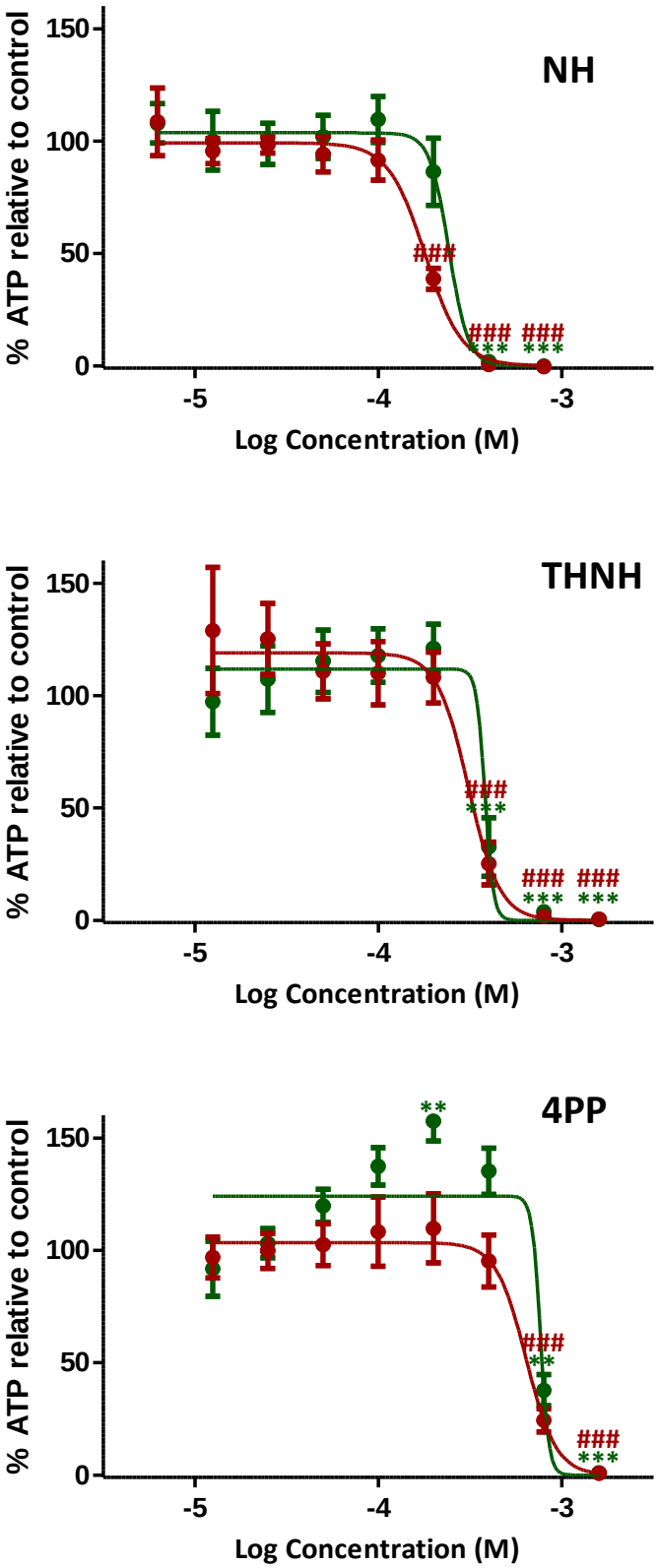

*Figure 5.4. Dose response curves of NH, THNH and 4PP following their incubation with SH-SY5Y cells (green circles) and S.NNMT.LP cells (red circles) for 5 days. Cell viability was determined via ATP assay. All data are mean ± SEM, n = 5. * = p < 0.05 vs untreated SH-SY5Y, ** = p < 0.01 vs untreated SH-SY5Y, *** = p < 0.001 vs untreated SH-SY5Y, ### = p < 0.001 vs untreated S.NNMT.LP.*

5.3.2.1. NH

NH was toxic to SH-SY5Y cells at concentrations of 400 µM and 800 µM (both $p <$ 0.001). In S.NNMT.LP cells, NH was toxic at concentrations of 200 µM, 400 µM and 800 µM (all $p < 0.001$). ATP content was significantly lower in S.NNMT.LP cells compared to SH-SY5Y at 200 µM (-3.7 on the log scale, $p <0.01$) only. The log $EC50_{ATP}$s (in M) for SH-SY5Y and S.NNMT.LP cells exposed to NH were -3.58 ± 0.05 (equivalent to 263 µM) and -3.76 ± 0.04 (equivalent to 174 µM) respectively. The difference between the 2 log $EC50_{ATP}$s was statistically significant ($p = 0.02$).

5.3.2.2. THNH

THNH was toxic to SH-SY5Y cells at concentrations of 400 µM, 800 µM and 1600 µM (all $p < 0.001$). In S.NNMT.LP cells, THNH was also toxic at concentrations of 400 µM, 800 µM and 1600 µM (all $p < 0.001$). No significant difference in toxicity was seen between cell lines at any individual dose. The log $EC50_{ATP}$s (in M) for SH-SY5Y and S.NNMT.LP cells exposed to THNH were -3.36 ± 0.06 (equivalent to 437 µM) and -3.46 ± 0.03 (equivalent to 348 µM) respectively. The difference between the two log $EC50_{ATP}$s was not significant ($p = 0.21$).

5.3.2.3. 4PP

4PP was toxic to SH-SY5Y cells at concentrations of 800 µM ($p < 0.01$) and 1600 µM ($p < 0.001$). In SH-SY5Y cells, 4PP also caused a significant increase in ATP content at 200 µM ($p < 0.01$). In S.NNMT.LP cells, 4PP was also toxic at concentrations of 800

µM and 1600 µM (both $p < 0.001$). 4PP did not increase ATP content in S.NNMT.LP cells. Significant differences in toxicity were seen between cell lines at 200 µM (-3.7 on the log scale, $p < 0.01$) and 400 µM (-3.4 on the log scale, $p < 0.05$). The log $EC50_{ATP}$s (in M) for SH-SY5Y and S.NNMT.LP cells exposed to 4PP were -3.13 ± 0.02 (equivalent to 741 µM) and -3.20 ± 0.04 (equivalent to 631 µM) respectively. The difference between the two log $EC50_{ATP}$s was not significant ($p = 0.12$). It should be noted that, due to the increased ATP content above untreated cells seen at low concentrations of 4PP, the calculated error of the $EC50_{ATP}$ in SH-SY5Y cells is likely to have been underestimated. This is due to a reduced fit of the data to the top of a traditional sigmoid curve.

5.3.1.4. Order of compound toxicity – ATP

In accordance with the data from the MTT assays, NH was most toxic to both cell lines. However, contrary to what was seen in the MTT assays, the second most-toxic compound was THNH followed by 4PP as illustrated by the $EC50_{ATP}$s (-3.58 ± 0.05 (263 µM), -3.36 ± 0.06 (437 µM) and -3.13 ± 0.02 (741 µM) respectively for SH-SY5Y and -3.76 ± 0.04 (174 µM), -3.46 ± 0.03 (348 µM) and -3.20 ± 0.04 (631 µM) respectively for S.NNMT.LP) and in figure 5.5, which shows the comparative toxicity profiles of all 3 compounds within each cell line. NH log $EC50_{ATP}$ was significantly lower than both THNH and 4PP in both cell lines ($p < 0.05$ *vs* THNH and $p < 0.001$ *vs* 4PP in SH-SY5Y, $p < 0.001$ for both in S.NNMT.LP). THNH $EC50_{ATP}$ was significantly lower than 4PP in both cell lines ($p < 0.05$ in SH-SY5Y, $p < 0.001$ in S.NNMT.LP).

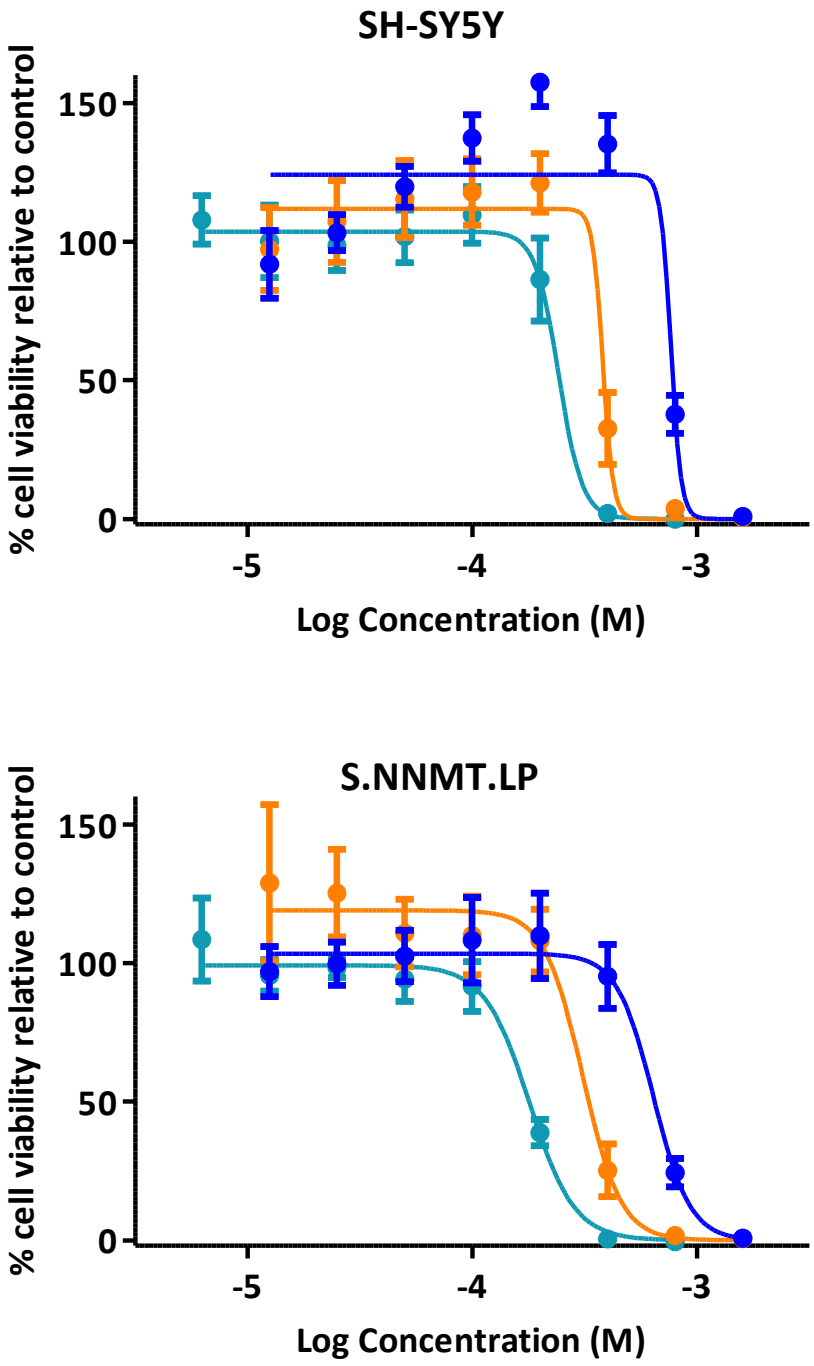

Figure 5.5. Comparative toxicity curves of NH (turquoise), 4PP (blue) and THNH (orange) in SH-SY5Y cells (top) and S.NNMT.LP cells (bottom) following a 5-day incubation. Cell viability was determined via ATP assay. All data are mean ± SEM, n = 5.

5.3.3. Toxicity differences existed between the MTT and ATP assays

A *t*-test analysing the differences in log EC50 from one assay to another revealed that the NH $EC50_{MTT}$ for SH-SY5Y cells was significantly lower than $EC50_{ATP}$ (-3.79 ± 0.06 (162 µM) *vs* -3.58 ± 0.05 (263 µM), $p = 0.03$). This was not the case for S.NNMT.LP cells (-3.81 ± 0.05 (155 µM) *vs* -3.76 ± 0.04 (174 µM), $p = 0.41$). THNH EC50s showed no difference between assays (-3.37 ± 0.02 (427 µM) *vs* -3.36 ± 0.06 (437 µM), $p = 0.91$ for SH-SY5Y and -3.44 ± 0.04 (363 µM) *vs* -3.46 ± 0.03 (348 µM), $p = 0.68$ for S.NNMT.LP). The $EC50_{MTT}$s of 4PP-treated SH-SY5Y and S.NNMT.LP cells were significantly lower than the corresponding $EC50_{ATP}$s (-3.47 ± 0.04 (339 µM) *vs* -3.132 ± 0.02 (741 µM), $p < 0.0001$ and -3.48 ± 0.03 (331 µM) *vs* -3.20 ± 0.04 (631 µM), $p < 0.0005$ for SH-SY5Y and S.NNMT.LP cells respectively).

5.4. Discussion

Summary of key findings

- ***No difference in toxicity between cell lines was seen following MTT assays***
- ***Differences between SH-SY5Y and S.NNMT.LP in onset of toxicity, toxicity at specific doses and EC50 were seen in the ATP assay for NH***
- ***4PP had significantly greater protective effects in SH-SY5Y cells than S.NNMT.LP cells following the ATP assay***

5.4.1. βC-toxicity in SH-SY5Y and S.NNMT.LP cells

When measured by MTT cell viability assay, all compounds exhibited similar toxicity responses in both cell lines, although NH showed significant toxicity towards SH-SY5Y at 6.25 µM and 100 µM but not S.NNMT.LP cells. However, the fact that there was neither a difference in toxicity between cell lines at these concentrations, nor a difference in $EC50_{MTT}$, indicated that the 2 cell lines did not possess meaningful differences in cell viability when incubated with NH.

Furthermore, the toxicity seen in SH-SY5Y cells at the lowest dose may be due to experimental, rather than biochemical, factors. This is supported by the observation that in the MTT assays, the lowest dose of every compound, particularly in SH-SY5Y cells, showed a lower viability than doses thereafter (figure 5.2). This is likely due to the fact that the lowest dose given to the SH-SY5Y cells was consistently applied to the wells at the bottom left corner of the 96-well plate. A study investigating location-dependent biases in plate readers found that, in some cases, row H

columns 1-4 exhibit lower absorbances relative to the grand mean of the plate. This is in contrast to row D columns 9-12 which typically exhibited greater than average absorbances (Harrison & Hammock 1988). While the differences in absorbances observed in Harrison and Hammock's study were generally low (5%-10% either side of the grand mean depending on the plate reader) this may have been sufficient to contribute to the unexpected difference seen between the lowest NH dose and untreated SH-SY5Y cells in this study. Why this difference was only significant to the SH-SY5Y cells incubated with NH is unclear and may be coincidental.

Differences in toxicity between both cell lines were more apparent when measuring ATP content. While, again, no differences were seen when either cell line was exposed to THNH, the NNMT-V5-expressing S.NNMT.LP cells appeared to be significantly more susceptible to NH-mediated loss of ATP than the non-NNMT-expressing SH-SY5Y cells. This was supported by the fact that significant reductions in ATP content began at a lower NH dose (200 µM) in S.NNMT.LP cells; S.NNMT.LP ATP content compared to SH-SY5Y cells was significantly lower at this dose and the overall $EC50_{ATP}$ for NH was significantly lower in the S.NNMT.LP cells. The significant difference in $EC50_{ATP}$ was paralleled by a significant increase in the NH $EC50_{ATP}$ compared with $EC50_{MTT}$ in the SH-SY5Y cells, but not S.NNMT.LP cells. This unilateral difference in inter-assay EC50 suggests that the SH-SY5Y cells may have been able to protect themselves against NH-mediated ATP depletion by a mechanism that was absent or overcome in S.NNMT.LP cells incubated with NH.

The precise mechanism for this increased susceptibility of S.NNMT.LP cells to NH-mediated ATP-dependent toxicity is unclear. It is also unclear whether this

difference in toxicity was due to the production of *N*-methylated NH in S.NNMT.LP cells or an alternative mechanism that simply renders NNMT-V5-expressing SH-SY5Y cells more susceptible to ATP-dependent NH toxicity. Regardless of the exact mechanism, the fact that this difference was only detected in the more sensitive of the 2 assays (ATP analysis) may suggest that NH toxicity was only marginally more severe to S.NNMT.LP cells over the time-course of the study. However, whilst during the 5-day timeframe of the MTT assay no toxicological differences were found, over a longer period of time differences in energy availability may manifest themselves into more pronounced toxicity. Accordingly, a situation could arise in the brain whereby cells with higher NNMT expression, exposed to NH over many years, are subjected to a slow yet increasing toxicity that may only become fully manifest at a later stage. This long-term build-up of toxicity is in line with the development of PD pathophysiology, as the gradual degeneration of SNpc neurons in the brain typically spans several years.

It should be noted that the increased susceptibility of S.NNMT.LP cells to NH-mediated ATP reduction is in contrast to the overall enhanced viability of S.NNMT.LP cells seen in the previous chapter. Given that NNMT is thought to be cytoprotective to many different cell-types, including SH-SY5Y (see chapter 4), it is possible that the upregulation of NNMT as a cytoprotective response in the brain could have long-term unwanted toxic consequences in the presence of sufficient quantities of NH. This raises the possibility that NNMT expression in PD could be a double-edged sword, resulting in a situation in which the initially protective effects of NNMT are counteracted by the effects of long-term exposure of NNMT-

expressing cells to NH. Over time this balance of toxicity *vs* protection could shift towards greater harm due to the slow, but steady, accumulation of NNMT-dependent NH toxicity, eventually surpassing the neuron's cytotoxic threshold and initiating cell death.

The lack of toxicological differences between SH-SY5Y and S.NNMT.LP cells as well as the significant differences in EC50 between THNH and NH suggest that THNH has no direct relevance as a toxin to either cell line. Furthermore studies involving the injection of 2*N*-methylated THNH into rat brains found no dopaminergic neuron-specific toxicity (Perry *et al.* 1986). Thus, THNH is unlikely to play a direct role in either PD toxicity or toxicity derived from the expression of NNMT. However, due its place in the biosynthetic pathway for the production of 2,9-diMeNH, THNH may yet play an indirect role in the disease *via* its oxidation to NH (section 1.3.5.2, figure 1.10).

5.4.2. 4PP-exposure in SH-SY5Y and S.NNMT.LP cells

While there was no apparent difference in cell viability following 4PP incubation at any dose, and the $EC50_{MTT}$s and $EC50_{ATP}$s of the 2 cell lines were not significantly different, the ATP content of SH-SY5Y cells was significantly higher at 200 µM and 400 µM 4PP compared with that observed in S.NNMT.LP cells. In particular, 200 µM 4PP significantly enhanced ATP content in SH-SY5Y cells above the level in untreated cells, an effect that was absent in the S.NNMT.LP. To the author's knowledge, there are currently no other experimental reports of 4PP-mediated

enhancement of ATP. However, 4PP-mediated cytoprotection against MPP^+ toxicity has previously been reported *in vivo* (Irwin, Langston & DeLanney 1987).

The fact that this enhancement was only measured in the ATP assay suggests that 4PP may initially exert its cytoprotective properties by acting as a mediator of increased ATP production. Over a longer period of time, this increased ATP content may manifest itself as greater overall cell viability and survival. Thus, increased cell viability mediated by 4PP may be detectable *via* MTT assay over an incubation time longer than 5 days. While exposure of NNMT-expressing cells to 4PP did not appear to be toxic, the lack of protective effect seen compared to non-expressing cells may, over time, result in lower cell viability due to comparatively lower ATP content in S.NNMT.LP. However, the mechanism for this is unclear, although it is unlikely that the lack of protection seen in the NNMT-expressing cells is due to the simultaneous production of MPP^+. Had this been the case, MPP^+ production would have occurred intracellularly and, thus, would have provided the neurotoxin with immediate access to its primary target, mitochondrial CxI (Nicklas, Vyas & Heikkila 1985, Cleeter, Cooper & Schapira 1992). This would have resulted in a substantially increased - and more noticeable - toxicity towards S.NNMT.LP cells.

Interestingly, 4PP exposure to both cell lines showed a significant increase in $EC50_{ATP}$ compared with $EC50_{MTT}$. The precise reason for this in unclear but it may indicate that 4PP-mediated cell death at higher doses occurs principally *via* an ATP-independent mechanism as approximately twice as much 4PP was required to reduce cellular ATP by half than to halve the cell viability. The significantly higher 4PP $EC50_{ATP}$s compared with $EC50_{MTT}$s appear to explain the change in order of

toxicity that occurred, as THNH, which was less toxic than 4PP in the MTT assays, did not have a significantly increased $EC50_{ATP}$. More studies are required in order to fully elucidate why 4PP shows such a strong variation in toxicity between assays.

5.4.3. The physiological relevance of the compound concentrations used in the study

Unfortunately, for comparative purposes, there are currently no published data that provide an indication of the concentration 4PP can reach in the mammalian brain. While data exist reporting THNH concentrations in rat brain (370 – 1510 pg/g of tissue, approximately 2.15 – 8.78 nM) (Faull *et al.* 1982, Peura *et al.* 1989), no human data have been published. On the other hand data does exist for NH which suggests that the NH concentrations used in this study were higher than those that have been reported in healthy human brains. Matsubara *et al*. (1993) reported a NH concentration of 16 +/- 8 nM in the SN of non-PD human brains (16.00 +/- 8 pmol/g, equivalent to 16 +/- 8 nM, assuming 1 g = 1 ml). Currently, there are no data reporting the concentration of NH in the PD brain but it is assumed that its concentration would be substantially higher than the one reported in non-PD brains. This is supported by the finding that NH concentration showed a significant 2.1-fold increase in the CSF of PD patients compared with controls (134 +/- 107 pM *vs* 64.1 +/- 57 pM) (Kuhn *et al*. 1996).

Similar results to those reported in this study may be achievable using lower NH concentrations but with significantly longer incubation times. Should the S.NNMT.LP cells indeed be converting NH to its *N*-methylated forms, the slow but

gradual sequestration of any *N*-methylated products in mitochondria would lead to the cytotoxic threshold of the cell eventually being reached. This could occur even with low substrate concentrations and rates of *N*-methylation. This is due to the fact that that positively charged ions, like MPP^+ or the *2N*-methylated β-carbolinium ions, are known to sequester within mitochondria (Ramsay *et al.* 1989), with some cationic compounds reaching concentrations up to 1000-fold higher inside the mitochondria than outside (Hoppel *et al.* 1987). Indeed, with PD being associated primarily with age, this very slow but gradual accumulation could be occurring over several decades in human brains.

However, due to the impracticalities of the long-term culture of immortalised cells, whether because of cost, overgrowing or the inability to keep conditions constant, it is often necessary to perform assays over a shorter space of time *in vitro*. Thus, the process can be accelerated by using supra-physiological concentrations in order to determine possible effects of exposure more rapidly. In this case, the higher NH concentration may also function to force the hypothetical *N*-methylation reaction to completion. While this may not be indicative of ideal physiological conditions for the reaction, should the toxicity seen in this study be confirmed to be due to the production of *N*-methylated NH, the data can be seen as a proof of concept rather than a direct indicator of the capability of NNMT-expressing neurons in the human brain to form *N*-methylated NH products. As such, in future, *in vivo* studies should be carried out to further investigate the susceptibility of of NNMT-expressing cells' to NH.

5.4.4. Summary

In conclusion, S.NNMT.LP cells were significantly more susceptible to NH-mediated ATP reduction compared to SH-SY5Y cells. The precise mechanism for this increased susceptibility is unclear. The absence of this observation in the MTT assay suggested that the reduction in ATP content mediated by NH was insufficient to affect cell viability over the time course of the study. THNH showed no differences in toxicity to either cell line. 4PP was found to be significantly better at enhancing the ATP content of SH-SY5Y cells compared with S.NNMT.LP cells. The precise mechanism of this protection is not currently known.

6. The determination of the role of NNMT in 2-MeNH toxicity and biosynthesis

6.1. Introduction

The previous chapter discussed the increased susceptibility of the NNMT-V5-expressing S.NNMT.LP cells to NH toxicity compared with SH-SY5Y cells which do not express the enzyme. However, it was unclear whether this toxicity was due to the S.NNMT.LP's inherent susceptibility to NH or to the possible conversion of NH into one of its more toxic, *N*-methylated forms. Figure 1.10 in Chapter 1 illustrated that there are 2 possible NH *N*-methylation products, 2-MeNH or 2,9-diMeNH. A study by Matsubara, Collins & Neafsey (1992) suggested that 2,9-diMeNH, the end product of NH di-*N*-methylation, arises from sequential NH *N*-methylation, initially at the 2*N* position followed by the *9N* position. Thus, *N*-methylation of the pyridine moiety appears to be the first step towards the production of the endogenous neurotoxin, and it is this particular moiety in other compounds, such as 3-acetylpyridine, that NNMT has been shown to *N*-methylate (Alston & Abeles 1988).

While 2,9-diMeNH has been reported to be the most toxic of all the naturally-occurring βC derivatives (Hamann *et al.* 2006, Pavlovic *et al.* 2006, Wernicke *et al.* 2007), 2-MeNH has also been reported to be toxic, particularly to cells expressing DAT (Wernicke *et al.* 2007). Thus, given the concomitant elevation of both NNMT expression and the concentration of *N*-methylated βCs in PD, the toxicity of 2-MeNH and 2,9-diMeNH to SH-SY5Y and S.NNMT.LP cells was determined *via* MTT and ATP assays. Due to the lack of commercially-available 2-MeNH and 2,9-diMeNH, both compounds were synthesised using published methods (figure 6.1, discussed in more detail in section 6.2.1).

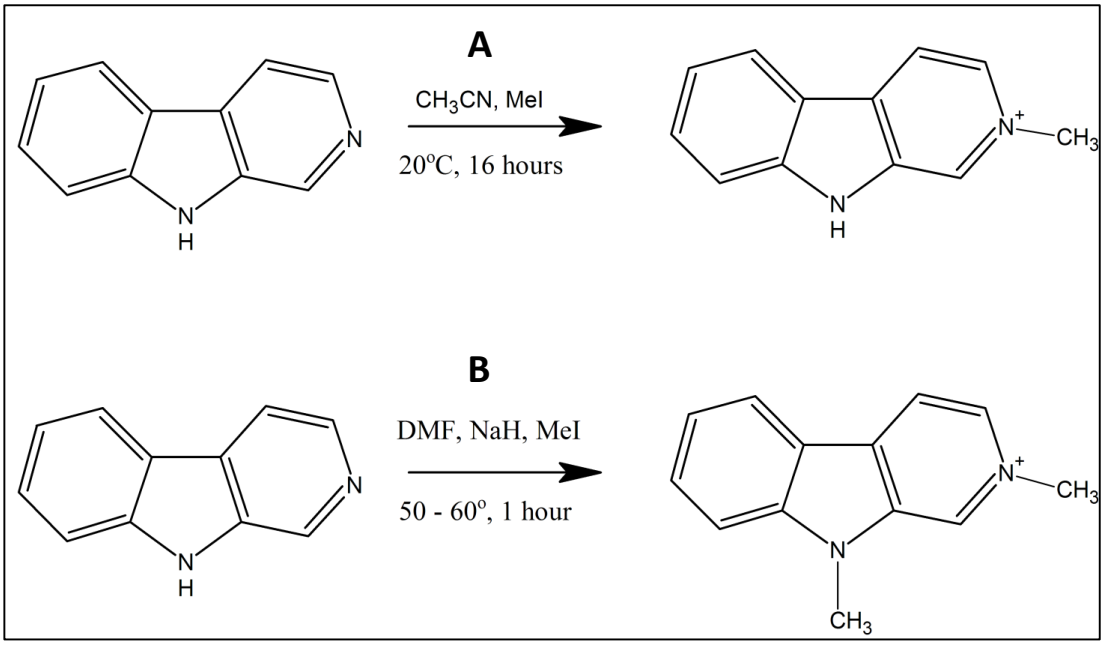

Figure 6.1. The reaction conditions for the synthesis of 2-MeNH, as described by Thatcher et al. 2012 (A) and 2,9-diMeNH, as described by Cao et al. 2005 (B). CH_3CN = acetonitrile, MeI = methyl iodide, DMF = N,N-dimethylformamide, NaH = sodium hydride

In addition, the possibility of NNMT catalysing NH 2*N*-methylation was determined. This was achieved *via* a cell free NNMT enzyme activity assay in the presence of NH and SAM cofactor. The results were analysed *via* liquid chromatography-mass spectrometry (LC-MS) in order to definitively determine whether the enzyme is capable of catalysing the 2*N*-methylation of NH to 2-MeNH. In particular, the detection of 2-MeNH was performed using a triple quadrupole mass spectrometer, as this allowed improved identification of specific analytes *via* MS-MS selected reaction monitoring (SRM) and also provided a sufficient signal-to-noise ratio for quantification at low concentrations should NH only be a poor substrate for NNMT.

6.2. Methods

6.2.1. Synthesis

6.2.1.1. Synthesis of 2-MeNH

The synthesis of 2-MeNH was based upon the method of Thatcher *et al.* (2012) and was carried out as follows within the confines of a fume cupboard. Five hundred mg of NH was added to a 50 mL round-bottomed flask. A magnetic flea was added to the flask which was then clamped above a magnetic stirrer (Nickel Electro Ltd, Weston-super-Mare, UK). Ten mL of acetonitrile (ACN, Fisher Scientific, Loughborough, UK) were added to the flask and gently stirred for 30 minutes at room temperature, before 0.5 mL methyl iodide (MI) were added using a needle and syringe. The flask was firmly stoppered and the reaction was left to stir at room temperature for 16 hours, during which time a light yellow precipitate was formed. The stopper was removed and the solution was left to stir for an additional 30 minutes to allow any residual MI to evaporate.

The reaction solution was then poured into a sintered funnel and was filtered under vacuum, resulting in the collection of a yellow powder. The filtrate was collected into a conical flask. The precipitate was washed with 5 ml of diethyl ether followed by filtration under vacuum for 1 minute to ensure as much solvent as possible was drawn off. The remaining solid was scraped off the funnel and collected into a beaker. The filtrate was then added to the top of the sintered funnel and filtered once more under vacuum for 1 minute, with any additional precipitate pooled with the previously collected precipitate. The pooled precipitate was then added back onto the filter and washed with diethyl ether a further three times. The remaining

precipitate was then scraped off and dried under reduced pressure in a desiccator overnight.

6.2.1.2. Synthesis of 2,9-diMeNH

The synthesis of 2,9-diMeNH was based upon the method by Cao *et al.* (2005) and was carried out as follows within the confines of a fume cupboard. Four hundred and twenty mg of NH was added to a 100 mL round-bottomed flask inside a fume hood. A magnetic flea was added to the flask which was then clamped above a magnetic stirrer (Nickel Electro Ltd, Weston-super-Mare, UK). Fifteen ml of anhydrous DMF was added to the flask which was then stoppered and gently stirred until the NH dissolved. An oil bath upon a temperature-controlled stirring plate was pre-heated to 60^{o}C before 0.3 g of sodium hydride (NaH) was added to the NH-DMF solution. One mL of MI was then added *via* needle and syringe and the flask was submerged in the oil bath. A condenser was attached to the top of the flask and the water supply was switched on. The reaction was then left for 1 hour.

The condenser was disassembled and the flask was removed from the oilbath and clamped over a stirring plate. The flask was then stirred un-stoppered for 30 minutes to allow it to cool and to allow any excess, un-reacted MI to evaporate. Ten mL of deionised water was added before the solution was poured into a 500 mL separating funnel. Thirty mL of ethyl acetate (EA) were added to the separating funnel which was then stoppered and shaken vigorously. The separating funnel was inverted and the tap opened periodically to relieve the pressure during shaking. The funnel was then left to rest for 30 seconds to allow the solvents to partition. The

lower (aqueous) and upper (EA) layers were then collected into separate conical flasks. The EA-containing flask was set aside and the flask containing the aqueous layer was poured back into the separating funnel. Thirty mL of fresh EA was added to the funnel and the shaking and draining process was repeated a total of 3 times as described above, pooling the aqueous and EA layers into their respective flasks each time.

The conical flask containing the aqueous partition was set aside. The entire volume of the EA-containing conical flask was then added to the separating funnel before 10 mL of deionised water was added. The funnel was then shaken and drained as described above and the process was repeated once more. Both the aqueous layer and EA layer were drained into clean conical flasks. The aqueous-layer flask was again set aside. The EA layer was then added back into the separating funnel a final time in order to wash and shake with 15 mL of brine. The brine layer was drained and set aside before the EA layer was collected into a clean conical flask.

Excess water was removed from the EA solution by adding several heaped spatula measures of anhydrous magnesium sulphate and swirling the flask. The contents were then filtered using a sintered funnel attached to the vacuum supply. No wash was performed after filtration. The filtrate was then evaporated using a Rotavapor V800 rotary evaporator (Buchi, Oldham, UK) to produce a golden paste.

6.2.1.3. Confirmation of the identities of the synthetic products

The identification of synthetic products was performed using nuclear magnetic resonance (NMR), mass spectrometry and melting point analysis.

6.2.1.3.1. NMR

Analysis of synthetic products was performed using proton (^{1}H-NMR) and carbon (^{13}C-NMR) NMR. Samples were prepared for NMR by dissolving 10 mg of product in 700 µL of deuterated DMSO (Santa Cruz Biotechnology, Heidelberg, Germany).

^{1}H-NMR spectra were recorded at 400 MHz and ^{13}C-NMR spectra were recorded at 100.6 MHz using an Ultrashield 400 NMR spectrometer (Bruker, Coventry, UK). NMR spectra were then compared with spectra reported in the literature (Thatcher *et al*. 2012, Cao *et al*. 2005).

6.2.1.3.2. Melting point analysis

Melting point was determined by placing a small amount of product into a capillary tube. This was then inserted into a digital melting point apparatus (Electrothermal, Stone, UK) with the temperature initially set to 180^{o}C, increasing by 0.2^{o}C every 10 seconds. The temperatures at the commencement of melting and the completion of melting were recorded and compared with those reported in the literature (Rook *et al*. 2010, Cao *et al*. 2005).

6.2.1.3.3. Mass spectrometry

Confirmation of synthesis was performed *via* infusion of 1 ng/mL product in methanol into a TSQ Quantum Access triple quadrupole (Thermo Scientific, Loughborough, UK) followed by full scan analysis to provide confirmation of product size and purity.

6.2.2. MTT assay of SH-SY5Y cells and S.NNMT.LP cells incubated with 2-MeNH

SH-SY5Y and S.NNMT.LP cells were prepared for MTT assay as described in section 2.4.1. Cell solutions were seeded at a density of 15,000 cells/well as per the plate layout described in figure 2.3.

A 100 mM solution of 2-MeNH was made according to section 2.4.2, table 2.3. The dosing procedure (section 2.4.2) was followed, resulting in both cell lines being exposed to 8 different concentrations of 2-MeNH: 2000 µM, 1000 µM, 500 µM, 250 µM, 125 µM, 62.5 µM, 31.25 µM, 15.625 µM. Control wells were given media only. All plates were then incubated with 2-MeNH for a total of 120 hours as described in section 5.2. Toxicity, *via* MTT assay, was assessed using the method described in section 2.4.3.1.

6.2.3. ATP assay of SH-SY5Y cells and S.NNMT.LP cells incubated with 2-MeNH

SH-SY5Y and S.NNMT.LP cells were prepared for ATP assay as described in section 2.4.1. Cell solutions were seeded at a density of 15,000 cells/well as per the plate layout described in figure 2.3.

The dosing procedure was identical to that used in section 6.2.2. Toxicity, *via* ATP assay, was assessed using the method described in section 2.4.3.1.

6.2.4. Determination of NNMT NH *N*-methyltransferase activity

6.2.4.1. Proof-of-concept study

It has been hypothesised that NNMT may catalyse the first stage of NH's *N*-methylation pathway (section 1.3.5.2, figure 1.10); as such, the elevated expression of NNMT observed in the PD patient brain (Parsons *et al*. 2002, Parsons *et al*. 2003) may facilitate local increases in the levels of *N*-methylated βCs. Accordingly, an enzyme assay (Patel *et al.* 2013) in which NH was substituted for nicotinamide as substrate, using purified, active, recombinant NNMT protein (a kind gift from Prof. M. Emanuelli, Università Politecnica delle Marche, Ancona, Italy) was carried out in order to assess whether NNMT can catalyse the formation of 2-MeNH.

Prior to beginning the reaction, 5 750 µL aliquots of ACN were prepared in 1.5 mL Eppendorf tubes and placed on ice. A reaction mix was prepared in a 1.5 mL Eppendorf tube containing the following components (table 6.1): 694 µL deionised water, 8 µL of 100 mM NH (section 2.4.2, table 2.3, 1 mM final concentration), 40

µL of 1 M, pH 8.6 Tris (50 mM final concentration), 8 µL of 100 mM dithiothreitol (DTT, 1 mM final concentration) and 10 µL of 1.7 µg/µL NNMT protein in DMSO (21.25 ng/µL final concentration).

Table 6.1. The compositions of solutions used in the NNMT enzyme assay.

Compound	Concentration	Composition
Tris	1 M	12.1 g Trizma HCL in 90 mL deionised H_2O, adjusted to pH 8.6 before making up to 100 mL.
DTT	100 mM	15.4 mg/mL (Sigma-Aldrich, Dorset, UK) in deionised H_2O.
SAM cofactor	100 mM	3.98 mg/mL (Sigma-Aldrich, Dorset, UK) in deionised H_2O.

The reaction mix was vortexed and inserted into a pre-heated Eppendorf heater (Grant Instruments, Shepreth, Cambridgeshire) set to 37^{o}C. The reaction mix was incubated for 5 minutes to reach temperature prior to the addition of 40 µL 10 mM SAM cofactor (0.5 mM final concentration) to start the reaction. The reaction tube was vortexed immediately following the addition of SAM and a 150 µL aliquot was transferred to one of the ACN aliquots, vortexed and placed on ice in order to terminate the enzyme reaction and precipitate the protein. The reaction tube was placed back onto the heater and the time was noted. One hundred and fifty µL reaction aliquots were transferred to ACN every 15 minutes for 1 hour.

In order to quantify the production of 2-MeNH, a range of 2-MeNH standards were produced from a 5 mg/mL DMSO stock of synthesised 2-MeNH (equivalent to 8.5 mg/ml of 2-MeNH iodide). The standards were made as outlined in table 6.2.

Table 6.2. The composition of 2-MeNH standards made from a 5 mg/mL stock of 2-MeNH in DMSO.

Solution	Concentration	Name and volume of standard solution used	Volume of DMSO added
A	5 µg/mL	Stock, 5 µL	4995 µL
B	2 µg/mL	Solution A, 400 µL	600 µL
C	1 µg/mL	Solution B, 500 µL	500 µL
D	500 ng/mL	Solution C, 500 µL	500 µL
E	200 ng/mL	Solution D, 400 µL	600 µL
F	100 ng/mL	Solution E, 500 µL	500 µL
G	20 ng/mL	Solution F, 200 µL	800 µL

Eight µL of each standard were transferred into an Eppendorf containing 744 µL deionised water, 40 µL Tris and 8 µL DTT. Accordingly, the final concentrations of the standards were 50 ng/mL, 20 ng/mL, 10 ng/mL, 5 ng/mL, 2 ng/mL, 1 ng/mL and 0.2 ng/mL. Once each solution had been prepared and vortexed, a 150 µL aliquot of each sample was transferred into 750 µL ACN as described above.

Upon collection of all samples and standards, the Eppendorf tubes were centrifuged (1-14 Microfuge, Sigma Centrifuges, Wem, UK) for 10 minutes at 16,000 x *g*. Eight hundred µL of supernatant were then carefully transferred into a fresh Eppendorf, taking care not to disturb the protein pellet.

6.2.4.2. Detection of 2-MeNH

6.2.4.2.1. Determination of 2-MeNH and THNH parent → product ion transitions

Prior to beginning LC-MS analysis of the enzyme assay samples, parent and product ion transitions for selected reaction monitoring (SRM) were determined for 2-MeNH and THNH (internal standard) following their infusion into a TSQ Quantum Access triple quadrupole mass spectrometer (Thermo Scientific, Loughborough, UK). Determination of ions fragments was performed by analysing the full scan MS-MS spectrum of 1 µg/mL (in a 0.1% FA, 50% methanol solution) infusions of 2-MeNH and THNH. Collision energies for the MS-MS were 33 V and 12 V for 2-MeNH and THNH respectively.

6.2.4.2.2. Sample preparation and LC-MS

One hundred µL of each enzyme assay sample were transferred into an extraction tube. A 1 mg/mL stock solution of THNH in methanol was made to be used as an internal standard. The solution was diluted to 1 µg/mL in a 0.1% formic acid (FA), 50% methanol solution before 20 µL was added to each extraction tube (final

concentration 166 ng/mL). The tubes were evaporated to dryness under N_2 at 40°C for 30 minutes before being reconstituted in 200 µL of 0.1% FA, 50% methanol solution.

Ten µL of each solution was injected into a Thermo Accela Pump and Autosampler (Thermo Scientific, Loughborough, UK) coupled to a Thermo TSQ Quantum Access and separated using a C4 Thermo Hypersil Gold 50x2.1mm 1.9µ column (Thermo Scientific, Loughborough, UK) at a flow rate of 200 µL/min using the mobile phase gradient outlined in table 6.3. The total run time was 12 minutes.

Table 6.3. The gradient conditions of the LC analysis of 2-MeNH following the NNMT enzyme assay.

Time (min)	% Solvent A (0.1% FA in H_2O)	% Solvent B (0.1% FA in ACN)
0.00	95	5
0.50	95	5
5.00	50	50
6.00	50	50
6.20	95	5
12.00	95	5

Eluted reaction components were analysed using triple quadrupole, positive electrospray ionisation, with a spray voltage of 3000 kV and a capillary temperature of 350°C. Identification of 2-MeNH and THNH were performed *via* the detection of their parent → product ion transitions.

6.2.4.2.3. Analysis of LC-MS data

A 2-MeNH calibration curve was generated by plotting the normalised peak area (NPA), determined by dividing the peak area for 2-MeNH by the corresponding peak area for the THNH internal standard, against the amount of 2-MeNH injected. NPA was calculated for each sample before NNMT activity was calculated and expressed as nmoles 2-MeNH produced/mg protein. Linearity of the reaction over time was determined using linear regression analysis.

6.2.4.3. Calculation of Michaelis-Menten kinetic parameters of NNMT NH 2-N-methylation

In order to calculate the Michaelis-Menten kinetic constants K_m and V_{max} for the conversion of NH to 2-MeNH by NNMT, the assay was repeated as described above using NH in the concentration range of 0.05 mM, 0.1 mM, 0.25 mM, 0.5 mM and 1 mM. Each dilution into the reaction mix was made directly from a 100 mM NH stock (section 2.4.2, table 2.3) and 150µL aliquots were taken at 30 seconds, 1 minute, 2 minutes, 4 minutes and 8 minutes. In addition, a no-enzyme control was prepared, replacing protein with 10 µL deionised water to control for non-enzymatic conversion of NH to 2-MeNH. Samples were taken at 0 minutes and 8 minutes and prepared for LC-MS as described above.

Initial velocity (expressed as NPA/min) was determined for each substrate concentration, corrected for no-enzyme control and then expressed as specific activity (nmoles 2-MeNH produced/hour/mg NNMT protein). K_m (expressed as mM)

and V_{max} (nmoles 2-MeNH produced/hour/mg protein) were calculated using (1) non-linear regression analysis using a Michaelis-Menten plot (v vs [S]), (2) linear regression analysis of a Eadie-Hofstee plot (v vs. v/[S]), which also allows for the determination of the presence of substrate inhibition, a property demonstrated by NNMT when using nicotinamide as a substrate (Patel *et al*. 2013), and (3) linear regression analysis of a Hanes-Woolf plot ([S]/v vs. [S]), each using GraphPad Prism.

6.2.5. Statistical Analysis

Enzyme kinetic data were analysed via non-linear and linear regression as described above. Toxicity data were analysed using the methods described in section 2.4.4.

6.3. Results

6.3.1. Analysis of syntheses: 2-MeNH

6.3.1.1. Characteristics of the synthetic product

The synthesis of 2-MeNH produced a light yellow powder with a yield of 90% which was close to the 97% yield reported by Thatcher *et al*. 2012. The melting point of 2-MeNH powder was 236 - 238^{o}C, which matched the previously reported melting point of 236 - 238^{o}C (Rook *et al.* 2010).

6.3.1.2. NMR spectra for 2-MeNH matched those previously reported

The ^{1}H-NMR spectrum for the 2-MeNH synthesis was as follows:

400 MHz (DMSO d_6): δ 12.78 (1H, s, NH), 9.36 (1H, s, aromatic), 8.81 (1H, s (br), aromatic), 8.65 (1H, s (br), aromatic), 8.50 (1H, s (br), aromatic), 7.80 (2H, s (br), aromatic, aromatic), 7.46 (1H, s (br), aromatic), 4.49 (3H, s, $N^{+}CH_3$).

Chemical shifts (δ) are quoted in parts per million (ppm) and are referenced to the residual protonated solvent peak. The order of citation in parentheses is (1) number of equivalent nuclei by integration, (2) multiplicity of peak (s, singlet; br, broad), and (3) assignment of proton environment.

The ^{13}C-NMR spectrum for the 2-MeNH synthesis was as follows:

100 MHz (DMSO d_6): δ 143.9 (aromatic), 134.8 (aromatic), 134.8 (aromatic), 133.4 (aromatic), 131.87 (aromatic), 130.4 (aromatic), 123.6 (aromatic), 121.5 (aromatic),

119.2 (aromatic), 117.6 (aromatic), 113.0 (aromatic), 47.7 (N^+CH_3). Chemical shifts (δ) are quoted in parts per million (ppm) and are referenced to the appropriate solvent peak.

Both of these spectra matched the spectra previously reported for the synthesis (Thatcher *et al*. 2012), thus demonstrating the successful synthesis of 2-MeNH.

6.3.1.3. The 2-MeNH mass to charge ratio (m/z) was confirmed using mass spectrometry

Infusion of a 1 mg/mL solution of 2-MeNH in methanol into the triple quadrupole mass spectrometer confirmed the *m/z* of 2-MeNH as 183.1, concurrent with its calculated molecular mass of 183.1 ($C_{12}H_{11}N_2^+$, figure 6.2).

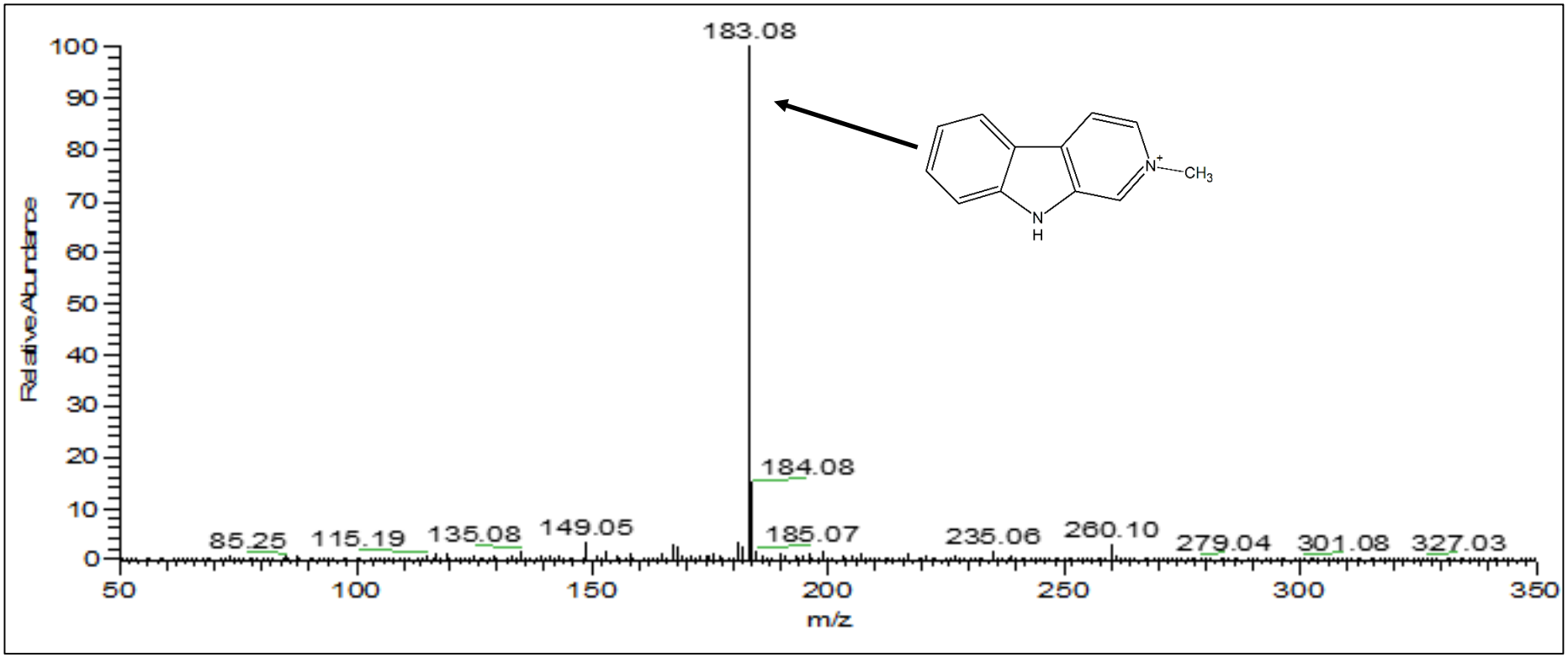

Figure 6.2. The full scan spectrum of synthesised 2-meNH following its infusion into a TSQ Triple quadrupole (Thermo Scientific, Loughborough, UK) mass spectrometer.

6.3.2. Analysis of syntheses: 2,9-diMeNH

6.3.2.1. Characteristics of the synthetic product

The synthesis of 2,9-diMeNH yielded a golden paste with a yield of <5%. This did not match the 73% yield published by Cao *et al*. 2005. Due to the low yield, there was insufficient sample to perform melting point and MS analysis.

6.3.2.2. NMR spectra for 2,9-diMeNH did not match those previously reported

The ^{1}H-NMR spectrum for the 2,9-diMeNH synthesis was as follows:

400 MHz (DMSO d6): δ 8.05 (1H, d, J = 7.9 Hz, aromatic), 7.61 (1H, d, J = 8.4 Hz, aromatic), 7.47-7.51 (1H, m, aromatic), 7.41 (1H, d, J = 7.0 Hz, aromatic), 7.21-7.25 (1H, m, aromatic), 7.02 (1H, d, J = 7.0 Hz, aromatic), 4.24 (3H, s, CH_3), 3.57 (3H, s, CH_3).

Chemical shifts (δ) are quoted in parts per million (ppm) and are referenced to the residual protonated solvent peak. The order of citation in parentheses is (1) number of equivalent nuclei by integration, (2) multiplicity of peak (s, singlet; d, doublet; t, triplet; and m, multiplet), (3) the coupling constant (J) quoted in Hertz (Hz) and (4) assignment of proton environment.

The ^{13}C-NMR spectrum for the 2,9-diMeNH synthesis was as follows:

100 MHz (DMSO d6): δ 155.85 (aromatic), 140.38 (aromatic), 130.04 (aromatic), 126.53 (aromatic), 126.36 (aromatic), 123.94 (aromatic), 121.33 (aromatic), 120.89

(aromatic), 119.86 (aromatic), 110.53 (aromatic), 99.57 (aromatic), 36.19 (CH_3), 31.10 (CH_3).

The ^{13}C-NMR spectrum for the synthesis of 2,9-diMeNH indicated that the product contained 13 carbon atoms and thus confirmed that di-methylation had taken place. However, while the ^{1}H-NMR spectrum confirmed the presence of 2 methyl groups *via* 2 aliphatic singlets (δ 4.24 and δ 3.57) with an integrated size of 3 protons, it also revealed that only 6 aromatic protons were present in the product (rather than 7), suggesting that 1 methyl group had become attached to an aromatic carbon, rather than the aliphatic nitrogen. As a result, the combined spectra did not match the one reported by Cao *et al*. (2005). Repeated attempts at synthesis resulted in no resolution of this, therefore, the synthesis and subsequent investigation of 2,9-diMeNH was not pursued further.

6.3.2. Toxicity assays of SH-SY5Y and S.NNMT.LP cells incubated with 2-MeNH

6.3.2.1. S.NNMT.LP cell viability was significantly less susceptible to the toxicity of 2-MeNH compared with SH-SY5Y cells

A dose-response curve of cell viability, as measured using the MTT assay, derived from mean data from each experimental repeat (n = 4), is shown in figure 6.3. The individual curves from each experimental repeat, which were used to generate 1 $EC50_{MTT}$ per cell line and 1 set of mean data for each of the individual experiments, are shown in Appendix 2.

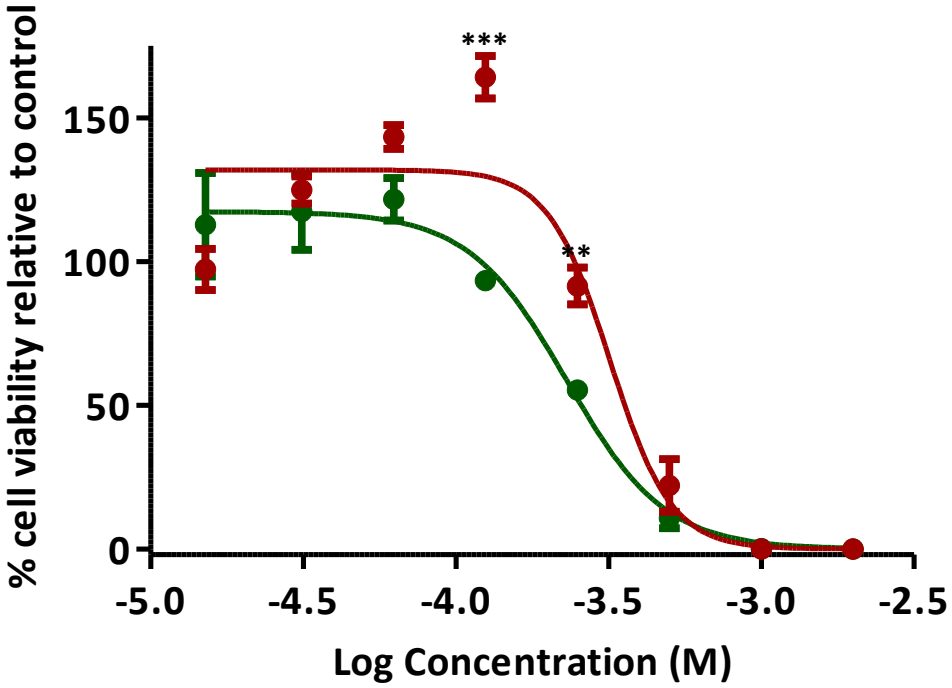

Figure 6.3. The dose response curve of 2-meNH toxicity towards SH-SY5Y cells (green circles) and S.NNMT.LP cells (red circles) after a 5 day incubation. Cell viability was determined via MTT assay. All data are mean ± SEM, n = 4. ** = p < 0.01 S.NNMT.LP vs SH-SY5Y, *** = p < 0.001 S.NNMT.LP vs SH-SY5Y.

As summarised in table 6.4, 2-MeNH was toxic to SH-SY5Y cells at concentrations of 250 µM, 500 µM, 1mM and 2 mM (all $p < 0.001$). For S.NNMT.LP cells, 2-MeNH was toxic at concentrations of 500 µM, 1mM and 2 mM (all $p < 0.001$). 2-MeNH also caused a significant increase in cell viability in S.NNMT.LP cells at 62.5 µM and 125 µM (both $p < 0.001$), which was not observed for SH-SY5Y cells. The maximum increase in viability (+64 ± 7.3%) was measured at 125 µM.

Table 6.4 The dose-dependent effects of 2-MeNH on SH-SY5Y and S.NNMT.LP cell viability.

Cell line	Toxicity (µM)	Significance	Increased viability (µM)	Significance
SH-SY5Y	250, 500, 1000, 2000	$p < 0.001$	N/A	N/A
S.NNMT.LP	500, 1000, 2000	$p < 0.001$	62.5, 125	$p < 0.001$

A significant difference in toxicity was seen between cell lines at 125 µM (-3.9 on the log scale, $p < 0.001$) and 250 µM (-3.6 on the log scale, $p < 0.01$). The log $EC50_{MTT}$s (in M) for SH-SY5Y and S.NNMT.LP cells exposed to 2-MeNH were -3.59 ± 0.02 (equivalent to 257 µM) and -3.45 ± 0.03 (equivalent to 355 µM) respectively. The difference between the $EC50_{MTT}$s was significant ($p = 0.009$).

A statistical comparison of the log $EC50_{MTT}$s for NH from Chapter 5 with those presented here revealed that NH was more toxic than 2-MeNH to both SH-SY5Y cells (NH: –3.79 ± 0.06 (162 µM) vs 2-MeNH: -3.59 ± 0.02 (257 µM), $p = 0.02$) and

S.NNMT.LP (NH: -3.81 ± 0.05 (155 µM) vs 2-MeNH: -3.45 ± 0.03 (355 µM), p = 0.0005). Comparisons between individual concentrations were not possible due to the differing concentration ranges used to produce the dose-response curves; these differences were necessitated in order to obtain optimal maxima and minima in cell viability for each toxin. Figure 6.4 shows the comparative toxicity profiles of the 2 compounds towards each cell line.

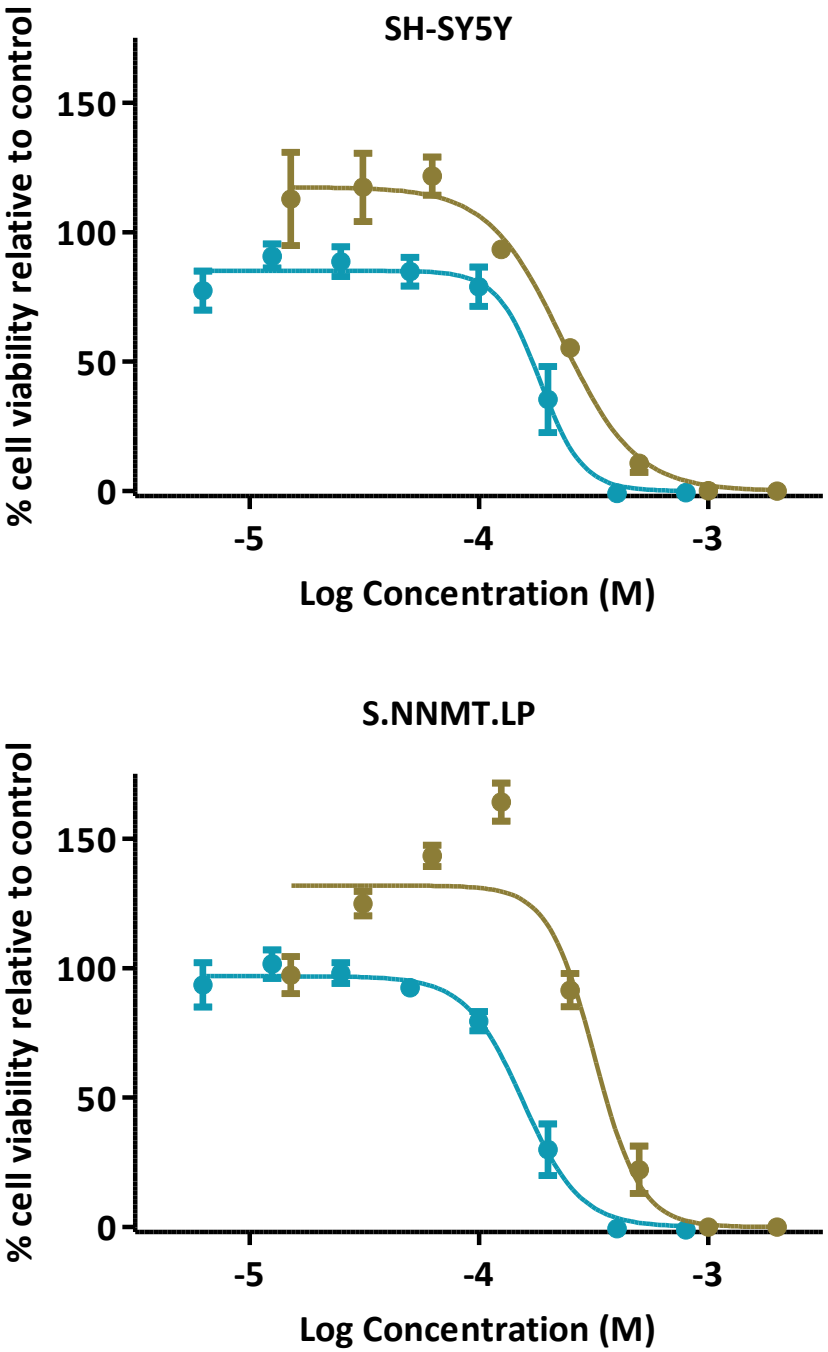

Figure 6.4. Comparative toxicity curves of NH (turquoise) and 2-meNH (brown) in SH-SY5Y cells (top) and S.NNMT.LP cells (bottom) following 5-day incubations. Cell viability was determined via MTT assay. All data are mean ± SEM, n = 4.

6.3.2.2. The ATP content of S.NNMT.LP cells was significantly protected against 2-MeNH compared with SH-SY5Y cells

A dose-response curve of ATP content, derived from mean data from each experimental repeat (n = 4), is shown in figure 6.5. The individual curves from each experimental repeat, which were used to generate 1 $EC50_{ATP}$ per cell line and 1 set of mean data for each of the individual dose comparisons, are shown in Appendix 2.

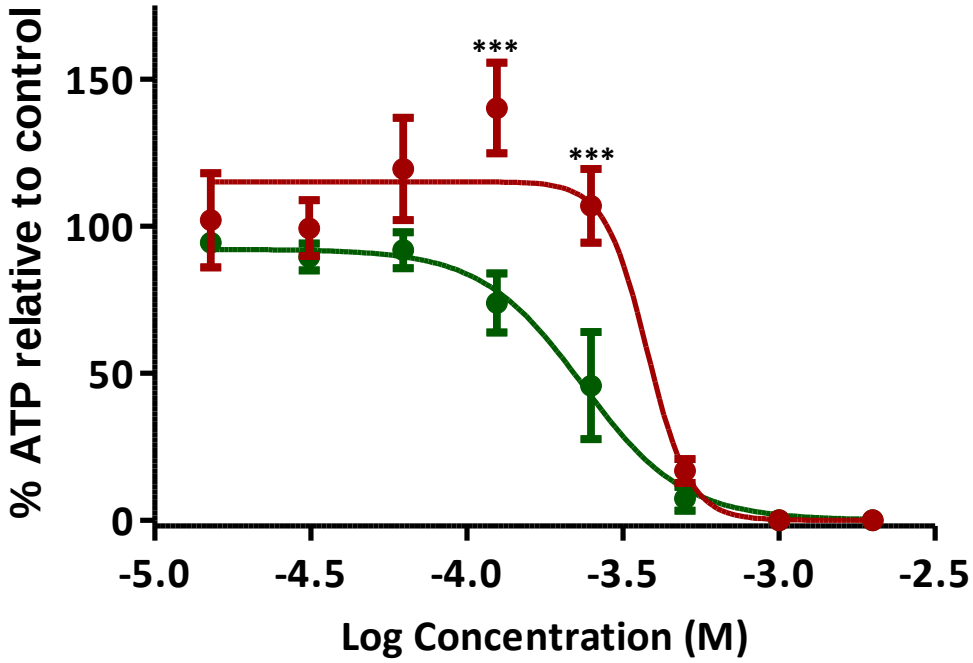

Figure 6.5. The dose response curve of 2-meNH toxicity towards SH-SY5Y cells (green circles) and S.NNMT.LP cells (red circles) after a 5 day incubation. Cell viability was determined via ATP assay. All data are mean ± SEM, n = 4. *** = p < 0.001 S.NNMT.LP vs SH-SY5Y.

As summarised in table 6.5, 2-MeNH significantly reduced ATP content in SH-SY5Y cells at concentrations of 250 µM, 500 µM, 1mM and 2 mM (all $p < 0.001$). In S.NNMT.LP cells, 2-MeNH significantly reduced ATP content at 500 µM, 1mM and 2 mM (all $p < 0.001$). 2-MeNH also caused a significant increase in ATP content in S.NNMT.LP cells 125 µM ($p < 0.05$). This effect was absent in SH-SY5Y cells. The maximum increase in ATP content (+40 ± 15%) was observed at 125 µM.

Table 6.5. The dose-dependent effects of 2-MeNH on the ATP content of SH-SY5Y and S.NNMT.LP cells.

Cell line	Reduced ATP content occurred (µM)	Significance	Increased ATP content occurred (µM)	Significance
SH-SY5Y	250, 500, 1000, 2000	$p < 0.001$	N/A	N/A
S.NNMT.LP	500, 1000, 2000	$p < 0.001$	125	$p < 0.05$

A significant difference in ATP content was seen between cell lines at 125 µM (-3.9 on the log scale) and 250 µM (-3.6 on the log scale, figure 6.5, both $p < 0.001$). The log $EC50_{ATP}$s (in M) for SH-SY5Y and S.NNMT.LP cells incubated with 2-MeNH were -3.67 ± 0.114 (equivalent to 214 µM) and -3.41 ± 0.0321 (equivalent to 389 µM) respectively. The difference between the 2 log $EC50_{ATP}$s was not significant ($p = 0.07$).

A comparison of the NH ATP data from the previous chapter with the data presented here showed that NH was more effective at reducing ATP content by

50% than 2-MeNH in S.NNMT.LP cells as illustrated by the $EC50_{ATP}$s (NH: -3.76 ± 0.04 (174 µM) vs 2-MeNH: -3.41 ± 0.03 (389 µM), p = 0.0002). However, for SH-SY5Y cells, there was no difference between the NH and 2-MeNH log $EC50_{ATP}$s (NH: –3.58 ± 0.05 (263 µM) vs 2me-NH: -3.67 ± 0.11 (214 µM), p = 0.47). Figure 6.6 shows the comparative profiles of the 2 compounds towards each cell line.

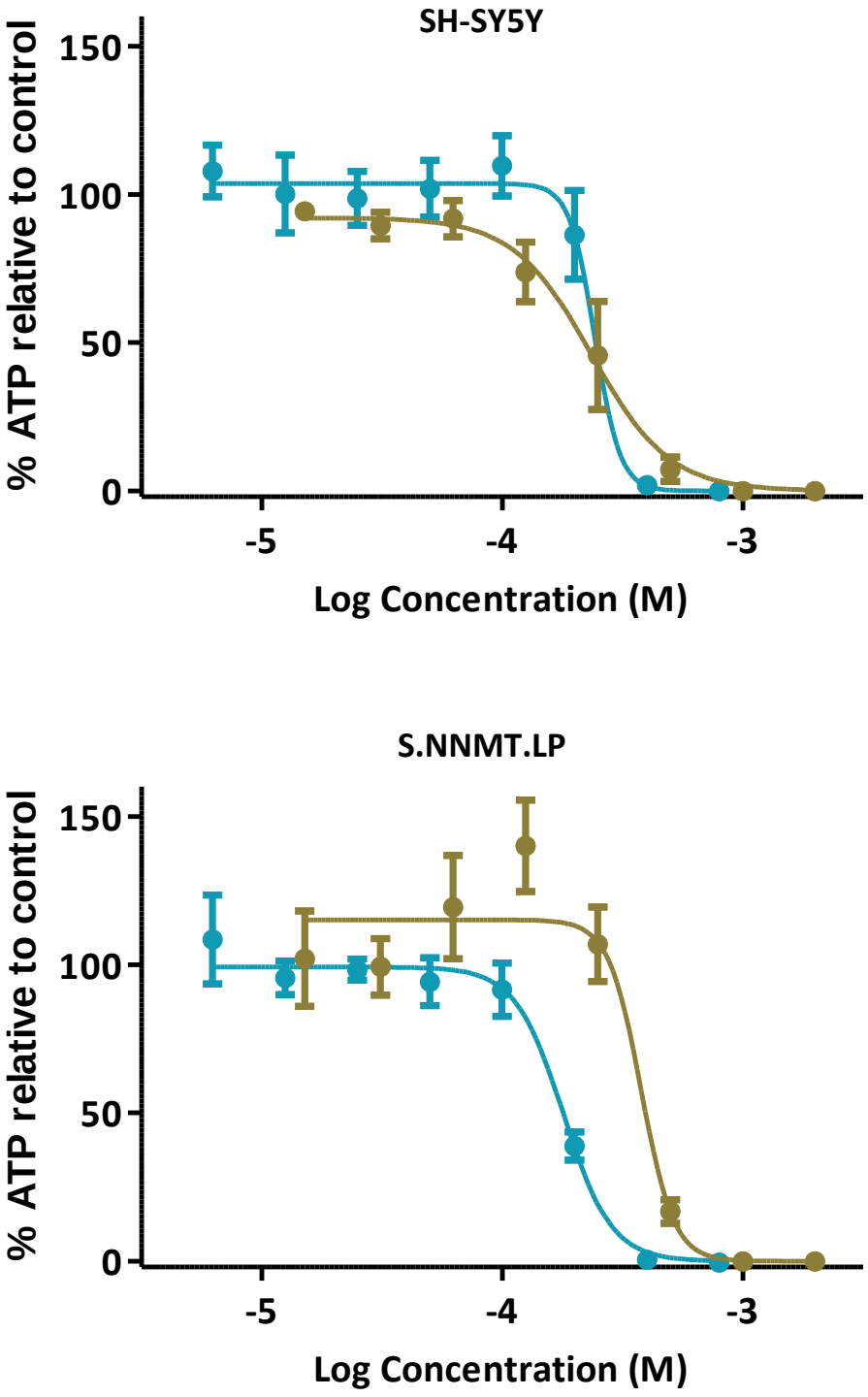

Figure 6.6. Comparative toxicity curves of NH (turquoise) and 2-meNH (brown) in SH-SY5Y cells (top) and S.NNMT.LP cells (bottom) following 5-day incubations. Cell viability was determined via ATP assay. All data are mean ± SEM, n = 4.

A *t*-test analysing the differences in 2-MeNH log $EC50_{MTT}$ and log $EC50_{ATP}$ showed that the 2-MeNH log EC50s were the same across the 2 assays in both SH-SY5Y cells ($EC50_{MTT}$: -3.59 ± 0.02 (257 µM) *vs* $EC50_{ATP}$: -3.67 ± 0.11 (214 µM), p = 0.51) and S.NNMT.LP cells ($EC50_{MTT}$: -3.45 ± 0.03 (355 µM) *vs* $EC50_{ATP}$: -3.41 ± 0.03 (389 µM), p = 0.38).

6.3.3. Investigation of NNMT's NH *2N*-methyltransferase activity

6.3.3.1. SRM transitions of 2-MeNH and THNH

The infusion of 1 µg/mL synthesised 2-MeNH standard, followed by MS/MS at a collision energy of 33 V resulted in the identification of the following parent-product ion transitions (in *m/z*): 183 → 168, 183 →140, 183 → 115. The full scan MS/MS spectrum showing these transitions is shown in figure 6.7.

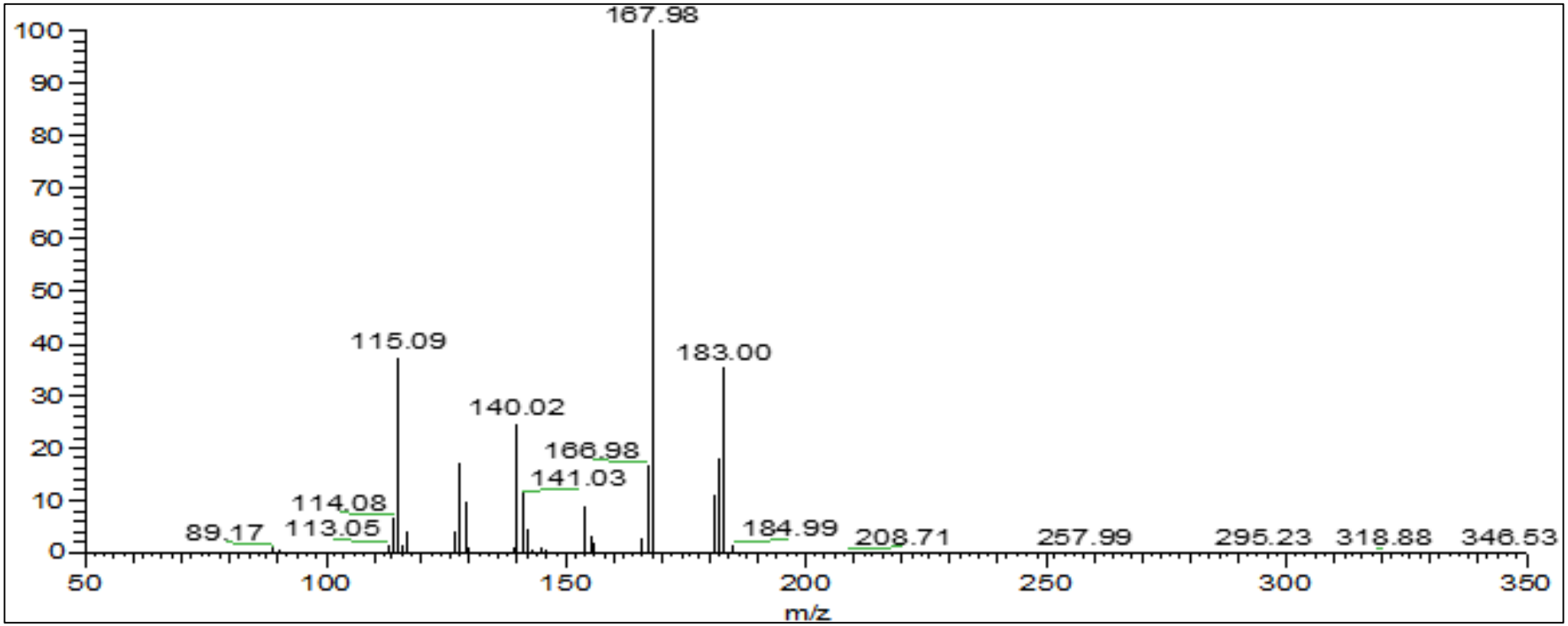

Figure 6.7. Full scan spectrum of 2-meNH m/z following fragmentation of the 183 m/z parent ion via MSMS. Three specific transitions were identified: 183 → 168, 183 →140 and 183 → 115.

The infusion of 1 µg/mL THNH standard, followed by MS/MS at a collision energy of 12 V resulted in the identification of a single parent-product ion transition (in *m/z*): 173.1 → 144.

6.3.3.2. Determination of NNMT NH 2N-methyltransferase specific activity

2-MeNH was quantified *via* the 183 → 168 transition. 2-MeNH production increased with time in the proof-of-concept enzyme assay (figure 6.8). v_i was determined as 0.63 nmol 2-MeNH/minute/mg NNMT. Accordingly, specific activity was determined as 38.1 nmol 2-MeNH/hour/mg NNMT. Data from t = 60 minutes were not included as peak-splitting and saturation of signal had occurred.

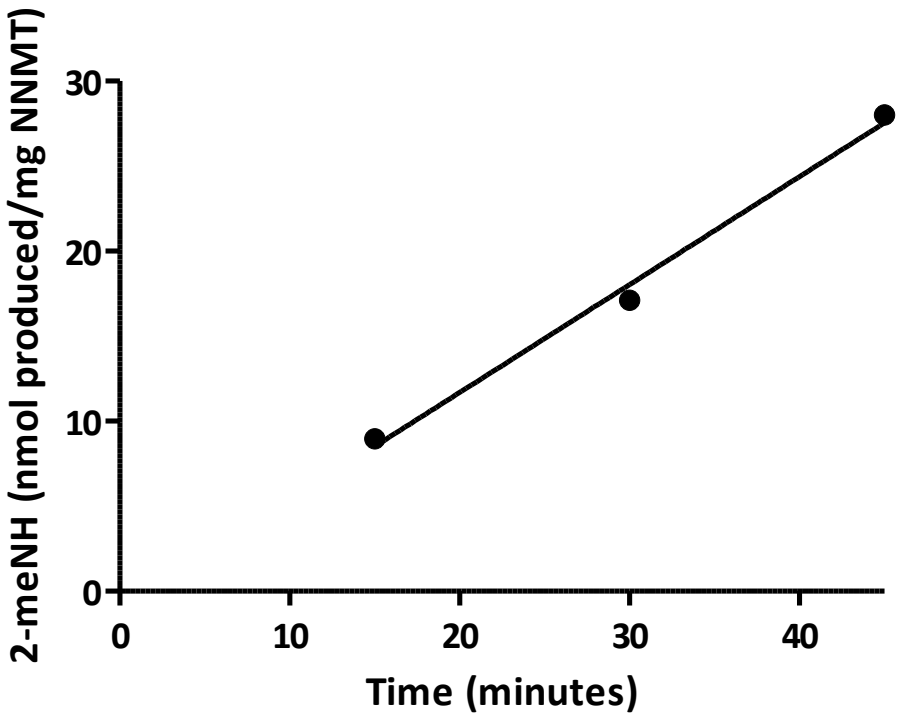

Figure 6.8. The NNMT-mediated production of 2-MeNH over time

6.3.4. The kinetic parameters of NNMT NH 2*N*-methylation

The Michaelis-Menten, Eadie-Hofstee and Hanes-Woolf plots of 2-MeNH production by NNMT are shown in figures 6.9, 6.10 and 6.11 respectively. The individual graphs at each NH concentration that were used to determine the points on the Michaelis-Menten plot can be found in appendix 3.

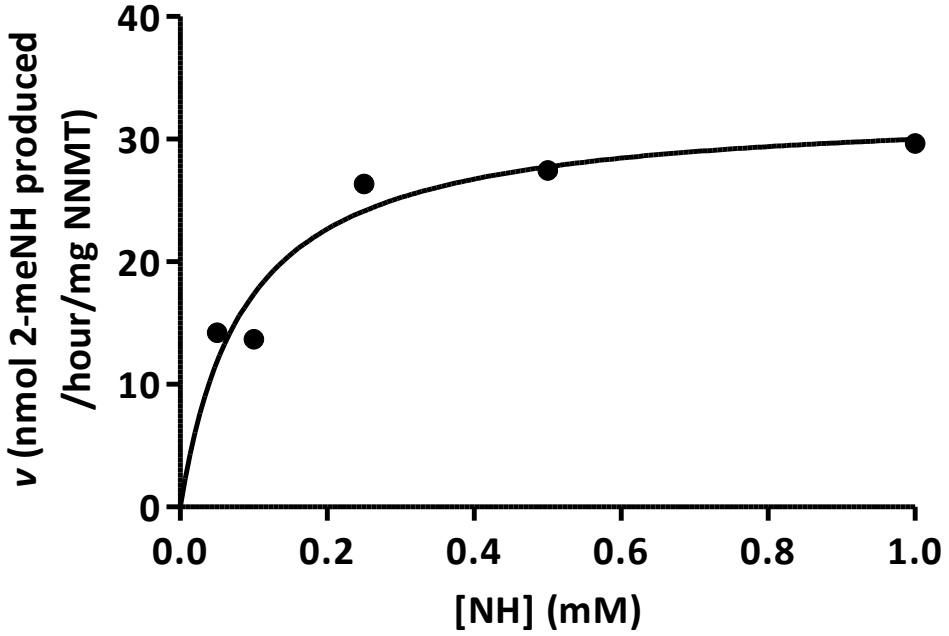

Figure 6.9. Michaelis-Menten plot of NH 2N-methyltransferase activity of NNMT.

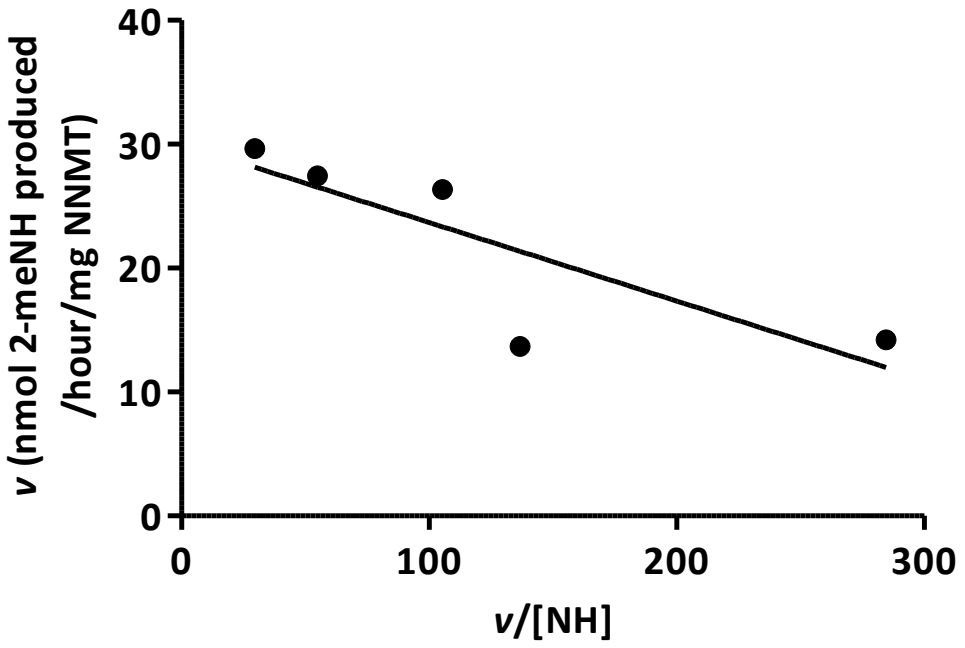

Figure 6.10. Eadie-Hofstee plot of NH 2N-methyltransferase activity of NNMT.

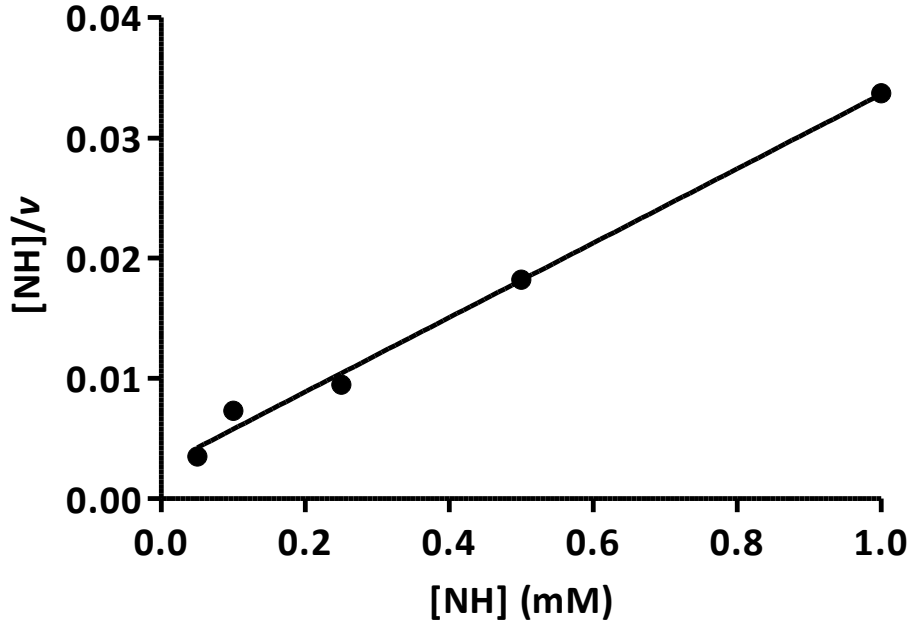

Figure 6.11. Hanes-Woolf plot of NH 2N-methyltransferase activity of NNMT.

The calculations of V_{max} and a K_m derived from each plot are shown in table 6.6. Initially data were modelled using the standard Michaelis-Menten equation:

$$v = \frac{Vmax[S]}{Km + [S]}$$

The transformations for the Eadie-Hofstee and Hanes-Woolf plots (detailed in section 6.2.4.3) were used to determine K_m and V_{max} *via* the axes of each plot. In the Eadie-Hofstee plot V_{max} was derived from the Y-intercept. Subsequently K_m, was determined from the X-intercept by solving the equation:

$$X - intercept = \frac{Vmax}{Km}$$

In the Hanes-Woolf plot, the x-intercept was used to obtain -Km. Subsequently, V_{max}, was determined from the Y-intercept by solving the equation:

$$Y - intercept = \frac{Km}{Vmax}$$

Table 6.6. K_m and Vmax calculations from various plots of enzyme assay data for the determination of NNMT's NH 2N-methyltransferase activity.

Plot	K_m (mM)	Vmax (nmol 2-MeNH/hour/mg NNMT)
Michaelis-Menten	0.0878	32.6
Eadie-Hofstee	0.0634	30.0
Hanes-Woolf	0.0872	32.3

6.4. Discussion

Summary of key findings

- ***Synthesis of 2-MeNH was successful. However, the synthesis of 2,9-diMeNH was unsuccessful***
- ***S.NNMT.LP cell viability and ATP content were less susceptible to 2-MeNH toxicity than SH-SY5Y***
- ***NNMT demonstrated NH methyltransferase activity***

6.4.1. The synthesis of 2-MeNH, but not 2,9-diMeNH, was successful

The 2 NMR spectra, melting point analysis and *m/z* ratio all confirmed the successful synthesis of 2-MeNH. Unfortunately, this was not the case for 2,9-diMeNH which did not show matching NMR spectra to the literature, nor was there a significant yield synthesised. The reasons for this are unclear but could be due to a lack of detail in the Cao *et al*. (2005) published method. The method described by Cao *et al*. produced a yield of 73%, vastly exceeding the yield achieved by the synthesis in this study (<5%). Furthermore, the small amount of product that was eventually produced did not match the published NMR spectra.

There are 2 possible reasons for these differences. Firstly, the extraction in the reported method may have included and additional, unreported, step to further enhance the yield. Thus, in this study it is possible that the product remained in the aqueous phase following extraction. However, the fact that the extract did not

show matching NMR spectra suggests that even a better extraction may not have yielded the desired product. The second explanation is that the successful synthetic procedure performed by Cao *et al*. (2005) contained additional steps or conditions to ensure the correct product was formed that were omitted from the manuscript in error. This may have occurred as a result of the 2,9-diMeNH being a modification of another synthesis (2,9-Dibenzyl-1-methyl-NH) in the manuscript. Thus, the synthesis of the wrong product in this study may have resulted in the extraction producing a low yield.

The NMR spectra of the product indicated that di-methylation had indeed occurred but likely not at both the 2*N* and 9*N* positions. This was unexpected considering that the aliphatic nitrogen was expected to more readily to bond the methyl group than an aromatic carbon due to its higher reactivity. However, considering, as mentioned above, that the 2,9-diMeNH method was based upon the synthesis and extraction of a 1-methyl NH derivative, it is possible that the 2nd methylation took place at the 1*C* position. However, this would need confirmation *via* additional experiments e.g. 2-dimensional NMR.

Unfortunately, due to time constraints, it was not possible to establish an alternative protocol for synthesis of 2,9-diMeNH. However, future work will look to refine the process in order to achieve a successful synthesis of 2,9-diMeNH. Furthermore, as the 2*N*-methyation at NH's pyridine ring is more likely for NNMT given its known activity, and due to the fact that it is the first step in the proposed methylation pathway, the successful synthesis of 2-MeNH is the more physiologically relevant.

6.4.2. S.NNMT.LP cell viability and ATP content were less susceptible to 2-MeNH toxicity than SH-SY5Y

Both assays used in this study revealed significant differences between SH-SY5Y and S.NNMT.LP cells following 2-MeNH incubation. Furthermore, the lack of significant difference between $EC50_{MTT}$ and $EC50_{ATP}$ for each cell line suggested that the effects of 2-MeNH to each cell line were consistent across both assays.

Not only did toxicity begin at significantly lower concentrations in SH-SY5Y cells, 125 µM 2-MeNH significantly enhanced MTT reduction and ATP content in S.NNMT.LP cells but not SH-SY5Y. This lead to a significant difference in log $EC50_{MTT}$ between the cell lines but not the log $EC50_{ATP}$. However, various other factors were significantly different in the ATP assay: the concentration at which a significant reduction of ATP began was higher in LP cells; the enhancement of ATP content occurred in S.NNMT.LP cells but not in SH-SY5Y cells; ATP content in S.NNMT.LP was significantly higher at 125 µM and 250 µM compared with SH-SY5Y. Furthermore the difference in $EC50_{ATP}$ ($p = 0.07$) was trending towards significance and thus, it is likely that, with further repetition, the difference in log $EC50_{ATP}$s would become significant.

The data discussed here are in line with previously reported data regarding the resistance of S.NNMT.LP cells to toxicity mediated by CxI inhibitors (Parsons *et al.* 2011, Milani, Ramsden & Parsons 2013). In these studies, S.NNMT.LP cells were significantly less susceptible to the toxicity of rotenone and MPP^+ compared with SH-SY5Y cells, an effect mediated by increased MeN production. Due to the fact that 2-MeNH is also a CxI inhibitor (Albores *et al.* 1990) it is, therefore, likely that

the S.NNMT.LP cells in this study were protected *via* similar mechanisms. S.NNMT.LP cells are protected by preventing the toxin-induced degradation of subunits of CxI (e.g. NDUFS3), thereby maintaining CxI activity and ATP production (Parsons *et al*. 2011). Maintenance of ATP content will conceivably also maintain cell viability, thus potentially explaining why the protective effects in this study were seen in both assays.

In addition to the reduced susceptibility of S.NNMT.LP cells to 2-MeNH toxicity, as mentioned above, they also showed significantly increased viability and ATP content above that observed in untreated cells at 125 µM and also to a lesser extent at 62.5 µM (which only demonstrated viability enhancement in the MTT assay) 2-MeNH. As these significant enhancements were seen in both assays, it is possible that the mechanisms for this phenomenon are inter-linked. Indeed, it is hypothesised that the increased viability seen in S.NNMT.LP cells incubated with 125 µM 2-MeNH arose as a result of the concomitantly increased ATP synthesis

As discussed in chapter 4, simply expressing NNMT-V5 in SH-SY5Y cells is sufficient to increase ATP synthesis *via* an increased CxI activity (Parsons *et al*. 2011). Furthermore, NNMT-V5 expression in SH-SY5Y induces cell signalling such as the cytoprotective EFNB2 and Akt pathways (Thomas *et al*. 2013). Thus, it is possible that the synergy between NNMT-V5 expression and 2-MeNH may involve these pathways. As mentioned above, 2-MeNH is a CxI inhibitor. However, 2-MeNH's activity at CxI is relatively weak with an IC50 almost 7-fold higher than MPP^+ (Albores *et al*. 1990). Thus, an explanation for the enhanced viability and ATP content in S.NNMT.LP cells could be that the inhibition of 2-MeNH of CxI at those

concentrations is sufficient to trigger additional protective mechanisms mediated by NNMT without being excessively damaging to ATP production as a whole, thus the cell is able to compensate for the presence of the CxI inhibitor. This, however, is speculative and future studies will be required to confirm this.

In general, 2-MeNH appeared to be less toxic to either cell line than its precursor, NH. This was true for both the $EC50_{MTT}$ and $EC50_{ATP}$ in S.NNMT.LP cells but only for the $EC50_{MTT}$ in SH-SY5Y cells. This may indicate that 2-MeNH and NH have different mechanisms of action and thus different toxicity. While Albores and colleagues (Albores *et al*. 1990) did not study NH specifically, they suggested that neutral βCs may act on complexes II and III of the mitochondrial respiratory machinery, in contrast to the cationic forms which predominantly work on CxI. However, a specific mechanism for NH toxicity is unknown as it is principally thought to be toxic following its di-*N*-methylation to 2,9-diMeNH (Pavlovic *et al*. 2006).

Another reason for the difference in toxicity between NH and 2-MeNH may be related to the route of the compounds' entry into the cell. Wernicke *et al*. (2007) reported that 2-MeNH toxicity is highly dependent upon the presence of DAT. In their study, 2-MeNH toxicity was equal to that of NH in HEK cells that did not express recombinant, human DAT. However, in HEK cells that did express DAT, 2-MeNH EC50 was over 7x lower (Wernicke *et al*. 2007). In this study, NH was significantly more toxic than 2-MeNH to cell viability (as measured according to $EC50_{MTT}$s). Thus, NH could be more readily getting into the cells than 2-MeNH and thus reaching higher intracellular concentrations. However, one caveat to comparing data from this study with the one performed by Wernicke and

colleagues is that the degree of DAT activity in the transfected HEK cells relative to that in the brain is not known. Therefore, it is possible that the successful transfection of DAT may have resulted in an overexpression and, thus, exaggeration of any DAT-dependent toxicity. Another caveat to comparing the data published by Wernicke and colleagues with the data shown here is that the HEK cells are derived from the kidney and are also embryonic rather than tumourigenic. Thus, cell line differences may be responsible for the differential toxicity observed.

It is widely assumed that SH-SY5Y neurons express DAT (Cheung *et al.* 2009, Xie, Hu & Li 2010, Korecka *et al.* 2013). However, SH-SY5Y that have not been differentiated into a neuronal phenotype only express low levels of DAT (Presgraves *et al.* 2004). This lower expression in undifferentiated SH-SY5Y cells has been suggested as the principal reason for a lower susceptibility to MPP^+ compared with cells with higher DAT expression (Fang, Zuo & Yu 1995, Presgraves *et al.* 2004). Therefore, in this study, it is possible that the lack of 2-MeNH toxicity in both cell lines occurred because low DAT expression did not permit sufficient 2-MeNH entry into the cell.

In order to confirm whether the low 2-MeNH toxicity is due to the absence of DAT, the toxicity experiments should be repeated using cells expressing recombinant human DAT *via* an inducible expression system. Any alteration in 2-MeNH toxicity following DAT expression could be further investigated in the presence of the DAT-inhibitor 1-(2-[bis(4-fluorophenyl)methoxy] ethyl)-4-(3 phenylpropyl) piperazine (GBR 12909).

While the possibility of 2-MeNH toxicity being potentiated by DAT warrants investigation, both cell lines are expected to express DAT to a degree. Furthermore,

despite a theoretically lowered 2-MeNH uptake, due to the relatively long duration of the study a significant amount of 2-MeNH is expected to have entered the cell. In particular, the charged nature of 2-MeNH may facilitate its eventual sequestration into the mitochondria (Ramsay *et al.* 1989). Thus, 2-MeNH may genuinely be less toxic than NH in these cells.

Should this indeed be the case, this raises interesting questions about the 2*N*-methylation of NH. Namely, is it actually a toxicity-enhancing event or is detoxification occurring? The lower toxicity of 2-MeNH compared with NH in these studies suggests that conversion of NH to 2-MeNH in the brain may in fact be a detoxification pathway. If this is indeed the case, the conversion of NH to 2-MeNH may be protecting cells from the toxicity mediated by elevated levels of NH in PD brains.

6.4.3. NNMT has NH *2N*-methyltransferase activity

The initial LC-MS data presented in section 6.3.3.1 confirmed the production of 2-MeNH. Furthermore, the linear increase in 2-MeNH production over time suggested that no product inhibition of the reaction was occurring, a phenomenon that can occur with other enzymes (e.g. cysteine dioxygenase (Parsons *et al.* 1998)) As such, this is the first demonstration that NNMT has NH *N*-methyltransferase activity.

The successful Michaelis-Menten curve fit of the specific activity data (figure 6.9) demonstrated that the reaction followed Michaelis-Menten kinetics, and allowed an estimation of K_m and V_{max}. However, the range of NH concentrations used in this

preliminary study did not include sufficient data points derived from concentrations within the linear portion of the curve, i.e. below 0.25 mM, although the plateau portion of the curve was well defined and a Michaelis-Menten curve with a good fit (r^2 = 0.99) was obtained. Nevertheless, further data points below 0.25 mM would improve the calculation of K_m and V_{max} by improving the gradient of the linear portion of the curve. Furthermore, the values for K_m and V_{max} were derived from a single experiment. Thus, repetition of the assay will permit more accurate determination of the kinetic constant. Accordingly, the K_m and V_{max} derived from these data should be viewed primarily as an estimate.

Due to the tendency for reciprocal data to amplify any experimental errors, the Km and Vmax of 0.0878 mM and 32.6 nmol/hour/mg NNMT respectively determined by the Michaelis-Menten plot, rather than the linear plots, should be viewed as the most reliable. The Hanes-Woolfe plot, which is often used as for confirmation of Michaelis-Menten-derived Km and Vmax (Nelson & Cox 2008), produced very similar constants. The Eadie-Hofstee-derived constants differed from the above 2 plots but the plot was principally created to determine whether substrate inhibition had occurred, as is observed when nicotinamide is a substrate (Patel *et al*. 2013). Accordingly, the lack of divergent points from the linear regression analysis suggested that substrate inhibition of the reaction was not occurring.

With the above considerations in mind, direct comparison of the Michaelis-Menten-derived K_m for NH reported here with other studies reporting K_m values for nicotinamide indicated that NNMT may have a higher affinity for NH than nicotinamide. For example, Patel *et al*. (2013) reported that the K_m for human

NNMT activity using nicotinamide was 1.36 mM, 15 times higher than the one reported here. However, in contrast, the V_{max} reported by Patel *et al*. (123.4 nmol/hour/mg protein) was almost 4-times higher despite being derived from homogenate and not isolated protein, and as such would be expected to be a lower estimate of V_{max} than one calculated using isolated protein. The same trend was seen in a study by Rini *et al*. (1990). Here, K_m of NNMT activity with nicotinamide as a substrate was 0.347 mM, 4-times higher than reported here. However, the V_{max} was reported to be 51.5 nmol/hour/mg protein, 1.6-times the value determined here.

Although the data presented here are only an estimate, the kinetic differences between NH and nicotinamide are in accordance with the detoxification theory presented above. While nicotinamide remains the primary substrate of NNMT, in the presence of growing concentrations of NH, the greater affinity of NH for NNMT will result in a favourable removal of NH from the cytosol, preventing its accumulation and limiting its ATP-reducing effects which occur at higher concentrations. Further experiments are required to confirm the kinetic differences between the 2 substrates.

This is the first demonstration of NNMT's ability to catalyse the 2*N*-methylation of NH, and is the first direct evidence of an *N*-methyltransferase with the capability to *N*-methylate NH. Coupled with the discovery that NNMT-V5-expressing cells are protected from 2-MeNH toxicity and that 2-MeNH was less toxic to all cells compared to its precursor NH, these findings reinforce the hypothesis that NNMT

expression in PD may be acting as a stress response to the disease pathogenesis. However, there are some caveats to this.

Firstly, the ability of NNMT to produce 2-MeNH has only been demonstrated in purified protein and may be significantly different in the more physiologically-relevant environment of the cell. For example, competition for the NNMT active site would likely occur between NH, nicotinamide and any other endogenous NNMT substrates. This would reduce the rate at which NNMT can produce 2-MeNH, especially as the apparent V_{max} is substantially lower than that for nicotinamide. This is in accordance with the finding in chapter 5 that 200 µM NH reduced ATP content to a significantly greater extent in S.NNMT.LP cells than SH-SY5Y cells. Thus, NH, which is more toxic to S.NNMT.LP cells at this dose was likely not converted to 2-MeNH at a sufficient rate to eliminate NH's ATP reducing effects. However, this difference, while statistically significant, was not very large. Also, as mentioned in chapter 5, the concentrations used in the study were supraphysiological. Therefore, in the presence of the lower, physiological concentrations, NNMT-mediated NH 2*N*-methylation may be sufficient to prevent an accumulation of NH to toxic concentrations.

Secondly, should NNMT-expressing cells indeed be capable of producing 2-MeNH *in situ*, they will have produced a compound that is only 1 step away from becoming a much more potent toxin (2,9-diMeNH). Thus, NNMT's ability to produce 2-MeNH could still implicate it in the bio-activation of βCs in PD. While NH 9*N*-methyltransferase is yet to be fully characterised and identified, the lack of toxicity observed in S.NNMT.LP cells incubated with 2-MeNH suggests that NNMT itself

does not catalyse the formation of 2,9-diMeNH. Moreover, there are no reports of NNMT catalysed *N*-methylation moiety besides pyridine groups. Thus, on its own, NNMT is likely to act as a detoxification mechanism for NH by producing 2-MeNH. However, in the presence of a 2-MeNH 9*N*-methyltransferase, this step could in fact potentiate toxicity. This supports the notion that, in certain circumstances, the expression of NNMT in PD may represent a double-edged sword by providing neuroprotection on the one hand, but potentiating toxicity on the other.

6.4.4. Summary

S.NNMT.LP cells were significantly less susceptible to 2-MeNH toxicity than SH-SY5Y cells. This is likely to be due to the ability of S.NNMT.LP cells to resist the toxicity of CxI inhibitors due to the expression of NNMT-V5. Considering that NNMT was found to possess 2*N*-methyltransferase activity and, thus, the ability to produce 2-MeNH, this raises interesting questions about the interaction of βCs and NNMT in PD.

Firstly, can NNMT catalyse the 2-*N*-methylation of NH *in situ*? Future work could determine this by replacing purified NNMT with homogenised S.NNMT.LP cells exposed to NH in a cell free assay. Also, S.NNMT.LP cells could be incubated with NH before being analysed for the production of 2-MeNH using mass spectrometry.

Secondly, is 2-MeNH not as toxic as previously reported, or is the lack of toxicity in this study due to insufficient entry into the cell? This could be answered *via* studies involving SH-SY5Y and S.NNMT.LP cells transfected with DAT.

Finally, what is the mechanism for the S.NNMT.LP cells' increased susceptibility to NH? It was originally hypothesised that the formation of 2-MeNH or possible downstream conversion to 2,9-diMeNH could have been responsible for the increased vulnerability of S.NNMT.LP cells to NH. However, these studies showing a decreased susceptibility to 2-MeNH by S.NNMT.LP cells cast doubt on this theory. Instead, it is possible that NH and 2-MeNH may have a different, but as of yet, undetermined action on NNMT-expressing cells, and that the conversion of NH to 2-MeNH is in fact a detoxification pathway. In order to provide the most compelling evidence for NNMTs role in PD, future studies involving upregulated NNMT expression *in vivo* and in the presence of βCs are required.

7. Discussion

7.1. The contribution of the project towards establishing the role of NNMT in PD

7.1.1. Summary of the project thus far

As discussed in chapter 1, PD is a disease in which the inherently high energy demands of SNpc dopaminergic neurons results in an innate degree of stress, both in terms of maintaining ATP production and in terms of limiting the production of ROS. As part of a multiple-hit hypothesis, many, sometimes minor, factors are thought to accumulate with time and gradually increase the strain upon SNpc neurons until they reach their cytotoxic threshold. This project investigated the possibility that NNMT is involved in this phenomenon, either as a propagator of toxicity or as a protective agent against the degenerative process.

The studies carried out in this project have yielded 5 key points about the role of NNMT in cell survival. Firstly, NNMT expression enhanced cell viability in SH-SY5Y cells. Secondly, NNMT expression conferred an increased susceptibility to NH toxicity *in vitro*. However, this susceptibility was confined to loss of ATP content and only occurred at 1 concentration. Thirdly, NNMT expression conferred protection against 2-MeNH toxicity *in vitro*. Fourthly, 2-MeNH was less toxic than NH in both cell lines. Finally, purified NNMT was able to convert NH to 2-MeNH.

7.1.2. The effects of NNMT expression on the cell

In light of chapter 4 and publications from other disease areas (Cuomo *et al.* 1994, Mateuszuk *et al.* 2009, Kim *et al.* 2010, Sternak *et al.* 2010, Tang *et al.* 2011, Zhang

et al. 2014) it appears that increasing NNMT expression in PD may be protective by enhancing CxI activity and subsequently ATP production. In the PD brain, this would be expected to mitigate neurodegeneration by enhancing ATP content and preventing ROS production *via* electron leakage from damaged CxI. The enhancement of ATP production will additionally help reduce the damage caused by ROS by increasing the ATP-dependent production of the antioxidant glutathione, which itself is reduced in PD (Zeevalk, Razmpour & Bernard 2008).

These findings raise interesting questions about the induction of NNMT expression in the brain of PD patients. Is the expression of NNMT, which is higher in the brains of patients with PD (Parsons *et al*. 2002, Parsons *et al*. 2003) induced as a protective response following the onset of PD or does the increased NNMT expression predate the onset of PD? If it is the former, then it would appear highly likely that NNMT expression can be induced to protect SNpc brain cells. However, if it is the latter and NNMT expression is elevated from birth then, considering its association with PD, the elevated expression of the enzyme could be contributing to the disease pathogenesis despite its protective effects. This could, therefore, implicate NNMT as a genetic susceptibility factor. Considering that the relative activity of NNMT is dependent solely on the levels of its mRNA rather than mutations in its gene coding region (Smith *et al.* 1998), genetic analysis of the NNMT gene in patients may not yield an answer to this question. Instead, it may be useful to investigate other genetic factors that could directly induce NNMT expression. Should SNPs in other genes become known that result in a higher production of NNMT mRNA, this could provide evidence for enhanced NNMT expression representing a genetic

predisposition rather than an adaptive response in PD. However, in the absence of this information, the current evidence suggests that NNMT may be upregulated by cells of the brain to protect CxI, maintain ATP content and promote Akt signalling in order to counteract the deleterious pathogenic mechanisms of PD.

7.1.3. The effect of NNMT expression on the toxicity of NH

While NNMT's role as a protective agent appears plausible, data from chapter 5 suggest that, in certain circumstances, NNMT expression may in fact be detrimental to the cell. The discovery that the NNMT-V5 expressing S.NNMT.LP cells were more susceptible than non-expressing cells to NH-mediated reduction in ATP content supports the hypothesis put forth by others that NNMT may increase the toxicity of βCs (Matsubara *et al.* 2002, Williams, Cartwright & Ramsden 2005). However, the difference in ATP content, while significant, only occurred at 1 concentration. Furthermore, this susceptibility was confined to the ATP assay, suggesting that NH did not reduce ATP content sufficiently to affect cell viability.

In section 5.4.1 it was hypothesised that, over time, NH-mediated depletion of ATP may become sufficient to affect viability. In addition the NH-mediated depletion of ATP may combine with other PD-causing factors as part of the multiple-hit hypothesis, to further exacerbate ATP loss to the extent where cell death is initiated. However, this would need to occur *via* the accumulation of NH in the SNpc (Östergren *et al.* 2004), something which may be counteracted by the conversion of NH to 2-MeNH by NNMT (discussed more below). Indeed, the data in chapter 6, showing NNMT-mediated production of 2-MeNH, significant protection

of both ATP content and cell viability in S.NNMT.LP cells incubated with 2-MeNH, and a reduced toxicity of 2-MeNH compared to NH in both cell lines, suggest that conversion of NH to 2-MeNH may be a detoxification process. Thus, the steady conversion of NH to 2-MeNH in the brain could be acting as a buffer to prevent the accumulation and eventual toxicity of NH.

7.1.4. The NNMT-mediated conversion of NH to 2-MeNH may be a detoxification pathway

The data in chapter 6 represent the first demonstration of NNMT's ability to convert NH to 2-MeNH. PNMT has previously also been reported as a βC 2*N*-methyltransferase (Gearhart, Neafsey & Collins 2002), though this was for the conversion of 9-MeNH to 2,9-diMeNH. While this may imply that PNMT may be able to also catalyse the conversion of NH to 2-MeNH, there is no experimental data to support this. Indeed, the physiological relevance of this finding is unclear, given that 9-MeNH is reported not to occur naturally in the brain (Matsubara, Neafsey & Collins 1992). Should the estimated K_m reported in chapter 6 for NNMT be confirmed in future studies, NNMT would appear to have a greater affinity for NH than nicotinamide. Accordingly, while nicotinamide concentration will always be in excess of NH, in the presence of rising intracellular concentrations of NH, NH will be able to out-compete nicotinamide for NNMT's active site. Thus, NH produced in the cell can be quickly removed, preventing its accumulation and allowing it to be maintained at low concentrations. Comparison of V_{max} suggests that NNMT's overall ability to 2*N*-methylate NH appears to be lower than that reported for nicotinamide

(Rini *et al.* 1990, Patel *et al.* 2013). Accordingly, NNMT may not be a prolific 2*N*-methylator of NH but may nevertheless favourably convert NH to 2-MeNH when the former is produced in the cell, allowing the mitigation of its potential toxicity.

Interestingly, not only was 2-MeNH less toxic than NH, it was also significantly less toxic to S.NNMT.LP cells than SH-SY5Y cells. Moreover, 2-MeNH at its lower doses enhanced both cell viability and ATP content in S.NNMT.LP. This was very surprising, considering a previous report that 2-MeNH is a neurotoxin, capable of depleting dopamine levels following injection into the SN (Neafsey *et al*. 1989). However, the dose used in this study was extremely high (440 nmol in a 5 µL injection, 88 mM). Even at this high dose dopamine content was only reduced to 40% of control. A later study using lower concentrations found that 40 mM 2-MeNH only reduced dopamine content to 64%. Moreover, injection of 8 mM 2-MeNH only reduced dopamine content to 80% of control (Neafsey *et al*. 1995). In, the study presented in chapter 6, the enhancement of cell viability and ATP content seen in the S.NNMT.LP cells occurred at concentrations of 125 µM and to a lesser extent 62.5 µM (which only demonstrated cell viability enhancement without ATP enhancement). Accordingly, while one cannot directly compare the *in vivo* studies carried out by Neafsey and colleagues to the *in vitro* data here, the finding that 2-MeNH may in fact be cytoprotective at low doses in S.NNMT.LP cells may be representative of an extension of the trend seen when lower doses of 2-MeNH were applied to rat brains, namely that at more physiologically relevant concentrations, 2-MeNH is not actually toxic at all. Instead, 2-MeNH may in fact be cytoprotective. It should, once again be noted that the concentrations used in the

toxicity assays of this project were likely higher than in the brain. However, as discussed in section 5.4.3, the concentrations used were high in order to determine the effects of these compounds over a much shorter space of time than will occur in PD. Accordingly, lower concentrations of 2-MeNH may also result in cytoprotection when acting over several years or decades.

The finding of 2-MeNH cytoprotection has interesting parallels to the debate about MeN toxicity. As mentioned in section 1.3.4, some studies claimed that MeN was toxic in the brain (Fukushima *et al.* 1995, Fukushima *et al.* 2002, Mori *et al.* 2012). However, investigation of significantly lower concentrations of MeN revealed that MeN may in fact be protective to the cell (Chlopicki *et al.* 2007, Slomka *et al.* 2008, Sternak *et al.* 2010, Parsons *et al.* 2011, Milani, Ramsden & Parsons 2013). Accordingly a similar situation may be occurring here. This is particularly interesting considering that both MeN and 2-MeNH possess a charged pyridine ring. Thus there may be some structural ambiguity to this moiety, conferring toxicity on the one hand (2,9-diMeNH, MPP^+, paraquat) yet protection/enhancement of cell viability on the other (MeN, 2-MeNH).

The key caveat to the hypothesis of 2-MeNH-mediated cytoprotection is that 2-MeNH, as discussed in section 1.3.5.2, is an intermediate in the biosynthetic pathway of 2,9-diMeNH, a compound that is considered significantly toxic both *in vitro* and *in vivo* (Bonnet *et al.* 2004, Hamann *et al.* 2006, Pavlovic *et al.* 2006, Wernicke *et al.* 2007). While, as discussed in chapter 6, the likelihood of NNMT-mediated further *N*-methylation of 2-MeNH to 2,9-diMeNH is low, the presence of additional *N*-methyltransferases which are capable of performing this 2nd *N*-

methylation reaction could lead to the eventual production of 2,9-diMeNH. Thus, while the conversion of NH to 2-MeNH may be a protective mechanism in NNMT expressing cells, in the presence of other enzymes this could still promote toxicity.

One phenomenon that warrants investigation is the effect of NNMT expression on the susceptibility of SH-SY5Y cells to 2,9-diMeNH toxicity. NNMT expression, which is protective against toxin-mediated CxI inhibition (Parsons *et al.* 2011, Milani, Ramsden & Parsons 2013), may protect cells from 2,9-diMeNH which possesses similar CxI inhibitory potential to MPP^+ (Albores *et al*. 1990). Unfortunately, the attempted synthesis of 2,9-diMeNH in this project was not successful and thus, it was not possible to test this hypothesis. However, should NNMT expression be protective against 2,9-diMeNH, this would provide the most compelling evidence for NNMT being a protective agent in PD to date.

7.1.5. NNMT-V5 expression did not alter the toxicity of THNH and 4PP

Other compounds studied in this project include THNH and 4PP. The fact that neither cell line showed any increased susceptibility to THNH during either MTT or ATP assays, and that it was significantly less toxic than NH, suggested that the compound may not be of great relevance to the toxicity of βCs. Instead, its relevance is derived from the fact that it can be oxidised to form the more toxic NH (Herraiz, Guillén & Arán 2008). However, there was no evidence to suggest that the expression of NNMT had an effect on this process. The degree of THNH conversion

to NH in both cell lines was not investigated further due to the desire to investigate the 2*N*-methylation of the more toxic NH in greater detail.

The lack of toxicity shown by THNH may be attributable to the lack of a fully aromatic pyridine ring. However, 4PP, which contains a fully aromatic pyridine ring, was significantly less toxic than THNH to both cell lines following the ATP assay, with no difference in toxicity between THNH and 4PP observed during the MTT assay. Thus, while the only difference between NH and THNH is the aromatic pyridine ring, it is not clear to what extent aromatisation of this ring alone influences the toxicity of the βCs.

The significant increase in ATP content seen when SH-SY5Y cells were incubated with 200 μM 4PP suggested that it may be able to sustain or increase ATP production in the cell. The absence of this increase in the S.NNMT.LP cells suggests that the expression of NNMT prevented this increase from occurring in response to 4PP, although why this is the case remains unclear.

The 4PP-mediated enhancement of ATP suggests that exposure to 4PP may be protective to some cells in the long term by preserving or increasing ATP levels. This is interesting considering that 4PP is found in oranges (Thomas & Bassols 1992) and mint (Snyder & D'Amato 1985) and is likely to be able to cross the blood brain barrier. Thus, consumption of 4PP as part of a healthy diet may have positive effects on the ATP production in the brain. Interestingly, 4PP has also been found in cigarette smoke (Heckman & Best 1981). Accordingly, these data may help to explain the reports that PD seems to be one of the few diseases that smoking appears to protect against (Kieburtz & Wunderle 2013). However, further research

is required to quantify the amount of 4PP that can reach the brain from both food and tobacco smoke and also whether 4PP can enhance ATP production *in vivo* in addition to *in vitro*.

7.1.6. Conclusions drawn from the project

Taking everything into account, the data presented in this project indicate that NNMT expression had a protective effect on SH-SY5Y cells, which occurred predominantly *via* increased CxI-mediated ATP production. In addition, NNMT appears to catalyse the detoxification of NH, as evidenced by (i) lower 2-MeNH toxicity compared with NH in both cell lines, (ii) S.NNMT.LP cells were significantly protected against 2-MeNH and (iii) 2-MeNH enhanced cell viability and ATP content in these cells. The caveat to this is that the conversion is yet to be demonstrated *in situ*. Furthermore, as indicated by the significantly lower ATP content of S.NNMT.LP cells compared with SH-SY5Y at 200 µM NH, the detoxification of NH may be overwhelmed at higher NH concentrations. However, at lower NH concentrations, such as those more likely to be found *in vivo*, NNMT may be able to remove sufficient NH from the cytoplasm to prevent NH accumulation and toxicity. It is possible that NNMT may be pro-toxic in certain circumstances, such as in the presence of sufficient NH substrate and enzymes that are capable of catalysing the 9*N*-methylation of 2-MeNH. However, there are currently no experimental data to demonstrate this. Furthermore, the degree to which these theoretically pro-toxic events would contrast with the existing NNMT-mediated cytoprotective benefits would need to be determined.

7.2. Future work

7.2.1. Further studies using established methods

7.2.1.1. Optimisation of the NNMT enzyme assay

As discussed in chapter 6, the K_m and V_{max} reported are only considered an estimate. This is due to the fact that the NH concentration range used in the study did not provide sufficient points in the linear portion of the Michaelis-Menten plot, although the data was successfully modelled using Michaelis-Menten non-linear regression analysis with a high degree of fit (r^2 = 0.9935). Future refinement of the assay would involve the use of additional concentrations below 0.25 mM to further improve the accuracy of the K_m and V_{max} calculations.

7.2.1.2. Synthesis of 2,9-diMeNH followed by repetition of enzyme assays and toxicity studies

As discussed in chapter 6, the synthesis of 2,9-diMeNH was unsuccessful. Future refinement of the synthetic process, either by determining an alternative method of synthesis or by troubleshooting the Cao et al. (2005) method, should result in its successful production. If successful, 2,9-dimenNH would be used to investigate whether the expression of NNMT-V5 could confer greater susceptibility to the S.NNMT.LP cells incubated with 2,9-diMeNH or if NNMT-V5 expression protects the S.NNMT.LP cells in a similar manner to that seen with 2-MeNH.

In addition, while the 9*N*-methylation of 2-MeNH is unlikely to be performed by NNMT (section 6.4.3), the possibility of this reaction still needs to be confirmed or

ruled out. Thus, synthesised 2,9-diMeNH would be used to create a MS-MS-based fingerprint such as that generated for 2-MeNH in chapter 6. This would then be used to determine whether purified NNMT can mediate the production of 2,9-diMeNH using either NH or 2-MeNH as the substrate.

7.2.1.3. Investigation of the mechanisms of βC toxicity/protection in S.NNMT.LP cells

As discussed in section 6.4.2, differences in the susceptibility of S.NNMT.LP cells to NH and to 2-MeNH may suggest that both of these compounds exert their toxicity *via* different mechanisms. Accordingly, NNMT-mediated production of 2-MeNH from NH may represent a detoxification pathway of NH. Elucidating their respective mechanisms of toxicity may provide insight into why S.NNMT.LP cells are protected against one (2-MeNH) yet show some form of ATP-dependent vulnerability to the other (NH).

The protection of S.NNMT.LP cells against 2-MeNH toxicity is likely due to the fact that it is a CxI inhibitor (Albores *et al*. 1990), something which NNMT expression has been shown to protect against (Parsons *et al*. 2011, Milani *et al*. 2013). However, the specific mechanisms of NH toxicity are yet to be determined. In addition to determining the apparently diverging mechanisms of the above 2 βCs it would be of interest to analyse the CxI inhibition of 2,9-diMeNH, which is more potent than 2-MeNH (Albores *et al*. 1990), in contrast to the CxI-protecting effects of NNMT expression.

7.2.1.4. Determination of NH 2N-methyltransferase activity in S.NNMT.LP cells

In addition to determining the NH 2*N*-methyltransferase activity of purified NNMT, it will be necessary to determine whether this reaction can take place *in situ* within S.NNMT.LP, for example by measuring 2-MeNH production in S.NNMT.LP cells incubated with NH.

In the context of the studies reported here, this discovery would build upon the chapter 5 and 6 discoveries that S.NNMT.LP cells were vulnerable to NH-mediated reduction in ATP content yet protected against 2-MeNH toxicity. Accordingly, a successful demonstration of S.NNMT.LP-mediated conversion of NH to 2-MeNH will strengthen the hypothesis that this reaction is a detoxification pathway in these cells.

7.2.2. Improvement of physiological relevance *via* new methods

7.2.2.1. Repetition of toxicity assays using differentiated cells

Cellular differentiation of SH-SY5Y cells has been shown to increase levels of TH, DAT and NeuN, markers which indicate the differentiation of SH-SY5Y cells into a more dopaminergic neuron-relevant cell line (Presgraves *et al*. 2004). In this project, the primary goal was the determination of the effects of NNMT expression alone (chapter 4) and in the presence of 4PP and βCs (chapters 5 and 6). As such, these studies were collectively a proof-of-concept study to demonstrate the

inherent protective effects of NNMT and the potential for NNMT to alter the toxicity of βCs. However, as acknowledged in chapter 6, this comes at a compromise of not being able to maximise the physiological relevance to PD. The use of undifferentiated cells, however, was justified due to the fact that chemical differentiation *via* numerous growth factors and mitotic inhibitors can have profound biochemical effects upon the cell, such as altering ATP content (Korecka *et al*. 2013). Thus, using differentiated cells may have limited the value of the characterisation studies (chapter 4) as many of the effects observed from NNMT expression may have been masked by the differentiation process.

Some attempts at inducing neuronal differentiation were made during the project but these were largely unsuccessful due to the fact that visual identification of neuronal differentiation under the microscope (reduced cell width, elongation and branching of neurites) was inconsistent. Furthermore, Western blotting analysis did not show any changes in neuronal markers (TH and NeuN). Therefore, due to time constraints, this part of the project was abandoned in favour of confirming the NH 2*N*-methyltransferase ability of NNMT.

Differentiation of SH-SY5Y cells is a frequently-discussed topic with multiple reported methods in existence (Encinas *et al.* 2000, Presgraves *et al.* 2004, Constantinescu *et al.* 2007, Cheung *et al.* 2009, Agholme *et al.* 2010, Lopes *et al.* 2010, Korecka *et al.* 2013). All these methods centre upon the use of retinoic acid (RA) to induce differentiation but the extent of its effects on the cell and whether it is best used alone, in combination with other agents or indeed how to culture RA-differentiated cells, are points of contention.

Lopes *et al*. (2010) reported that differentiation of SH-SY5Y cells into cells with higher expression of TH and NeuN as well as increased vulnerability to 6-hydroxydopamine (6OHDA, a frequently used dopaminergic neuron specific toxin) was achieved *via* incubation of SH-SY5Y cells with 10 µM RA over 7 days in media containing only 1% FBS. On the other hand, Cheung *et al*. (2009) used a similar protocol over 7 days and reported no increase in TH expression and that 6OHDA toxicity was, conversely, reduced in these cells. One possible explanation for this difference may be the serum content used in the respective studies as the Cheung *et al*. study only reduced FBS to 3% during differentiation but these differences highlight the general trend of various groups professing differences in opinion about the use of RA in differentiation protocols.

In a similar vein to Lopes *et al*. and Cheung *et al*., Korecka *et al*. (2013) used RA alone to produce differentiated SH-SY5Y cells. However, this was done at a 10-fold lower concentration of RA, 0.5% FBS and used SH-SY5Y cells cultured in matrigel. The result was the upregulation of numerous markers of neuronal differentiation (NeuN was not tested for), but no TH upregulation occurred. Other studies have used RA in combination with other factors and in different conditions. For example, Constantinescu *et al*. (2007), used a glass dish perfusion system of SH-SY5Y cells mounted on coverslips to produce differentiated cells with increased TH, NeuN and DAT expression following application of 10 µM RA followed by brain-derived neurotophic factor and various mitotic inhibitors. Finally, Presgraves *et al*. (2004) used SH-SY5Y cells grown in traditional cell culture plates but, after 3 days incubation with 10 µM RA, replaced RA with 12-O-tetradecanoyl-phorbol-13-

acetate for 3 days to produce cells with significantly higher TH and DAT expression and increased susceptibility to MPP^+. The large variability of differentiation methods and results highlights the fact that there is currently no gold standard protocol for the differentiation of SH-SY5Y cells. Accordingly, future work should focus on determining the most suitable and practical method for differentiating the SH-SY5Y and S.NNMT.LP cells, with particular reference to methods that increase DAT, TH and NeuN expression, in order for the toxicity assays in this study to be repeated with improved physiological relevance.

7.2.2.1. Assessment of the effects of NNMT expression in vivo

While determining the toxicity of NH, 2-MeNH and 2,9-diMeNH in differentiated SH-SY5Y and S.NNMT.LP cells will add to the physiological relevance of the model, the most compelling experimental evidence for NNMT's potential involvement in PD will come from *in vivo* studies. The most likely candidate for *in vivo* determination of the effects of increased NNMT expression would be transgenic mouse models, as the practicalities of their breeding coupled with their strong genomic similarity to humans make them the animal of choice for the genetic analysis of human disease (Doyle *et al.* 2012). In particular, the use of a topical transgenic model, in which the genome is altered only at the desired target organ/tissue *via* the direct administration of a recombinant adeno-associated virus (rAAV) containing a cDNA insert of, or siRNA sequence targeted to, the gene of interest, would allow the effects of NNMT overexpression to be determined exclusively within the SNpc. Moreover, this would occur without the time, expense

and complications arising from the generation of transgenic animals (i.e. embryo lethality of expressed target protein) (Klein *et al.* 1998).

Accordingly, the CxI protective, and overall cytoprotective effects of, NNMT expression could be investigated *in vivo* by injecting the brain with an rAAV containing a plasmid with a cDNA insert for NNMT, or an shRNA targeted to NNMT, under the control of a neuron-specific promoter, e.g. synapsin-1, in order to rapidly upregulate/downregulate NNMT expression. Furthermore, administration of βCs in high-expressing, endogenously-expressing, and NNMT knockdown models will allow the relationship between NNMT and βCs to be determined in a more physiological context.

7.3. Concluding remarks

This project has contributed to the field of PD research by reinforcing the findings made in other diseases that induction of NNMT expression enhances cell viability. Furthermore, this project has provided the first experimental evidence of NNMT's NH 2*N*-methyltransferase activity and that this ability to convert NH to 2-MeNH may be a protective detoxification response by NNMT-expressing cells. Given that 9*N*-methylation of 2-MeNH has been reported in the brain (Matsubara, Neafsey & Collins 1992, Gearhart *et al.* 2000), the possibility of NNMT and/or other *N*-methyltransferases producing 2,9-diMeNH *via* step-wise di-*N*-methylation of NH cannot be ruled out. However, in the absence of an identified 9*N*-methyltransferase and any *in vivo* data showing an increased susceptibility to NH when NNMT is

overexpressed, these data suggest upregulation of NNMT in PD, at least initially, may occur as a protective response to the underlying pathogenic process.

References

Agholme, L., Lindstrom, T., Kagedal, K., Marcusson, J. & Hallbeck, M. 2010. An *in vitro* model for neuroscience: differentiation of SH-SY5Y cells into cells with morphological and biochemical characteristics of mature neurons. *J Alzheimers Dis,* **20,** 1069-82.

Albores, R., Neafsey, E. J., Drucker, G., Fields, J. Z. & Collins, M. A. 1990. Mitochondrial respiratory inhibition by N-methylated β-carboline derivatives structurally resembling *N*-methyl-4-phenylpyridine. *Proc Natl Acad Sci U S A,* **87,** 9368-72.

Alston, T. A. & Abeles, R. H. 1988. Substrate specificity of nicotinamide methyltransferase isolated from porcine liver. *Arch Biochem Biophys,* **260,** 601-8.

Andén, N. E., Hfuxe, K., Hamberger, B. & Hokfelt, T. 1966. A quantitative study on the nigro-neostriatal dopamine neuron system in the rat. *Acta Physiol Scand,* **67,** 306-12.

Anderson, D. G., Mariappan, S. V., Buettner, G. R. & Doorn, J. A. 2011. Oxidation of 3,4-dihydroxyphenylacetaldehyde, a toxic dopaminergic metabolite, to a semiquinone radical and an *ortho*-quinone. *J Biol Chem,* **286,** 26978-86.

Andrews, Z. B., Diano, S. & Horvath, T. L. 2005. Mitochondrial uncoupling proteins in the CNS: in support of function and survival. *Nat Rev Neurosci,* **6,** 829-40.

Aoyama, K., Matsubara, K., Kondo, M., Murakawa, Y., Suno, M., Yamashita, K., Yamaguchi, S. & Kobayashi, S. 2001. Nicotinamide-*N*-methyltransferase is higher in the lumbar cerebrospinal fluid of patients with Parkinson's disease. *Neurosci Lett,* **298,** 78-80.

Attwell, D. & Laughlin, S. B. 2001. An energy budget for signaling in the grey matter of the brain. *J Cereb Blood Flow Metab,* **21,** 1133-45.

Baylor, S. M. & Hollingworth, S. 1990. Absorbance signals from resting frog skeletal muscle fibers injected with the pH indicator dye, phenol red. *J Gen Physiol,* **96,** 449-71.

Beltran, B., Mathur, A., Duchen, M. R., Erusalimsky, J. D. & Moncada, S. 2000. The effect of nitric oxide on cell respiration: a key to understanding its role in cell survival or death. *Proc Natl Acad Sci U S A,* **97,** 14602-7.

Bernas, T. & Dobrucki, J. 2002. Mitochondrial and nonmitochondrial reduction of MTT: interaction of MTT with TMRE, JC-1, and NAO mitochondrial fluorescent probes. *Cytometry,* **47,** 236-42.

Berridge, M. V. & Tan, A. S. 1993. Characterization of the cellular reduction of 3-(4,5-dimethylthiazol-2-yl)-2,5-diphenyltetrazolium bromide (MTT): subcellular localization, substrate dependence, and involvement of mitochondrial electron transport in MTT reduction. *Arch Biochem Biophys,* **303,** 474-82.

Berridge, M. V., Herst, P. M. & Tan, A. S. 2005. Tetrazolium dyes as tools in cell biology: new insights into their cellular reduction. *Biotechnol Annu Rev,* **11,** 127-52.

Blandini, F. & Armentero, M. T. 2012. Animal models of Parkinson's disease. *FEBS J,* **279,** 1156-66.

Bolam, J. P. & Pissadaki, E. K. 2012. Living on the edge with too many mouths to feed: why dopamine neurons die. *Mov Disord,* **27,** 1478-83.

Bonnet, R., Pavlovic, S., Lehmann, J. & Rommelspacher, H. 2004. The strong inhibition of triosephosphate isomerase by the natural β-carbolines may explain their neurotoxic actions. *Neuroscience,* **127,** 443-53.

Braak, H., Del Tredici, K., Rub, U., De Vos, R. A., Jansen Steur, E. N. & Braak, E. 2003. Staging of brain pathology related to sporadic Parkinson's disease. *Neurobiol Aging,* **24,** 197-211.

Bras, J., Guerreiro, R., Darwent, L., Parkkinen, L., Ansorge, O., Escott-Price, V., Hernandez, D. G., Nalls, M. A., Clark, L. N., Honig, L. S., Marder, K., Van Der Flier, W. M., Lemstra, A., Scheltens, P., Rogaeva, E., St George-Hyslop, P., Londos, E., Zetterberg, H., Ortega-Cubero, S., Pastor, P., Ferman, T. J., Graff-Radford, N. R., Ross, O. A., Barber, I., Braae, A., Brown, K., Morgan, K., Maetzler, W., Berg, D., Troakes, C., Al-Sarraj, S., Lashley, T., Compta, Y., Revesz, T., Lees, A., Cairns, N., Halliday, G. M., Mann, D., Pickering-Brown, S., Dickson, D. W., Singleton, A. & Hardy, J. 2014. Genetic analysis implicates *APOE*, *SNCA* and suggests lysosomal dysfunction in the etiology of dementia with Lewy bodies. *Hum Mol Genet***,** doi: 10.1093/hmg/ddu334.

Bülbring, E. & Burn, J. H. 1949. Formation of adrenaline from noradrenaline in the perfused suprarenal gland. *Br J Pharmacol Chemother,* **4,** 245-7.

Burke, R. E. 2007. Inhibition of mitogen-activated protein kinase and stimulation of Akt kinase signaling pathways: two approaches with therapeutic potential in the treatment of neurodegenerative disease. *Pharmacol Ther,* **114,** 261-77.

Bus, J. S. & Gibson, J. E. 1984. Paraquat: model for oxidant-initiated toxicity. *Environ Health Perspect,* **55,** 37-46.

Cao, R., Chen, H., Peng, W., Ma, Y., Hou, X., Guan, H., Liu, X. & Xu, A. 2005. Design, synthesis and in vitro and in vivo antitumor activities of novel β-carboline derivatives. *Eur J Med Chem,* **40,** 991-1001.

Chaudhuri, K. R., Healy, D. G. & Schapira, A. H. 2006. Non-motor symptoms of Parkinson's disease: diagnosis and management. *Lancet Neurol,* **5,** 235-45.

Chen, H. & Chan, D. C. 2009. Mitochondrial dynamics--fusion, fission, movement, and mitophagy--in neurodegenerative diseases. *Hum Mol Genet,* **18,** R169-76.

Chen, L., Ding, Y., Cagniard, B., Van Laar, A. D., Mortimer, A., Chi, W., Hastings, T. G., Kang, U. J. & Zhuang, X. 2008. Unregulated cytosolic dopamine causes neurodegeneration associated with oxidative stress in mice. *J Neurosci,* **28,** 425-33.

Chen, L. B. 1988. Mitochondrial membrane potential in living cells. *Annu Rev Cell Biol,* **4,** 155-81.

Cheng, H. C., Ulane, C. M. & Burke, R. E. 2010. Clinical progression in Parkinson disease and the neurobiology of axons. *Ann Neurol,* **67,** 715-25.

Cheung, Y. T., Lau, W. K., Yu, M. S., Lai, C. S., Yeung, S. C., So, K. F. & Chang, R. C. 2009. Effects of all-trans-retinoic acid on human SH-SY5Y neuroblastoma as in vitro model in neurotoxicity research. *Neurotoxicology,* **30,** 127-35.

Chlopicki, S., Swies, J., Mogielnicki, A., Buczko, W., Bartus, M., Lomnicka, M., Adamus, J. & Gebicki, J. 2007. 1-Methylnicotinamide (MNA), a primary metabolite of nicotinamide, exerts anti-thrombotic activity mediated by a cyclooxygenase-2/prostacyclin pathway. *Br J Pharmacol,* **152,** 230-9.

Chu, Y. & Kordower, J. H. 2007. Age-associated increases of α-synuclein in monkeys and humans are associated with nigrostriatal dopamine depletion: is this the target for Parkinson's disease? *Neurobiol Dis,* **25,** 134-49.

Cleeter, M. W., Cooper, J. M. & Schapira, A. H. 1992. Irreversible inhibition of mitochondrial complex I by 1-methyl-4-phenylpyridinium: evidence for free radical involvement. *J Neurochem,* **58,** 786-9.

Collier, T. J., Kanaan, N. M. & Kordower, J. H. 2011. Ageing as a primary risk factor for Parkinson's disease: evidence from studies of non-human primates. *Nat Rev Neurosci,* **12,** 359-66.

Collins, M. A., Neafsey, E. J., Matsubara, K., Cobuzzi, R. J., Jr. & Rollema, H. 1992. Indole-*N*-methylated β-carbolinium ions as potential brain-bioactivated neurotoxins. *Brain Res,* **570,** 154-60.

Constantinescu, R., Constantinescu, A. T., Reichmann, H. & Janetzky, B. 2007. Neuronal differentiation and long-term culture of the human neuroblastoma line SH-SY5Y. *J Neural Transm Suppl***,** 17-28.

Crotti, A. E., Gates, P. J., Lopes, J. L. & Lopes, N. P. 2010. Electrospray MS-based characterization of β-carbolines--mutagenic constituents of thermally processed meat. *Mol Nutr Food Res,* **54,** 433-9.

Crouch, S. P., Kozlowski, R., Slater, K. J. & Fletcher, J. 1993. The use of ATP bioluminescence as a measure of cell proliferation and cytotoxicity. *J Immunol Methods,* **160,** 81-8.

Cuomo, R., Dattilo, M., Pumpo, R., Capuano, G., Boselli, L. & Budillon, G. 1994. Nicotinamide methylation in patients with cirrhosis. *J Hepatol,* **20,** 138-42.

Dawson, T. M. & Dawson, V. L. 2010. The role of *parkin* in familial and sporadic Parkinson's disease. *Mov Disord,* **25 Suppl 1,** S32-9.

De Lau, L. M. & Breteler, M. M. 2006. Epidemiology of Parkinson's disease. *Lancet Neurol,* **5,** 525-35.

De Vries, R. L. & Przedborski, S. 2013. Mitophagy and Parkinson's disease: be eaten to stay healthy. *Mol Cell Neurosci,* **55,** 37-43.

Deitrich, R. & Erwin, V. 1980. Biogenic amine-aldehyde condensation products: tetrahydroisoquinolines and tryptolines (β-carbolines). *Annu Rev Pharmacol Toxicol,* **20,** 55-80.

Dexter, D. T., Wells, F. R., Agid, F., Agid, Y., Lees, A. J., Jenner, P. & Marsden, C. D. 1987. Increased nigral iron content in postmortem parkinsonian brain. *Lancet,* **2,** 1219-20.

Dexter, D. T., Wells, F. R., Lees, A. J., Agid, F., Agid, Y., Jenner, P. & Marsden, C. D. 1989. Increased nigral iron content and alterations in other metal ions occurring in brain in Parkinson's disease. *J Neurochem,* **52,** 1830-6.

Dexter, D. T. & Jenner, P. 2013. Parkinson disease: from pathology to molecular disease mechanisms. *Free Radic Biol Med,* **62,** 132-44.

Dick, F. D., De Palma, G., Ahmadi, A., Scott, N. W., Prescott, G. J., Bennett, J., Semple, S., Dick, S., Counsell, C., Mozzoni, P., Haites, N., Wettinger, S. B., Mutti, A., Otelea, M., Seaton, A., Soderkvist, P. & Felice, A. 2007. Environmental risk factors for Parkinson's disease and parkinsonism: the Geoparkinson study. *Occup Environ Med,* **64,** 666-72.

Dodel, R., Jonsson, B., Reese, J. P., Winter, Y., Martinez-Martin, P., Holloway, R., Sampaio, C., Ruzicka, E., Hawthorne, G., Oertel, W., Poewe, W., Stebbins, G., Rascol, O., Goetz, C. G. & Schrag, A. 2014. Measurement of costs and scales for outcome evaluation in health economic studies of Parkinson's disease. *Mov Disord,* **29,** 169-76.

Dorsey, E. R., Constantinescu, R., Thompson, J. P., Biglan, K. M., Holloway, R. G., Kieburtz, K., Marshall, F. J., Ravina, B. M., Schifitto, G., Siderowf, A. & Tanner, C. M. 2007. Projected number of people with Parkinson disease in the most populous nations, 2005 through 2030. *Neurology,* **68,** 384-6.

Doty, R. L. 2012. Olfactory dysfunction in Parkinson disease. *Nat Rev Neurol,* **8,** 329-39.

Doyle, A., Mcgarry, M. P., Lee, N. A. & Lee, J. J. 2012. The construction of transgenic and gene knockout/knockin mouse models of human disease. *Transgenic Res,* **21,** 327-49.

Dredge, B. K. & Jensen, K. B. 2011. NeuN/Rbfox3 nuclear and cytoplasmic isoforms differentially regulate alternative splicing and nonsense-mediated decay of Rbfox2. *PLoS One,* **6,** e21585.

Eguchi, Y., Shimizu, S. & Tsujimoto, Y. 1997. Intracellular ATP levels determine cell death fate by apoptosis or necrosis. *Cancer Res,* **57,** 1835-40.

Encinas, M., Iglesias, M., Liu, Y., Wang, H., Muhaisen, A., Cena, V., Gallego, C. & Comella, J. X. 2000. Sequential treatment of SH-SY5Y cells with retinoic acid and brain-derived neurotrophic factor gives rise to fully differentiated, neurotrophic factor-dependent, human neuron-like cells. *J Neurochem,* **75,** 991-1003.

Erb, C., Seidel, A., Frank, H., Platt, K. L., Oesch, F. & Klein, J. 1999. Formation of *N*-methylnicotinamide in the brain from a dihydropyridine-type prodrug: effect on brain choline. *Biochem Pharmacol,* **57,** 681-4.

Exner, N., Treske, B., Paquet, D., Holmstrom, K., Schiesling, C., Gispert, S., Carballo-Carbajal, I., Berg, D., Hoepken, H. H., Gasser, T., Kruger, R., Winklhofer, K. F., Vogel, F., Reichert, A. S., Auburger, G., Kahle, P. J., Schmid, B. & Haass, C. 2007. Loss-of-function of human PINK1 results in mitochondrial pathology and can be rescued by parkin. *J Neurosci,* **27,** 12413-8.

Exner, N., Lutz, A. K., Haass, C. & Winklhofer, K. F. 2012. Mitochondrial dysfunction in Parkinson's disease: molecular mechanisms and pathophysiological consequences. *EMBO J,* **31,** 3038-62.

Fang, J., Zuo, D. & Yu, P. H. 1995. Comparison of cytotoxicity of a quaternary pyridinium metabolite of haloperidol (HP^+) with neurotoxin *N*-methyl-4-phenylpyridinium (MPP^+) towards cultured dopaminergic neuroblastoma cells. *Psychopharmacology (Berl),* **121,** 373-8.

Faull, K., Holman, R., Gr, E. & Barchas, J. 1982. *Tryptolines: artifact or reality? A new method of analysis using GC/MS.,* New York, NY, USA Alan R. Liss, Inc.

Fekkes, D. & Bode, W. T. 1993. Occurrence and partition of the β-carboline norharman in rat organs. *Life Sci,* **52,** 2045-54.

Fields, J. Z., Albores, R. R., Neafsey, E. J. & Collins, M. A. 1992. Inhibition of mitochondrial succinate oxidation-similarities and differences between *N*-methylated β-carbolines and MPP^+. *Arch Biochem Biophys,* **294,** 539-43.

Fitzmaurice, A. G., Rhodes, S. L., Cockburn, M., Ritz, B. & Bronstein, J. M. 2014. Aldehyde dehydrogenase variation enhances effect of pesticides associated with Parkinson disease. *Neurology,* **82,** 419-26.

Foltynie, T. & Kahan, J. 2013. Parkinson's disease: an update on pathogenesis and treatment. *J Neurol,* **260,** 1433-40.

Fotakis, G. & Timbrell, J. A. 2006. *In vitro* cytotoxicity assays: comparison of LDH, neutral red, MTT and protein assay in hepatoma cell lines following exposure to cadmium chloride. *Toxicol Lett,* **160,** 171-7.

Fukushima, T., Tawara, T., Isobe, A., Hojo, N., Shiwaku, K. & Yamane, Y. 1995. Radical formation site of cerebral complex I and Parkinson's disease. *J Neurosci Res,* **42,** 385-90.

Fukushima, T., Kaetsu, A., Lim, H. & Moriyama, M. 2002. Possible role of 1-methylnicotinamide in the pathogenesis of Parkinson's disease. *Exp Toxicol Pathol,* **53,** 469-73.

Fuxe, K. 1965. Evidence for the Existence of Monoamine Neurons in the Central Nervous System. 3. The Monoamine Nerve Terminal. *Z Zellforsch Mikrosk Anat,* **65,** 573-96.

Gai, W. P., Geffen, L. B., Denoroy, L. & Blessing, W. W. 1993. Loss of C1 and C3 epinephrine-synthesizing neurons in the *medulla oblongata* in Parkinson's disease. *Ann Neurol,* **33,** 357-67.

Gearhart, D. A., Collins, M. A., Lee, J. M. & Neafsey, E. J. 2000. Increased β-carboline 9N-methyltransferase activity in the frontal cortex in Parkinson's disease. *Neurobiol Dis,* **7,** 201-11.

Gearhart, D. A., Neafsey, E. J. & Collins, M. A. 2002. Phenylethanolamine *N*-methyltransferase has β-carboline 2*N*-methyltransferase activity: hypothetical relevance to Parkinson's disease. *Neurochem Int,* **40,** 611-20.

Gerlach, M., Double, K. L., Ben-Shachar, D., Zecca, L., Youdim, M. B. & Riederer, P. 2003. Neuromelanin and its interaction with iron as a potential risk factor for dopaminergic neurodegeneration underlying Parkinson's disease. *Neurotox Res,* **5,** 35-44.

Gilks, W. P., Abou-Sleiman, P. M., Gandhi, S., Jain, S., Singleton, A., Lees, A. J., Shaw, K., Bhatia, K. P., Bonifati, V., Quinn, N. P., Lynch, J., Healy, D. G., Holton, J. L., Revesz, T. & Wood, N. W. 2005. A common *LRRK2* mutation in idiopathic Parkinson's disease. *Lancet,* **365,** 415-6.

Goldstein, D. S., Sullivan, P., Holmes, C., Miller, G. W., Alter, S., Strong, R., Mash, D. C., Kopin, I. J. & Sharabi, Y. 2013. Determinants of buildup of the toxic dopamine metabolite DOPAL in Parkinson's disease. *J Neurochem,* **126,** 591-603.

Goris, A., Williams-Gray, C. H., Clark, G. R., Foltynie, T., Lewis, S. J., Brown, J., Ban, M., Spillantini, M. G., Compston, A., Burn, D. J., Chinnery, P. F., Barker, R. A. & Sawcer, S. J. 2007. Tau and α-synuclein in susceptibility to, and dementia in, Parkinson's disease. *Ann Neurol,* **62,** 145-53.

Grahame-Smith, D. G. 1967. The biosynthesis of 5-hydroxytryptamine in brain. *Biochem J,* **105,** 351-60.

Gu, M., Cooper, J. M., Taanman, J. W. & Schapira, A. H. 1998. Mitochondrial DNA transmission of the mitochondrial defect in Parkinson's disease. *Ann Neurol,* **44,** 177-86.

Guzman, J. N., Sanchez-Padilla, J., Chan, C. S. & Surmeier, D. J. 2009. Robust pacemaking in *substantia nigra* dopaminergic neurons. *J Neurosci,* **29,** 11011-9.

Guzman, J. N., Sanchez-Padilla, J., Wokosin, D., Kondapalli, J., Ilijic, E., Schumacker, P. T. & Surmeier, D. J. 2010. Oxidant stress evoked by pacemaking in dopaminergic neurons is attenuated by DJ-1. *Nature,* **468,** 696-700.

Hamann, J., Rommelspacher, H., Storch, A., Reichmann, H. & Gille, G. 2006. Neurotoxic mechanisms of 2,9-dimethyl-β-carbolinium ion in primary dopaminergic culture. *J Neurochem,* **98,** 1185-99.

Hamann, J., Wernicke, C., Lehmann, J., Reichmann, H., Rommelspacher, H. & Gille, G. 2008. 9-Methyl-β-carboline up-regulates the appearance of differentiated dopaminergic neurones in primary mesencephalic culture. *Neurochem Int,* **52,** 688-700.

Hancock, A. A., Bush, E. N., Stanisic, D., Kyncl, J. J. & Lin, C. T. 1988. Data normalization before statistical analysis: keeping the horse before the cart. *Trends Pharmacol Sci,* **9,** 29-32.

Harrison, R. O. & Hammock, B. D. 1988. Location dependent biases in automatic 96-well microplate readers. *J Assoc Off Anal Chem,* **71,** 981-7.

Hayflick, L. 1965. The Limited in Vitro Lifetime of Human Diploid Cell Strains. *Exp Cell Res,* **37,** 614-36.

Healy, D. G., Falchi, M., O'sullivan, S. S., Bonifati, V., Durr, A., Bressman, S., Brice, A., Aasly, J., Zabetian, C. P., Goldwurm, S., Ferreira, J. J., Tolosa, E., Kay, D. M., Klein, C., Williams, D. R., Marras, C., Lang, A. E., Wszolek, Z. K., Berciano, J., Schapira, A. H., Lynch, T., Bhatia, K. P., Gasser, T., Lees, A. J. & Wood, N. W. 2008. Phenotype, genotype, and worldwide genetic penetrance of *LRRK2*-associated Parkinson's disease: a case-control study. *Lancet Neurol,* **7,** 583-90.

Heckman, R. & Best, F. 1981. An investigation of the lipophilic bases of cigarette smoke condensate. *Tobacco Science,* **183,** 83-89.

Herraiz, T. 2004. Relative exposure to β-carbolines norharman and harman from foods and tobacco smoke. *Food Addit Contam,* **21,** 1041-50.

Herraiz, T., Guillén, H. & Galisteo, J. 2007. *N*-methyltetrahydro-β-carboline analogs of 1-methyl-4-phenyl-1,2,3,6-tetrahydropyridine (MPTP) neurotoxin are oxidized to

neurotoxic β-carbolinium cations by heme peroxidases. *Biochem Biophys Res Commun,* **356,** 118-23.

Herraiz, T., Guillén, H. & Arán, V. J. 2008. Oxidative metabolism of the bioactive and naturally occurring β-carboline alkaloids, norharman and harman, by human cytochrome P450 enzymes. *Chem Res Toxicol,* **21,** 2172-80.

Hirsch, E. C., Jenner, P. & Przedborski, S. 2013. Pathogenesis of Parkinson's disease. *Mov Disord,* **28,** 24-30.

Ho, P. W., Chu, A. C., Kwok, K. H., Kung, M. H., Ramsden, D. B. & Ho, S. L. 2006. Knockdown of uncoupling protein-5 in neuronal SH-SY5Y cells: Effects on MPP+-induced mitochondrial membrane depolarization, ATP deficiency, and oxidative cytotoxicity. *J Neurosci Res,* **84,** 1358-66.

Honegger, A. & Humbel, R. E. 1986. Insulin-like growth factors I and II in fetal and adult bovine serum. Purification, primary structures, and immunological cross-reactivities. *J Biol Chem,* **261,** 569-75.

Hood, E. 2004. RNAi: What's all the noise about gene silencing? *Environ Health Perspect,* **112,** A224-9.

Hoppel, C. L., Grinblatt, D., Kwok, H. C., Arora, P. K., Singh, M. P. & Sayre, L. M. 1987. Inhibition of mitochondrial respiration by analogs of 4-phenylpyridine and 1-methyl-4-phenylpyridinium cation (MPP_+), the neurotoxic metabolite of MPTP. *Biochem Biophys Res Commun,* **148,** 684-93.

Hornykiewicz, O. 1989. Ageing and neurotoxins as causative factors in idiopathic Parkinson's disease-a critical analysis of the neurochemical evidence. *Prog Neuropsychopharmacol Biol Psychiatry,* **13,** 319-28.

Irwin, I., Langston, J. W. & Delanney, L. E. 1987. 4-Phenylpyridine (4PP) and MPTP: the relationship between striatal MPP+ concentrations and neurotoxicity. *Life Sci,* **40,** 731-40.

Kamel, F. 2013. Epidemiology. Paths from pesticides to Parkinson's. *Science,* **341,** 722-3.

Kanaan, N. M., Kordower, J. H. & Collier, T. J. 2008. Age-related changes in dopamine transporters and accumulation of 3-nitrotyrosine in rhesus monkey midbrain dopamine neurons: relevance in selective neuronal vulnerability to degeneration. *Eur J Neurosci,* **27,** 3205-15.

Kandel, E., Schwartz, J. & Jessel, T. 2000. *Principals of Neural Science, 4th edition.* New York, NY, USA. McGraw-Hill.

Kaneko, I., Yamada, N., Sakuraba, Y., Kamenosono, M. & Tutumi, S. 1995. Suppression of mitochondrial succinate dehydrogenase, a primary target of β-amyloid, and its derivative racemized at Ser residue. *J Neurochem,* **65,** 2585-93.

Kieburtz, K. & Wunderle, K. B. 2013. Parkinson's disease: evidence for environmental risk factors. *Mov Disord,* **28,** 8-13.

Kim, H. C., Mofarrahi, M., Vassilakopoulos, T., Maltais, F., Sigala, I., Debigare, R., Bellenis, I. & Hussain, S. N. 2010. Expression and functional significance of nicotinamide *N*-methyl transferase in skeletal muscles of patients with chronic obstructive pulmonary disease. *Am J Respir Crit Care Med,* **181,** 797-805.

Kish, S. J., Shannak, K., Rajput, A., Deck, J. H. & Hornykiewicz, O. 1992. Aging produces a specific pattern of striatal dopamine loss: implications for the etiology of idiopathic Parkinson's disease. *J Neurochem,* **58,** 642-8.

Klein, C., Lohmann-Hedrich, K., Rogaeva, E., Schlossmacher, M. G. & Lang, A. E. 2007. Deciphering the role of heterozygous mutations in genes associated with parkinsonism. *Lancet Neurol,* **6,** 652-62.

Klein, R. L., Meyer, E. M., Peel, A. L., Zolotukhin, S., Meyers, C., Muzyczka, N. & King, M. A. 1998. Neuron-specific transduction in the rat septohippocampal or nigrostriatal pathway by recombinant adeno-associated virus vectors. *Exp Neurol,* **150,** 183-94.

Koh, J. Y. & Choi, D. W. 1987. Quantitative determination of glutamate mediated cortical neuronal injury in cell culture by lactate dehydrogenase efflux assay. *J Neurosci Methods,* **20,** 83-90.

Kopp, N., Denoroy, L., Renaud, B., Pujol, J. F., Tabib, A. & Tommasi, M. 1979. Distribution of adrenaline-synthesizing enzyme activity in the human brain. *J Neurol Sci,* **41,** 397-409.

Kordower, J. H., Chu, Y., Hauser, R. A., Freeman, T. B. & Olanow, C. W. 2008. Lewy body-like pathology in long-term embryonic nigral transplants in Parkinson's disease. *Nat Med,* **14,** 504-6.

Korecka, J. A., Van Kesteren, R. E., Blaas, E., Spitzer, S. O., Kamstra, J. H., Smit, A. B., Swaab, D. F., Verhaagen, J. & Bossers, K. 2013. Phenotypic characterization of retinoic acid differentiated SH-SY5Y cells by transcriptional profiling. *PLoS One,* **8,** e63862.

Kowal, S. L., Dall, T. M., Chakrabarti, R., Storm, M. V. & Jain, A. 2013. The current and projected economic burden of Parkinson's disease in the United States. *Mov Disord,* **28,** 311-8.

Kuhn, W., Muller, T., Grosse, H. & Rommelspacher, H. 1996. Elevated levels of harman and norharman in cerebrospinal fluid of parkinsonian patients. *J Neural Transm,* **103,** 1435-40.

Kwok, K. H., Ho, P. W., Chu, A. C., Ho, J. W., Liu, H. F., Yiu, D. C., Chan, K. H., Kung, M. H., Ramsden, D. B. & Ho, S. L. 2010. Mitochondrial UCP5 is neuroprotective by

preserving mitochondrial membrane potential, ATP levels, and reducing oxidative stress in MPP^+ and dopamine toxicity. *Free Radic Biol Med,* **49,** 1023-35.

Langston, J. W., Ballard, P., Tetrud, J. W. & Irwin, I. 1983. Chronic Parkinsonism in humans due to a product of meperidine-analog synthesis. *Science,* **219,** 979-80.

Langston, J. W., Irwin, I., Langston, E. B. & Forno, L. S. 1984. 1-Methyl-4-phenylpyridinium ion (MPP^+): identification of a metabolite of MPTP, a toxin selective to the *substantia nigra*. *Neurosci Lett,* **48,** 87-92.

Lesage, S. & Brice, A. 2009. Parkinson's disease: from monogenic forms to genetic susceptibility factors. *Hum Mol Genet,* **18,** R48-59.

Lesage, S., Anheim, M., Condroyer, C., Pollak, P., Durif, F., Dupuits, C., Viallet, F., Lohmann, E., Corvol, J. C., Honore, A., Rivaud, S., Vidailhet, M., Durr, A. & Brice, A. 2011. Large-scale screening of the Gaucher's disease-related glucocerebrosidase gene in Europeans with Parkinson's disease. *Hum Mol Genet,* **20,** 202-10.

Lesage, S. & Brice, A. 2012. Role of mendelian genes in "sporadic" Parkinson's disease. *Parkinsonism Relat Disord,* **18 Suppl 1,** S66-70.

Lew, M. 2007. Good statistical practice in pharmacology. Problem 2. *Br J Pharmacol,* **152,** 299-303.

Li, S. W., Lin, T. S., Minteer, S. & Burke, W. J. 2001. 3,4-Dihydroxyphenylacetaldehyde and hydrogen peroxide generate a hydroxyl radical: possible role in Parkinson's disease pathogenesis. *Brain Res Mol Brain Res,* **93,** 1-7.

Liu, S. & Lu, B. 2010. Reduction of protein translation and activation of autophagy protect against *PINK1* pathogenesis in *Drosophila melanogaster*. *PLoS Genet,* **6,** e1001237.

Liu, Y., Peterson, D. A., Kimura, H. & Schubert, D. 1997. Mechanism of cellular 3-(4,5-dimethylthiazol-2-yl)-2,5-diphenyltetrazolium bromide (MTT) reduction. *J Neurochem,* **69,** 581-93.

Lopes, F. M., Schroder, R., Da Frota, M. L., Jr., Zanotto-Filho, A., Muller, C. B., Pires, A. S., Meurer, R. T., Colpo, G. D., Gelain, D. P., Kapczinski, F., Moreira, J. C., Fernandes Mda, C. & Klamt, F. 2010. Comparison between proliferative and neuron-like SH-SY5Y cells as an in vitro model for Parkinson disease studies. *Brain Res,* **1337,** 85-94.

Lowry, O. H., Rosebrough, N. J., Farr, A. L. & Randall, R. J. 1951. Protein measurement with the Folin phenol reagent. *J Biol Chem,* **193,** 265-75.

Macleod, D. A., Rhinn, H., Kuwahara, T., Zolin, A., Di Paolo, G., Mccabe, B. D., Marder, K. S., Honig, L. S., Clark, L. N., Small, S. A. & Abeliovich, A. 2013. *RAB7L1* interacts with *LRRK2* to modify intraneuronal protein sorting and Parkinson's disease risk. *Neuron,* **77,** 425-39.

Maraganore, D. M., De Andrade, M., Elbaz, A., Farrer, M. J., Ioannidis, J. P., Kruger, R., Rocca, W. A., Schneider, N. K., Lesnick, T. G., Lincoln, S. J., Hulihan, M. M., Aasly, J. O., Ashizawa, T., Chartier-Harlin, M. C., Checkoway, H., Ferrarese, C., Hadjigeorgiou, G., Hattori, N., Kawakami, H., Lambert, J. C., Lynch, T., Mellick, G. D., Papapetropoulos, S., Parsian, A., Quattrone, A., Riess, O., Tan, E. K. & Van Broeckhoven, C. 2006. Collaborative analysis of α-synuclein gene promoter variability and Parkinson disease. *JAMA,* **296,** 661-70.

Martins, J. B., Bastos Mde, L., Carvalho, F. & Capela, J. P. 2013. Differential Effects of Methyl-4-Phenylpyridinium Ion, Rotenone, and Paraquat on Differentiated SH-SY5Y Cells. *J Toxicol,* **2013,** 347312.

Mateuszuk, L., Khomich, T. I., Slominska, E., Gajda, M., Wojcik, L., Lomnicka, M., Gwozdz, P. & Chlopicki, S. 2009. Activation of nicotinamide *N*-methyltrasferase and increased formation of 1-methylnicotinamide (MNA) in atherosclerosis. *Pharmacol Rep,* **61,** 76-85.

Matharu, B., Gibson, G., Parsons, R., Huckerby, T. N., Moore, S. A., Cooper, L. J., Millichamp, R., Allsop, D. & Austen, B. 2009. Galantamine inhibits β-amyloid aggregation and cytotoxicity. *J Neurol Sci,* **280,** 49-58.

Matsubara, K., Collins, M. A. & Neafsey, E. J. 1992. Mono-N-methylation of 1,2,3,4-tetrahydro-β-carbolines in brain cytosol: absence of indole methylation. *J Neurochem,* **59,** 505-10.

Matsubara, K., Neafsey, E. J. & Collins, M. A. 1992. Novel *S*-adenosylmethionine-dependent indole-*N*-methylation of β-carbolines in brain particulate fractions. *J Neurochem,* **59,** 511-8.

Matsubara, K., Collins, M. A., Akane, A., Ikebuchi, J., Neafsey, E. J., Kagawa, M. & Shiono, H. 1993. Potential bioactivated neurotoxicants, *N*-methylated β-carbolinium ions, are present in human brain. *Brain Res,* **610,** 90-6.

Matsubara, K., Idzu, T., Kobayashi, Y., Nakahara, D., Maruyama, W., Kobayashi, S., Kimura, K. & Naoi, M. 1995. *N*-methyl-4-phenylpyridinium and an endogenously formed analog, *N*-methylated β-carbolinium, inhibit striatal tyrosine hydroxylation in freely moving rats. *Neurosci Lett,* **199,** 199-202.

Matsubara, K., Gonda, T., Sawada, H., Uezono, T., Kobayashi, Y., Kawamura, T., Ohtaki, K., Kimura, K. & Akaike, A. 1998. Endogenously occurring β-carboline induces parkinsonism in nonprimate animals: a possible causative protoxin in idiopathic Parkinson's disease. *J Neurochem,* **70,** 727-35.

Matsubara, K., Aoyama, K., Suno, M. & Awaya, T. 2002. *N*-methylation underlying Parkinson's disease. *Neurotoxicol Teratol,* **24,** 593-8.

Matsuda, W., Furuta, T., Nakamura, K. C., Hioki, H., Fujiyama, F., Arai, R. & Kaneko, T. 2009. Single nigrostriatal dopaminergic neurons form widely spread and highly dense axonal arborizations in the neostriatum. *J Neurosci,* **29,** 444-53.

Michiorri, S., Gelmetti, V., Giarda, E., Lombardi, F., Romano, F., Marongiu, R., Nerini-Molteni, S., Sale, P., Vago, R., Arena, G., Torosantucci, L., Cassina, L., Russo, M. A., Dallapiccola, B., Valente, E. M. & Casari, G. 2010. The Parkinson-associated protein PINK1 interacts with Beclin1 and promotes autophagy. *Cell Death Differ,* **17,** 962-74.

Milani, Z. H., Ramsden, D. B. & Parsons, R. B. 2013. Neuroprotective effects of nicotinamide N-methyltransferase and its metabolite 1-methylnicotinamide. *J Biochem Mol Toxicol,* **27,** 451-6.

Misawa, H., Ishii, K. & Deguchi, T. 1992. Gene expression of mouse choline acetyltransferase. Alternative splicing and identification of a highly active promoter region. *J Biol Chem,* **267,** 20392-9.

Mochizuki, H. & Yasuda, T. 2012. Iron accumulation in Parkinson's disease. *J Neural Transm,* **119,** 1511-4.

Mori, Y., Sugawara, A., Tsuji, M., Kakamu, T., Tsuboi, S., Kanda, H., Hayakawa, T. & Fukushima, T. 2012. Toxic effects of nicotinamide methylation on mouse brain striatum neuronal cells and its relation to manganese. *Environ Health Prev Med,* **17,** 371-6.

Mosharov, E. V., Larsen, K. E., Kanter, E., Phillips, K. A., Wilson, K., Schmitz, Y., Krantz, D. E., Kobayashi, K., Edwards, R. H. & Sulzer, D. 2009. Interplay between cytosolic dopamine, calcium, and α-synuclein causes selective death of *substantia nigra* neurons. *Neuron,* **62,** 218-29.

Mueller, H., Kassack, M. U. & Wiese, M. 2004. Comparison of the usefulness of the MTT, ATP, and calcein assays to predict the potency of cytotoxic agents in various human cancer cell lines. *J Biomol Screen,* **9,** 506-15.

Murphy, M. P. 2009. How mitochondria produce reactive oxygen species. *Biochem J,* **417,** 1-13.

Myers, A. J., Kaleem, M., Marlowe, L., Pittman, A. M., Lees, A. J., Fung, H. C., Duckworth, J., Leung, D., Gibson, A., Morris, C. M., De Silva, R. & Hardy, J. 2005. The H1c haplotype at the *MAPT* locus is associated with Alzheimer's disease. *Hum Mol Genet,* **14,** 2399-404.

Nachmansohn, D. & Berman, M. 1946. Studies on choline acetylase; on the preparation of the coenzyme and its effect on the enzyme. *J Biol Chem,* **165,** 551-63.

Nagatsu, T. 1995. Tyrosine hydroxylase: human isoforms, structure and regulation in physiology and pathology. *Essays Biochem,* **30,** 15-35.

Nagatsu, T. & Sawada, M. 2007. Biochemistry of postmortem brains in Parkinson's disease: historical overview and future prospects. *J Neural Transm Suppl***,** 113-20.

Nalls, M. A., Plagnol, V., Hernandez, D. G., Sharma, M., Sheerin, U. M., Saad, M., Simon-Sanchez, J., Schulte, C., Lesage, S., Sveinbjornsdottir, S., Stefansson, K., Martinez, M., Hardy, J., Heutink, P., Brice, A., Gasser, T., Singleton, A. B. & Wood, N. W. 2011. Imputation of sequence variants for identification of genetic risks for Parkinson's disease: a meta-analysis of genome-wide association studies. *Lancet,* **377,** 641-9.

Neafsey, E. J., Drucker, G., Raikoff, K. & Collins, M. A. 1989. Striatal dopaminergic toxicity following intranigral injection in rats of 2-methyl-norharman, a β-carbolinium analog of *N*-methyl-4-phenylpyridinium ion (MPP^+). *Neurosci Lett,* **105,** 344-9.

Neafsey, E. J., Albores, R., Gearhart, D., Kindel, G., Raikoff, K., Tamayo, F. & Collins, M. A. 1995. Methyl-β-carbolinium analogs of MPP^+ cause nigrostriatal toxicity after *substantia nigra* injections in rats. *Brain Res,* **675,** 279-88.

Nelson, D. & Cox, M. 2008. *Principles of Biochemistry, 5th edition.* New York, NY, USA. W.H. Freeman and Company.

Nicklas, W. J., Vyas, I. & Heikkila, R. E. 1985. Inhibition of NADH-linked oxidation in brain mitochondria by 1-methyl-4-phenyl-pyridine, a metabolite of the neurotoxin, 1-methyl-4-phenyl-1,2,5,6-tetrahydropyridine. *Life Sci,* **36,** 2503-8.

Noonan, C. W., Reif, J. S., Yost, M. & Touchstone, J. 2002. Occupational exposure to magnetic fields in case-referent studies of neurodegenerative diseases. *Scand J Work Environ Health,* **28,** 42-8.

Oda, Y. 1999. Choline acetyltransferase: the structure, distribution and pathologic changes in the central nervous system. *Pathol Int,* **49,** 921-37.

Orrenius, S., Zhivotovsky, B. & Nicotera, P. 2003. Regulation of cell death: the calcium-apoptosis link. *Nat Rev Mol Cell Biol,* **4,** 552-65.

Östergren, A., Annas, A., Skog, K., Lindquist, N. G. & Brittebo, E. B. 2004. Long-term retention of neurotoxic β-carbolines in brain neuromelanin. *J Neural Transm,* **111,** 141-57.

Ott, M., Gogvadze, V., Orrenius, S. & Zhivotovsky, B. 2007. Mitochondria, oxidative stress and cell death. *Apoptosis,* **12,** 913-22.

Palacino, J. J., Sagi, D., Goldberg, M. S., Krauss, S., Motz, C., Wacker, M., Klose, J. & Shen, J. 2004. Mitochondrial dysfunction and oxidative damage in *parkin*-deficient mice. *J Biol Chem,* **279,** 18614-22.

Pals, P., Lincoln, S., Manning, J., Heckman, M., Skipper, L., Hulihan, M., Van Den Broeck, M., De Pooter, T., Cras, P., Crook, J., Van Broeckhoven, C. & Farrer, M. J. 2004. α-Synuclein promoter confers susceptibility to Parkinson's disease. *Ann Neurol,* **56,** 591-5.

Park, J., Lee, S. B., Lee, S., Kim, Y., Song, S., Kim, S., Bae, E., Kim, J., Shong, M., Kim, J. M. & Chung, J. 2006. Mitochondrial dysfunction in *Drosophila PINK1* mutants is complemented by *parkin*. *Nature,* **441,** 1157-61.

Parsons, R. B., Ramsden, Waring, R. H., Barber, P. C., Williams, A. C. 1998. Hepatic localisation of rat cysteine dioxygenase. *J Hepatol,* **29,** 595-602.

Parsons, R. B., Waring, R. H., Williams, A. C. & Ramsden, D. B. 2001. Cysteine dioxygenase: regional localisation of protein and mRNA in rat brain. *J Neurosci Res,* **65,** 78-84.

Parsons, R. B., Smith, M. L., Williams, A. C., Waring, R. H. & Ramsden, D. B. 2002. Expression of nicotinamide *N*-methyltransferase (E.C. 2.1.1.1) in the Parkinsonian brain. *J Neuropathol Exp Neurol,* **61,** 111-24.

Parsons, R. B., Smith, S. W., Waring, R. H., Williams, A. C. & Ramsden, D. B. 2003. High expression of nicotinamide *N*-methyltransferase in patients with idiopathic Parkinson's disease. *Neurosci Lett,* **342,** 13-6.

Parsons, R. B., Price, G. C., Farrant, J. K., Subramaniam, D., Adeagbo-Sheikh, J. & Austen, B. M. 2006. Statins inhibit the dimerization of β-secretase via both isoprenoid- and cholesterol-mediated mechanisms. *Biochem J,* **399,** 205-14.

Parsons, R. B., Aravindan, S., Kadampeswaran, A., Evans, E. A., Sandhu, K. K., Levy, E. R., Thomas, M. G., Austen, B. M. & Ramsden, D. B. 2011. The expression of nicotinamide *N*-methyltransferase increases ATP synthesis and protects SH-SY5Y neuroblastoma cells against the toxicity of Complex I inhibitors. *Biochem J,* **436,** 145-55.

Patel, M., Vasaya, M. M., Asker, D. & Parsons, R. B. 2013. HPLC-UV method for measuring nicotinamide *N*-methyltransferase activity in biological samples: evidence for substrate inhibition kinetics. *J Chromatogr B Analyt Technol Biomed Life Sci,* **921-922,** 87-95.

Pavlovic, S., Schulze, G., Wernicke, C., Bonnet, R., Gille, G., Badiali, L., Kaminska, A., Lorenc-Koci, E., Ossowska, K. & Rommelspacher, H. 2006. 2,9-Dimethyl-β-carbolinium, a neurotoxin occurring in human brain, is a potent inducer of apoptosis as 1-methyl-4-phenylpyridinium. *Neuroscience,* **139,** 1525-37.

Perry, T. L., Yong, V. W., Wall, R. A. & Jones, K. 1986. Paraquat and two endogenous analogues of the neurotoxic substance *N*-methyl-4-phenyl-1,2,3,6-tetrahydropyridine do not damage dopaminergic nigrostriatal neurons in the mouse. *Neurosci Lett,* **69,** 285-9.

Perry, T. L., Jones, K., Hansen, S. & Wall, R. A. 1987. 4-phenylpyridine and three other analogues of 1-methyl-4-phenyl-1,2,3,6-tetrahydropyridine lack dopaminergic nigrostriatal neurotoxicity in mice and marmosets. *Neurosci Lett,* **75,** 65-70.

Peura, P., Johnson, J. V., Yost, R. A. & Faull, K. F. 1989. Concentrations of tryptoline and methtryptoline in rat brain. *J Neurochem,* **52,** 847-52.

Pezzoli, G. & Cereda, E. 2013. Exposure to pesticides or solvents and risk of Parkinson disease. *Neurology,* **80,** 2035-41.

Pissadaki, E. K. & Bolam, J. P. 2013. The energy cost of action potential propagation in dopamine neurons: clues to susceptibility in Parkinson's disease. *Front Comput Neurosci,* **7,** 13.

Polymeropoulos, M. H., Lavedan, C., Leroy, E., Ide, S. E., Dehejia, A., Dutra, A., Pike, B., Root, H., Rubenstein, J., Boyer, R., Stenroos, E. S., Chandrasekharappa, S., Athanassiadou, A., Papapetropoulos, T., Johnson, W. G., Lazzarini, A. M., Duvoisin, R. C., Di Iorio, G., Golbe, L. I. & Nussbaum, R. L. 1997. Mutation in the α-synuclein gene identified in families with Parkinson's disease. *Science,* **276,** 2045-7.

Poole, A. C., Thomas, R. E., Andrews, L. A., Mcbride, H. M., Whitworth, A. J. & Pallanck, L. J. 2008. The PINK1/Parkin pathway regulates mitochondrial morphology. *Proc Natl Acad Sci U S A,* **105,** 1638-43.

Presgraves, S. P., Ahmed, T., Borwege, S. & Joyce, J. N. 2004. Terminally differentiated SH-SY5Y cells provide a model system for studying neuroprotective effects of dopamine agonists. *Neurotox Res,* **5,** 579-98.

Purves, D., Augustine, G., Fitzpatrick, D., Katz, L., Lamantia, A., Mcnamara, J. & Williams, S. 2001. *Neuroscience, 2nd edition.* Sunderland, MA, USA. Sinauer Associates.

Puschmann, A. 2013. Monogenic Parkinson's disease and parkinsonism: clinical phenotypes and frequencies of known mutations. *Parkinsonism Relat Disord,* **19,** 407-15.

Ramsay, R. R., Youngster, S. K., Nicklas, W. J., Mckeown, K. A., Jin, Y. Z., Heikkila, R. E. & Singer, T. P. 1989. Structural dependence of the inhibition of mitochondrial respiration and of NADH oxidase by 1-methyl-4-phenylpyridinium (MPP^+) analogs and their energized accumulation by mitochondria. *Proc Natl Acad Sci U S A,* **86,** 9168-72.

Rees, J. N., Florang, V. R., Eckert, L. L. & Doorn, J. A. 2009. Protein reactivity of 3,4-dihydroxyphenylacetaldehyde, a toxic dopamine metabolite, is dependent on both the aldehyde and the catechol. *Chem Res Toxicol,* **22,** 1256-63.

Rini, J., Szumlanski, C., Guerciolini, R. & Weinshilboum, R. M. 1990. Human liver nicotinamide *N*-methyltransferase: ion-pairing radiochemical assay, biochemical properties and individual variation. *Clin Chim Acta,* **186,** 359-74.

Roede, J. R. & Jones, D. P. 2014. Thiol-reactivity of the fungicide maneb. *Redox Biol,* **2,** 651-5.

Rook, Y., Schmidtke, K. U., Gaube, F., Schepmann, D., Wunsch, B., Heilmann, J., Lehmann, J. & Winckler, T. 2010. Bivalent β-carbolines as potential multitarget anti-Alzheimer agents. *J Med Chem,* **53,** 3611-7.

Ross, O. A., Braithwaite, A. T., Skipper, L. M., Kachergus, J., Hulihan, M. M., Middleton, F. A., Nishioka, K., Fuchs, J., Gasser, T., Maraganore, D. M., Adler, C. H., Larvor, L., Chartier-Harlin, M. C., Nilsson, C., Langston, J. W., Gwinn, K., Hattori, N. & Farrer, M. J. 2008. Genomic investigation of α-synuclein multiplication and parkinsonism. *Ann Neurol,* **63,** 743-50.

Saha, S., Guillily, M. D., Ferree, A., Lanceta, J., Chan, D., Ghosh, J., Hsu, C. H., Segal, L., Raghavan, K., Matsumoto, K., Hisamoto, N., Kuwahara, T., Iwatsubo, T., Moore, L., Goldstein, L., Cookson, M. & Wolozin, B. 2009. *LRRK2* modulates vulnerability to mitochondrial dysfunction in *Caenorhabditis elegans*. *J Neurosci,* **29,** 9210-8.

Sakowski, S. A., Geddes, T. J., Thomas, D. M., Levi, E., Hatfield, J. S. & Kuhn, D. M. 2006. Differential tissue distribution of tryptophan hydroxylase isoforms 1 and 2 as revealed with monospecific antibodies. *Brain Res,* **1085,** 11-8.

Satoh, T., Isobe, H., Ayukawa, K., Sakai, H. & Nawata, H. 1996. The effects of pravastatin, an HMG-CoA reductase inhibitor, on cell viability and DNA production of rat hepatocytes. *Life Sci,* **59,** 1103-8.

Scarffe, L. A., Stevens, D. A., Dawson, V. L. & Dawson, T. M. 2014. Parkin and PINK1: much more than mitophagy. *Trends Neurosci,* **37,** 315-24.

Schapira, A. H., Cooper, J. M., Dexter, D., Jenner, P., Clark, J. B. & Marsden, C. D. 1989. Mitochondrial complex I deficiency in Parkinson's disease. *Lancet,* **1,** 1269.

Schapira, A. H., Cooper, J. M., Dexter, D., Clark, J. B., Jenner, P. & Marsden, C. D. 1990. Mitochondrial complex I deficiency in Parkinson's disease. *J Neurochem,* **54,** 823-7.

Schapira, A. H. 2008. Mitochondria in the aetiology and pathogenesis of Parkinson's disease. *Lancet Neurol,* **7,** 97-109.

Seidler, A., Hellenbrand, W., Robra, B. P., Vieregge, P., Nischan, P., Joerg, J., Oertel, W. H., Ulm, G. & Schneider, E. 1996. Possible environmental, occupational, and other etiologic factors for Parkinson's disease: a case-control study in Germany. *Neurology,* **46,** 1275-84.

Shimura, H., Hattori, N., Kubo, S., Mizuno, Y., Asakawa, S., Minoshima, S., Shimizu, N., Iwai, K., Chiba, T., Tanaka, K. & Suzuki, T. 2000. Familial Parkinson disease gene product, parkin, is a ubiquitin-protein ligase. *Nat Genet,* **25,** 302-5.

Sidransky, E., Nalls, M. A., Aasly, J. O., Aharon-Peretz, J., Annesi, G., Barbosa, E. R., Bar-Shira, A., Berg, D., Bras, J., Brice, A., Chen, C. M., Clark, L. N., Condroyer, C., De Marco, E. V., Durr, A., Eblan, M. J., Fahn, S., Farrer, M. J., Fung, H. C., Gan-Or, Z., Gasser, T., Gershoni-Baruch, R., Giladi, N., Griffith, A., Gurevich, T., Januario, C.,

Kropp, P., Lang, A. E., Lee-Chen, G. J., Lesage, S., Marder, K., Mata, I. F., Mirelman, A., Mitsui, J., Mizuta, I., Nicoletti, G., Oliveira, C., Ottman, R., Orr-Urtreger, A., Pereira, L. V., Quattrone, A., Rogaeva, E., Rolfs, A., Rosenbaum, H., Rozenberg, R., Samii, A., Samaddar, T., Schulte, C., Sharma, M., Singleton, A., Spitz, M., Tan, E. K., Tayebi, N., Toda, T., Troiano, A. R., Tsuji, S., Wittstock, M., Wolfsberg, T. G., Wu, Y. R., Zabetian, C. P., Zhao, Y. & Ziegler, S. G. 2009. Multicenter analysis of glucocerebrosidase mutations in Parkinson's disease. *N Engl J Med,* **361,** 1651-61.

Sidransky, E. & Lopez, G. 2012. The link between the GBA gene and parkinsonism. *Lancet Neurol,* **11,** 986-98.

Simons, J. W. & Van Den Broek, C. 1970. Comparison of ageing *in vitro* and ageing *in vivo* by means of cell size analysis using a Coulter counter. *Gerontologia,* **16,** 340-51.

Slomka, M., Zieminska, E., Salinska, E. & Lazarewicz, J. W. 2008. Neuroprotective effects of nicotinamide and 1-methylnicotinamide in acute excitotoxicity in vitro. *Folia Neuropathol,* **46,** 69-80.

Smeitink, J., Van Den Heuvel, L. & Dimauro, S. 2001. The genetics and pathology of oxidative phosphorylation. *Nat Rev Genet,* **2,** 342-52.

Smith, M. L., Burnett, D., Bennett, P., Waring, R. H., Brown, H. M., Williams, A. C. & Ramsden, D. B. 1998. A direct correlation between nicotinamide *N*-methyltransferase activity and protein levels in human liver cytosol. *Biochim Biophys Acta,* **1442,** 238-44.

Snyder, S. H. & D'amato, R. J. 1985. Predicting Parkinson's disease. *Nature,* **317,** 198-9.

Sofic, E., Riederer, P., Heinsen, H., Beckmann, H., Reynolds, G. P., Hebenstreit, G. & Youdim, M. B. 1988. Increased iron (III) and total iron content in post mortem *substantia nigra* of parkinsonian brain. *J Neural Transm,* **74,** 199-205.

Sternak, M., Khomich, T. I., Jakubowski, A., Szafarz, M., Szczepanski, W., Bialas, M., Stojak, M., Szymura-Oleksiak, J. & Chlopicki, S. 2010. Nicotinamide *N*-methyltransferase (NNMT) and 1-methylnicotinamide (MNA) in experimental hepatitis induced by concanavalin A in the mouse. *Pharmacol Rep,* **62,** 483-93.

Stöckigt, J., Antonchick, A. P., Wu, F. & Waldmann, H. 2011. The Pictet-Spengler reaction in nature and in organic chemistry. *Angew Chem Int Ed Engl,* **50,** 8538-64.

Surmeier, D. J., Guzman, J. N., Sanchez-Padilla, J. & Schumacker, P. T. 2011. The role of calcium and mitochondrial oxidant stress in the loss of *substantia nigra* pars compacta dopaminergic neurons in Parkinson's disease. *Neuroscience,* **198,** 221-31.

Surmeier, D. J., Guzman, J. N., Sanchez, J. & Schumacker, P. T. 2012. Physiological phenotype and vulnerability in Parkinson's disease. *Cold Spring Harb Perspect Med,* **2,** a009290.

Susilo, R., Damm, H., Rommelspacher, H. & Hofle, G. 1987. Biotransformation of 1-methyl-1,2,3,4-tetrahydro-β-carboline-1-carboxylic acid to harmalan, tetrahydroharman and harman in rats. *Neurosci Lett,* **81,** 325-30.

Susilo, R. & Rommelspacher, H. 1987. Formation of a β-carboline (1,2,3,4-tetrahydro-1-methyl-β-carboline-1-carboxylic acid) following intracerebroventricular injection of tryptamine and pyruvic acid. *Naunyn Schmiedebergs Arch Pharmacol,* **335,** 70-6.

Takahashi, S., Abe, T., Gotoh, J. & Fukuuchi, Y. 2002. Substrate-dependence of reduction of MTT: a tetrazolium dye differs in cultured astroglia and neurons. *Neurochem Int,* **40,** 441-8.

Tang, S. W., Yang, T. C., Lin, W. C., Chang, W. H., Wang, C. C., Lai, M. K. & Lin, J. Y. 2011. Nicotinamide *N*-methyltransferase induces cellular invasion through activating matrix metalloproteinase-2 expression in clear cell renal cell carcinoma cells. *Carcinogenesis,* **32,** 138-45.

Tanner, C. M., Kamel, F., Ross, G. W., Hoppin, J. A., Goldman, S. M., Korell, M., Marras, C., Bhudhikanok, G. S., Kasten, M., Chade, A. R., Comyns, K., Richards, M. B., Meng, C., Priestley, B., Fernandez, H. H., Cambi, F., Umbach, D. M., Blair, A., Sandler, D. P. & Langston, J. W. 2011. Rotenone, paraquat, and Parkinson's disease. *Environ Health Perspect,* **119,** 866-72.

Tayebi, N., Walker, J., Stubblefield, B., Orvisky, E., Lamarca, M. E., Wong, K., Rosenbaum, H., Schiffmann, R., Bembi, B. & Sidransky, E. 2003. Gaucher disease with parkinsonian manifestations: does glucocerebrosidase deficiency contribute to a vulnerability to parkinsonism? *Mol Genet Metab,* **79,** 104-9.

Thatcher, R. J., Johnson, D. G., Slattery, J. M. & Douthwaite, R. E. 2012. Charged behaviour from neutral ligands: synthesis and properties of *N*-heterocyclic pseudo-amides. *Chemistry,* **18,** 4329-36.

Thiruchelvam, M., Richfield, E. K., Baggs, R. B., Tank, A. W. & Cory-Slechta, D. A. 2000. The nigrostriatal dopaminergic system as a preferential target of repeated exposures to combined paraquat and maneb: implications for Parkinson's disease. *J Neurosci,* **20,** 9207-14.

Thomas, A. F. & Bassols, F. 1992. Occurrence of Pyridines and Other Bases in Orange Oil. *Journal of Agricultural and Food Chemistry,* **40,** 2236-2243.

Thomas, M. G., Saldanha, M., Mistry, R. J., Dexter, D. T., Ramsden, D. B. & Parsons, R. B. 2013. Nicotinamide *N*-methyltransferase expression in SH-SY5Y neuroblastoma and N27 mesencephalic neurones induces changes in cell morphology *via* ephrin-B2 and Akt signalling. *Cell Death Dis,* **4,** e669.

Thompson, M. A. & Weinshilboum, R. M. 1998. Rabbit lung indolethylamine *N*-methyltransferase. cDNA and gene cloning and characterization. *J Biol Chem,* **273,** 34502-10.

Triarhou, L. 2002. *Dopaminergic Neuron Transplantation in the Weaver Mouse Model of Parkinson's Disease,* New York, NY, USA. Springer, Kluwer Academic / Plenum Publishers and Landes Bioscience. With kind permisison by Springer Science + Business Media.

Ulanovskaya, O. A., Zuhl, A. M. & Cravatt, B. F. 2013. NNMT promotes epigenetic remodeling in cancer by creating a metabolic methylation sink. *Nat Chem Biol,* **9,** 300-6.

Van Der Helm, H. 1962. A simplified method of demonstrating lactic dehydrogenase isoenzymes in serum. *Clin Chim Acta,* **7,** 124-8.

Van Meerloo, J., Kaspers, G. J. & Cloos, J. 2011. Cell sensitivity assays: the MTT assay. *Methods Mol Biol,* **731,** 237-45.

Vives-Bauza, C., Zhou, C., Huang, Y., Cui, M., De Vries, R. L., Kim, J., May, J., Tocilescu, M. A., Liu, W., Ko, H. S., Magrane, J., Moore, D. J., Dawson, V. L., Grailhe, R., Dawson, T. M., Li, C., Tieu, K. & Przedborski, S. 2010. PINK1-dependent recruitment of Parkin to mitochondria in mitophagy. *Proc Natl Acad Sci U S A,* **107,** 378-83.

Votyakova, T. V. & Reynolds, I. J. 2001. $\Delta\psi_m$-dependent and -independent production of reactive oxygen species by rat brain mitochondria. *J Neurochem,* **79,** 266-77.

Walther, D. J. & Bader, M. 2003. A unique central tryptophan hydroxylase isoform. *Biochem Pharmacol,* **66,** 1673-80.

Wernicke, C., Schott, Y., Enzensperger, C., Schulze, G., Lehmann, J. & Rommelspacher, H. 2007. Cytotoxicity of β-carbolines in dopamine transporter expressing cells: structure-activity relationships. *Biochem Pharmacol,* **74,** 1065-77.

White, L. D. & Lawson, E. E. 1997. Effects of chronic prenatal hypoxia on tyrosine hydroxylase and phenylethanolamine *N*-methyltransferase messenger RNA and protein levels in *medulla oblongata* of postnatal rat. *Pediatr Res,* **42,** 455-62.

Williams, A. C., Cartwright, L. S. & Ramsden, D. B. 2005. Parkinson's disease: the first common neurological disease due to auto-intoxication? *QJM,* **98,** 215-26.

Wirdefeldt, K., Adami, H. O., Cole, P., Trichopoulos, D. & Mandel, J. 2011. Epidemiology and etiology of Parkinson's disease: a review of the evidence. *Eur J Epidemiol,* **26 Suppl 1,** S1-58.

Xie, H. R., Hu, L. S. & Li, G. Y. 2010. SH-SY5Y human neuroblastoma cell line: in vitro cell model of dopaminergic neurons in Parkinson's disease. *Chin Med J (Engl),* **123,** 1086-92.

Yao, D., Gu, Z., Nakamura, T., Shi, Z. Q., Ma, Y., Gaston, B., Palmer, L. A., Rockenstein, E. M., Zhang, Z., Masliah, E., Uehara, T. & Lipton, S. A. 2004.

Nitrosative stress linked to sporadic Parkinson's disease: *S*-nitrosylation of parkin regulates its E3 ubiquitin ligase activity. *Proc Natl Acad Sci U S A,* **101,** 10810-4.

Zecca, L., Casella, L., Albertini, A., Bellei, C., Zucca, F. A., Engelen, M., Zadlo, A., Szewczyk, G., Zareba, M. & Sarna, T. 2008. Neuromelanin can protect against iron-mediated oxidative damage in system modeling iron overload of brain aging and Parkinson's disease. *J Neurochem,* **106,** 1866-75.

Zeevalk, G. D., Razmpour, R. & Bernard, L. P. 2008. Glutathione and Parkinson's disease: is this the elephant in the room? *Biomed Pharmacother,* **62,** 236-49.

Zhang, J., Wang, Y., Li, G., Yu, H. & Xie, X. 2014. Down-regulation of nicotinamide *N*-methyltransferase induces apoptosis in human breast cancer cells *via* the mitochondria-mediated pathway. *PLoS One,* **9,** e89202.

Ziegler, M. G., Bao, X., Kennedy, B. P., Joyner, A. & Enns, R. 2002. Location, development, control, and function of extraadrenal phenylethanolamine *N*-methyltransferase. *Ann N Y Acad Sci,* **971,** 76-82.

Zimran, A. 2011. How I treat Gaucher disease. *Blood,* **118,** 1463-71.

Appendix 1

Listed below are the individual dose response curves that were used to cumulatively produce the n = 5 for all the data presented in chapter 5. The mean data set from each curve below was input as a single repeat into the curves seen in chapter 5. The same is true for the 1-way ANOVAs that were calculated using the mean raw data from each of these curves. One EC50 was calculated from each curve and input as a single repeat into the comparison of $EC50_{MTT}$ and $EC50_{ATP}$ *via* Student's *t*-test reported in chapter 5. Dark green curves and circles are indicative of the SH-SY5Y data while dark red curves are indicative of the S.NNMT.LP data.

MTT data

Norharman

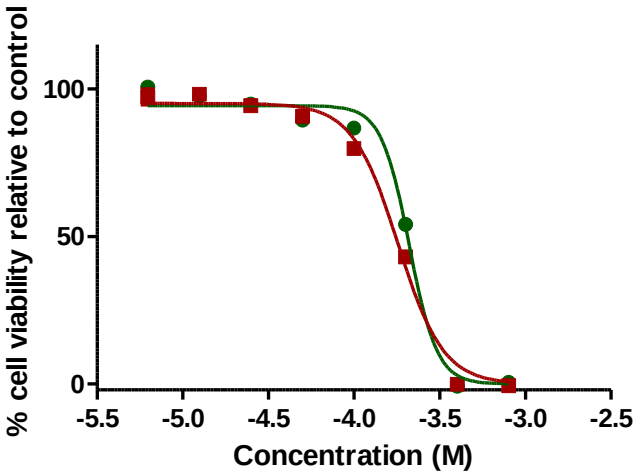

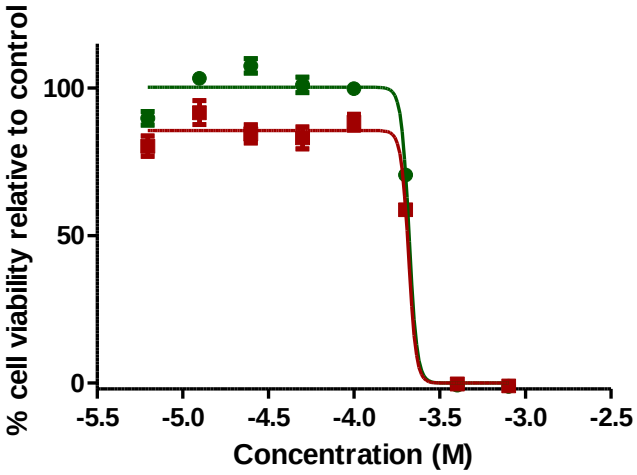

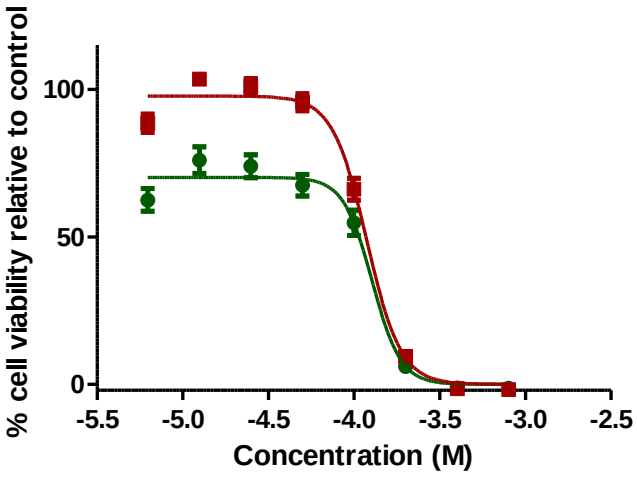

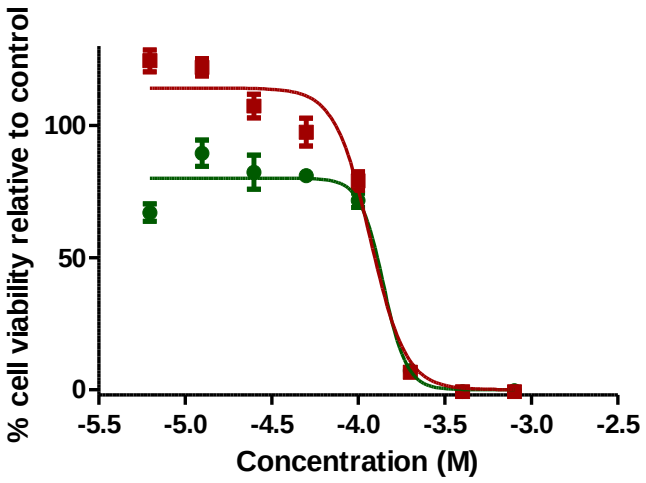
% cell viability relative to control
100
50
0
-5.5
-5.0
-4.5
-4.0
-3.5
-3.0
-2.5
Concentration (M)

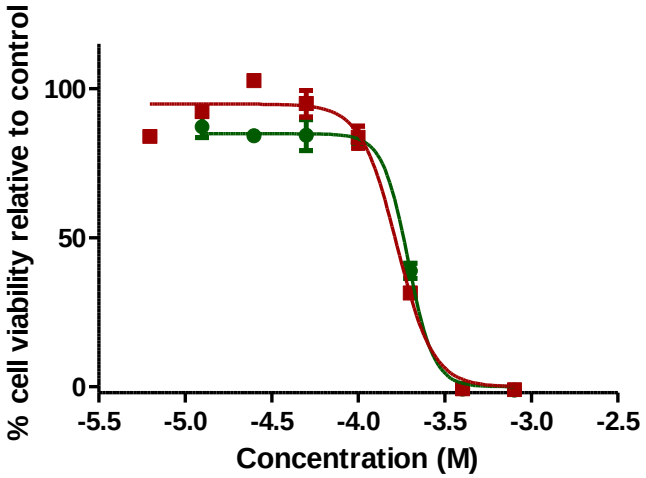
% cell viability relative to control
100
50
0
-5.5
-5.0
-4.5
-4.0
-3.5
-3.0
-2.5
Concentration (M)

Tetrahydronorharman

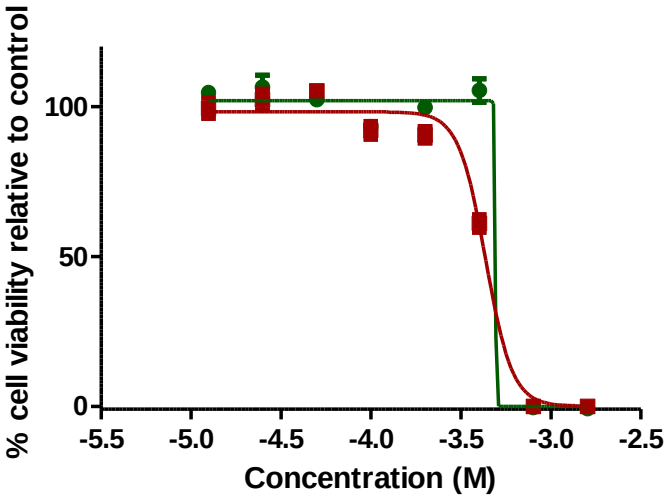

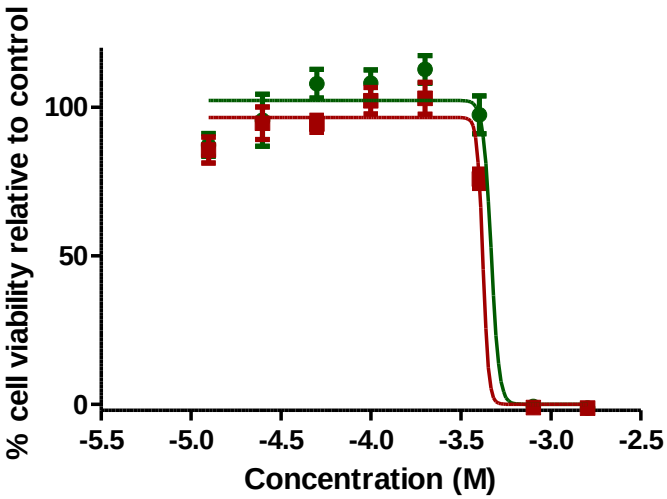

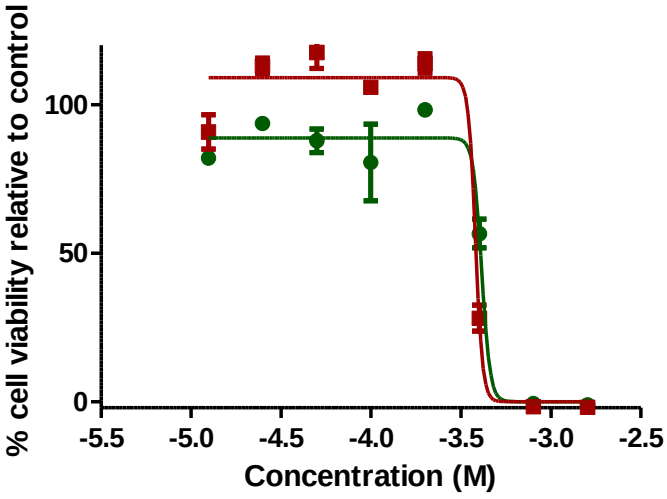

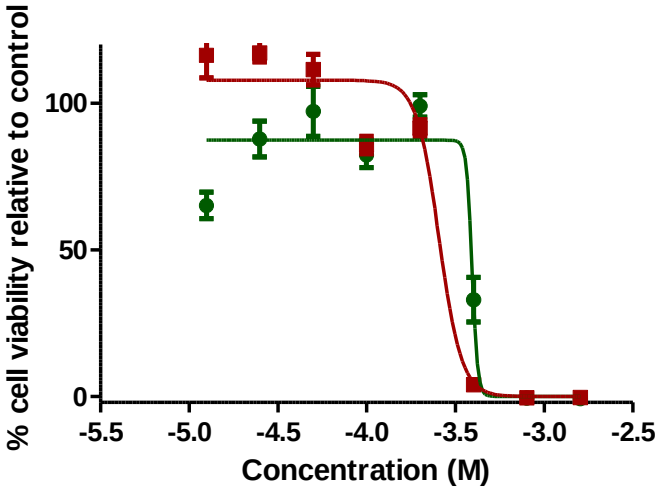
% cell viability relative to control
100
50
0
-5.5
-5.0
-4.5
-4.0
-3.5
-3.0
-2.5
Concentration (M)

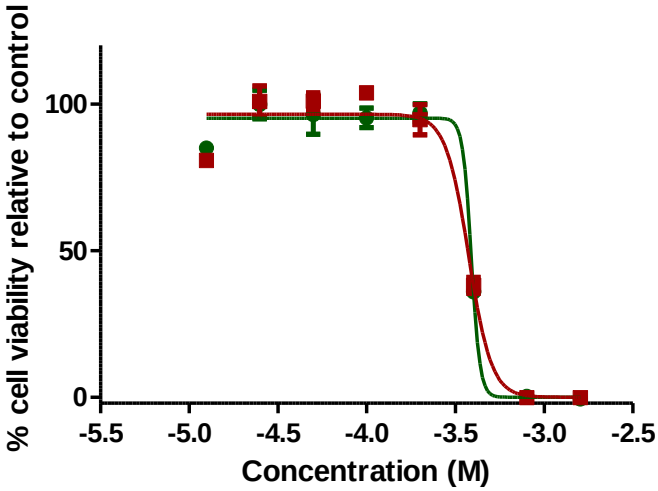
% cell viability relative to control
100
50
0
-5.5
-5.0
-4.5
-4.0
-3.5
-3.0
-2.5
Concentration (M)

4-phenylpyridine

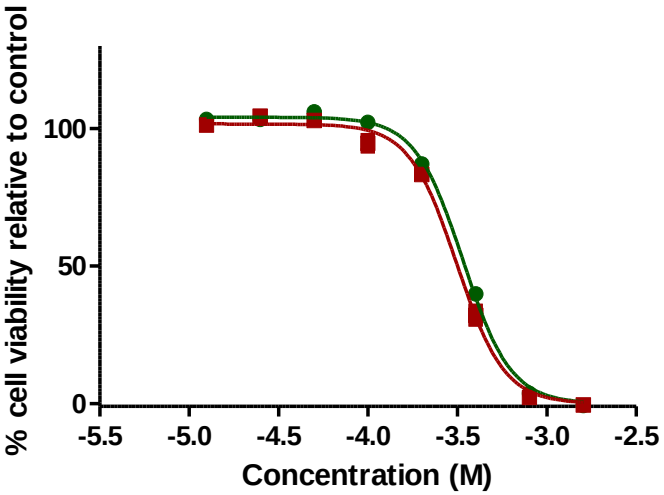

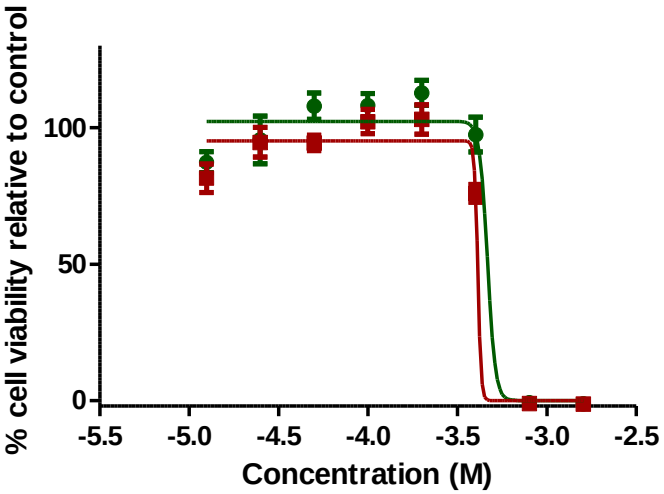

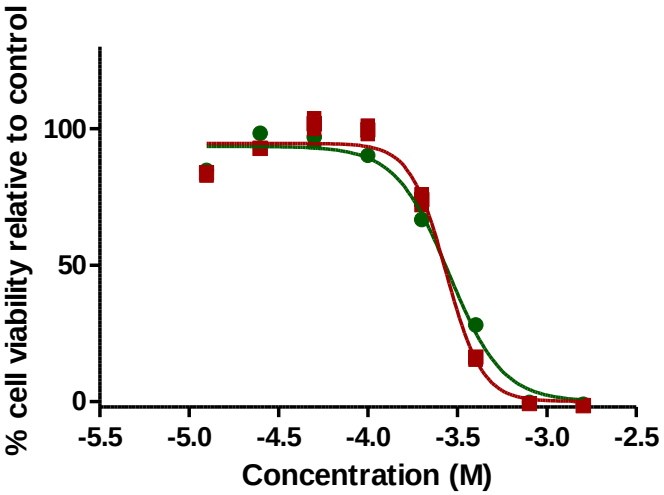

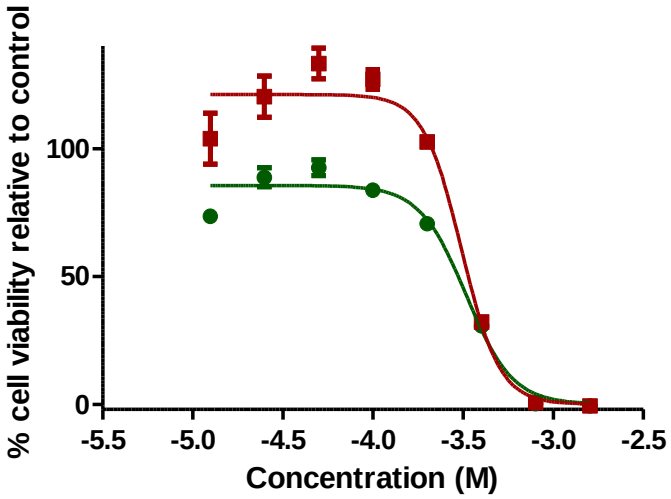
% cell viability relative to control
100
50
0
-5.5
-5.0
-4.5
-4.0
-3.5
-3.0
-2.5
Concentration (M)

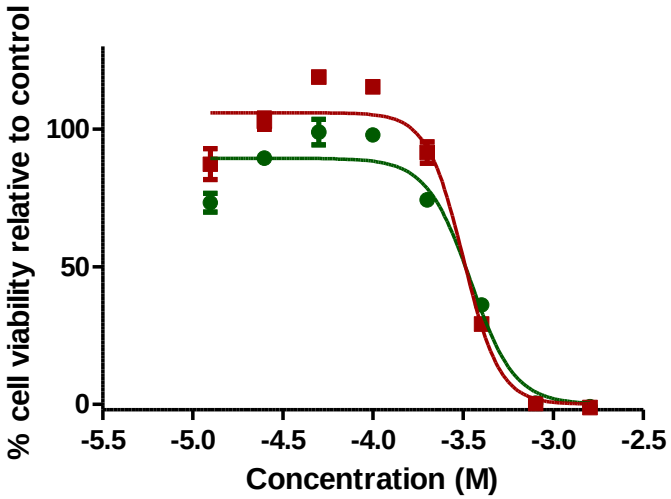
% cell viability relative to control
100
50
0
-5.5
-5.0
-4.5
-4.0
-3.5
-3.0
-2.5
Concentration (M)

ATP data

Norharman

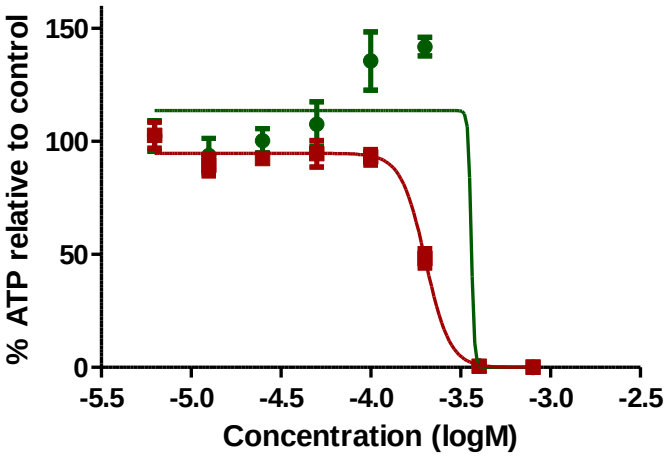

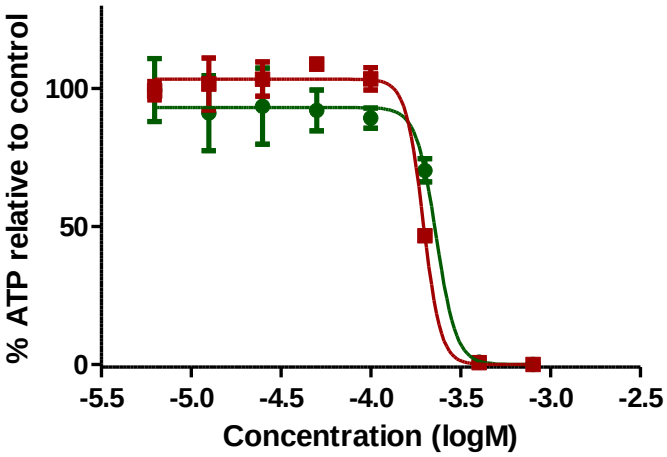

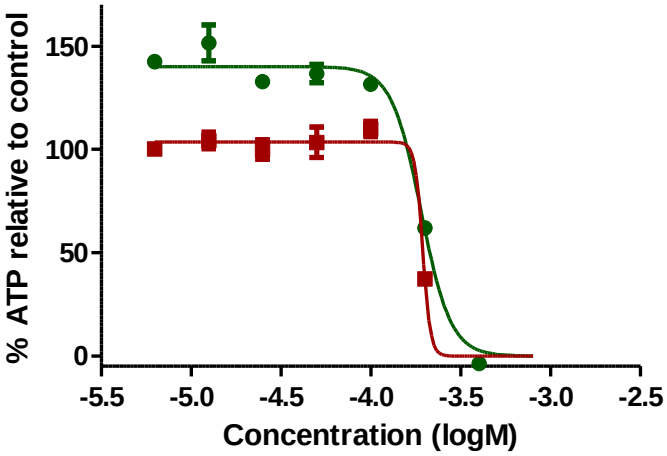

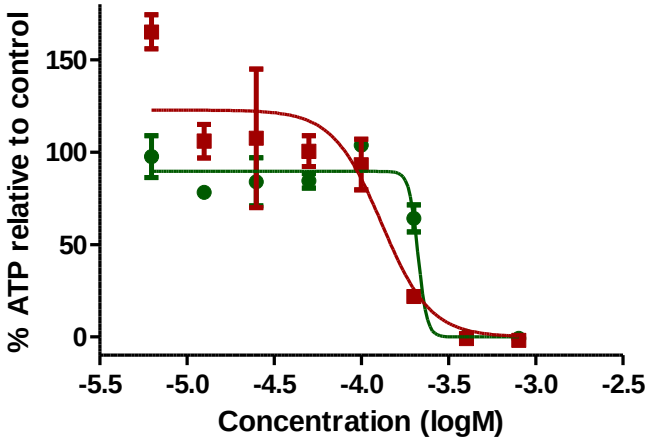
% ATP relative to control
150
100
50
0
-5.5
-5.0
-4.5
-4.0
-3.5
-3.0
-2.5
Concentration (logM)

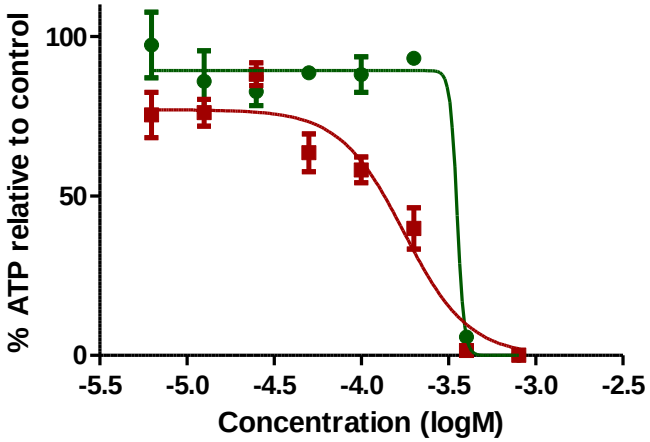
% ATP relative to control
100
50
0
-5.5
-5.0
-4.5
-4.0
-3.5
-3.0
-2.5
Concentration (logM)

Tetrahydronorharman

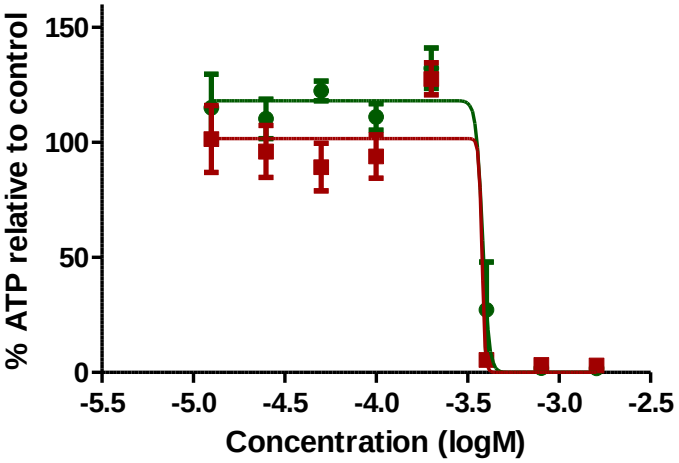

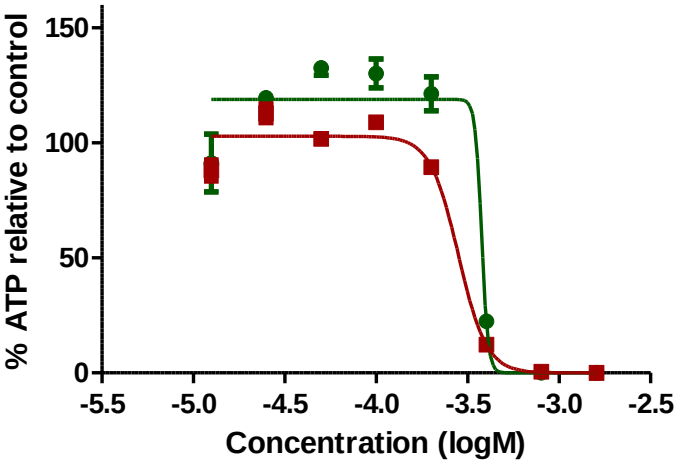

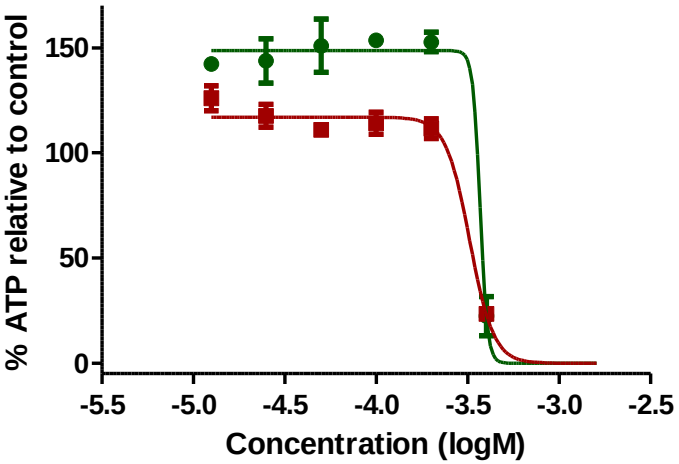

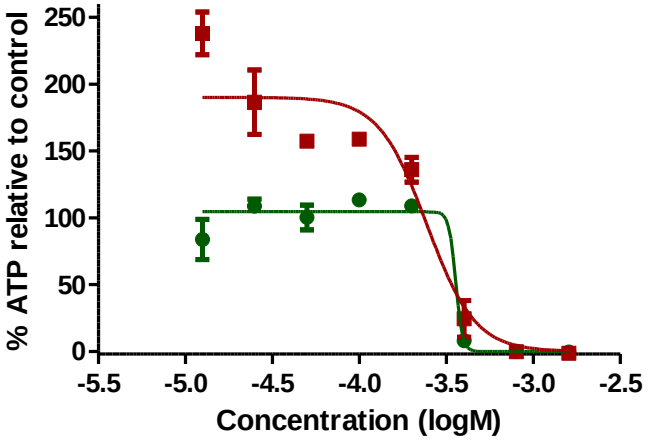
% ATP relative to control
250
200
150
100
50
0
-5.5
-5.0
-4.5
-4.0
-3.5
-3.0
-2.5
Concentration (logM)

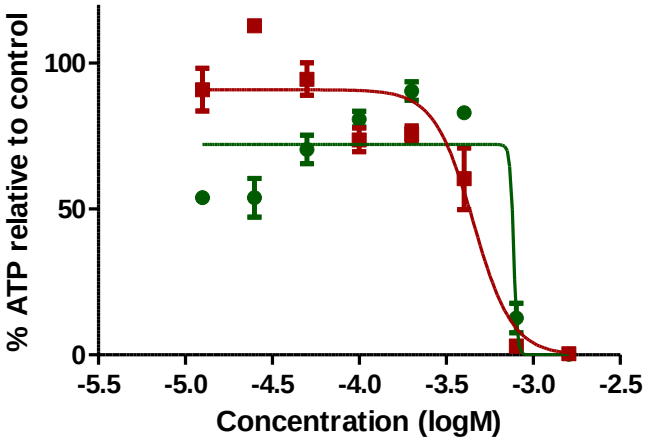
% ATP relative to control
100
50
0
-5.5
-5.0
-4.5
-4.0
-3.5
-3.0
-2.5
Concentration (logM)

4-Phenylpyridine

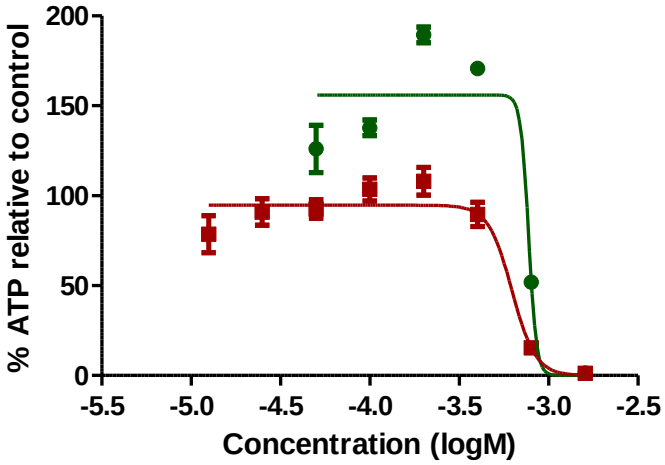

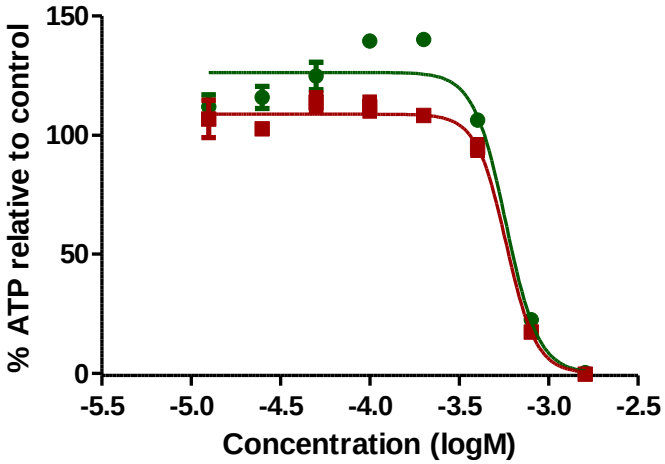

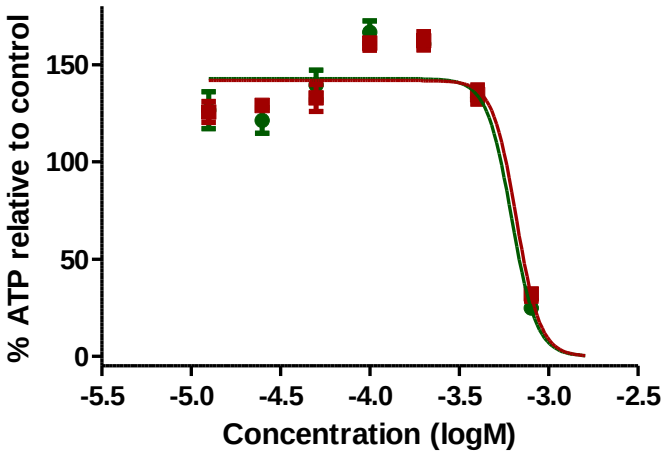

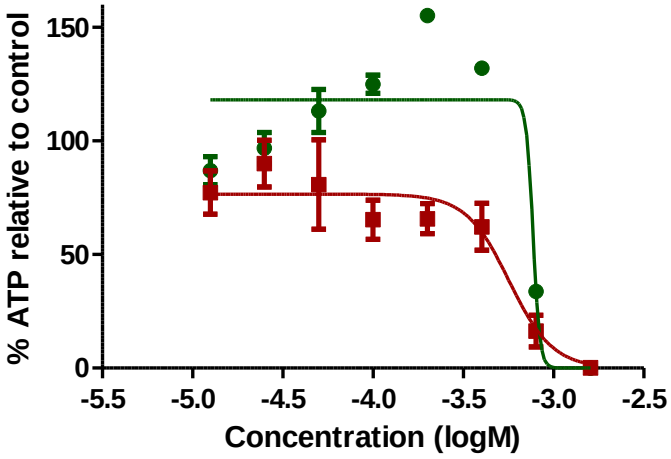
% ATP relative to control
150
100
50
0
-5.5
-5.0
-4.5
-4.0
-3.5
-3.0
-2.5
Concentration (logM)

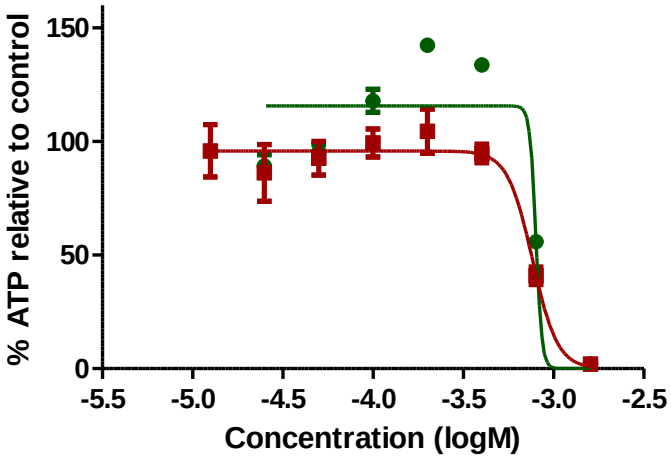
% ATP relative to control
150
100
50
0
-5.5
-5.0
-4.5
-4.0
-3.5
-3.0
-2.5
Concentration (logM)

Appendix 2

Listed below are the individual 2-methylnorharman dose response curves that were used to cumulatively produce the n = 4 for all the data presented in chapter 6. The mean data set from each curve below was input as a single repeat into the curves seen in chapter 6. The same is true for the 1-way ANOVAs that were calculated using the mean raw data from each of these curves. One EC50 was calculated from each curve and input as a single repeat into the comparison of $EC50_{MTT}$ and $EC50_{ATP}$ *via* Student's *t*-test reported in chapter 6. Dark green curves and circles are indicative of the SH-SY5Y data while dark red curves are indicative of the S.NNMT.LP data.

MTT data

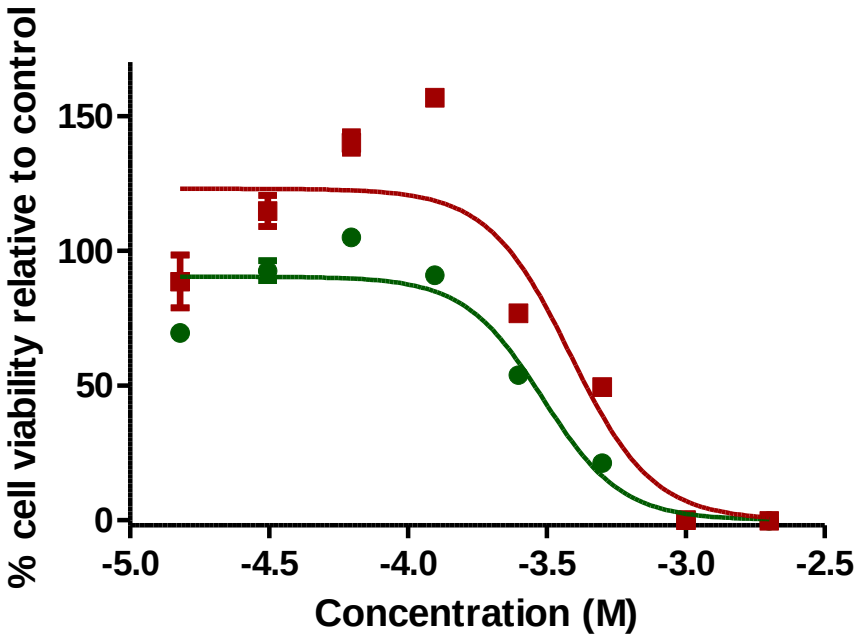
% cell viability relative to control
150
100
50
0
-5.0
-4.5
-4.0
-3.5
-3.0
-2.5
Concentration (M)

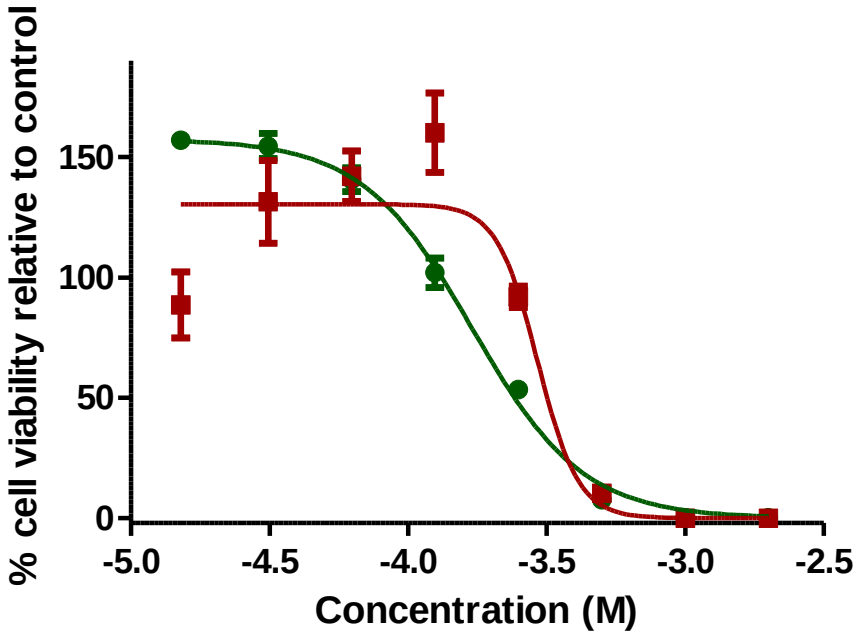
% cell viability relative to control
150
100
50
0
-5.0
-4.5
-4.0
-3.5
-3.0
-2.5
Concentration (M)

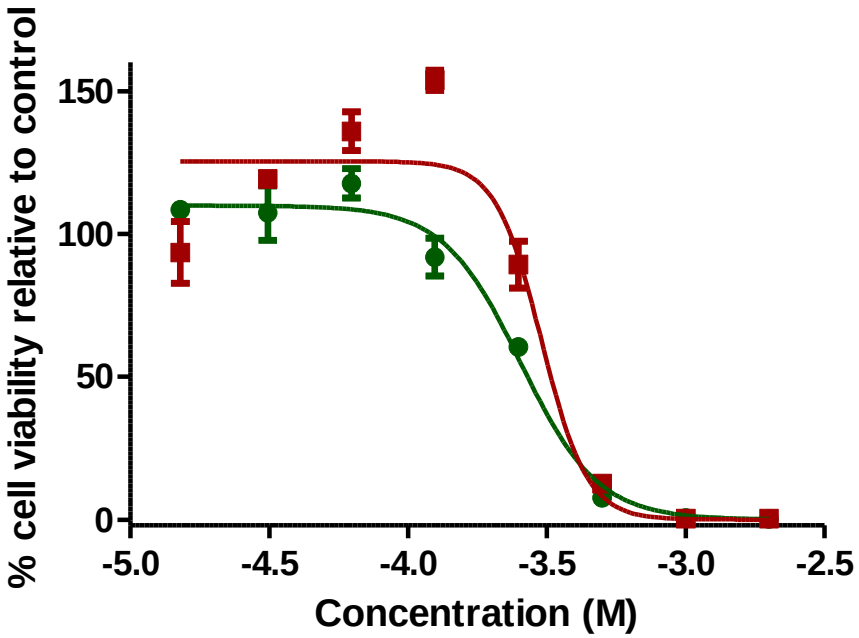
% cell viability relative to control
150
100
50
0
-5.0
-4.5
-4.0
-3.5
-3.0
-2.5
Concentration (M)

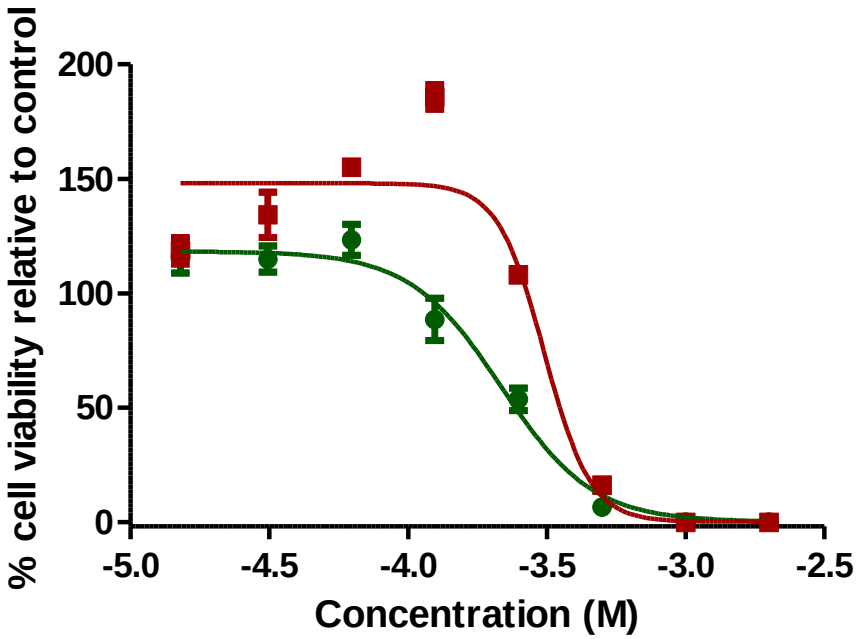
% cell viability relative to control
200
150
100
50
0
-5.0
-4.5
-4.0
-3.5
-3.0
-2.5
Concentration (M)

ATP data

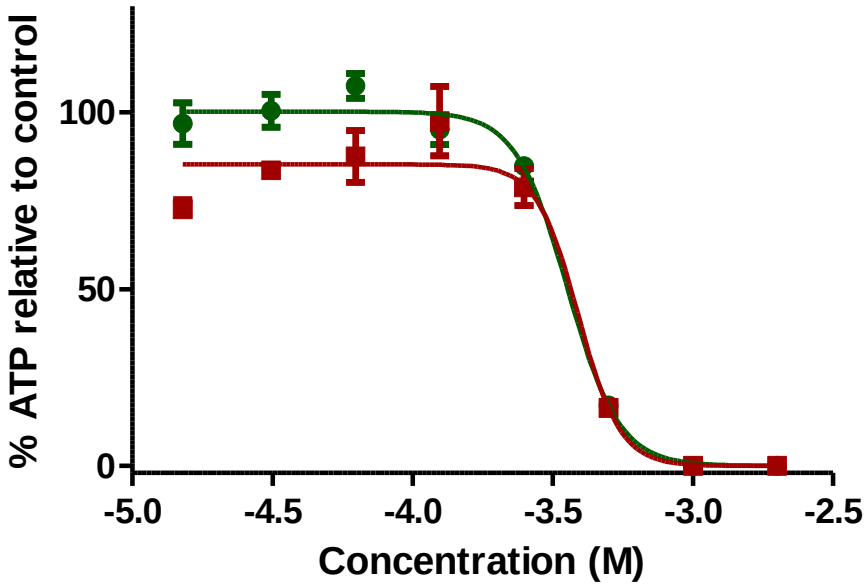
% ATP relative to control
100
50
0
-5.0
-4.5
-4.0
-3.5
-3.0
-2.5
Concentration (M)

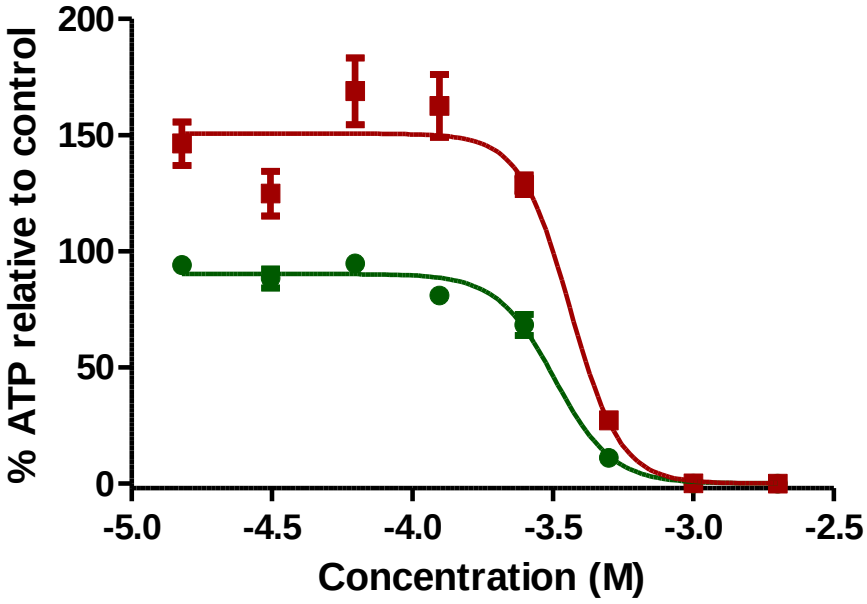
% ATP relative to control
200
150
100
50
0
-5.0
-4.5
-4.0
-3.5
-3.0
-2.5
Concentration (M)

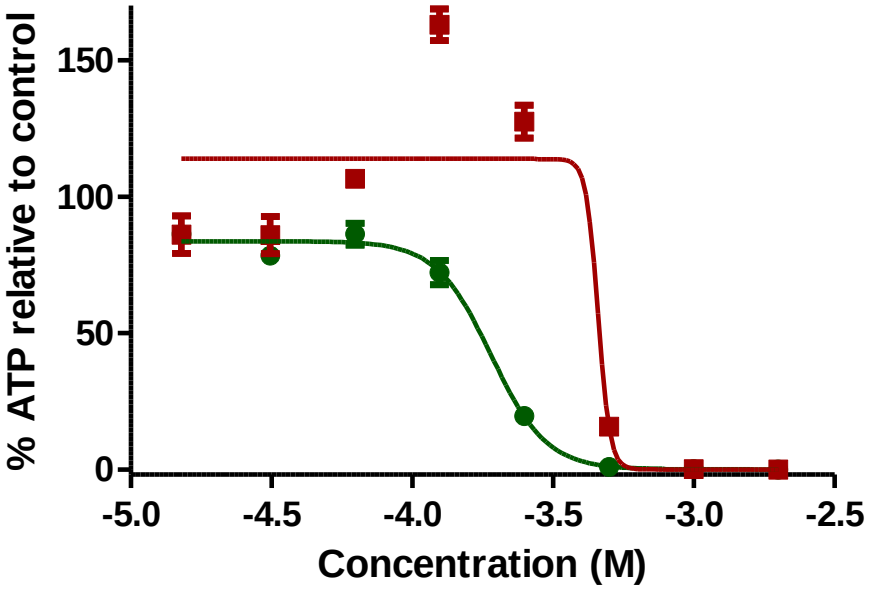
% ATP relative to control
150
100
50
0
-5.0
-4.5
-4.0
-3.5
-3.0
-2.5
Concentration (M)

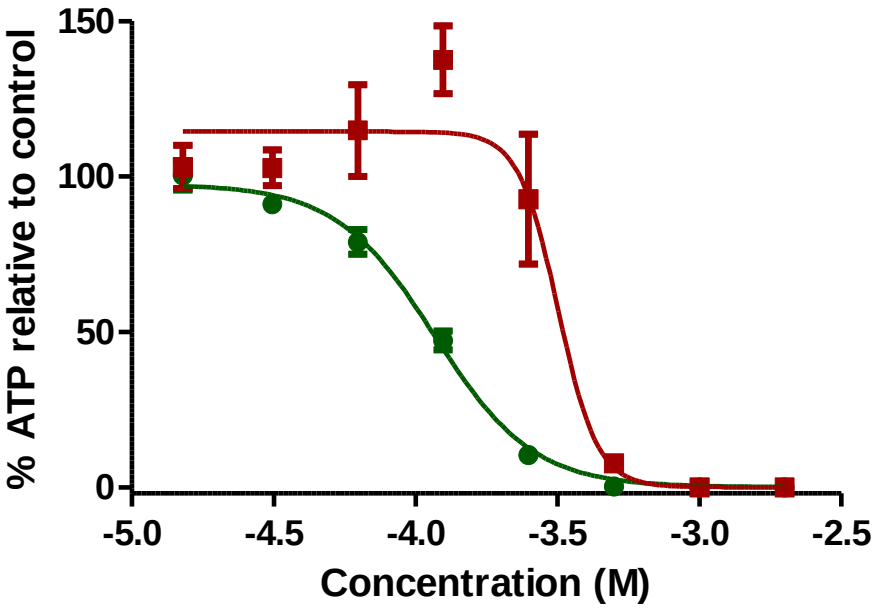
% ATP relative to control
150
100
50
0
-5.0
-4.5
-4.0
-3.5
-3.0
-2.5
Concentration (M)

Appendix 3

Listed below are the individual enzyme assay time course graphs that were used to calculated specific activity for each NH concentration and subsequently used to produce the Michaelis-Menten plot and linear derivations thereof presented in chapter 6.

No enzyme control

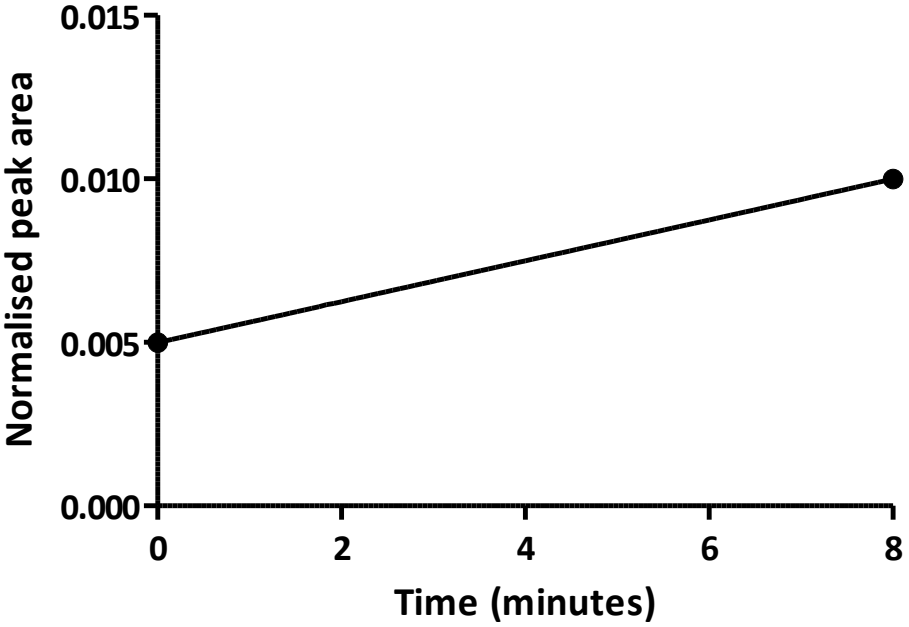

0.05 mM NH

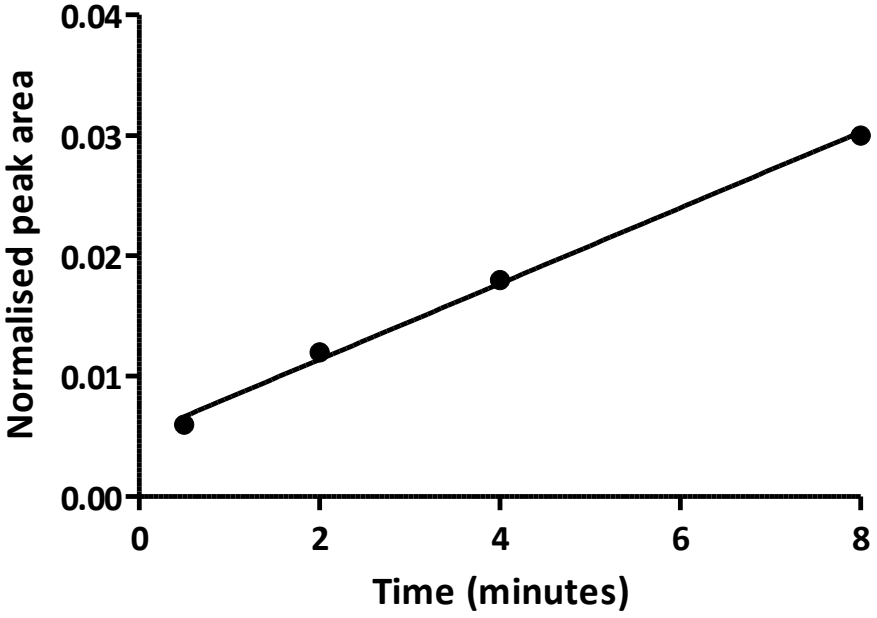

0.1 mM NH

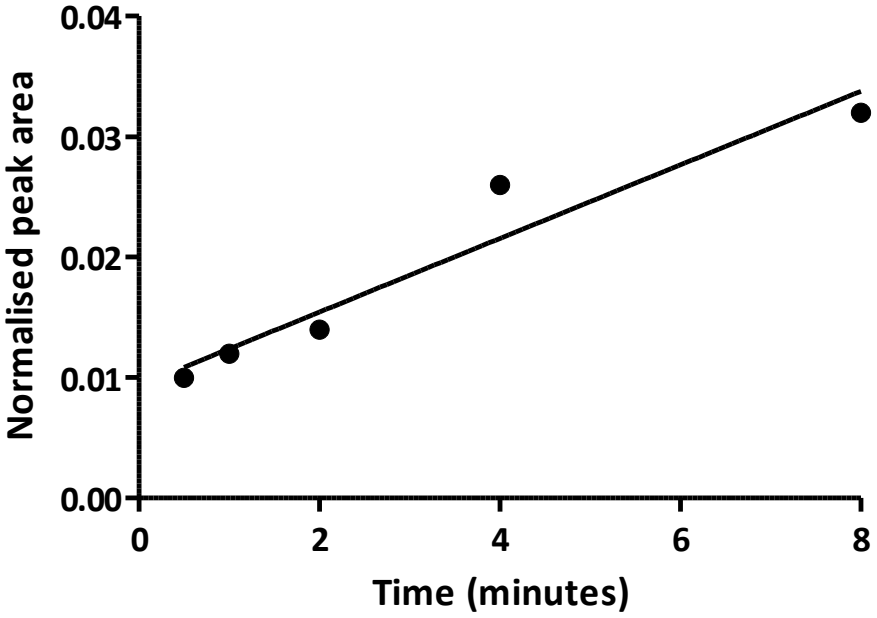

0.25 mM NH

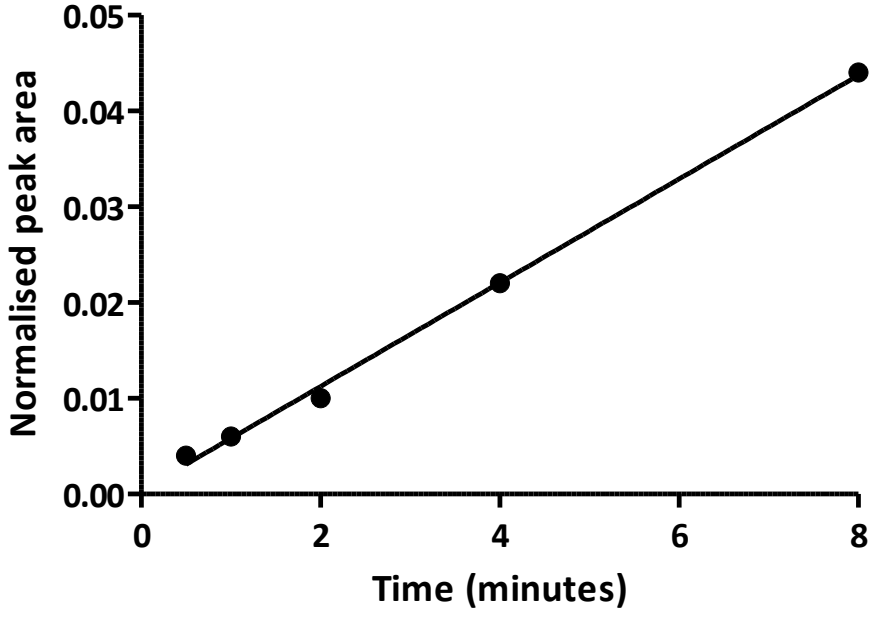

0.5 mM NH

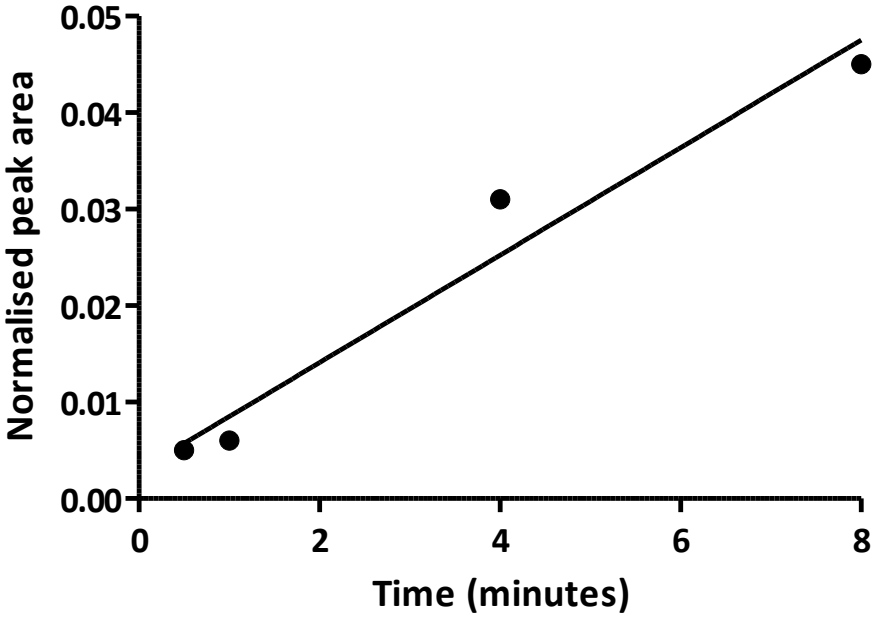

1.0 mM NH

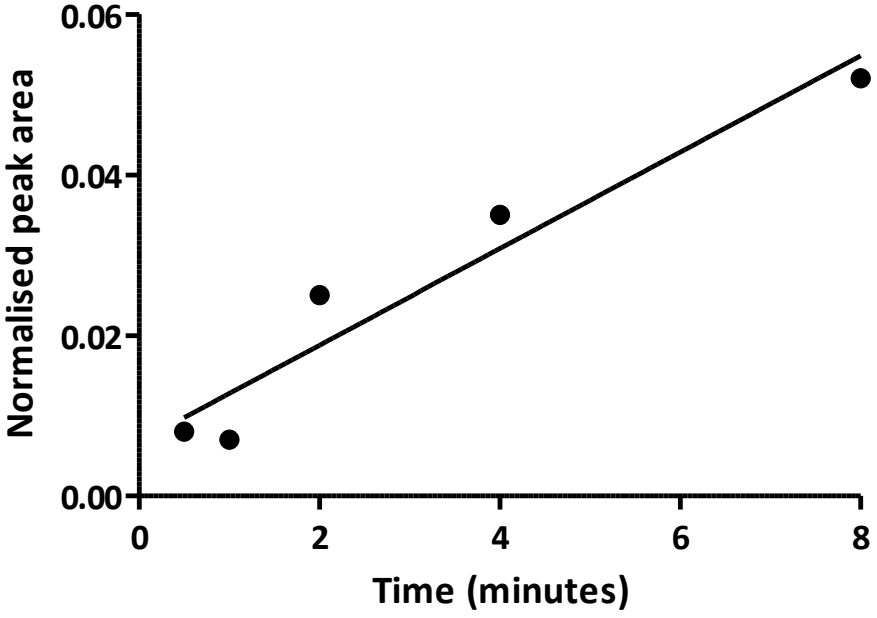

Appendix 4

Included below are publications that contain data obtained in this project.

Parsons, R. B., Aravindan, S., Kadampeswaran, A., Evans, E. A., Sandhu, K. K., Levy, E. R., Thomas, M. G., Austen, B. M. & Ramsden, D. B. 2011. The expression of nicotinamide N-methyltransferase increases ATP synthesis and protects SH-SY5Y neuroblastoma cells against the toxicity of Complex I inhibitors. *Biochem J,* **436,** 145-55: ***Western blotting, ATP content, JC-1 staining and oxygen consumption data from chapter 4 are featured in figures 1 and 3.***

Thomas, M. G., Saldanha, M., Mistry, R. J., Dexter, D. T., Ramsden, D. B. & Parsons, R. B. 2013. Nicotinamide N-methyltransferase expression in SH-SY5Y neuroblastoma and N27 mesencephalic neurones induces changes in cell morphology via ephrin-B2 and Akt signalling. *Cell Death Dis,* **4,** e669: ***Neuronal lineage data from chapter 4 are featured in figure 5.***